COURSE 1

ATOMIC MOTION IN LASER LIGHT

C. COHEN-TANNOUDJI

Collège de France
and
Département de Physique de
l'Ecole Normale Supérieure
Paris, France

J. Dalibard, J.M. Raimond and J. Zinn-Justin, eds.
Les Houches, Session LIII, 1990
Systèmes Fondamentaux en Optique Quantique
/Fundamental Systems in Quantum Optics

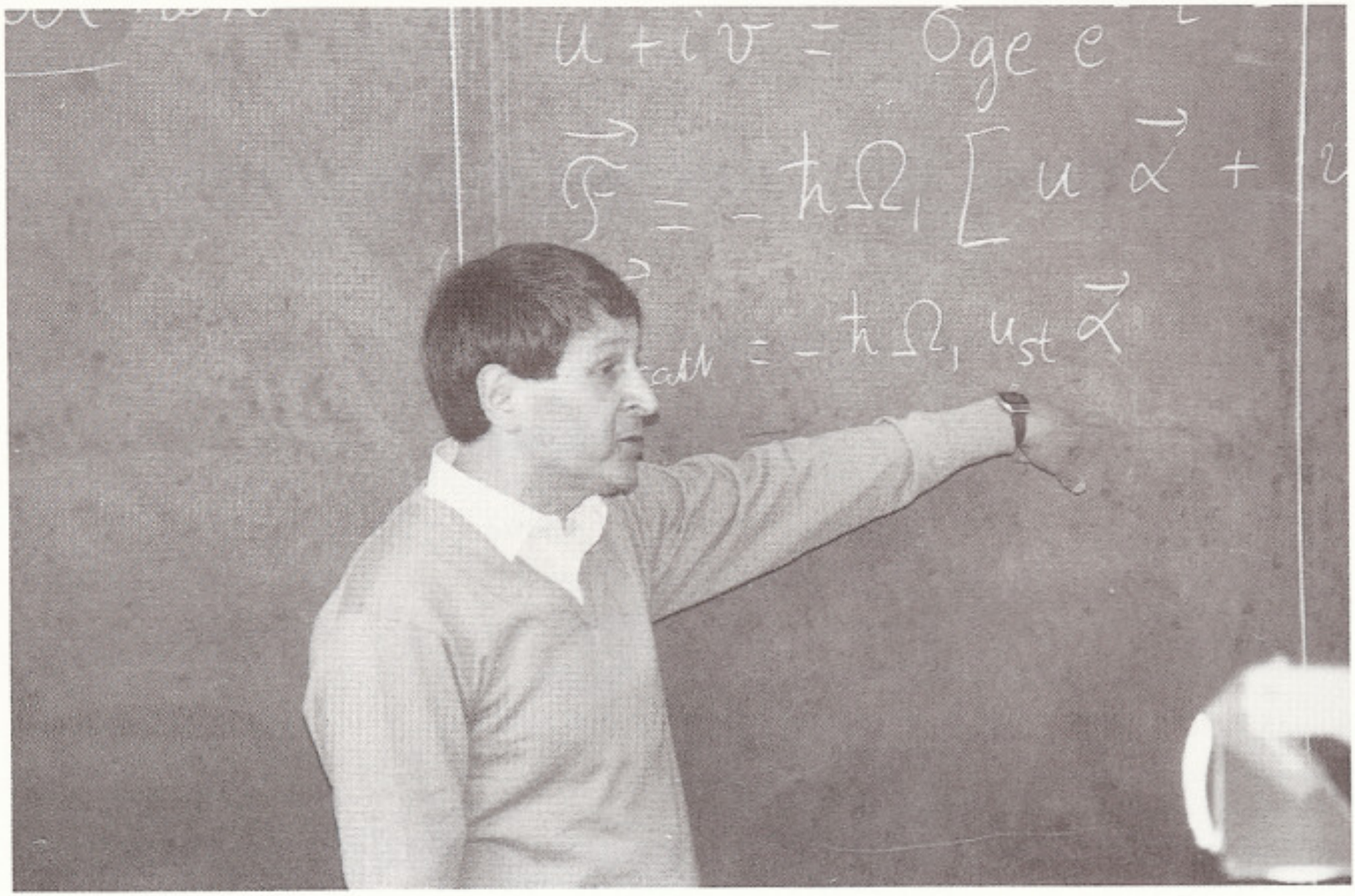
u + i v = 6ge e
F = - h Ω, [u α +
= - h Ω, u_st α

Contents

1. General introduction

1.1. Purpose of this course

The purpose of this course is to discuss the basic processes and the physical mechanisms which govern atomic motion in laser light. During the last few years, spectacular results have been obtained concerning the possibility to "manipulate" atoms with laser light. A new expanding research field, called laser cooling and trapping, has come out (see for example the courses of W. Phillips, R. Blatt and H. Walther in this volume). In order to explore the limits of these new methods, several theoretical approaches have been developed. In this course, we review some of these approaches and we compare their advantages, their difficulties and their domains of validity.

The emphasis will be put here on physical ideas and physical mechanisms. The details of the calculations will not be given when they are available in the literature. We will just recall the principle of such calculations, devoting more time to the interpretation of the results and to the discussion of the various approximations which are introduced. We will consider only the case of neutral atoms. Laser cooling of ions is discussed in detail in the courses of R. Blatt and H. Walther.

1.2. The interacting systems

The atomic medium is supposed to be very dilute, so that one can ignore atom–atom interactions. We thus consider here a single atom A, with an excited state e and a ground state g separated by an energy interval

$$E_e - E_g = \hbar\omega_A, \tag{1.1}$$

ω_A being called the atomic frequency. Important atomic observables are the electric dipole moment $\boldsymbol{d}$, the position $\boldsymbol{R}$ and the momentum $\boldsymbol{P}$ of the center of mass. This atom A is coupled, on the one hand, to the laser field L, and on the other hand to all the other modes of the radiation field which initially do not contain any photon and which form what we call the quantum vacuum field V (see fig. 1).

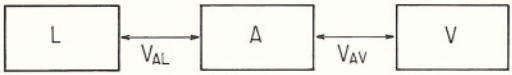

Fig. 1. The interacting systems and their various couplings.

The laser field L is assumed to be monochromatic, with a frequency ω_L. If the initial state of the laser field is a coherent state, one can show (see ref. [1] and exercise 17 in ref. [2]) that it is legitimate to describe it as a c-number external field

$$\boldsymbol{E}_L(\boldsymbol{r},t) = \boldsymbol{\epsilon}(\boldsymbol{r})\mathcal{E}(\boldsymbol{r})\cos[\omega_L t + \Phi(\boldsymbol{r})], \tag{1.2}$$

where $\boldsymbol{\epsilon}(\boldsymbol{r})$, $\mathcal{E}(\boldsymbol{r})$ and $\Phi(\boldsymbol{r})$ are, respectively, the polarization, the amplitude and the phase of the laser field in $\boldsymbol{r}$. The atom–laser coupling V_{AL} is characterized by the Rabi frequency Ω_1, which is proportional to the scalar product of the dipole moment matrix element $\langle e \mid \boldsymbol{d} \mid g\rangle$ and the laser field $\boldsymbol{E}_L(\boldsymbol{r},t)$. The Hamiltonian evolution due to V_{AL} can be analyzed in terms of elementary processes of absorption and stimulated emission of laser photons by the atom.

The atom–vacuum field coupling V_{AV} is responsible for spontaneous emission of photons by the excited atom. It is characterized by the natural width Γ of the excited state e, which is also equal to the spontaneous emission rate of photons from e. Since V is a large system with an infinite number of degrees of freedom, the coupling V_{AV} introduces damping and fluctuations in the evolution of A. One of the main objectives of this course is to study the limits introduced by these fluctuations and to explain how it is possible to reduce them to their minimum value, and even to circumvent them.

Two extreme regimes can be considered for the evolution of A. For very short interaction times, i.e., for $t \ll \Gamma^{-1}$, one can neglect spontaneous emission, and the evolution of A+L is described by a Schrödinger equation. For very long interaction times, i.e., for $t \gg \Gamma^{-1}$, several spontaneous emission processes occur during the interaction time t, and the "reduced" evolution of A (traced over the vacuum field degrees of freedom) is then described by a master equation or by a Langevin equation. This second case is the most frequently studied and it will be analyzed in detail in the following.

1.3. Characteristic times

For subsequent discussions, it will be useful to introduce here a few characteristic times and to compare their orders of magnitude.

The shortest time of the problem is the correlation time τ_c of the vacuum field. Vacuum fluctuations (see ref. [3], Chap. 3 and ref. [4], Chap. III)

have a very broad frequency spectrum $J(\omega)$, which varies very slowly with ω around the atomic frequency ω_A: the typical frequency scale for the variations of $J(\omega)$ is ω_A itself. It follows that

$$\tau_c \simeq 1/\omega_A. \tag{1.3}$$

The fact that τ_c is much shorter than all other characteristic times will allow us to consider the vacuum field V as a "reservoir" and to describe its effect on the evolution of the atom A as a relaxation process (see ref. [5], Chap. 4 and references therein and ref. [2], Chap. IV).

For the atomic internal degrees of freedom, the most obvious characteristic time is the radiative lifetime τ_R of the excited state e

$$\tau_R = 1/\Gamma, \tag{1.4}$$

which is the inverse of the natural width Γ of e and which can be considered as the relaxation time associated with spontaneous emission. The well known relation $\Gamma \ll \omega_A$ implies that $\tau_R \gg \tau_c$.

The existence of several Zeeman sublevels in the ground state gives rise to other internal relaxation times which are associated with optical pumping [6]. Absorption–spontaneous emission cycles, which are also called fluorescence cycles, can transfer the atom from one Zeeman sublevel g_m of g to another one $g_{m'}$. At low laser intensity I_L, it is possible to define a rate Γ' for the occurrence of such optical pumping cycles, which is proportional to I_L. The inverse of this rate

$$\tau_P = 1/\Gamma' \tag{1.5}$$

is called the optical pumping time τ_P and can be considered as the mean time the atom has to wait before undergoing an optical pumping cycle. At low laser intensity I_L,

$$\tau_P \gg \tau_R. \tag{1.6}$$

We will show in the second part of this course how the existence of such long internal relaxation times for multilevel atoms can give rise to very efficient new cooling mechanisms.

Note that, for two-level atoms, one can still define at low intensity a fluorescence rate Γ' and a mean time $1/\Gamma'$ between two fluorescence cycles experienced by the same atom, a mean time which is much longer than τ_R. But such fluorescence cycles bring back the atom into the same ground state and they do not give rise to additional internal relaxation times. Actually,

for a two-level atom, the only damping times appearing in the optical Bloch equations which describe the evolution of the internal degrees of freedom are all on the order of τ_R.

For the external (i.e., translational) atomic degrees of freedom, a very important characteristic time is the damping time of the atomic velocity. We will show in chapter 4 (section 4.1) that it is on the order of

$$T_{ext} = \hbar/E_R, \tag{1.7}$$

where

$$E_R = \hbar^2 k_L^2/2M \tag{1.8}$$

is the recoil energy of the atom when it absorbs or emits a single laser photon. In eq. (1.8), M is the total mass of the atom and $k_L = \omega_L/c$.

For most allowed atomic transitions,

$$\hbar\Gamma \gg E_R. \tag{1.9}$$

For example, for the resonance line of sodium, $\hbar\Gamma = 400E_R$. When there is a single internal time $T_{int} = \tau_R$, it follows from eqs. (1.4), (1.7) and (1.9) that

$$T_{ext} \gg T_{int}. \tag{1.10}$$

This separation of time scales introduces great simplifications in the analysis of atomic motion. As shown in the next chapters, one can then adiabatically eliminate the fast internal variables and derive reduced equations of motion for external variables.

However, it must be kept in mind that condition (1.10) is not always fulfilled. For atoms with a degenerate ground state, the internal time τ_P can become, at low intensity, comparable to the external time (1.7), and even longer. External times shorter than T_{ext} can also appear, such as the oscillation period T_{osc} of the atom at the bottom of an optical potential well. In such cases, it is no longer possible to eliminate the internal variables, and the theoretical analysis is more complicated. But, as shown in the last part of this course, such situations are also quite interesting, since they generally lead to much lower limits for the temperatures which can be achieved by laser cooling.

1.4. Outline of the course

In the first part of this course, i.e., from chapter 2 to chapter 7, we restrict ourselves to atoms with a non-degenerate ground state. This is for example

the case for a transition $J_g = 0 \longleftrightarrow J_e = 1$. If we suppose in addition that a high static magnetic field $\boldsymbol{B}$ is applied, which pushes the two Zeeman sublevels $|e, m = \pm 1\rangle$ very far away from resonance, we are left with a two-level atom $\{|e\rangle, |g\rangle\}$, with $|e\rangle = |e, m = 0\rangle$ and $|g\rangle = |g, m = 0\rangle$. The only non-zero matrix elements of the dipole moment operator $\boldsymbol{d}$ can then be written

$$\langle e \mid \boldsymbol{d} \mid g \rangle = d\, \boldsymbol{\epsilon}_z = \langle g \mid \boldsymbol{d} \mid e \rangle, \tag{1.11}$$

where we have assumed that d is real and where $\boldsymbol{\epsilon}_z$ is the unit vector along the Oz-axis. Note however that some papers [7] keep the three Zeeman sublevels $|e, m = -1, 0, +1\rangle$ of the excited state with $\boldsymbol{B} = \boldsymbol{0}$.

Assuming that the atomic wave packet is very well localized in the laser wave (semi-classical limit), we first derive in chapter 2 the expression of the radiative force operator which governs the motion of the center of the wave packet. The mean value of the force operator is then analyzed for an atom initially at rest (chapter 3) and for a moving atom (chapter 4), which allows us to introduce the notions of reactive, dissipative and friction forces. The fluctuations of the radiative force around its mean value are responsible for a diffusion of atomic momentum which heats the atom and which limits the efficiency of laser cooling. These fluctuations are studied both in the Heisenberg picture and in the Schrödinger picture (chapter 5). All these results are now well known and we just present here a brief sketch of their derivation, referring the reader to existing publications for more details. On the other hand, we devote more time to the discussion of the physical mechanisms. In particular, we present in chapter 6 original results concerning the intriguing problem of an atom put at the node of a laser standing wave. We show that the anomalously large momentum diffusion which occurs in such a place (where there is no light) is due to interference effects between different scattering amplitudes and reveals the existence of a new kind of "*correlated redistribution*" process. The physical mechanisms occurring at high intensity are also analyzed in chapter 7, using the so called dressed atom approach.

The second part of the course (chapters 8 to 11) deals with atoms having several Zeeman sublevels in the ground state. We consider for example simple atomic transitions with $J_g = 1/2$ or $J_g = 1$. We first recall in chapter 8 a few basic results concerning the effect of weak intensity light irradiation on the internal dynamics of a slowly moving multilevel atom. Several effects, such as optical pumping and light shifts are briefly reviewed. We then show how these effects can conspire to improve the efficiency of laser cooling by orders of magnitude. Two recent developments are studied in

detail. The first one concerns laser cooling with laser configurations exhibiting strong polarization gradients (chapter 9 and 10). The physical mechanisms responsible for the very low temperatures which have been recently measured (a few micro Kelvins) are analyzed. Some new results concerning the limits of polarization gradient cooling are presented. Finally, we discuss in chapter 11 a method using velocity selective coherent population trapping for cooling atoms below the so called recoil limit.

I Two-level atoms

2. Radiative force in the semi-classical limit

We will follow in this chapter the presentation of ref. [8].

2.1. Hamiltonian

The Hamiltonian H of the global system represented in fig. 1 can be written

$$H = H_{\mathrm{A}} + H_{\mathrm{V}} + V_{\mathrm{AL}} + V_{\mathrm{AV}}. \tag{2.1}$$

The first term

$$H_{\mathrm{A}} = H_{\mathrm{A}}^{\mathrm{ext}} + H_{\mathrm{A}}^{\mathrm{int}} = \frac{\boldsymbol{P}^2}{2M} + \hbar\omega_{\mathrm{A}}|e\rangle\langle e| \tag{2.2}$$

is the atomic Hamiltonian, which is the sum of the kinetic energy of the center of mass and of the internal energy (we take $E_g = 0$). The second term

$$H_{\mathrm{V}} = \sum_j \hbar\omega_j (a_j^+ a_j + \tfrac{1}{2}) \tag{2.3}$$

is the energy of the quantum radiation field (see ref. [4], Chap. III), initially in the vacuum state, expressed as a sum of contributions of the various modes j. Note that, since the laser field L is treated here as a c-number external field, there is no Hamiltonian H_L for L in eq. (2.1). The third term of eq. (2.1) is the coupling

$$V_{\mathrm{AL}} = -\,\boldsymbol{d}\cdot\boldsymbol{E}_{\mathrm{L}}(\boldsymbol{R},t) \tag{2.4}$$

between the atomic dipole moment $\boldsymbol{d}$ and the laser electric field $\boldsymbol{E}_{\mathrm{L}}(\boldsymbol{R}, t)$ given in eq. (1.2) and evaluated at the position $\boldsymbol{R}$ of the center of mass (electric dipole approximation). Finally, the last term of eq. (2.1) describes the atom–vacuum field coupling

$$V_{\mathrm{AV}} = -\,\boldsymbol{d}\cdot\boldsymbol{E}(\boldsymbol{R}), \tag{2.5}$$

where the mode expansion of the electric field operator (see ref. [4], Chap. III) is given by

$$\boldsymbol{E}(\boldsymbol{r}) = i\sum_j \mathcal{E}_j a_j \boldsymbol{\epsilon}_j\, \mathrm{e}^{\mathrm{i}\boldsymbol{k}_j\cdot\boldsymbol{r}} + \mathrm{h.c.}, \tag{2.6}$$

a_j^+ (and a_j) being the creation (and annihilation) operators of a photon of momentum $\hbar\boldsymbol{k}_j$, energy $\hbar\omega_j = \hbar c k_j$ and polarization $\boldsymbol{\epsilon}_j$, and $\mathcal{E}_j$ being a normalization constant equal to

$$\mathcal{E}_j = \sqrt{\frac{\hbar\omega_j}{2\epsilon_0 L^3}} \tag{2.7}$$

(L^3 is the quantization volume).

One very often uses the so called "rotating wave approximation" (r.w.a.) which consists of neglecting the "antiresonant" terms of V_{AL} and V_{AV}. Using for $\boldsymbol{d}$ the expression

$$\boldsymbol{d} = d\,\boldsymbol{\epsilon}_z\,(\,|e\rangle\langle g| + (|g\rangle\langle e|\,), \tag{2.8}$$

which results from eq. (1.11), introducing the *Rabi frequency* Ω_1 given by

$$\hbar\Omega_1(\boldsymbol{r}) = -d\,\mathcal{E}(\boldsymbol{r})\,\boldsymbol{\epsilon}_z\cdot\boldsymbol{\epsilon}(\boldsymbol{r}) \tag{2.9}$$

and neglecting the antiresonant terms $\mathrm{e}^{-\mathrm{i}\omega_{\mathrm{L}}t}\,|g\rangle\langle e|$ (and h.c.) of V_{AL} then leads to

$$V_{\mathrm{AL}} = \frac{\hbar\Omega_1(\boldsymbol{R})}{2}\left[\mathrm{e}^{-\mathrm{i}\Phi(\boldsymbol{R})}\,\mathrm{e}^{-\mathrm{i}\omega_{\mathrm{L}}t}\;|e\rangle\langle g| + \mathrm{h.c.}\right] \tag{2.10}$$

One can similarly neglect the antiresonant terms $a_j|g\rangle\langle e|$ (and h.c.) of V_{AV}.

2.2. Heisenberg equations

In order to study the dynamics of the center of mass of A, we start from the Heisenberg equations for $\boldsymbol{R}$ and $\boldsymbol{P}$. The equation of motion of $\boldsymbol{R}$ is

$$\dot{\boldsymbol{R}} = \frac{1}{i\hbar}[\,\boldsymbol{R}, H\,] = \frac{\partial H}{\partial \boldsymbol{P}} = \frac{\boldsymbol{P}}{M}, \tag{2.11a}$$

and shows that $\boldsymbol{P}/M$ is the velocity of the center of mass. It follows that the force operator, $\boldsymbol{F}(\boldsymbol{R}) = M\ddot{\boldsymbol{R}} = \dot{\boldsymbol{P}}$, is given by the Heisenberg equation for $\boldsymbol{P}$

$$\begin{aligned}\dot{\boldsymbol{P}} = M\ddot{\boldsymbol{R}} &= \frac{1}{\mathrm{i}\hbar}[\boldsymbol{P}, H] = -\frac{\partial H}{\partial \boldsymbol{R}} \\ &= -\boldsymbol{\nabla} V_{\mathrm{AL}}(\boldsymbol{R}) - \boldsymbol{\nabla} V_{\mathrm{AV}}(\boldsymbol{R}) \\ &= \text{Force operator } \boldsymbol{F}(\boldsymbol{R}). \end{aligned} \tag{2.11b}$$

The quantum electric field operator $\boldsymbol{E}(\boldsymbol{R})$ appearing in $\boldsymbol{\nabla} V_{\mathrm{AV}}(\boldsymbol{R})$ can be transformed using the Heisenberg equation for $a_j(t)$. The general solution of this equation, which is a linear differential equation with a source term, can be written (see ref. [9] and ref. [2], Complement A_V)

$$a_j(t) = a_j(0)\ \mathrm{e}^{-\mathrm{i}\omega_j t} + a_j^{\mathrm{source}}(t) \tag{2.12}$$

where the first term

$$a_j^{\mathrm{vac}}(t) = a_j(0)\ e^{-i\omega_j t} \tag{2.13}$$

is the general solution of the homogeneous equation and corresponds to the vacuum field evolving freely between the initial time $t = 0$ and t, and where the second term is a particular solution of the inhomogeneous equation which corresponds to the "source field" originating from the atomic dipole moment between $t = 0$ and t. Inserting eq. (2.12) into the mode expansion (2.6) of $\boldsymbol{E}(\boldsymbol{R}, t)$ allows one to separate two contributions in the electric field operator

$$\boldsymbol{E}(\boldsymbol{R}, t) = \boldsymbol{E}^{\mathrm{vac}}(\boldsymbol{R}, t) + \boldsymbol{E}^{\mathrm{source}}(\boldsymbol{R}, t), \tag{2.14}$$

corresponding, respectively, to the vacuum free field and to the source field.

In all previous expressions, the *total* field operator $a_j(t)$ commutes with all atomic operators taken at the same time, since field and atomic operators commute at $t = 0$ (they act in different spaces), and since the unitary Hamiltonian evolution between 0 and t preserves the commutation relations. All possible orders between $a_j(t)$ and atomic operators are thus equivalent. This is no longer true for $a_j^{\mathrm{vac}}(t)$ and $a_j^{\mathrm{source}}(t)$ separately. Depending on the choice made initially for ordering the $a_j(t)$ and the atomic operators, the respective contributions of the vacuum field and of the source field will appear to be different, whereas their *sum* of course does not depend on this initial choice (see ref. [9] and ref. [2], Complement A_V). From

now on, we will choose the *normal order*, where all the annihilation operators $a_j(t)$ are put at the extreme right, and all the creation operators $a_j^+(t)$ at the extreme left. Such an order leads in general to simpler calculations, in particular when one takes average values in the vacuum state $|0\rangle$ of the quantum field. As a consequence of the well known relations

$$a_j(0)|0\rangle = 0, \qquad \langle 0|a_j^+(0) = 0, \tag{2.15}$$

the contribution of the vacuum field to the vacuum average values vanishes. It must be kept in mind however that other orders may be useful. For example, the completely symmetrical order is more convenient for physical interpretations [10].

We insert now eq. (2.14) into the second term, $-\boldsymbol{\nabla} V_{\mathrm{AV}}(\boldsymbol{R})$, of the second line of eq. (2.11.b). One can show that the source field $\boldsymbol{E}^{\mathrm{source}}(\boldsymbol{r}, t)$ due to the atomic dipole moment $\boldsymbol{d}$ has no gradient at the position $\boldsymbol{R}$ where this dipole moment is located (this field is an even function of $\boldsymbol{r} - \boldsymbol{R}$). The contribution of the source field to the force operator thus vanishes, and we get finally

$$\boldsymbol{F}(\boldsymbol{R}, t) = -\boldsymbol{\nabla} V_{\mathrm{AL}}(\boldsymbol{R}, t) - : \boldsymbol{\nabla} V_{\mathrm{AV}}^{\mathrm{vac}}(\boldsymbol{R}, t) : \tag{2.16}$$

where $V_{\mathrm{AV}}^{\mathrm{vac}}$ is obtained from V_{AV} by replacing the total field by the vacuum field and where the notation $: X :$ means that the normal order has been chosen for ordering X.

2.3. Semiclassical limit

Up to now, no assumption has been made concerning the atomic wave packet. We now assume, as in refs. [8] and [11], that such a wave packet is sufficiently well localized in position space and in momentum space to allow the quantum description of atomic motion to be as close as possible to the classical description where the atom has a well defined position and a well defined momentum.

2.3.1. Localization conditions

At $t = 0$, the external atomic state is supposed to be described by a wave function $\psi(\boldsymbol{r})$ centered on

$$\boldsymbol{r}_0 = \langle \boldsymbol{R}(0) \rangle \tag{2.17}$$

and having a width $\Delta R(0)$. In momentum space, the same state is described by a wave function centered on

$$\boldsymbol{p}_0 = \langle \boldsymbol{P}(0) \rangle \tag{2.18}$$

with a width $\Delta P(0)$ related to $\Delta R(0)$ by the Heisenberg inequality

$$\Delta R(0)\ \Delta P(0)\ \geqslant\ \hbar. \tag{2.19}$$

We will say a few words below (in subsection 2.3.2) on the more general case where the external state is a stastistical mixture described by a density operator rather than a pure state described by a wave function.

The force exerted by the laser wave on the atom varies over distances on the order of the laser wavelength λ_{L}, or larger. It also depends on the velocity v of the atom because of the Doppler effect $k_{\mathrm{L}}v$, where $k_{\mathrm{L}} = 2\pi/\lambda_{\mathrm{L}}$. The velocity change δv producing an appreciable change of the atomic response to the laser excitation is such that $k_L \delta v$ is on the order of the natural width Γ of the excited state, or larger.

If one wants the force experienced by the atomic wave packet to be quasi-classical, i.e., with very small fluctuations around its mean value, two conditions must be fulfilled. First, the position spread $\Delta R(0)$ must be small compared to λ_{L}

$$\Delta R(0) \ll \lambda_{\mathrm{L}} \qquad \text{or equivalently} \qquad k_{\mathrm{L}} \Delta R(0) \ll 1. \tag{2.20}$$

Secondly, the velocity spread $\Delta v(0) = \Delta P(0)/M$ must be small enough to allow the corresponding spread of Doppler shifts to be negligible compared to Γ.

$$\frac{k_{\mathrm{L}} \Delta P(0)}{M} \ll \Gamma. \tag{2.21}$$

Note that condition (2.21) does not imply any relation between Γ and the mean Doppler effect $k_{\mathrm{L}} p_0/M$ of the wave packet. Such a mean Doppler effect may be large compared to Γ. Condition (2.21) bears on the spread of Doppler shifts, not on the mean Doppler shift.

Equations (2.20) and (2.21), which express the localization of the wave packet in position space and in momentum space, impose upper bounds on $\Delta R(0)$ and $\Delta P(0)$, which can be in conflict with the Heisenberg inequality (2.19). Multiplying both sides of eq. (2.20) by the corresponding sides of eq. (2.21) and using eq. (2.19), we get the compatibility condition

$$\frac{\hbar k_{\mathrm{L}}^2}{M} \ll \Gamma. \tag{2.22}$$

One finds again the condition $E_{\mathrm{R}} \ll \hbar\Gamma$, written in eq. (1.9), and equivalent to $T_{\mathrm{ext}} \gg T_{\mathrm{int}}$ (see eq. (1.10)). The existence of two time scales thus appears as a necessary condition for the semi-classical limit.

2.3.2. Is localization maintained at later times?
Conditions (2.20) and (2.21) have been imposed at time $t = 0$. Can we still consider the atom as well localized both in position and momentum at a later time τ?

Suppose first that $\tau \ll T_{\text{ext}}$, so that one can neglect the change of atomic momentum between $t = 0$ and $t = \tau$ (remember that T_{ext} is the damping time of $\mathbf{P}$). One can thus write

$$P(\tau) \simeq P(0), \tag{2.23a}$$

from which one deduces, using eq. (2.11.a)

$$R(\tau) \simeq R(0) + \frac{P(0)}{M}\tau. \tag{2.23b}$$

It follows that

$$\Delta P(\tau) \simeq \Delta P(0), \tag{2.24a}$$

$$\Delta R(\tau) \simeq \Delta R(0) + \frac{\Delta P(0)}{M}\tau. \tag{2.24b}$$

Because of eq. (2.24.a), momentum localization is unchanged. Equation (2.24.b) describes the well known spatial spreading of the wave packet. In order to maintain spatial localization at time $t = \tau$, one must have

$$\frac{k_{\text{L}}\Delta P(0)}{M}\tau \ll 1, \tag{2.25}$$

which means that τ must not be too long. If $\tau \simeq T_{\text{int}} \simeq \Gamma^{-1}$, one easily checks that eq. (2.25) is equivalent to eq. (2.21). The spatial spreading of the atomic wave packet during a time on the order of Γ^{-1}, or a few Γ^{-1}, is thus negligible. It follows that one can choose time intervals τ such that

$$T_{\text{int}} \ll \tau \ll T_{\text{ext}} \tag{2.26}$$

which are short enough compared to T_{ext} so that one can neglect the variations of atomic momentum during τ, and sufficiently long compared to T_{int} to allow the internal degrees of freedom to reach an equilibrium state. It is therefore possible to use the concept of steady-state force for a well localized wave packet.

At much longer times, $\tau \gg T_{\text{ext}}$, it is no longer possible to consider that the atomic momentum has not changed. Because of the random character

of the momentum exchanges between the atom and the field, there is a momentum diffusion which tends to increase ΔP. But if the laser frequency is properly tuned, there is also a laser cooling which tends to reduce ΔP. One can show (see subsection 5.2.4) that, as a result of the competition between these two processes, ΔP tends to values which still satisfy eq. (2.21). There are therefore situations where the atomic momentum remains well localized. By contrast, and except for a few special cases where the atom is strongly confined by a trapping potential (for example, near the nodes of an intense standing wave), it seems impossible to maintain eq. (2.20) for all times. Spatial diffusion tends in general to increase ΔR well above λ_L.

There is however an important point which is overlooked by such an analysis. At long times, the state of the center of mass can certainly no longer be described by a wave function, even if this was true at $t = 0$. Several fluorescence cycles have occurred and quantum non-separable correlations have appeared between the various degrees of freedom, with the result that the reduced state of the center of mass is a statistical mixture of states described by a density operator σ_A^{ext}, rather than a pure state described by a wave function. In such a case, the characterization of spatial localization by condition (2.20) is too crude, and a more precise definition must be given. Let $\langle \boldsymbol{r}' \mid \sigma_A^{ext} \mid \boldsymbol{r}'' \rangle$ be the density matrix representing σ_A^{ext} in the basis of the eigenstates of the position operator $\boldsymbol{R}$ of the center of mass. The width of the spatial distribution $\mathcal{R}(\boldsymbol{r}) = \langle \boldsymbol{r} \mid \sigma_A^{ext} \mid \boldsymbol{r} \rangle$, given by the diagonal elements of σ_A^{ext}, is the width ΔR considered above, which can increase well above λ_L. But there is also another important characteristic length, called the spatial coherence length ξ_A, and defined as the typical distance beyond which the off-diagonal elements of σ_A^{ext} (spatial atomic coherences) vanish

$$\langle \boldsymbol{r}' \mid \sigma_A^{ext} \mid \boldsymbol{r}'' \rangle \simeq 0 \qquad \text{if} \qquad \mid \boldsymbol{r}' - \boldsymbol{r}'' \mid \gg \xi_A. \tag{2.27}$$

Now, one can show that, in the problem considered here, ξ_A remains always much smaller than λ_L. This is due to the fact that photon scattering destroys atomic spatial coherences [12]. Consider a target particle $\mathcal{T}$ that scatters at random times projectile particles $\mathcal{P}$ having a de Broglie wavelength λ_P. One can show [12] that the spatial coherence length of $\mathcal{T}$ is reduced to values much shorter than λ_P by these scattering processes. Here, the target is the atom A, the projectiles are the laser photons with wavelength λ_L, and the scattering processes correspond to fluorescence cycles occurring at random times. It follows that

$$\xi_A \ll \lambda_L. \tag{2.28}$$

In order to understand the implications of eq. (2.28), imagine that we express $\sigma_{\rm A}^{\rm ext}$ at time $t = \tau$ as a statistical mixture of wave packets. Each of these individual wave packets must have a spatial extension much smaller than $\lambda_{\rm L}$ since, otherwise, eq. (2.28) would be violated; and the centers of these wave packets are distributed over an interval ΔR, which is the width of the spatial distribution and which can be much larger than $\lambda_{\rm L}$. Such an analysis shows that we can consider that localization is maintained for all times, but this localization concerns the individual wave packets in terms of which the statistical mixture can be expressed, and not the whole spatial distribution. The fact that we are obliged to consider several wave packets at time $t = \tau$, even if we start from a single wave packet at $t = 0$, is due to the randomness of fluorescence cycles, which introduces fluctuations in the atomic evolution. Actually, the various wave packets into which $\sigma_{\rm A}^{\rm ext}$ can be decomposed at time $t = \tau$, can be considered as a statistical ensemble, in the classical sense, representing the various possible "histories" which can happen to the atom between $t = 0$ and $t = \tau$.

2.4. Mean force and Langevin force

Suppose that, at $t = 0$, the atomic wave packet is well localized around $\boldsymbol{r}_0$, with a sufficiently small velocity spread around

$$\boldsymbol{v}_0 = \frac{\boldsymbol{p}_0}{M}. \tag{2.29}$$

If we are interested in the rate of variation of the mean value of $\boldsymbol{P}$, $\mathrm{d}\langle \boldsymbol{P} \rangle / \mathrm{d}t$, and of the variance of $\boldsymbol{P}$, $\mathrm{d}(\Delta P)^2/\mathrm{d}t$, in the neighborhood of $t = 0$, we must calculate one-time average values such as $\langle \boldsymbol{F}(\boldsymbol{R}(\tau), \tau) \rangle$ and two-time average values such as $\langle \boldsymbol{F}(\boldsymbol{R}(\tau), \tau) \cdot \boldsymbol{F}(\boldsymbol{R}(\tau'), \tau') \rangle$ where $\boldsymbol{F}$ is the force operator defined in eq. (2.16) and where τ and τ' are times close enough to 0, i.e., much smaller than $T_{\rm ext}$ (but which can eventually be as large as a few $T_{\rm int} = \Gamma^{-1}$). Since $\tau, \tau' \ll T_{\rm ext}$, we can use eq. (2.23.b) for re-expressing $\boldsymbol{R}(\tau)$ and $\boldsymbol{R}(\tau')$ as a function of $\boldsymbol{R}(0)$, $\boldsymbol{P}(0)$, τ, τ'. Furthermore, since the wave packet is well localized in position and in momentum, we can replace in the one-time and two-time averages the operators $\boldsymbol{R}(0)$ and $\boldsymbol{P}(0)$ by the c-numbers $\boldsymbol{r}_0$ and $\boldsymbol{p}_0$. It thus appears that, for calculating $\mathrm{d}\langle \boldsymbol{P} \rangle / \mathrm{d}t$ and $\mathrm{d}(\Delta P)^2/\mathrm{d}t$ around $t = 0$, we can replace $\boldsymbol{F}(\boldsymbol{R}(\tau), \tau)$ by $\boldsymbol{F}(\boldsymbol{r}_0 + \boldsymbol{v}_0\tau, \tau)$. Note that $\boldsymbol{F}(\boldsymbol{r}_0 + \boldsymbol{v}_0\tau, \tau)$ acts only on internal atomic variables and field variables whereas $\boldsymbol{F}(\boldsymbol{R}(\tau), \tau)$ acts also on external variables.

The rate of variation of $\langle \boldsymbol{P} \rangle$ is equal to the mean value of $\boldsymbol{F}(\boldsymbol{r}_0 + \boldsymbol{v}_0 t, t)$, which we note $\boldsymbol{\mathcal{F}}(\boldsymbol{r}_0 + \boldsymbol{v}_0 t, t)$. Since the mean value of the second term of the right-hand side of eq. (2.16) vanishes because of the normal order (see

eq. (2.15)), we get for the mean force

$$\boldsymbol{\mathcal{F}}(\boldsymbol{r}_0+\boldsymbol{v}_0t,t) = -\langle \boldsymbol{\nabla} V_{\mathrm{AL}}(\boldsymbol{r},t)\rangle|_{\boldsymbol{r}=\boldsymbol{r}_0+\boldsymbol{v}_0t}. \tag{2.30}$$

The fluctuating part of $\boldsymbol{F}(\boldsymbol{r}_0+\boldsymbol{v}_0t,t)$, i.e., the difference between the force and its mean value,

$$\delta\boldsymbol{F}(\boldsymbol{r},t) = \boldsymbol{F}(\boldsymbol{r},t) - \boldsymbol{\mathcal{F}}(\boldsymbol{r},t), \tag{2.31}$$

plays an important role in the calculation of $\mathrm{d}(\Delta P)^2/\mathrm{d}t$. Such a fluctuating force, with zero mean value, is called a Langevin force. Using eqs. (2.16) and (2.30), we get

$$\delta\boldsymbol{F}(\boldsymbol{r},t) = \delta\boldsymbol{F}_{\mathrm{las}}(\boldsymbol{r},t) + \delta\boldsymbol{F}_{\mathrm{vac}}(\boldsymbol{r},t), \tag{2.32}$$

where

$$\delta\boldsymbol{F}_{\mathrm{las}}(\boldsymbol{r},t) = -\boldsymbol{\nabla} V_{\mathrm{AL}}(\boldsymbol{r},t) - \boldsymbol{\mathcal{F}}(\boldsymbol{r},t), \tag{2.33a}$$

$$\delta\boldsymbol{F}_{\mathrm{vac}}(\boldsymbol{r},t) = - :\boldsymbol{\nabla} V_{\mathrm{AV}}(\boldsymbol{r},t): \tag{2.33b}$$

represent, respectively, the contributions of the laser field and of the vacuum field to the Langevin force.

We finally re-express $-\boldsymbol{\nabla} V_{\mathrm{AL}}(\boldsymbol{r},t)$. Using eq. (2.10), we get

$$-\boldsymbol{\nabla} V_{\mathrm{AL}}(\boldsymbol{r},t) = -\frac{\hbar}{2}|e\rangle\langle g|\ \mathrm{e}^{-\mathrm{i}\omega_{\mathrm{L}}t}\ \boldsymbol{\nabla}[\,\Omega_1(\boldsymbol{r})\ \mathrm{e}^{-\mathrm{i}\Phi(\boldsymbol{r})}\,] + \text{ h.c.} \tag{2.34}$$

The calculation of the gradient gives

$$\boldsymbol{\nabla}[\Omega_1(\boldsymbol{r})\ \mathrm{e}^{-\mathrm{i}\Phi(\boldsymbol{r})}] = \Omega_1(\boldsymbol{r})\ \mathrm{e}^{-\mathrm{i}\Phi(\boldsymbol{r})}[\,\boldsymbol{\alpha}(\boldsymbol{r}) - \mathrm{i}\boldsymbol{\beta}(\boldsymbol{r})\,], \tag{2.35}$$

where

$$\boldsymbol{\alpha}(\boldsymbol{r}) = \frac{\boldsymbol{\nabla}\Omega_1(\boldsymbol{r})}{\Omega_1(\boldsymbol{r})}, \tag{2.36a}$$

$$\boldsymbol{\beta}(\boldsymbol{r}) = \boldsymbol{\nabla}\Phi(\boldsymbol{r}) \tag{2.36b}$$

characterize, respectively, the spatial variations of the Rabi frequency and of the phase. If we insert eqs. (2.35) and (2.36) in eq. (2.34) and if we use eq. (2.30) and the fact that the mean value of $|e\rangle\langle g|$ is $\sigma_{ge}(t)$ where σ is the

internal atomic density operator, we finally get the following expression for the mean force

$$\begin{aligned}\boldsymbol{\mathcal{F}}(\boldsymbol{r},t) &= \mathrm{Re}\left\{\sigma_{ge}(t)\,\hbar\Omega_1(\boldsymbol{r})\,\mathrm{e}^{-\mathrm{i}[\omega_L t+\Phi(\boldsymbol{r})]}[\,\boldsymbol{\alpha}(\boldsymbol{r})-\mathrm{i}\boldsymbol{\beta}(\boldsymbol{r})\,]\right\}\\ &= -\hbar\Omega_1(\boldsymbol{r})\,[\,u(t)\boldsymbol{\alpha}(\boldsymbol{r})+v(t)\boldsymbol{\beta}(\boldsymbol{r})\,],\end{aligned} \tag{2.37}$$

with

$$u(t) = \mathrm{Re}\;\sigma_{ge}(t)\;\mathrm{e}^{-\mathrm{i}[\omega_L t+\Phi(\boldsymbol{r})]}, \tag{2.38a}$$

$$v(t) = \mathrm{Im}\;\sigma_{ge}(t)\;\mathrm{e}^{-\mathrm{i}[\omega_L t+\Phi(\boldsymbol{r})]}\,. \tag{2.38b}$$

In all these equations, $\boldsymbol{r}$ means $\boldsymbol{r}_0+\boldsymbol{v}_0 t$.

2.5. Optical Bloch equations (OBE)

The force operator (2.34) depends on the internal atomic operator $|e\rangle\langle g|$, and the mean force (2.37) depends on the average value of $|e\rangle\langle g|$, i.e., on the off-diagonal element σ_{ge} of the internal atomic density matrix σ. We now briefly explain how it is possible to derive the equations of motion of σ, which are called the optical Bloch equations (for more details, see ref. [9] and ref. [2], Complement A_V).

We start from the equations of motion of the four operators

$$\Pi_{ab} = |a\rangle\langle b|, \tag{2.39}$$

with $a, b = e$ or g, which can be written

$$i\hbar\,\dot{\Pi}_{ab} = [\,\Pi_{ab},\,H\,] = [\,\Pi_{ab},\,H_{\mathrm{A}}^{\mathrm{int}} + V_{\mathrm{AL}} + V_{\mathrm{AV}}], \tag{2.40}$$

since Π_{ab} commutes with $H_{\mathrm{A}}^{\mathrm{ext}} = \boldsymbol{P}^2/2M$ and H_{V}. As in section 2.2 above, we replace the field operator $a_j(t)$ appearing in the mode expansion of V_{AV} [see eqs. (2.5) and (2.6)] by the solution (2.12) of the Heisenberg equation for $a_j(t)$. One can then show that, if normal order has been chosen in eq. (2.40), the contribution of the source field, $a_j^{\mathrm{source}}(t)$, to the rate of variation of Π_{ab} reduces to damping terms, proportional to the spontaneous emission rate Γ. On the other hand, the contribution of the free field appears as a Langevin force with zero average value. The structure of the equation of motion of Π_{ab} is thus the following

$$\begin{aligned}\dot{\Pi}_{ab} = &-\frac{i}{\hbar}[\,\Pi_{ab},\,H_{\mathrm{A}}^{\mathrm{int}} + V_{\mathrm{AL}}\,]\\ &+ \text{Damping terms} \;+\; \text{Langevin force.}\end{aligned} \tag{2.41}$$

Taking the average value of eq. (2.41) and using the fact that the Langevin force has a zero average value, we get

$$\dot{\sigma}_{ba} = -\frac{\mathrm{i}}{\hbar}\,\langle b|[\,H_{\mathrm{A}}^{\mathrm{int}} + V_{\mathrm{AL}}\,,\sigma\,]|a\rangle + \left(\frac{\mathrm{d}}{\mathrm{d}t}\sigma_{ba}\right)_{\mathrm{sp}}, \tag{2.42}$$

where the damping terms (due to spontaneous emission) have the following form

$$\left(\frac{\mathrm{d}}{\mathrm{d}t}\sigma_{ee}\right)_{\mathrm{sp}} = -\,\Gamma\,\sigma_{ee}, \tag{2.43a}$$

$$\left(\frac{\mathrm{d}}{\mathrm{d}t}\sigma_{gg}\right)_{\mathrm{sp}} = +\,\Gamma\,\sigma_{ee}, \tag{2.43b}$$

$$\left(\frac{\mathrm{d}}{\mathrm{d}t}\sigma_{eg}\right)_{\mathrm{sp}} = -\,\frac{\Gamma}{2}\,\sigma_{eg}, \tag{2.43c}$$

$$\left(\frac{\mathrm{d}}{\mathrm{d}t}\sigma_{ge}\right)_{\mathrm{sp}} = -\,\frac{\Gamma}{2}\,\sigma_{ge}. \tag{2.43d}$$

Equations (2.43.a) and (2.43.b) describe the departure of the atom from e by spontaneous emission and its transfer to g with a rate Γ. Equations (2.43.c) and (2.43.d) describe the damping of optical coherences with a rate $\Gamma/2$. (Strictly speaking, there are also terms describing a radiative shift of the evolution frequency of the optical coherences, but this shift is supposed to be reincluded in the atomic frequency ω_{A}.)

From eqs. (2.42) and (2.43), it is clear that

$$\frac{\mathrm{d}}{\mathrm{d}t}(\sigma_{ee} + \sigma_{gg}) = 0, \tag{2.44}$$

since the trace of a commutator is zero. It follows that $\sigma_{ee}+\sigma_{gg}$ is constant and equal to 1 and that the four matrix elements σ_{ab} are not independent. We introduce the so-called Bloch vector with three independent components u, v, w, where u and v are given by eqs. (2.38.a) and (2.38.b) and where

$$w(t) = \tfrac{1}{2}\,[\,\sigma_{ee}(t) - \sigma_{gg}(t)\,]\,. \tag{2.45}$$

Note that $u(t)$ and $v(t)$ depend on t, not only through $\sigma_{ge}(t)$ and $\sigma_{eg}(t)$, but also through $\Phi(\boldsymbol{r}) = \Phi(\boldsymbol{r}_0 + \boldsymbol{v}_0 t)$.

From eqs. (2.38), (2.45), (2.42) and (2.43), we get, using eqs. (2.2) and (2.10), the following equations of motion of u, v, w, written in matrix form

$$\begin{pmatrix} \dot{u} \\ \dot{v} \\ \dot{w} \end{pmatrix} = \begin{pmatrix} -\Gamma/2 & \delta + \dot{\Phi} & 0 \\ -(\delta + \dot{\Phi}) & -\Gamma/2 & -\Omega_1 \\ 0 & \Omega_1 & -\Gamma \end{pmatrix} \begin{pmatrix} u \\ v \\ w \end{pmatrix} + \begin{pmatrix} 0 \\ 0 \\ -\Gamma/2 \end{pmatrix}. \tag{2.46}$$

In these equations,

$$\dot{\Phi} = \boldsymbol{v}_0 \cdot \boldsymbol{\nabla}\Phi = \boldsymbol{v}_0 \cdot \boldsymbol{\beta} \tag{2.47}$$

and Ω_1 and Φ are evaluated at $\boldsymbol{r} = \boldsymbol{r}_0 + \boldsymbol{v}_0 t$.

Equations (2.46) look like the usual Bloch equations of NMR. The components u, v, w of the Bloch vector can be considered as the components S_x, S_y, S_z of a fictitious spin 1/2 submitted (in the rotating frame) to two static fields, one along Oz, proportional to $-(\delta + \dot{\Phi})$, one along Ox, proportional to Ω_1.

3. Mean radiative force for a two-level atom initially at rest

The general results of chapter 2 are applied here to the particular case of an atom initially at rest, at a point which we take as the origin of coordinates

$$\boldsymbol{r}_0 = \boldsymbol{0}, \tag{3.1a}$$

$$\boldsymbol{v}_0 = \boldsymbol{0}. \tag{3.1b}$$

The origin of time can always be chosen in such a way that the phase $\Phi(\boldsymbol{0})$ of the laser field in $\boldsymbol{r} = \boldsymbol{0}$ is zero. The laser electric field (1.2) at the position of the atom can then be written

$$\boldsymbol{E}_{\mathrm{L}}(\boldsymbol{0}, t) = \boldsymbol{\epsilon}(\boldsymbol{0})\, \mathcal{E}(\boldsymbol{0}) \cos \omega_{\mathrm{L}} t = \boldsymbol{\mathcal{E}}_0 \cos \omega_{\mathrm{L}} t, \tag{3.2}$$

where $\boldsymbol{\mathcal{E}}_0 = \boldsymbol{\epsilon}(\boldsymbol{0})\, \mathcal{E}(\boldsymbol{0})$. We use in the following the simpler notation

$$\Omega_1(\boldsymbol{0}) = \Omega_1, \tag{3.3a}$$

$$\boldsymbol{\alpha}(\boldsymbol{0}) = \left. \frac{\boldsymbol{\nabla}\Omega_1}{\Omega_1} \right|_{\boldsymbol{r}=\boldsymbol{0}} = \boldsymbol{\alpha}, \tag{3.3b}$$

$$\boldsymbol{\beta}(\boldsymbol{0}) = \boldsymbol{\nabla}\Phi\,|_{\boldsymbol{r}=\boldsymbol{0}} = \boldsymbol{\beta}. \tag{3.3c}$$

Note finally that, as a consequence of eq. (3.1.b)

$$\dot{\Phi} = \boldsymbol{v}_0 \cdot \boldsymbol{\nabla} \Phi \,\big|_{\boldsymbol{r}=\boldsymbol{0}} = 0. \tag{3.4}$$

3.1. Steady-state solution of optical Bloch equations

Using eq. (3.4) and the fact that the Rabi frequency (3.3.a) is time independent (since the atom is at rest at $\boldsymbol{r} = \boldsymbol{0}$), we see that the optical Bloch equations given in eq. (2.46) are here a set of coupled linear differential equations with time independent coefficients. They thus admit a steady-state solution which is easily found to be (see ref. [2], Chap. V)

$$u_{\mathrm{st}} = \frac{\delta}{\Omega_1} \frac{s}{1+s}, \tag{3.5a}$$

$$v_{\mathrm{st}} = \frac{\Gamma}{2\Omega_1} \frac{s}{1+s}, \tag{3.5b}$$

$$w_{\mathrm{st}} = -\frac{1}{2(1+s)}, \tag{3.5c}$$

where

$$s = \frac{\Omega_1^2/2}{\delta^2 + (\Gamma^2/4)} \tag{3.6}$$

is called the saturation parameter.

We will also need in the following the steady-state value $\sigma_{ee}^{\mathrm{st}}$ of the population of the upper state, which can be deduced from eqs. (2.45), (3.5.c) and the relation $\sigma_{ee}^{\mathrm{st}} + \sigma_{gg}^{\mathrm{st}} = 1$

$$\sigma_{ee}^{\mathrm{st}} = \frac{1}{2} + w_{\mathrm{st}} = \frac{1}{2} \frac{s}{1+s}. \tag{3.7}$$

It clearly appears in eq. (3.7) that $\sigma_{ee}^{\mathrm{st}}$ tends to $1/2$ for high saturation parameters ($s \gg 1$).

3.2. Reactive response and dissipative response

Equation (2.37) shows that the mean force $\boldsymbol{\mathcal{F}}$ is the sum of two contributions, respectively proportional to u and v. In order to interpret physically these two contributions in steady-state, we first show in this section that

$u_{\rm st}$ and $v_{\rm st}$ describe, respectively, the reactive response and the dissipative response of the atom to the laser excitation.

We take the steady-state average value of the dipole moment operator $\boldsymbol{d}$ given in eq. (2.8). This gives, using eq. (2.39)

$$\begin{aligned}\langle \boldsymbol{d} \rangle_{\rm st} &= d\,\boldsymbol{\epsilon}_z \langle\, \Pi_{eg} + \Pi_{ge} \rangle_{\rm st} \\ &= d\,\boldsymbol{\epsilon}_z (\sigma_{ge}^{\rm st} + \sigma_{eg}^{\rm st}) = 2d\,\boldsymbol{\epsilon}_z\ {\rm Re}\ \sigma_{ge}^{\rm st}. \end{aligned} \tag{3.8}$$

On the other hand, the definition (2.38) of u and v and the fact that $\Phi(\mathbf{0}) = 0$ lead to

$$u_{\rm st} + {\rm i}\, v_{\rm st} = \sigma_{ge}^{\rm st}\ {\rm e}^{-{\rm i}\omega_{\rm L} t}\ {\rm e}^{-{\rm i}\Phi(\mathbf{0})} = \sigma_{ge}^{\rm st}\ {\rm e}^{-{\rm i}\omega_{\rm L} t}, \tag{3.9}$$

so that

$$\begin{aligned}{\rm Re}\ \sigma_{ge}^{\rm st} &= {\rm Re}\,\{[\,u_{\rm st} + {\rm i}\, v_{\rm st}\,]\ {\rm e}^{+{\rm i}\omega_{\rm L} t}\} \\ &= u_{\rm st} \cos\omega_{\rm L} t - v_{\rm st} \sin\omega_{\rm L} t. \end{aligned} \tag{3.10}$$

From eqs. (3.8) and (3.10) it follows that

$$\langle \boldsymbol{d} \rangle_{\rm st} = 2d\,\boldsymbol{\epsilon}_z [\, u_{\rm st} \cos\omega_{\rm L} t - v_{\rm st} \sin\omega_{\rm L} t\,]. \tag{3.11}$$

Comparing eq. (3.11) with the expression (3.2) of the laser electric field at the position of the atom, we conclude that $u_{\rm st}$ and $v_{\rm st}$ are proportional to the components of the mean dipole moment, respectively, in phase and in quadrature with the driving laser field. They thus describe the reactive response and the dissipative response of the atom to the laser excitation.

The previous result suggests that, in steady-state, the mean energy absorbed per unit time by the atom, and consequently the mean number of photons absorbed per unit time $\langle {\rm d}N/{\rm d}t \rangle_{\rm st}$, are related to the dissipative response $v_{\rm st}$. For the following discussion, it will be useful to establish the equation relating $\langle {\rm d}N/{\rm d}t \rangle_{\rm st}$ to $v_{\rm st}$.

The work ${\rm d}W$ done during ${\rm d}t$ by the laser electric field (3.2) acting upon the charge q of the atomic electron is

$${\rm d}W = q \cos\omega_{\rm L} t\ \boldsymbol{\mathcal{E}}_0 \cdot {\rm d}\boldsymbol{r}, \tag{3.12}$$

where ${\rm d}\boldsymbol{r}$ is the displacement of the charge during ${\rm d}t$. Using $\dot{\boldsymbol{d}} = q\dot{\boldsymbol{r}}$, we conclude that the mean energy absorbed by the atom per unit time in steady-state is given by

$$\left\langle \frac{{\rm d}W}{{\rm d}t} \right\rangle_{\rm st} = \cos\omega_{\rm L} t\ \ \boldsymbol{\mathcal{E}}_0 \cdot \langle\, \dot{\boldsymbol{d}}\, \rangle_{\rm st}. \tag{3.13}$$

If we now use the expression (3.11) of $\langle \boldsymbol{d} \rangle_{\text{st}}$, we get

$$\left\langle \frac{\mathrm{d}W}{\mathrm{d}t} \right\rangle_{\text{st}} = -2d\,\boldsymbol{\epsilon}_z \cdot \boldsymbol{\mathcal{E}}_0\,\omega_{\text{L}}[\,v_{\text{st}}\cos^2\omega_{\text{L}}t + u_{\text{st}}\sin\omega_{\text{L}}t\cos\omega_{\text{L}}t\,]. \tag{3.14}$$

Averaging over one optical period gives

$$\left\langle \frac{\mathrm{d}W}{\mathrm{d}t} \right\rangle_{\text{st}} = \hbar\Omega_1\,\omega_{\text{L}}\,v_{\text{st}}, \tag{3.15}$$

where we have used the definition $\hbar\Omega_1 = -d\,\boldsymbol{\epsilon}_z \cdot \boldsymbol{\mathcal{E}}_0$ of the Rabi frequency. Since each absorbed photon provides an energy $\hbar\omega_{\text{L}}$, the mean number of photons absorbed per unit time in steady-state is given by

$$\left\langle \frac{\mathrm{d}N}{\mathrm{d}t} \right\rangle_{\text{st}} = \frac{1}{\hbar\omega_{\text{L}}} \left\langle \frac{\mathrm{d}W}{\mathrm{d}t} \right\rangle_{\text{st}} = \Omega_1\,v_{\text{st}}, \tag{3.16}$$

or equivalently

$$\left\langle \frac{\mathrm{d}N}{\mathrm{d}t} \right\rangle_{\text{st}} = \Gamma\,\sigma_{ee}^{\text{st}}, \tag{3.17}$$

since it follows from eqs. (3.5.b) and (3.7) that

$$\Omega_1 v_{\text{st}} = \Gamma\sigma_{ee}^{\text{st}}. \tag{3.18}$$

Equation (3.17) has a clear physical meaning. It expresses that, in steady-state, the mean number of photons absorbed per unit time (left-hand side) is equal to the mean number of photons spontaneously emitted per unit time (right-hand side).

3.3. Dissipative force - Radiation pressure

We will call dissipative force the component of the mean force (2.37) which, in steady-state, is proportional to v_{st}

$$\boldsymbol{\mathcal{F}}_{\text{dissip}} = -\hbar\Omega_1\,v_{\text{st}}\,\boldsymbol{\beta}. \tag{3.19}$$

The physical meaning of $\boldsymbol{\mathcal{F}}_{\text{dissip}}$ is particularly clear when the laser wave is a plane wave with a wave vector $\boldsymbol{k}_{\text{L}}$

$$\boldsymbol{E}_{\text{L}}(\boldsymbol{r},t) = \boldsymbol{\mathcal{E}}_{\circ}\cos(\omega_{\text{L}}t - \boldsymbol{k}_{\text{L}}\cdot\boldsymbol{r}). \tag{3.20}$$

It follows from eq. (3.20) that the phase of the field is then

$$\Phi(\boldsymbol{r}) = -\boldsymbol{k}_{\mathrm{L}} \cdot \boldsymbol{r}, \tag{3.21}$$

so that

$$\boldsymbol{\beta} = \boldsymbol{\nabla}\Phi|_{\boldsymbol{r}=\boldsymbol{0}} = -\boldsymbol{k}_{\mathrm{L}}. \tag{3.22}$$

Inserting eq. (3.22) into eq. (3.19) gives in this case, using eq. (3.16)

$$\boldsymbol{\mathcal{F}}_{\mathrm{dissip}} = \hbar\Omega_1 \, \boldsymbol{k}_{\mathrm{L}} \, v_{\mathrm{st}} = \hbar \boldsymbol{k}_{\mathrm{L}} \left\langle \frac{\mathrm{d}N}{\mathrm{d}t} \right\rangle_{\mathrm{st}}. \tag{3.23}$$

The interpretation of eq. (3.23) is straightforward. During the time interval $\mathrm{d}t$, the atom absorbs $\mathrm{d}N$ photons and gets a momentum $\mathrm{d}\boldsymbol{P} = \mathrm{d}N\hbar\boldsymbol{k}_{\mathrm{L}}$ corresponding to a steady-state mean force

$$\left\langle \frac{\mathrm{d}\boldsymbol{P}}{\mathrm{d}t} \right\rangle_{\mathrm{st}} = \hbar \boldsymbol{k}_{\mathrm{L}} \left\langle \frac{\mathrm{d}N}{\mathrm{d}t} \right\rangle_{\mathrm{st}} \tag{3.24}$$

In the previous argument, we have not considered the momentum associated with spontaneously emitted photons. The reason is that spontaneous emission occurs with equal probabilities in two opposite directions so that the loss of momentum due to the re-emission process is zero on the average. The dissipative force is also called radiation pressure force, or scattering force, since it originates from absorption–spontaneous emission cycles.

If one uses the expression (3.5.b) of v_{st} and the definition (3.6) of the saturation parameter s, one can write eq. (3.23) in an equivalent form,

$$\boldsymbol{\mathcal{F}}_{\mathrm{dissip}} = \hbar \boldsymbol{k}_{\mathrm{L}} \frac{\Gamma}{2} \, \frac{\Omega_1^2/2}{\delta^2 + (\Gamma^2/4) + (\Omega_1^2/2)}, \tag{3.25}$$

which displays more clearly the dependence of $\boldsymbol{\mathcal{F}}_{\mathrm{dissip}}$ on the various parameters. Plotted as a function of the detuning $\delta = \omega_{\mathrm{L}} - \omega_{\mathrm{A}}$, $\boldsymbol{\mathcal{F}}_{\mathrm{dissip}}$ varies as a Lorentz absorption curve centered about $\delta = 0$, as expected for a dissipative process. Let us consider now the variations of $\boldsymbol{\mathcal{F}}_{\mathrm{dissip}}$ with the laser intensity I_{L}, which is proportional to Ω_1^2. At low intensity (more precisely for $s \ll 1$), one finds that $\boldsymbol{\mathcal{F}}_{\mathrm{dissip}}$ is proportional to I_{L}. At high intensity (more precisely for $s \gg 1$), $\boldsymbol{\mathcal{F}}_{\mathrm{dissip}}$ tends to a maximum value given by $\hbar \boldsymbol{k}_{\mathrm{L}} \, \Gamma/2$, corresponding to a maximum acceleration

$$\boldsymbol{a}_{\max} = \frac{\hbar \boldsymbol{k}_{\mathrm{L}}}{M} \, \frac{\Gamma}{2}. \tag{3.26}$$

It is interesting to discuss some orders of magnitude. In eq. (3.26), $\hbar \boldsymbol{k}_L/M$ is the recoil velocity $\boldsymbol{v}_{rec}$ associated with the absorption or the emission of a single photon. Such velocities are usually quite small, for example on the order of 3 cm/s for sodium or 3 mm/s for cesium. But the number of fluorescence cycles per second can reach (for $s \gg 1$) values equal to $\Gamma/2$ which can be quite high since Γ^{-1} is on the order of a few 10^{-9} s. For example, for sodium, $\Gamma^{-1} = 16 \times 10^{-9}$ s, so that a_{max} is on the order of 10^6 m/s^2, i.e., on the order of $10^5\, g$, where g is the acceleration due to gravity. This explains how it is possible to stop an atomic beam with resonant radiation pressure in a small distance, on the order of one meter (see W.D. Phillips' lectures).

3.4. Reactive force – Dipole force

We will call $\boldsymbol{\mathcal{F}}_{react}$ the component of the mean force (2.37) which, in steady-state, is proportional to u_{st}

$$\boldsymbol{\mathcal{F}}_{react} = -\hbar \Omega_1 \, u_{st} \, \boldsymbol{\alpha}. \tag{3.27}$$

In a laser plane wave, $\boldsymbol{\epsilon}\, \mathcal{E} \cos(\omega_L t - \boldsymbol{k}_L \cdot \boldsymbol{r})$, the amplitude $\mathcal{E}$ and the polarization $\boldsymbol{\epsilon}$ of the laser field are independent of $\boldsymbol{r}$, so that $\boldsymbol{\nabla} \Omega_1$, and consequently $\boldsymbol{\alpha}$, vanish [see the definitions (2.9) of Ω_1 and (2.36.a) of $\boldsymbol{\alpha}$]. It follows that $\boldsymbol{\mathcal{F}}_{react} = \boldsymbol{0}$ in a plane wave. The reactive force can appear only if the laser wave is a linear superposition of several plane waves. On the other hand, $\boldsymbol{\mathcal{F}}_{react}$ cannot involve a net absorption of energy by the atom since it is associated with the reactive response of the atom. These two properties suggest that $\boldsymbol{\mathcal{F}}_{react}$ is associated with a *redistribution* of photons between the various plane waves forming the laser wave. Photons are removed from one plane wave by absorption processes and transferred into *another* plane wave by stimulated emission processes. During such a redistribution, the energy of the field does not change since all plane waves have the same frequency ω_L. There is no net absorption of energy by the atom. But, since the momenta of the photons associated with the various plane waves are not the same, such a redistribution changes the total momentum of the field, and consequently the momentum of the atom.

In order to make such an argument more explicit, let us consider the simple case where the laser wave is formed by two plane waves with wave vectors $\boldsymbol{k}_1$ and $\boldsymbol{k}_2$ (see also ref. [2], chapter V, subsection C.2.d). Figure 2 represents, in the complex plane, the complex amplitudes $\boldsymbol{E}_1$ and $\boldsymbol{E}_2$ of the two fields at a point $\boldsymbol{r}$ where they are assumed to be in quadrature, so that the two vectors $\boldsymbol{E}_1$ and $\boldsymbol{E}_2$ are perpendicular. We will consider only the

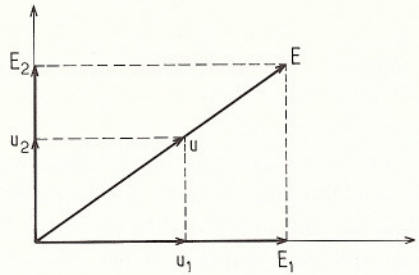

Fig. 2. Representation in the complex plane of a laser field $\boldsymbol{E}$ resulting from the superposition of two fields $\boldsymbol{E}_1$ and $\boldsymbol{E}_2$ in quadrature. The vectors $\boldsymbol{u}$, $\boldsymbol{u}_1$ and $\boldsymbol{u}_2$ represent the dipoles in phase respectively with $\boldsymbol{E}$, $\boldsymbol{E}_1$ and $\boldsymbol{E}_2$.

reactive response $\boldsymbol{u}$ of the atom to the total field $\boldsymbol{E}$, which has the same phase as $\boldsymbol{E}$ (or the opposite phase, depending on the detuning). Let $\boldsymbol{u}_1$ and $\boldsymbol{u}_2$ be the projections of $\boldsymbol{u}$ onto $\boldsymbol{E}_1$ and $\boldsymbol{E}_2$. The component $\boldsymbol{u}_1$ of $\boldsymbol{u}$ in phase with $\boldsymbol{E}_1$ does not absorb energy on the wave 1. The same argument holds for $\boldsymbol{u}_2$ and $\boldsymbol{E}_2$. On the other hand, $\boldsymbol{u}_2$ is advanced in phase by $\pi/2$ with respect to $\boldsymbol{E}_1$, whereas $\boldsymbol{u}_1$ is retarded by $\pi/2$ with respect to $\boldsymbol{E}_2$. It follows that if $\boldsymbol{E}_1$ gains energy by interacting with $\boldsymbol{u}_2$, $\boldsymbol{E}_2$ loses energy by interacting with $\boldsymbol{u}_1$. Furthermore, since $\mid \boldsymbol{E}_1 \mid\mid \boldsymbol{u}_2 \mid = \mid \boldsymbol{E}_2 \mid\mid \boldsymbol{u}_1 \mid$, the energy gained by one wave is exactly equal to the energy lost by the other wave. We understand in this way, on the one hand the existence of a redistribution between the two waves, on the other hand the coherent character of such a redistribution which has a sense ($1 \rightarrow 2$ or $2 \rightarrow 1$) depending on the relative phases of the two waves at the point where the atom is located. Note finally that, depending whether $\boldsymbol{u}$ has the same phase as $\boldsymbol{E}$ or the opposite phase, the sense of the redistribution is different. This explains why the reactive force is an odd function of the detuning.

If one uses the expression (3.5.a) of u_{st} and the definition (3.6) of s, one gets for $\boldsymbol{\mathcal{F}}_{\mathrm{react}}$ the following expression

$$\boldsymbol{\mathcal{F}}_{\mathrm{react}} = -\frac{\hbar\delta}{4} \frac{\boldsymbol{\nabla}\Omega_1^2}{\delta^2 + (\Gamma^2/4) + (\Omega_1^2/2)}. \tag{3.28}$$

The reactive force varies with $\delta = \omega_{\mathrm{L}} - \omega_{\mathrm{A}}$ as a Lorentz dispersion curve, as expected for a reactive process. For $\delta < 0$ ($\omega_{\mathrm{L}} < \omega_{\mathrm{A}}$), the reactive force pushes the atom towards the regions of higher intensity since it has the same sign as $\boldsymbol{\nabla}\Omega_1^2$. The opposite result holds for $\delta > 0$ ($\omega_{\mathrm{L}} > \omega_{\mathrm{A}}$). For each value of Ω_1^2 (with $\Omega_1 \gg \Gamma$), the value of δ which optimizes $\boldsymbol{\mathcal{F}}_{\mathrm{react}}$ is on the order of Ω_1, the corresponding maximal value of $\boldsymbol{\mathcal{F}}_{\mathrm{react}}$ being on the

order of

$$(\boldsymbol{\mathcal{F}}_{\text{react}})_{\max} \simeq \frac{\hbar \boldsymbol{\nabla} \Omega_1^2}{\Omega_1} \simeq \hbar \boldsymbol{\nabla} \Omega_1. \tag{3.29}$$

Contrary to $\boldsymbol{\mathcal{F}}_{\text{dissip}}$, which remains bounded when the laser intensity I_{L} increases, $\boldsymbol{\mathcal{F}}_{\text{react}}$ increases indefinitely with I_{L}. Equation (3.29) shows that $\boldsymbol{\mathcal{F}}_{\text{react}}$ can reach values on the order of $\hbar \boldsymbol{k}_{\text{L}} \Omega_1$ since $\boldsymbol{\nabla} \Omega_1$ can be on the order of $\boldsymbol{k}_{\text{L}} \Omega_1$, for example in a standing wave. Such a result corresponds to exchanges of momentum $\hbar \boldsymbol{k}_{\text{L}}$ occurring at a rate Ω_1, as expected for a redistribution process involving absorption–stimulated emission cycles. It has to be compared with the corresponding result for $\boldsymbol{\mathcal{F}}_{\text{dissip}}$ which reaches maximum values on the order of $\hbar \boldsymbol{k}_{\text{L}}$ times the spontaneous emission rate Γ.

Note finally that the reactive force (3.28) derives from a potential U since one can write

$$\boldsymbol{\mathcal{F}}_{\text{react}} = -\boldsymbol{\nabla} U, \tag{3.30}$$

where

$$U(\boldsymbol{r}) = \frac{\hbar \delta}{2} \ln \left[1 + \frac{\Omega_1^2(\boldsymbol{r})/2}{\delta^2 + (\Gamma^2/4)} \right]. \tag{3.31}$$

For $\delta < 0$ ($\omega_{\text{L}} < \omega_{\text{A}}$), a region of maximum intensity appears as an attractive potential well for the atom. For a given Ω_1, the maximum depth of such a potential well occurs for a saturation parameter $s \simeq 4$, and corresponds to $|U_{\max}| \simeq 0.3 \, |\hbar \, \Omega_1^{\max}|$.

In the following chapters, we will present other physical pictures for the reactive force, which is also called the dipole force. In chapter 6, we will interpret the redistribution process at low intensity as resulting from interferences between different scattering amplitudes. The high intensity limit will be considered in chapter 7, and the dipole force will be interpreted in this limit in terms of gradients of dressed state energies.

4. Moving atom. Friction force

We consider now an atom moving with a velocity $\boldsymbol{v}_0$, so that its position $\boldsymbol{r}$ is given by

$$\boldsymbol{r} = \boldsymbol{v}_0 \, t \tag{4.1}$$

if we take $\boldsymbol{r} = \boldsymbol{0}$ at $t = 0$.

4.1. Simple case of a laser plane wave

The laser wave is supposed to be a plane wave with wave vector $\boldsymbol{k}_{\mathrm{L}}$ [see eq. (3.20)]. Since the amplitude and the polarization of the laser electric field do not depend on $\boldsymbol{r}$, the Rabi frequency is position independent and consequently does not depend on time

$$\Omega_1(\boldsymbol{r} = \boldsymbol{v}_0\, t) = \Omega_1 = \text{constant}. \tag{4.2}$$

On the other hand, the phase Φ varies linearly with $\boldsymbol{r}$

$$\Phi(\boldsymbol{r}) = -\boldsymbol{k}_{\mathrm{L}} \cdot \boldsymbol{r} \tag{4.3}$$

so that

$$\dot{\Phi} = \frac{\mathrm{d}\boldsymbol{r}}{\mathrm{d}t} \cdot \boldsymbol{\nabla}\Phi = \boldsymbol{v}_0 \cdot \boldsymbol{\nabla}\Phi = -\boldsymbol{k}_{\mathrm{L}} \cdot \boldsymbol{v}_0. \tag{4.4}$$

Since Ω_1 and $\dot{\Phi}$ are time independent, the optical Bloch equations are still a set of coupled linear differential equations with time independent coefficients. They thus have a steady-state solution which is derived from the solution obtained in section 3.1 (where $\boldsymbol{v}_0$ was equal to zero) by the substitution

$$\delta \longrightarrow \delta + \dot{\Phi} = \delta - \boldsymbol{k}_{\mathrm{L}} \cdot \boldsymbol{v}_0, \tag{4.5}$$

or equivalently, since $\delta = \omega_{\mathrm{L}} - \omega_{\mathrm{A}}$, by the substitution

$$\omega_{\mathrm{L}} \longrightarrow \omega_{\mathrm{L}} - \boldsymbol{k}_{\mathrm{L}} \cdot \boldsymbol{v}_0. \tag{4.6}$$

Such a result means that the atom moving with velocity $\boldsymbol{v}_0$ "sees " the laser frequency shifted by the *Doppler shift* $-\boldsymbol{k}_{\mathrm{L}} \cdot \boldsymbol{v}_0$.

Figure 3a represents an atom moving with velocity $\boldsymbol{v}_0$ in a laser plane wave propagating along the negative direction of the Ox-axis, so that its wave vector can be written $\boldsymbol{k}_{\mathrm{L}} = -k_{\mathrm{L}}\, \boldsymbol{\epsilon}_x$. If $v_0 = \boldsymbol{\epsilon}_x \cdot \boldsymbol{v}_0$ is the projection of $\boldsymbol{v}_0$ along the Ox-axis, we have $-\boldsymbol{k}_{\mathrm{L}} \cdot \boldsymbol{v}_0 = k_{\mathrm{L}}\, v_0$. Figure 3b represents the component along Ox of the mean force experienced by the atom plotted versus $k_{\mathrm{L}} v_0$ [we just replace in eq. (3.25) δ by $\delta + k_{\mathrm{L}}\, v_0$]. We have assumed that δ is negative. The force is negative and reaches its maximum value when $\delta = -k_{\mathrm{L}}\, v_0$, i.e., when the apparent laser frequency $\omega_{\mathrm{L}} + k_{\mathrm{L}}\, v_0$ coincides with the atomic frequency ω_{A}. Near $v_0 = 0$ we can write

$$\mathcal{F}_x(v_0) = \mathcal{F}_x(v_0 = 0) - \alpha\, v_0 + \cdots, \tag{4.7}$$

where the term linear in v_0 is a friction force, since it is proportional to v_0 with the opposite sign. The coefficient α is called the *friction coefficient*.

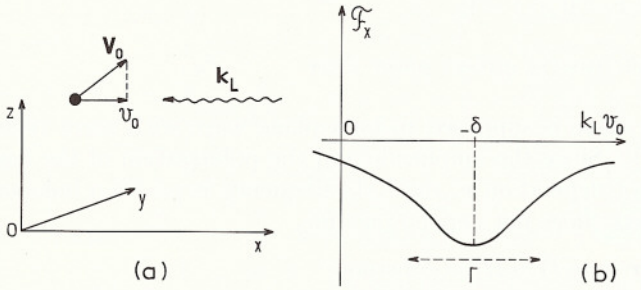

Fig. 3. (a) Atom moving with velocity $\boldsymbol{v}_0$ in a laser plane wave with wave vector $\boldsymbol{k}_{\mathrm{L}}$. (b) Mean force experienced by the atom versus $k_{\mathrm{L}} v_0$.

Replacing δ by $\delta - k_{\mathrm{L}}\, v_0$ in eq. (3.25) and expanding the result obtained for $\mathcal{F}_x(v_0)$ in powers of $k_{\mathrm{L}}\, v_0/\Gamma$, we get for α the following expression

$$\alpha = -\hbar k_{\mathrm{L}}^2 \frac{s}{(1+s)^2} \frac{\delta\, \Gamma}{\delta^2 + (\Gamma^2/4)}, \tag{4.8}$$

where s is the saturation parameter defined in eq. (3.6). It clearly appears from eq. (4.8) that α is positive for $\delta < 0$. For a fixed value of s, the value of δ which optimizes eq. (4.8) is $\delta = -\Gamma/2$. Taking this value of δ, we can then look for the optimal value of s which is found to be $s = 1$, corresponding to $\Omega_1 = \Gamma$. Taking these values of δ and Ω_1, we determine the maximum value of α

$$\alpha_{\max} = \frac{\hbar k_{\mathrm{L}}^2}{4}. \tag{4.9}$$

If we come back to eq. (4.7), and if we suppose that $\mathcal{F}_x(v_0 = 0)$ is compensated for by a static external force, we find that the equation of motion of the center of the atomic wave packet is

$$M \frac{\mathrm{d}v_0}{\mathrm{d}t} = \mathcal{F} = -\alpha\, v_0, \tag{4.10}$$

which means that the atomic velocity is damped with a rate

$$\gamma = \frac{\alpha}{M} = \frac{\hbar k_{\mathrm{L}}^2}{4M} = \frac{E_{\mathrm{R}}}{2\hbar}. \tag{4.11}$$

where E_{R} is the recoil energy defined in eq. (1.8). We have thus established the result announced in section 1.3 according to which external variables,

such as the atomic velocity, have a characteristic damping time on the order of $T_{\rm ext} = \gamma^{-1} \simeq \hbar/E_{\rm R}$ (ranging typically between 1 μs and 100 μs).

4.2. Laser standing wave

The laser wave is supposed now to be a standing wave along the Ox-axis, linearly polarized along Oz, so that eq. (1.2) becomes

$$\boldsymbol{E}_{\rm L}(\boldsymbol{r},t) = \boldsymbol{\epsilon}_z\, \mathcal{E}_0(x) \cos\omega_{\rm L} t, \tag{4.12}$$

where the amplitude $\mathcal{E}_0(x)$ is given by

$$\mathcal{E}_0(x) = 2\,\mathcal{E}_0 \cos k_{\rm L} x. \tag{4.13}$$

Inserting eq. (4.13) into eq. (4.12), we get

$$\boldsymbol{E}_{\rm L}(\boldsymbol{r},t) = \boldsymbol{\epsilon}_z\, \mathcal{E}_0[\cos(\omega_{\rm L} t - k_{\rm L} x) + \cos(\omega_{\rm L} t + k_{\rm L} x)], \tag{4.14}$$

which shows that the laser wave can be considered as the superposition of two counterpropagating plane waves, with the same amplitude $\mathcal{E}_0$. It must be emphasized however that the force exerted by the standing wave is not simply the sum of the radiation pressures of the two counterpropagating waves. There are interference effects between these two waves which play an essential role.

In a standing wave, the phase of the field is the same everywhere, so that $\boldsymbol{\beta} = \boldsymbol{\nabla}\Phi = \boldsymbol{0}$. On the other hand, the Rabi frequency is position dependent and can be written

$$\Omega_1(x) = -\frac{d\,\mathcal{E}_0(x)}{\hbar} = 2\,\Omega_1 \cos k_{\rm L} x, \tag{4.15}$$

where

$$\Omega_1 = -\frac{d\,\mathcal{E}_0}{\hbar} \tag{4.16}$$

is the Rabi frequency associated with each of the two counterpropagating plane waves forming the standing wave. It follows that

$$\boldsymbol{\alpha} = \frac{\boldsymbol{\nabla}\Omega_1(x)}{\Omega_1(x)} = \frac{\boldsymbol{\nabla}\mathcal{E}_0(x)}{\mathcal{E}_0(x)} = -k_{\rm L} \tan k_{\rm L} x\; \boldsymbol{\epsilon}_x \tag{4.17}$$

is different from zero. According to eq. (2.37), the mean force experienced by the atom depends only on the component u of the Bloch vector.

In order to find u, we have to solve the optical Bloch equations (2.46). If the atom is moving with velocity v_0 along Ox, we can replace x by $v_0 t$. We then see from eq. (4.15) that $\Omega_1(x)$ becomes a sinusoidal function of t, with frequency $k_L v_0$. On the other hand, $\dot{\Phi}$ vanishes since Φ does not depend on x. We conclude that, for an atom moving in a standing wave, the optical Bloch equations form a set of coupled linear differential equations with coefficients depending sinusoidally on time. Contrary to what happens for a plane running wave, it is in general impossible to solve analytically these equations, and we must use some approximations.

4.2.1. Limit of small velocities ($k_L v_0 \ll \Gamma$)

We present here a method of resolution of optical Bloch equations, first introduced in ref. [8], and which consists of looking for an expansion of the solution in powers of kv_0/Γ. The zeroth order term represents the "adiabatic" solution, corresponding to a situation where the atom is moving so slowly along Ox that its internal state, when it passes x, is the same as the one associated with an atom at rest in x. The first order term gives the first correction to the adiabatic approximation. It is linear in v_0, more precisely in kv_0/Γ which is the non-adiabaticity parameter, equal to the ratio between the distance $v_0\Gamma^{-1}$ over which the atom travels during the internal response time Γ^{-1} and the laser wavelength k^{-1} which characterizes the spatial variations of the laser field. When inserted into the expression (2.37) of the force, this first order correction gives rise to a force linear in v_0, which is precisely the friction force.

In order to find the terms linear in v in the solution of the optical Bloch equations, we first write eq. (2.46) in a compact matrix form

$$(\dot{X}) = \left(\frac{\partial}{\partial t} + v_0 \frac{\partial}{\partial x}\right)(X) = (\mathcal{B})(X) - (X_s), \tag{4.18}$$

where the column vectors X (Bloch vector) and X_s (source term) and the square matrix $\mathcal{B}$ (Bloch matrix) are given by

$$(X) = \begin{pmatrix} u \\ v \\ w \end{pmatrix}, \quad (X_s) = \begin{pmatrix} 0 \\ 0 \\ \Gamma/2 \end{pmatrix}, \quad (\mathcal{B}) = \begin{pmatrix} -\Gamma/2 & \delta & 0 \\ -\delta & -\Gamma/2 & -\Omega_1(x) \\ 0 & \Omega_1(x) & -\Gamma \end{pmatrix}. \tag{4.19}$$

In eq. (4.18), we have used the "hydrodynamic derivative" $\mathrm{d}/\mathrm{d}t = (\partial/\partial t) + v_0(\partial/\partial x)$. After a transient regime which lasts a time on the order of Γ^{-1}, the contributions of $\partial X/\partial t$ vanish and we have

$$v_0 \frac{\partial}{\partial x}(X) = (\mathcal{B})(X) - (X_s). \tag{4.20}$$

We now insert the expansion

$$(X) = (X^{(0)}) + (X^{(1)}) + \dots \tag{4.21}$$

of X in powers of kv_0/Γ into eq. (4.20). To order 0 in kv_0/Γ, the left-hand side vanishes and we get

$$0 = (\mathcal{B})\,(X^{(0)}) - (X_s), \tag{4.22a}$$

or equivalently

$$(X^{(0)}) = (\mathcal{B})^{-1}(X_s), \tag{4.22b}$$

which is just the steady-state Bloch vector for an atom at rest in x. To order 1 in kv_0/Γ, we then get

$$v_0 \frac{\partial}{\partial x}(X^{(0)}) = (\mathcal{B})\,(X^{(1)}), \tag{4.23}$$

which can be transformed, using eq. (4.22.b) into

$$(X^{(1)}) = (\mathcal{B})^{-1} v_0 \frac{\partial}{\partial x}(X^{(0)}) = (\mathcal{B})^{-1} v_0 \frac{\partial}{\partial x}(\mathcal{B})^{-1}(X_s). \tag{4.24}$$

Finally, we insert the expansion $u = u^{(0)} + u^{(1)} + \dots$ of the first component of X into the expression (2.37) of the force. We do not give here the expression of the friction force which results from such a calculation, since it can be found in ref. [8]. We just point out a few important characteristics of such a friction force.

Consider first the weak intensity limit: $s_0 \ll 1$, where s_0 is the saturation parameter associated with each of the two couterpropagating waves forming the standing wave. One finds in this limit that the friction force, averaged over one wavelength, coincides with the sum of the two friction forces exerted by the two counterpropagating plane waves. It thus appears that, at weak intensity, the interference effects between the two counterpropagating waves acting upon a moving atom vanish when averaged over one wavelength. One gets, for $k_L|v_0| \ll \gamma$ and $s_0 \ll 1$, $\mathcal{F} = -\alpha\, v_0$ with

$$\alpha = -\hbar\, k_L^2\, \Omega_1^2\, \frac{\delta\, \Gamma}{\left[\delta^2 + (\Gamma^2/4)\right]^2}. \tag{4.25}$$

Such an important result, which remains valid for arbitrary velocities, will be rederived in section 6.5 from a different point of view using scattering amplitudes. It actually provides the justification for the physical

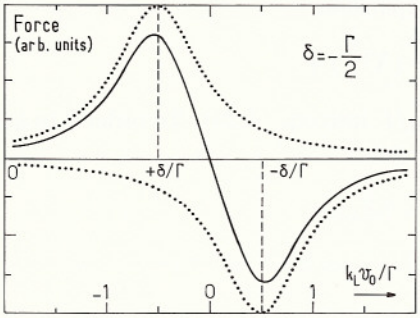

Fig. 4. Principle of Doppler cooling. Because of the Doppler effect, the radiation pressures exerted by the two counterpropagating waves forming the standing wave get unbalanced (curves in dotted lines), resulting in a net force opposite to the atomic velocity (curve in solid line).

picture usually given for Doppler cooling [13]. Consider an atom moving with velocity v_0 along a weak standing wave, formed by two counterpropagating waves $+\boldsymbol{k}_{\mathrm{L}}$ and $-\boldsymbol{k}_{\mathrm{L}}$, slightly detuned to the red side of the atomic frequency (fig. 4). Because of the Doppler effect, the atom gets closer to resonance with the wave opposing its motion, and farther from resonance with the other wave, so that the two forces exerted by the two waves become unbalanced, resulting in a net force opposite to v_0.

At high intensity ($s_0 \gg 1$), one finds that, contrary to what happens at low intensity, the friction force $\mathcal{F}(x,v)$, averaged over one wavelength, becomes an "antidamping" force for a red detuning ($\omega_{\mathrm{L}} < \omega_{\mathrm{A}}$) and a friction force for a blue detuning ($\omega_L > \omega_{\mathrm{A}}$). The physical interpretation of such a surprising result will be given later on, using the dressed-atom approach (see chapter 7, section 7.4).

4.2.2. Arbitrary velocity. Method of continued fractions

When kv becomes on the order of Γ, or larger than Γ, it is no longer possible to use the expansion (4.21) of the Bloch vector in powers of kv_0/Γ. We present in this section another approach to the problem, first introduced in ref. [14], and using the fact that the components of the Bloch vector are periodic functions of time, which itself is a consequence of the sinusoidal dependence on t of $\Omega_1(x) = \Omega_1(v_0 t)$ [see eq. (4.15)].

Since u, v, w are periodic functions of time, we can expand them in Fourier series. Inserting these expansions in the optical Bloch equations (4.18) leads to a set of recurrence relations between the various coefficients of the Fourier series expansions of u, v, w. It turns out that these equations can be formally solved in terms of continued fractions, which are very

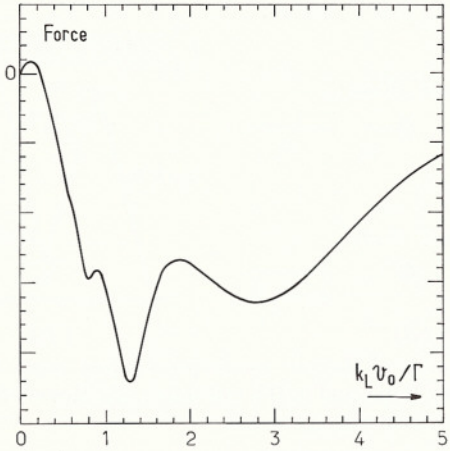

Fig. 5. Variations with $k_L v_0$ of the static part of the mean force experienced by an atom moving in a high intensity standing wave. This curve corresponds to $\delta = -2\Gamma$, $\Omega_1 = 5\Gamma$. The radiative shifts of the Doppleron resonances are already quite large.

convenient for computer calculations. We will not give here the details of such calculations, which can be found in ref. [14]. We just mention a few important results obtained in this way, and give their physical meaning.

In fig. 5, we have sketched the variations with $k_L v_0$ of the static part of the force $\boldsymbol{\mathcal{F}} = -\hbar\Omega_1(x)\, u(x,v)\, \boldsymbol{\alpha}$, averaged over one wavelength. We have supposed a red detuning ($\delta < 0$), and an intensity high enough so that the slope at $v_0 = 0$ is positive, contrarily to what happens at low intensity where we have a friction force for $\delta < 0$ (see end of the previous subsection 4.2.1). For larger values of $k_L v_0$, we see in fig. 5 that the force changes sign and exhibits resonant variations around values of $k_L v_0$ which correspond to $kv_0 = -\delta/3, -\delta/5 \ldots$

The resonances appearing in fig. 5 can be simply interpreted in terms of resonant multiphoton processes. For example, figure 6 represents such a multiphoton process, responsible for the resonance $k_L v_0 = -\delta/3$. In the atomic rest frame, the apparent frequencies of the two counterpropagating waves forming the standing wave are Doppler shifted to $\omega_L + k_L v_0$ and $\omega_L - k_L v_0$, respectively (fig. 6a). The atom can make a resonant transition from g to e by a three-photon process involving the absorption of one $\omega_L + k_L v_0$ photon, the stimulated emission of one $\omega_L - k_L v_0$ photon and the absorption of a second $\omega_L + k_L v_0$ photon (straight arrows of fig. 6b). Such a process is resonant if

$$2(\omega_L + k_L v_0) - (\omega_L - k_L v_0) = \omega_A, \tag{4.26}$$

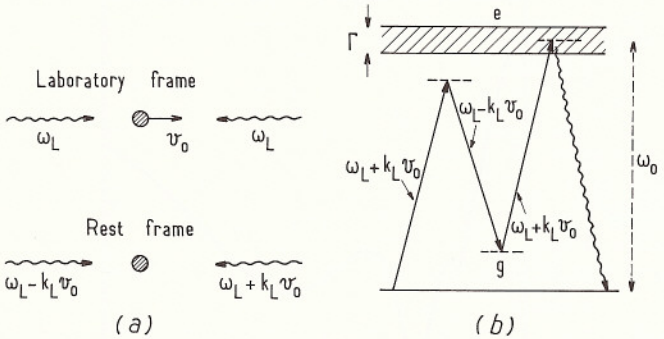

Fig. 6. (a) Frequencies of the two counterpropagating waves forming the standing wave in the laboratory frame and in the rest frame. (b) Resonant multiphoton process responsible for the resonance $k_L v_0 = -\delta/3$.

i.e., if

$$\omega_L - \omega_A = -3k_L v_0. \tag{4.27}$$

The width of the resonance is determined by the natural width Γ of the upper state. Once in e, the atom falls back in g by a spontaneous emission process (wavy arrow of fig. 6b). Similar diagrams involving $n+1$ absorptions, n stimulated emissions and one spontaneous emission could be given explaining the resonance $k_L v_0 = -\delta/(2n+1)$. Such resonant multiphoton processes involving photons with Doppler shifted frequencies are called "Dopplerons" [15].

4.3. The $\sigma^+ - \sigma^-$ configuration for a $J_g = 0 \leftrightarrow J_e = 1$ transition

Figure 6b clearly shows that redistribution processes play an important role in the resonances appearing in fig. 5, since we have absorption of photons from one wave followed by stimulated emission of photons in the counterpropagating wave. Actually, all the difficulties encountered in the theoretical description of the force experienced by an atom in a standing wave come from these redistribution processes, which involve interference effects between the two waves. We will come back to these problems in chapter 6. We present now another laser configuration and another atomic transition, for which there are no redistribution processes, and which consequently lead to much simpler results for the velocity dependent force [7].

We consider an atom with a transition $J_g = 0 \leftrightarrow J_e = 1$, having a single Zeeman sublevel g_0 in the ground state and three Zeeman sublevels e_{-1}, e_0 and e_{+1} in the excited state (fig. 7a). This atom is moving with

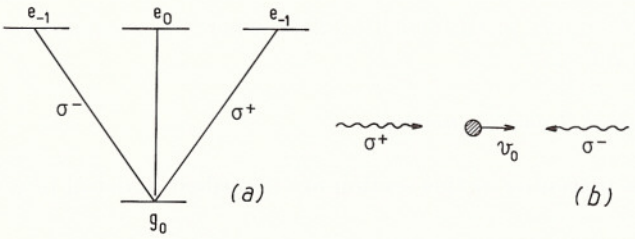

Fig. 7. (a) Zeeman sublevels for an atomic transition $J_g = 0 \longleftrightarrow J_e = 1$. (b) Laser configuration formed by two counterpropagating waves having, respectively right circular (σ^+) and left circular (σ^-) polarization.

velocity v along the same axis as two counterpropagating waves having respectively a right circular (σ^+) and a left circular (σ^-) polarization (fig. 7b). Because of angular momentum conservation, the σ^+ wave excites only the transition $g_0 \leftrightarrow e_{+1}$ and the σ^- wave excites only the transition $g_0 \leftrightarrow e_{-1}$. It follows that if the atom absorbs a σ^+ photon and goes from g_0 to e_{+1}, it cannot come back to g_0 by stimulated emission of a photon in the other σ^- wave. In other words, conservation of angular momentum prevents any redistribution of photons between the two counterpropagating waves. This explains why the calculation of the velocity dependent force is, in this case, much simpler than for a two-level atom. As shown in ref. [7], the force can be exactly calculated. For a red detuning ($\omega_L < \omega_A$), it remains a friction force for all intensities. No resonances, corresponding to Doppleron multiphoton processes, appear in the curve giving the variations of the force with the velocity.

5. Fluctuations of radiative forces

After having studied in the preceding two chapters 3 and 4 the mean value $\boldsymbol{\mathcal{F}}$ of the force, we consider now the fluctuating part $\delta\boldsymbol{F}$ of this force given by eqs. (2.32) and (2.33). Such a fluctuating force introduces noise in atomic motion and is responsible for a diffusion of atomic momentum which limits the efficiency of laser cooling and laser trapping. In this chapter, we explain how it is possible to describe theoretically such fluctuations and we discuss the physical content of the results.

Since atomic motion in laser light presents great similarities with Brownian motion, we have thought it would be useful to recall first (section 5.1) a few basic results concerning classical Brownian motion. We then approach the problem of fluctuations of radiative forces, first in the Heisenberg picture (section 5.2), where we follow closely the presentation of ref. [8], then

in the Schrödinger picture (section 5.3), where we summarize the results derived in ref. [17].

5.1. *Classical Brownian motion*

The topics presented in this section are described in detail in ref. [16].

5.1.1. *Langevin equation*

In order to describe the random motion of a heavy particle, with mass M and momentum $\boldsymbol{p}$, immersed in a fluid of light particles, Langevin introduced the following equation (for each component p of $\boldsymbol{p}$)

$$\frac{\mathrm{d}}{\mathrm{d}t}p(t) = -\gamma p(t) + F(t). \tag{5.1}$$

The total force acting on the particle is split into two parts: a friction force, $-\gamma p(t)$, representing the cumulative effect of collisions which damp the particle momentum with a "relaxation time"

$$T_R = \gamma^{-1} \tag{5.2}$$

and a fluctuating force $F(t)$, called the "Langevin force", responsible for the fluctuations of $p(t)$ about its mean value. In eq. (5.1), $F(t)$ is considered as an external force, independent of $p(t)$, having a zero average value

$$\overline{F(t)} = 0 \tag{5.3a}$$

and a correlation function equal to

$$\overline{F(t)F(t')} = 2D\, g(t - t'), \tag{5.3b}$$

where D is a coefficient which will be interpreted later on, and where $g(t-t')$ is a normalized function of $t - t'$

$$\int_{-\infty}^{+\infty} g(\tau)\, d\tau = 1, \tag{5.4}$$

which is an even function of $t - t'$ (since $F(t)$ is stationary), and which has a width on the order of the collision time τ_c.

Usually, the collision time τ_c is much smaller than the relaxation time T_R

$$\tau_c \ll T_R, \tag{5.5}$$

which means that we have two well separated time scales in the problem. It follows that, with respect to functions of $t-t'$ varying with a characteristic time T_R, eq. (5.3.b) can be approximated, taking into account eq. (5.4), by

$$\overline{F(t)F(t')} \simeq 2D\,\delta(t-t'). \tag{5.6}$$

5.1.2. Momentum diffusion coefficient

The solution of eq. (5.1) corresponding to $p(t_0) = p_0$ can be written

$$p(t) = p_0 e^{-\gamma(t-t_0)} + \int_{t_0}^{t} \mathrm{d}t'\, F(t')\, e^{-\gamma(t-t')}. \tag{5.7}$$

From eq. (5.3.a), it follows that

$$\overline{p(t)} = p_0 e^{-\gamma(t-t_0)}, \tag{5.8}$$

which means that the mean momentum of the particle is damped with a time constant $T_{\mathrm{R}} = \gamma^{-1}$.

We now evaluate the variance $\sigma_p^2(t)$ of p

$$\sigma_p^2(t) = \overline{\left[p(t) - \overline{p(t)}\right]^2}. \tag{5.9}$$

Using eqs. (5.7), (5.8), (5.3.b) and (5.6), and assuming $t - t_0 \gg \tau_{\mathrm{c}}$, we get

$$\begin{aligned} \sigma_p^2(t) &= \int_{t_0}^{t} \mathrm{d}t' \int_{t_0}^{t} \mathrm{d}t''\, \overline{F(t')F(t'')}\, \mathrm{e}^{-\gamma(t-t')}\, \mathrm{e}^{-\gamma(t-t'')} \\ &\simeq \frac{D}{\gamma}\left[1 - \mathrm{e}^{-2\gamma(t-t_0)}\right]. \end{aligned} \tag{5.10}$$

For time intervals short compared to the relaxation time ($t - t_0 \ll \gamma^{-1}$), we can expand the exponential of eq. (5.10) and we get

$$\tau_{\mathrm{c}} \ll t - t_0 \ll \gamma^{-1} \qquad \longrightarrow \qquad \sigma_p^2(t) \simeq 2D\,(t - t_0). \tag{5.11}$$

It follows that, at short times, the variance of $p(t)$ increases linearly with $t - t_0$, with a rate $2D$. This shows that D is a momentum diffusion coefficient. For long time intervals ($t - t_0 \gg \gamma^{-1}$), the exponential of eq. (5.10) becomes negligible and we get, using eq. (5.8)

$$t - t_{\circ} \gg \gamma^{-1} \qquad \longrightarrow \qquad \sigma_p^2 = \overline{p^2} - \overline{p}^2 = \overline{p^2} = \frac{D}{\gamma}. \tag{5.12}$$

The variance of p tends to a fixed value equal to D/γ. On the other hand, if the particle is assumed to reach an equilibrium at the temperature T of the surrounding fluid, we have

$$\frac{\overline{p^2}}{2M} = \frac{1}{2} k_B T. \tag{5.13}$$

Equating (5.12) and (5.13) gives the Einstein equation

$$D = M\gamma k_B T, \tag{5.14}$$

which relates the fluctuations of F, characterized by D, to the damping rate γ which characterizes the dissipative force damping the particle momentum.

5.1.3. Classical regression theorem

In this section, we present a simple method for calculating the correlation function of $p(t)$, which can be easily extended to quantum correlation functions.

We first calculate the correlation function $\overline{F(t)p(t')}$, involving both $F(t)$ and $p(t')$. If we let t_0 go to $-\infty$ in eq. (5.7), we get a steady-state correlation function given by

$$\overline{F(t)\,p(t')} = \int_{-\infty}^{t'} \mathrm{d}t'' \underbrace{\overline{F(t)F(t'')}}_{2D\delta(t-t'')} \mathrm{e}^{-\gamma(t'-t'')}. \tag{5.15}$$

If $t \gg t'$, more precisely if $t - t' \gg \tau_c$, the delta function $\delta(t - t'')$ of eq. (5.15) is outside the domain of integration, so that

$$t - t' \gg \tau_c \quad \longrightarrow \quad \overline{F(t)\,p(t')} = 0. \tag{5.16}$$

Such a result means that $p(t')$, which depends on the Langevin force $F(t'')$ in the past of t', cannot be correlated with the Langevin force $F(t)$ in the future of t'. On the other hand, if $t \ll t'$, more precisely if $t' - t \gg \tau_c$, we can extend to $+\infty$ the upper limit of the integral of eq. (5.15) which is then easily evaluated

$$t' - t \gg \tau_c \quad \longrightarrow \quad \overline{F(t)\,p(t')} = 2D\ \mathrm{e}^{-\gamma(t'-t)}. \tag{5.17}$$

Finally, for t close to t', $\overline{F(t)\,p(t')}$ varies rapidly between $2D$ and 0 over an interval of width τ_c, taking the value D for $t = t'$ (since $\overline{F(t)F(t'')}$ is an even function of $t - t''$). All these results are regrouped in fig. 8.

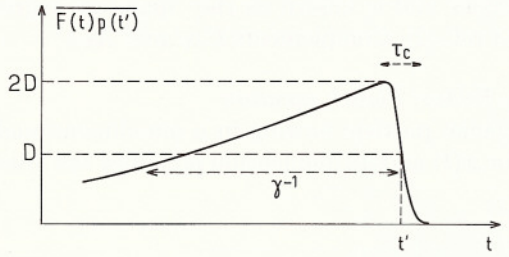

Fig. 8. Variations of $\overline{F(t)\,p(t')}$ versus t.

We calculate now the autocorrelation function $\overline{p(t)\,p(t')}$ of $p(t)$. For this purpose, we multiply both sides of eq. (5.1) by $p(t')$ and we take the average value

$$\frac{\mathrm{d}}{\mathrm{d}t}\,\overline{p(t)\,p(t')} = -\gamma\,\overline{p(t)\,p(t')} + \overline{F(t)\,p(t')}. \tag{5.18}$$

For $t-t' \gg \tau_c$, the last term of eq. (5.18) vanishes, according to eq. (5.16), and we get

$$t - t' \gg \tau_c \qquad \longrightarrow \qquad \frac{\mathrm{d}}{\mathrm{d}t}\,\overline{p(t)\,p(t')} = -\gamma\,\overline{p(t)\,p(t')}. \tag{5.19}$$

For $0 \leqslant t - t' \leqslant \tau_c$, $\overline{F(t)\,p(t')}$ is on the order of D, according to fig. 8, so that the contribution of the last term of eq. (5.18) to $\overline{p(t)\,p(t')}$, which is equal to the integral over t'' from t' to t of $\overline{F(t)\,p(t'')}$, remains bounded by $D\tau_c$. Since $\tau_c \ll \gamma^{-1}$, this contribution is very small compared to $D\gamma^{-1}$, which is nothing but the initial value $\overline{p^2}$ of $\overline{p(t)\,p(t')}$, for $t = t'$ (see eq. (5.12)). We can therefore ignore, for $t > t'$, the last term of eq. (5.18) and consider that the "two-time average " $\overline{p(t)\,p(t')}$ obeys the equation

$$\frac{\mathrm{d}}{\mathrm{d}t}\,\overline{p(t)\,p(t')} \simeq -\gamma\,\overline{p(t)\,p(t')}, \tag{5.20}$$

which is quite similar to the equation

$$\frac{\mathrm{d}}{\mathrm{d}t}\,\overline{p(t)} = -\gamma\,\overline{p(t)} \tag{5.21}$$

obeyed by the "one-time average" $\overline{p(t)}$. In other words, the fluctuations "regress" as the mean values. Such a result can be extended to quantum

correlation functions and is known as the "quantum regression theorem" (see ref. [18] and ref. [2], Complements C_{IV} and A_V).

5.1.4. Kramers–Fokker–Planck equation

Consider a Brownian particle moving in a one-dimensional potential well $U(x)$. Its position $x(t)$ and its momentum $p(t)$ obey the following equations

$$\frac{dx}{dt} = +\frac{p(t)}{M}, \tag{5.22a}$$

$$\frac{dp}{dt} = -\gamma p(t) - \frac{d}{dx}U(x) + F(t), \tag{5.22b}$$

which are a straightforward extension of the Langevin equation (5.1). We want here to give the principle of the derivation of the evolution equation of the distribution function $\mathcal{P}(x,p,t)$, which is the probability density of finding the particle with position x and momentum p at time t.

It is clear from eq. (5.22) that the rates of variation of $x(t)$ and $p(t)$ depend only on the state of the system at the same instant t, and not on its "history" in the past of t. For that reason, the stochastic process $\{x(t), p(t)\}$ is called a "Markov" process. Note that $\{p(t)\}$ alone would not be a Markov process, since $dp(t)/dt$ depends, according to eq. (5.22.b) on $dU(x)/dx$, i.e., on $x(t) = \int_{-\infty}^{t} dt' p(t')/M$ which involves the whole history of $p(t)$.

The distribution function $\mathcal{P}(x,p,t)$ associated with the Markov process $\{x(t), p(t)\}$ obeys the equation

$$\mathcal{P}(x,p,t) = \int\int dx'\, dp'\; \Pi(x,p,t/x',p',t')\, \mathcal{P}(x',p',t'), \tag{5.23}$$

where $\Pi(x,p,t/x',p',t')$ is the conditional probability for ending in x,p at time t if one starts from x',p' at time t'. This probability is normalized, so that

$$\int\int dx\, dp\; \Pi(x,p,t/x',p',t') = 1. \tag{5.24}$$

We now choose a time interval δt such that $\tau_c \ll \delta t \ll T_R$. Replacing in eqs. (5.23) and (5.24) t by $t+\delta t$ and t' by t, we derive from eq. (5.23) the following equation

$$\begin{aligned}\mathcal{P}(x,p,t+\delta t) - \mathcal{P}(x,p,t) &= +\int\int dx'\, dp'\; \Pi(x,p,t+\delta t/x',p',t)\, \mathcal{P}(x',p',t) \\ &\quad - \int\int dx''\, dp''\; \Pi(x'',p'',t+\delta t/x,p,t)\, \mathcal{P}(x,p,t),\end{aligned} \tag{5.25}$$

which has a clear physical meaning. After division by δt, such an equation expresses that the rate of variation of $\mathcal{P}(x,p,t)$ in x,p is equal to the rate in minus the rate out. It can thus be considered as a master equation for $\mathcal{P}(x,p,t)$.

We suppose now that the variations

$$\begin{aligned}\delta x &= x(t+\delta t) - x(t),\\ \delta p &= p(t+\delta t) - p(t)\end{aligned} \tag{5.26}$$

of $x(t)$ and $p(t)$ between t and $t+\delta t$ are small compared to the widths Δx and Δp of $\mathcal{P}(x,p,t)$ in x and p, respectively (limit of small jumps). By expanding in eq. (5.25) $\mathcal{P}(x',p',t)$ in powers of $x'-x$ and $p'-p$, it is then possible to approximate the master equation (5.25) by a partial differential equation. If the Taylor series expansion of $\mathcal{P}(x',p',t)$ is stopped after order two, one gets

$$\begin{aligned}\frac{\partial}{\partial t}\mathcal{P}(x_1,x_2,t) = &-\frac{\partial}{\partial x_1}M_1\mathcal{P} - \frac{\partial}{\partial x_2}M_2\mathcal{P}\\ &+\sum_{i,j=1,2}\frac{\partial^2}{\partial x_i \partial x_j}D_{ij}\mathcal{P},\end{aligned} \tag{5.27}$$

where we have used the simplified notation $x_1 = x, x_2 = p$ and where M_i and D_{ij} are given by

$$M_i = \lim_{\tau_c \ll \delta t \ll T_R} \frac{\overline{\delta x_i}}{\delta t}, \tag{5.28a}$$

$$D_{ij} = \frac{1}{2!}\lim_{\tau_c \ll \delta t \ll T_R} \frac{\overline{\delta x_i \delta x_j}}{\delta t}. \tag{5.28b}$$

In order to calculate M_i and D_{ij} we come back to eqs. (5.22), and we derive, after calculations similar to those of subsection 5.1.2., the following relations

$$\begin{aligned}&\frac{\overline{\delta x}}{\delta t} = \frac{p}{M}, && \frac{\overline{\delta p}}{\delta t} = -\gamma p - \frac{\mathrm{d}U}{\mathrm{d}x},\\ &\frac{\overline{\delta x^2}}{\delta t} = 0 = \frac{\overline{\delta x \delta p}}{\delta t}, && \frac{\overline{\delta p^2}}{\delta t} = 2D,\end{aligned} \tag{5.29}$$

which inserted into eq. (5.27) give the Kramers–Fokker–Planck equation

$$\begin{aligned}\frac{\partial}{\partial t}\mathcal{P}(x,p,t) = &-\frac{p}{M}\frac{\partial}{\partial x}\mathcal{P}(x,p,t)\\ &+\frac{\partial}{\partial p}\left[\gamma p + \frac{\mathrm{d}U}{\mathrm{d}x}\right]\mathcal{P}(x,p,t) + D\frac{\partial^2}{\partial p^2}\mathcal{P}(x,p,t).\end{aligned} \tag{5.30}$$

5.2. Analysis of momentum diffusion in the Heisenberg picture

5.2.1. Momentum diffusion coefficient and Langevin force operator
By definition, the momentum diffusion coefficient D is related to the rate of increase of the momentum variance

$$2D = \frac{\mathrm{d}}{\mathrm{d}t}\Delta P^2(t), \tag{5.31}$$

with

$$\Delta P^2(t) = \left\langle \left[\boldsymbol{P}(t) - \langle \boldsymbol{P}(t)\rangle\right]^2\right\rangle. \tag{5.32}$$

Starting from the Heisenberg equation for $\boldsymbol{P}(t)$, given in section 2,

$$\frac{\mathrm{d}}{\mathrm{d}t}\boldsymbol{P}(t) = \boldsymbol{F}(t), \tag{5.33}$$

where $\boldsymbol{F}(t)$ is the force operator, we get

$$\begin{aligned}\frac{\mathrm{d}}{\mathrm{d}t}\left\langle \left[\boldsymbol{P}(t) - \langle \boldsymbol{P}(t)\rangle\right]^2\right\rangle &= \frac{\mathrm{d}}{\mathrm{d}t}\langle \boldsymbol{P}^2\rangle - 2\langle \frac{\mathrm{d}}{\mathrm{d}t}\boldsymbol{P}\rangle \cdot \langle \boldsymbol{P}\rangle \\ &= \langle \boldsymbol{F}\cdot\boldsymbol{P} + \boldsymbol{P}\cdot\boldsymbol{F}\rangle - 2\langle \boldsymbol{F}\rangle\cdot\langle \boldsymbol{P}\rangle.\end{aligned} \tag{5.34}$$

Inserting into eq. (5.34) the solution

$$\boldsymbol{P}(t) = \int_0^\infty \mathrm{d}\tau\ \boldsymbol{F}(t-\tau) \tag{5.35}$$

of eq. (5.33), and using eq. (5.31) leads to

$$\begin{aligned}2D &= 2\ \mathrm{Re}\int_0^\infty \mathrm{d}\tau\ \left[\langle \boldsymbol{F}(t)\cdot\boldsymbol{F}(t-\tau)\rangle - \langle \boldsymbol{F}(t)\rangle\cdot\langle \boldsymbol{F}(t-\tau)\rangle\right] \\ &= 2\ \mathrm{Re}\int_0^\infty \mathrm{d}\tau\ \langle \delta\boldsymbol{F}(t)\cdot\delta\boldsymbol{F}(t-\tau)\rangle,\end{aligned} \tag{5.36}$$

where $\delta\boldsymbol{F}(t)$ is the fluctuating part of $\boldsymbol{F}(t)$

$$\delta\boldsymbol{F}(t) = \boldsymbol{F}(t) - \langle \boldsymbol{F}(t)\rangle. \tag{5.37}$$

It thus appears that the momentum diffusion coefficient is related to the time integral of the correlation function of the Langevin force operator.

In the following subsection, we give a brief outline of the calculation of such a correlation function, leading to the expression (5.44) for D. The physical interpretation of this expression is then given in subsection 5.2.3. The reader, not interested in the method of calculation of eq. (5.36), can thus directly proceed to subsection 5.2.3.

5.2.2. Correlation function of the Langevin force operator

We have seen in chapter 2 (see eqs. (2.32) and (2.33)) that the Langevin force $\delta \boldsymbol{F}(\boldsymbol{r},t)$ is the sum of two forces $\delta \boldsymbol{F}_{\rm las}(\boldsymbol{r},t)$ and $\delta \boldsymbol{F}_{\rm vac}(\boldsymbol{r},t)$ representing, respectively, the contributions of the laser field and the vacuum field to the Langevin force. From the expression (2.4) of $V_{\rm AL}$ and the fact that only the z-component of $\boldsymbol{d}$ is non-zero, we easily get

$$\delta \boldsymbol{F}_{\rm las} = [\, d_z - \langle d_z \rangle] \boldsymbol{\nabla} E_{Lz}, \tag{5.38}$$

where $\delta d_z = d_z - \langle d_z \rangle$ is the fluctuating part of d_z. A similar calculation starting from eqs. (2.5) and (2.14), allows one to transform eq. (2.33.b) into

$$\delta \boldsymbol{F}_{\rm vac} = d_z \boldsymbol{\nabla} (E_z^{\rm vac})^+ + \left[\boldsymbol{\nabla} (E_z^{\rm vac})^- \right] d_z. \tag{5.39}$$

Replacing $\delta \boldsymbol{F}$ by $\delta \boldsymbol{F}_{\rm las} + \delta \boldsymbol{F}_{\rm vac}$ in eq. (5.36) shows that the correlation function $\langle\, \delta \boldsymbol{F}(t) \cdot \delta \boldsymbol{F}(t-\tau) \,\rangle$ is a sum of three contributions, one involving only $\delta \boldsymbol{F}_{\rm las}$, one involving only $\delta \boldsymbol{F}_{\rm vac}$ and one involving both $\delta \boldsymbol{F}_{\rm las}$ and $\delta \boldsymbol{F}_{\rm vac}$. One can show that this last cross term is zero as a result of the fact that the vacuum free field gradients, appearing in eq. (5.39) and evaluated at time t, commute with the dipole operator $d_z(t')$ evaluated at any other time t' *. This allows one to put $\boldsymbol{\nabla}(E_z^{\rm vac})^+$ at the extreme right, and $\boldsymbol{\nabla}(E_z^{\rm vac})^-$ at the extreme left, which then gives zero when the vacuum average value is taken (see eq. (2.15)). This shows that D can be written

$$D = D_{\rm las} + D_{\rm vac}, \tag{5.40}$$

where

$$D_{\rm las} = {\rm Re} \int_0^\infty {\rm d}\tau \, \langle\, \delta \boldsymbol{F}_{\rm las}(t) \cdot \delta \boldsymbol{F}_{\rm las}(t-\tau) \,\rangle, \tag{5.41}$$

* To demonstrate such a result, one can express the annihilation operators $a_j(t)$ appearing in the field gradients as a function of $a_j(t')$ and of the source field radiated between t' and t. $a_j(t')$ commutes with $d_z(t')$. The remaining commutator appears as an integral over the modes $\boldsymbol{k}\boldsymbol{\epsilon}$ of an odd function of $\boldsymbol{k}$ and thus vanishes.

$$D_{\text{vac}} = \text{Re} \int_0^\infty d\tau \, \langle \, \delta \boldsymbol{F}_{\text{vac}}(t) \cdot \delta \boldsymbol{F}_{\text{vac}}(t-\tau) \, \rangle. \tag{5.42}$$

In eq. (5.38), $\boldsymbol{\nabla} E_{Lz}$ is a c-number, so that the correlation function of $\delta \boldsymbol{F}_{\text{las}}$ is proportional to the correlation function of δd_z. To calculate $\langle \delta d_z(t) \delta d_z(t-\tau) \rangle$, one can first express δd_z in terms of $\delta \Pi_{eg}$ and $\delta \Pi_{ge}$ where $\Pi_{ab} = |a\rangle\langle b|$ with $a, b = e$ *or* g (see eq. (2.39)). Now, we have already mentioned in section 2.5 that the equation of motion of Π_{ab} has the structure of a Langevin equation with damping terms and a Langevin force (see eq. (2.41)). Multiplying both sides of the equation giving $\dot{\Pi}_{ab}(t)$ by $\Pi_{cd}(t')$, and taking the vacuum average value, one can then show, by an argument very similar to the one used above in subsection 5.1.3, that, for $t > t'$, the two-time averages $\langle \Pi_{ab}(t) \Pi_{cd}(t') \rangle$ obey the same equations as the one-time averages $\langle \Pi_{ab}(t) \rangle$ (c and d being fixed), i.e., optical Bloch equations. Such an important result, known as the "quantum regression theorem" (see ref. [18] and ref. [2], Complements C_{IV} and A_V) means that the correlation functions of the atomic dipole moment can be calculated from optical Bloch equations.

It remains to evaluate eq. (5.42). Inserting eq. (5.39) into eq. (5.42), one sees that, due to eq. (2.15), the only non-zero term is

$$\langle 0 | d_z(t) \left[\boldsymbol{\nabla} (E_z^{\text{vac}})^+(t) \right] \left[\boldsymbol{\nabla} (E_z^{\text{vac}})^-(t-\tau) \right] d_z(t-\tau) | 0 \rangle. \tag{5.43}$$

The order of the two field operators appearing in eq. (5.43) can be changed using their commutator, which is a c-number. The contribution of this commutator is therefore proportional to the correlation function of d_z, which can be calculated from optical Bloch equations. The remaining term can be transformed, using the fact mentioned above that the vacuum free field gradient operators commute with the dipole operators at any time. One can then easily show that this term is equal to zero, as a consequence of eq. (2.15).

To summarize, we have shown that D is a sum of two terms. The first one, D_{las}, involves $\delta \boldsymbol{F}_{\text{las}}$ and thus $\boldsymbol{\nabla} E_{Lz}$, i.e., $\boldsymbol{\alpha}$ and $\boldsymbol{\beta}$ given in eq. (2.36). The second one, D_{vac}, comes from the commutator of the vacuum free field, i.e., from the quantum nature of this field, and is independent of $\boldsymbol{\alpha}$ and $\boldsymbol{\beta}$. Both D_{las} and D_{vac} involve correlation functions of the atomic dipole moment which can be calculated from optical Bloch equations, using the quantum regression theorem.

5.2.3. Physical discussion

For a two-level atom at rest at $\boldsymbol{r} = \boldsymbol{0}$, the method of calculation outlined in the previous subsection leads to the following result [8]

$$
\begin{aligned}
D = &+ \hbar^2 k_{\mathrm{L}}^2 \frac{\Gamma}{4} \frac{s}{1+s} \\
&+ \hbar^2 \boldsymbol{\beta}^2 \frac{\Gamma}{4} \frac{s}{(1+s)^3} \left\{ 1 + \frac{12\delta^2 - \Gamma^2}{4\delta^2 + \Gamma^2} s + s^2 \right\} \\
&+ \hbar^2 \boldsymbol{\alpha}^2 \frac{\Gamma}{4} \frac{s}{(1+s)^3} \left\{ 1 + \frac{-4\delta^2 + 3\Gamma^2}{4\delta^2 + \Gamma^2} s + 3s^2 + \frac{4\delta^2 + \Gamma^2}{\Gamma^2} s^3 \right\} \\
&- \hbar^2 \boldsymbol{\alpha} \cdot \boldsymbol{\beta}\, \delta \frac{s^2}{(1+s)^3} \left\{ \frac{4\Gamma^2}{4\delta^2 + \Gamma^2} + s \right\},
\end{aligned} \tag{5.44}
$$

where s is the saturation parameter at $\boldsymbol{r} = \mathbf{0}$, given by eq. (3.6), and where $\boldsymbol{\alpha}$ and $\boldsymbol{\beta}$ are the logarithmic Rabi frequency gradient and phase gradient at $\boldsymbol{r} = \mathbf{0}$ given in eqs. (3.3.b) and (3.3.c).

The first line of eq. (5.44), which is independent of $\boldsymbol{\alpha}$ and $\boldsymbol{\beta}$ is D_{vac}, which comes from the non-commutation of the vacuum free field operators

$$
D_{\mathrm{vac}} = \hbar^2 k_{\mathrm{L}}^2 \frac{\Gamma}{4} \frac{s}{1+s}. \tag{5.45}
$$

Such a term describes the momentum diffusion due to the random direction of the spontaneously emitted photons. The atomic momentum $\boldsymbol{P}$ accomplishes a random walk in momentum space, the size of each step being $\hbar k_{\mathrm{L}}$, and the number of steps during δt being equal to $\Gamma \sigma_{ee}^{\mathrm{st}} \delta t$, where $\sigma_{ee}^{\mathrm{st}}$ is the steady-state population of the upper state, given by (3.7). It follows from the well-known properties of random walk that the increase of the variance of $\mathbf{p}$ during δt can be written

$$
\begin{aligned}
\overline{(\delta \boldsymbol{p}^2)} - \left(\overline{\delta \boldsymbol{p}}\right)^2 &= \hbar^2 k_{\mathrm{L}}^2 \Gamma \sigma_{ee}^{\mathrm{st}} \delta t \\
&= \hbar^2 k_{\mathrm{L}}^2 \frac{\Gamma}{2} \frac{s}{1+s} \delta t.
\end{aligned} \tag{5.46}
$$

The comparison of eqs. (5.45) and (5.46) then shows that the right-hand side of eq. (5.46) can be written as $2D_{\mathrm{vac}}\delta t$, which confirms the physical interpretation of D_{vac}.

The three other lines of eq. (5.44) correspond to D_{las}. For a laser plane wave, $\boldsymbol{\beta} = -\boldsymbol{k}_{\mathrm{L}}$ and $\boldsymbol{\alpha} = \mathbf{0}$, so that only the second line of eq. (5.44) contributes to D_{las}. Such a term then describes the momentum diffusion due to the fluctuations of radiation pressure, more precisely due to the fluctuations in the number of absorbed photons. It can be written, using eq. (3.6), as

$$
D_{\mathrm{abs}} = \frac{1}{4} \hbar^2 k_{\mathrm{L}}^2 \Gamma \frac{s}{1+s} (1+Q), \tag{5.47}
$$

where Q is a dimensionless factor given by

$$Q = \frac{2\Omega_1^2(4\delta^2 - 3\Gamma^2)}{(2\Omega_1^2 + 4\delta^2 + \Gamma^2)^2}. \tag{5.48}$$

In order to interpret eq. (5.47), we introduce the number δN of laser photons absorbed during δt, and the corresponding momentum transferred to the atom $\delta \boldsymbol{p} = \hbar \boldsymbol{k}_L \delta N$. Since δN is a random variable, there is an increase of the atomic momentum variance due to the fluctuations in the number of absorbed photons

$$\overline{(\delta \boldsymbol{p}^2)} - \left(\overline{\delta \boldsymbol{p}}\right)^2 = \hbar^2 k_L^2 \left[\overline{\delta N^2} - \left(\overline{\delta N}\right)^2\right]. \tag{5.49}$$

Consider first the mean number of photons absorbed during δt, which is given by (see eq. (3.17))

$$\overline{\delta N} = \Gamma \sigma_{ee}^{\mathrm{st}} \delta t = \frac{\Gamma}{2} \frac{s}{1+s} \delta t. \tag{5.50}$$

If δN was following a Poisson law, the variance of δN would be equal to $\overline{\delta N}$. Actually, this is not the case, and one can show [19] that there are corrections to the Poisson statistics in resonance fluorescence which are precisely described by the factor Q given in eq. (5.48)

$$\overline{\delta N^2} - \left(\overline{\delta N}\right)^2 = \overline{\delta N}\,(1+Q). \tag{5.51}$$

It thus appears that eq. (5.49) can be rewritten, using eqs. (5.51), (5.50) and (5.47) as

$$\overline{(\delta \boldsymbol{p}^2)} - \left(\overline{\delta \boldsymbol{p}}\right)^2 = 2\, D_{\mathrm{abs}}\, \delta t, \tag{5.52}$$

which confirms the physical interpretation of D_{abs} as being due to the fluctuations in the number of absorbed photons. The comparison of eqs. (5.45) and (5.47) shows that D_{vac} and D_{abs} have the same order of magnitude.

In a laser standing wave, $\boldsymbol{\beta} = \mathbf{0}$, so that only the third line of eq. (5.44) contributes to D_{las}. Such a term then describes the fluctuations of dipole forces and will be denoted by D_{dip}. We consider here a laser standing wave along the Ox-axis, linearly polarized along Oz, and having a node in $x = 0$

$$\boldsymbol{E}_L(x,t) = \boldsymbol{\epsilon}_z\, 2\mathcal{E}_0 \sin k_L x \cos \omega_L t, \tag{5.53}$$

In eq. (5.53), $\mathcal{E}_0$ is the amplitude of each of the two counterpropagating waves forming the standing wave, the corresponding Rabi frequency being equal to Ω_1. The standing wave Rabi frequency in x is thus equal to

$$\Omega_1(x) = 2\Omega_1 \sin k_{\mathrm{L}} x, \tag{5.54}$$

so that

$$\boldsymbol{\alpha} = \frac{\boldsymbol{\nabla}\Omega_1(x)}{\Omega_1(x)} = \boldsymbol{\epsilon}_x \, k_{\mathrm{L}} \, \frac{1}{\tan k_{\mathrm{L}} x}. \tag{5.55}$$

Finally, the saturation parameter in x, $s(x)$, is equal to

$$s(x) = 4s_0 \sin^2 k_{\mathrm{L}} x, \tag{5.56}$$

where

$$s_0 = \frac{\Omega_1^2/2}{\delta^2 + (\Gamma^2/4)} = \frac{s_{\max}}{4} \tag{5.57}$$

is the saturation parameter of each of the two counterpropagating waves and $s_{\max}$ the maximum value of $s(x)$. We will not discuss here the general expression of D_{dip} obtained when eqs. (5.55) and (5.56) are inserted into the third line of eq. (5.44). We will restrict ourselves to the low intensity limit ($s_0 \ll 1$) and to the high intensity limit ($s_0 \gg 1$).

If $s_0 \ll 1$, the third line of eq. (5.44) reduces to

$$D_{\mathrm{dip}} \simeq \hbar^2 k_{\mathrm{L}}^2 \, \Gamma \, s_0 \cos^2 k_{\mathrm{L}} x = \hbar^2 k_{\mathrm{L}}^2 \, \Gamma \, \frac{s_{\max}}{4} \cos^2 k_{\mathrm{L}} x, \tag{5.58}$$

whereas the first line is equal to

$$D_{\mathrm{vac}} \simeq \hbar^2 k_{\mathrm{L}}^2 \, \Gamma \, s_0 \sin^2 k_{\mathrm{L}} x. \tag{5.59}$$

Note that $D_{\mathrm{dip}} + D_{\mathrm{vac}}$ is independent of x and equal to the sum of the diffusion coefficients associated with each of the two counterpropagating waves. Near a node, for example near $x = 0$, we get a very surprising result. Since there is no light in a node, we expect that there are no fluorescence photons. Effectively, $D_{\mathrm{vac}} \to 0$ if $x \to 0$. But D_{dip} takes at $x = 0$ its maximum value, equal to $\hbar^2 k_{\mathrm{L}}^2 \, \Gamma \, s_0 = \hbar^2 k_{\mathrm{L}}^2 \, \Gamma \, s_{\max}/4$. We will come back to this problem in section 6.3 and show that, near a node, the large value of D_{dip} is due to a new kind of correlated redistribution.

If $s_0 \gg 1$, the third line of eq. (5.44) tends to*

$$D_{\text{dip}} \simeq \hbar^2 k_{\text{L}}^2 \cos^2 k_{\text{L}} x \frac{\Omega_1^2}{2\Gamma}. \tag{5.60}$$

Contrary to D_{vac} and to D_{abs} given in eqs. (5.45) and (5.47), D_{dip} does not saturate at high laser intensities. A dressed atom interpretation of this result will be given in section 7.3. We have seen above, in section 3.4, that the depth of the optical potential well associated with dipole forces increases linearly with Ω_1. The fact that the heating due to the fluctuations of dipole forces increases quadratically with Ω_1, as shown by eq. (5.60), introduces severe limitations for laser traps. Note however that it is always possible, as suggested in ref. [20], to alternate in time cooling and trapping phases.

5.2.4. The Doppler limit in laser cooling

The equilibrium temperature reached in laser cooling results from a competition between laser cooling which damps the atomic velocity with a rate $\gamma = \alpha/M$, where α is the friction coefficient (see eq. (4.7))

$$\delta p/\delta t = -\gamma p, \tag{5.61}$$

and the heating due to momentum diffusion

$$\left(\frac{\delta p^2}{\delta t}\right)_{\text{diffusion}} = 2D. \tag{5.62}$$

From eq. (5.61), it follows that

$$\left(\frac{\delta p^2}{\delta t}\right)_{\text{cooling}} = -2\gamma p^2. \tag{5.63}$$

In steady-state, the two rates (5.62) and (5.63) cancel out so that $\gamma p^2 = D$. The equilibrium temperature is thus

$$\frac{p^2}{2M} = \frac{1}{2} k_{\text{B}} T = \frac{D}{2M\gamma}. \tag{5.64}$$

* Equation (5.60) is not valid near a node, since $s(x) \to 0$ in such a place.

From eq. (4.8), it follows that, at low intensity, and for $\delta = -\Gamma/2$, $\alpha \sim \hbar^2 k_L^2 s_0$, so that

$$\gamma \sim \frac{\hbar k_L^2}{M} s_0. \tag{5.65}$$

On the other hand, from the results derived in this section (see eqs. (5.45), (5.47) and (5.58)), we have, at low intensity

$$D \sim \hbar^2 k_L^2 \Gamma s_0. \tag{5.66}$$

Inserting eqs. (5.65) and (5.66) into eq. (5.64) leads to

$$k_B T_D \sim \frac{D}{M\gamma} \sim \hbar\Gamma. \tag{5.67}$$

It thus appears that the temperature reached by laser cooling for two-level atoms is determined by Γ. The exact value of the minimum temperature which can be reached is given by $k_B T_D \sim \hbar\Gamma/2$ (see refs. [8, 21, 22]) and is called the Doppler limit. T_D is on the order of 240 μK for Na and 125 μK for Cs.

5.3. Quantum kinetic equation for the atomic Wigner function

We try now, using the Schrödinger picture, to derive an equation of motion for the reduced atomic density operator describing the translational degrees of freedom of the atom. We just give the outline of the derivation, putting the emphasis on the new results and on the new physical insights. More details may be found in refs. [17] and [23].

5.3.1. Atomic Wigner function

When both internal and external degrees of freedom are treated quantum-mechanically, the atomic density matrix is labelled by two types of quantum numbers. For example, if one uses the position representation for the center of mass, the atomic density matrix elements are $\langle i, \boldsymbol{r}'|\sigma|j, \boldsymbol{r}''\rangle$, where $i, j = e$ or g and $\boldsymbol{r}'$and $\boldsymbol{r}''$ are eigenvalues of the position operator $\boldsymbol{R}$. Similarly, if we use the momentum representation, we get $\langle i, \boldsymbol{p}'|\sigma|j, \boldsymbol{p}''\rangle$.

A very useful representation, which treats in a symmetrical way position and momentum, is the so called "Wigner representation" [24], which associates with the atomic density operator σ, a function of $\boldsymbol{r}$ and $\boldsymbol{p}$ given by

$$\begin{aligned} W_{ij}(\boldsymbol{r}, \boldsymbol{p}) &= \frac{1}{\hbar^3} \int \mathrm{d}^3 u \exp(-\mathrm{i}\boldsymbol{p}.\boldsymbol{u}/\hbar) \left\langle i, \boldsymbol{r} + \frac{\boldsymbol{u}}{2} |\sigma| j, \boldsymbol{r} - \frac{\boldsymbol{u}}{2} \right\rangle \\ &= \frac{1}{\hbar^3} \int \mathrm{d}^3 v \exp(+i\boldsymbol{r}.\boldsymbol{v}/\hbar) \left\langle i, \boldsymbol{p} + \frac{\boldsymbol{v}}{2} |\sigma| j, \boldsymbol{p} - \frac{\boldsymbol{v}}{2} \right\rangle. \end{aligned} \tag{5.68}$$

From eq. (5.68), one can introduce the Wigner function

$$f(\boldsymbol{r},\boldsymbol{p}) = W_{ee}(\boldsymbol{r},\boldsymbol{p}) + W_{gg}(\boldsymbol{r},\boldsymbol{p}), \tag{5.69}$$

which is a density of "quasi-probability" to find the atom in $\boldsymbol{r}$ with momentum $\boldsymbol{p}$, regardless of its internal state. The atomic Wigner function is real, normalized and appears as an ordinary probability density for all completely symmetrical functions of $\boldsymbol{R}$ and $\boldsymbol{P}$. For example,

$$\tfrac{1}{2}\langle \boldsymbol{R}\cdot\boldsymbol{P} + \boldsymbol{P}\cdot\boldsymbol{R}\rangle = \int \mathrm{d}^3r\,\mathrm{d}^3p\;\boldsymbol{r}\cdot\boldsymbol{p}\;f(\boldsymbol{r},\boldsymbol{p}). \tag{5.70}$$

Note however that $f(\boldsymbol{r},\boldsymbol{p})$ can take negative values, which shows that it is not a true probability.

5.3.2. Generalized optical Bloch equations

These equations of motion generalize those discussed in section 2.5 above, to the case where the external degrees of freedom are treated quantum-mechanically. They have the same structure as in eq. (2.42), i.e., the sum of Hamiltonian terms coming from the atomic Hamiltonian H_{A} and the atom–laser interaction Hamiltonian V_{AL}, and damping terms due to spontaneous emission. The new features are the appearance of the external quantum numbers.

For example, the equation of motion of $W_{gg}(\boldsymbol{r},\boldsymbol{p})$ is found to be

$$\begin{aligned}
&\frac{\partial}{\partial t}W_{gg}(\boldsymbol{r},\boldsymbol{p}) = \\
&-\frac{\boldsymbol{p}}{M}\cdot\frac{\partial}{\partial \boldsymbol{r}}\,W_{gg}(\boldsymbol{r},\boldsymbol{p}) \\
&+\frac{\mathrm{i}d}{\hbar}\int \mathrm{d}^3k\left[\mathcal{E}^-(\boldsymbol{k})\,\mathrm{e}^{-\mathrm{i}\boldsymbol{k}\cdot\boldsymbol{r}}\,W_{eg}(\boldsymbol{r},\boldsymbol{p}-\frac{\hbar\boldsymbol{k}}{2}) - \mathcal{E}^+(\boldsymbol{k})\,\mathrm{e}^{+\mathrm{i}\boldsymbol{k}\cdot\boldsymbol{r}}\,W_{ge}(\boldsymbol{r},\boldsymbol{p}+\frac{\hbar\boldsymbol{k}}{2})\right] \\
&+\Gamma\int \mathrm{d}^2\kappa\,\phi(\boldsymbol{\kappa})\,W_{ee}(\boldsymbol{r},\boldsymbol{p}+\hbar k_{\mathrm{A}}\boldsymbol{\kappa}).
\end{aligned} \tag{5.71}$$

The first term comes from the commutator of σ with $H_{\mathrm{A}}^{\mathrm{ext}} = \boldsymbol{P}^2/2M$, the second one from the commutator of σ with V_{AL}, $\mathcal{E}_L^+(\boldsymbol{k})$ and $\mathcal{E}_L^-(\boldsymbol{k})$ being, respectively, the Fourier transforms of the positive and negative frequency components of the laser field. Finally, the last term describes the feeding of the ground state from the excited state by spontaneous emission, $\phi(\boldsymbol{\kappa})$ being the relative probability of spontaneous emission of a photon in the direction $\boldsymbol{\kappa}$ and k_{A} being equal to ω_{A}/c.

It clearly appears from eq. (5.71) that the atomic momentum undergoes discrete changes during the absorption and emission processes. It follows that the generalized optical Bloch equations are finite difference equations coupling the four functions $W_{ij}(\boldsymbol{r},\boldsymbol{p})$ with $i,j = e$ or g. Such equations are not easy to deal with, other than numerically, and we introduce now some approximations to simplify them.

5.3.3. Approximations leading to a Kramers–Fokker–Planck equation
We begin by introducing two small parameters characterizing atomic motion

$$\epsilon_1 = \frac{\hbar k_{\mathrm{L}}}{\Delta p} = \frac{\text{recoil momentum}}{\text{momentum spread}}, \tag{5.72}$$

$$\epsilon_2 = \frac{k_{\mathrm{L}}\Delta p}{M\Gamma} = \frac{\text{Doppler effect}}{\text{natural width}}. \tag{5.73}$$

Condition $\epsilon_1 \ll 1$ means also that the atomic coherence length $\xi_{\mathrm{A}} = \hbar/\Delta p$ is small compared to the laser wavelength k_L^{-1}, which is equivalent to the localization assumption (2.28) introduced above and defining the semi-classical limit. Conditions $\epsilon_2 \ll 1$ means that the atomic velocity has been already damped enough (by laser cooling), so that one can treat the Doppler effect perturbatively. Such a condition is also equivalent to the localization assumption in momentum space, introduced above in eq. (2.21). Actually, near the Doppler cooling limit, we have, according to eq. (5.67), $\Delta p^2/2M \sim \hbar\Gamma$, which leads to

$$\epsilon_1 \sim \epsilon_2 \sim \sqrt{E_{\mathrm{R}}/\hbar\Gamma}. \tag{5.74}$$

By expanding the generalized optical Bloch equations in powers of ϵ_1 and ϵ_2, it is then possible to replace these finite difference equations by coupled partial differential equations, easier to deal with. Another important point is that, at order 0 in ϵ_1 and ϵ_2, the Wigner function (5.69) does not evolve whereas all other variables vary with a time scale on the order of Γ^{-1}. This means that, in the limit of zero photon momentum ($k_{\mathrm{L}} = 0$), photon–atom interactions cannot change the position or the velocity of the atom. This means also, since $\epsilon_1, \epsilon_2 \ll 1$, that there is a slow variable in the problem, $f(r,p)$, in terms of which all other variables can be adiabatically eliminated, leading to a single reduced evolution equation for $f(\boldsymbol{r},\boldsymbol{p})$, which is a quantum kinetic equation describing atomic motion.

Such a general procedure has been followed in several papers [25–28], and leads to a Kramers–Fokker–Planck equation for $f(\boldsymbol{r},\boldsymbol{p})$. The advantage of

the treatment presented in ref. [17] is that it uses an operatorial method not limited to two-level atoms, leading, for the diffusion and friction coefficients, to general expressions with a more transparent structure in terms of two-time averages of the Heisenberg force operators. It is then possible to prove the equivalence of the results obtained in the Schrödinger and in the Heisenberg pictures and to get new physical insights in the friction coefficient and in the equilibrium temperature.

5.3.4. Physical discussion

The equation of motion of $f(\boldsymbol{r},\boldsymbol{p})$, derived in ref. [17] has the following form

$$\begin{aligned}\frac{\partial f}{\partial t} = &- \frac{\boldsymbol{p}}{M}\cdot\frac{\partial f}{\partial \boldsymbol{r}} - \boldsymbol{\mathcal{F}}(\boldsymbol{r})\cdot\frac{\partial f}{\partial \boldsymbol{p}} \\ &+ \sum_{i,j=x,y,z} \frac{\partial^2 f}{\partial p_i \partial p_j}\left[D^{ij}_{\text{las}}(\boldsymbol{r}) + D^{ij}_{\text{vac}}(\boldsymbol{r})\right] \\ &+ \sum_{i,j=x,y,z} \gamma_{ij}(\boldsymbol{r})\frac{\partial}{\partial p_i}(p_j f) \\ &+ \text{Terms in } \partial^2 f/\partial p_i \partial r_j. \end{aligned} \tag{5.75}$$

The term $-(\boldsymbol{p}/M)\cdot(\partial f/\partial \boldsymbol{r})$, which is of order 0 in ϵ_1 and ϵ_2, describes the free flight of the atom. The next term $-(\partial f/\partial \boldsymbol{p})\cdot\boldsymbol{\mathcal{F}}(\boldsymbol{r})$, which is of order 1 in ϵ_1, describes the drift in momentum of the Wigner function due to the mean radiative force $\boldsymbol{\mathcal{F}}$, studied in section 3 for an atom at rest in $\boldsymbol{r}$. The remaining terms are all of order 2 in ϵ_1 and ϵ_2, the last one (in $\partial^2 f/\partial p_i \partial r_j$) being negligible in most cases.

The terms in $\partial^2 f/\partial p_i \partial p_j$ describe momentum diffusion. D^{ij}_{las} and D^{ij}_{vac} are diffusion tensors given by equations similar to eqs. (5.41) and (5.42), each of the two $\delta\boldsymbol{F}$ operators being replaced by its i or j component. This shows that the two diffusion coefficients D_{las} and D_{vac} introduced in subsection 5.2.2 are just the traces of the diffusion tensors appearing in eq. (5.75).

The term in $\partial(p_j f)/\partial p_i$, with

$$\gamma_{ij}(\boldsymbol{r}) = \frac{\mathrm{i}\hbar}{M}\int_0^\infty \tau\,\mathrm{d}\tau\ \langle[F_{Li}(\boldsymbol{r},\tau), F_{Lj}(\boldsymbol{r},0)]\rangle_{\text{st}}\,. \tag{5.76}$$

where $\boldsymbol{F}_L = -\boldsymbol{\nabla}V_{\text{AL}}$ is the force operator associated with V_{AL} (first term of eq. (2.16)), and where the average value is taken in the steady state of

an atom at rest in $\boldsymbol{r}$, describes the friction. Combining this term with the term in $\partial f/\partial \boldsymbol{p}$ indeed gives

$$\sum_i \frac{\partial}{\partial p_i} \left[\mathcal{F}_i(\boldsymbol{r}) - \sum_j \gamma_{ij} p_j \right] f(\boldsymbol{r}, \boldsymbol{p}), \tag{5.77}$$

so that $-\sum_j \gamma_{ij} p_j$ appears as a friction force, linear in p, correcting the force $\mathcal{F}_i$ obtained in chapter 3 for an atom at rest in $\boldsymbol{r}$. In order to interpret expression (5.76) of the friction tensor γ_{ij}, we first recall a well known result of linear response theory [29]. If a physical system $\mathcal{S}$ is in a stationary state σ_{eq}, and if it is perturbed by $V(t) = -\lambda(t)M$, where $\lambda(t)$ is a classical function of t and M an observable of $\mathcal{S}$, then, the mean value, at time t, of another observable N of $\mathcal{S}$ is given, to order 1 in λ, by

$$\langle N(t) \rangle = \langle N \rangle_{\text{eq}} + \int_{-\infty}^{+\infty} \mathrm{d}t' \, \chi_{NM}(t - t') \lambda(t'), \tag{5.78}$$

where $\chi_{NM}(\tau)$ is a linear response function equal to

$$\chi_{NM}(\tau) = \frac{\mathrm{i}}{\hbar} \theta(\tau) \, \langle [N(\tau), M(0)] \rangle_{\text{eq}} . \tag{5.79}$$

In eq. (5.79), $\theta(\tau)$ is the Heaviside function (equal to 1 for $\tau > 0$ and to 0 for $\tau < 0$) and $N(\tau)$ and $M(0)$ are free Heisenberg operators (evaluated in the absence of V). The fact that the mean value of a commutator appears in expression (5.76) of the friction tensor then suggests to interpret γ_{ij} as a linear response function. More precisely, the interaction Hamiltonian between the laser and a moving atom can be written

$$-\boldsymbol{d} \cdot \boldsymbol{E}_{\text{L}} \left(\boldsymbol{r} + \frac{\boldsymbol{p}}{M}(t - t_0) \right) \simeq -\boldsymbol{d} \cdot \boldsymbol{E}_{\text{L}}(\boldsymbol{r}) + \sum_{j=x,y,z} -\frac{p_j}{M}(t - t_0) \boldsymbol{\nabla}_j \boldsymbol{d} \cdot \boldsymbol{E}_{\text{L}}(\boldsymbol{r}). \tag{5.80}$$

The last term, where we recognize $F_{Lj} = \boldsymbol{\nabla}_j (\boldsymbol{d} \cdot \boldsymbol{E}_L)$, can be considered as a perturbation due to atomic motion and can be written as

$$-\sum_{j=x,y,z} \frac{p_j}{M}(t - t_\circ) F_{Lj}(\boldsymbol{r}), \tag{5.81}$$

i.e., as a sum of terms analogous to $V(t)$, with $\lambda(t) = -(t_0 - t)p_j/M$ and $M = F_{Lj}$. It follows then from eq. (5.78) that the mean value of $N = F_{Li}(\boldsymbol{r})$

at time t_0 is, to order 1 in p, equal to

$$\langle F_{Li}(\boldsymbol{r},\boldsymbol{p},t_0)\rangle = \langle F_{Li}(\boldsymbol{r},\boldsymbol{p}=\boldsymbol{0},t_0)\rangle + \sum_j \int_{-\infty}^{+\infty} \mathrm{d}t' \left[\chi_{F_{Li}F_{Lj}}(t_0-t')\right]\left[-(t_0-t')\frac{p_j}{M}\right], \tag{5.82}$$

where we have put $t = t_0$. Using eq. (5.79), one can then show that the last term of eq. (5.82) can be written $-\sum_j \gamma_{ij} p_j$ and coincides with the friction force found in eq. (5.77). The friction force thus appears as the linear response of the force to the perturbation due to atomic motion.

To summarize the results of this section, we see that there is a close analogy between atomic motion in laser light and Brownian motion in a potential well. Starting from the generalized optical Bloch equations, it is possible to derive for the atomic Wigner function a kinetic equation quite analogous to the Kramers–Fokker–Planck equation (5.30) and to get simple physical interpretations for the diffusion and friction tensors in terms of correlation functions and linear susceptibilities. Finally, the equilibrium temperature can be written, according to eq. (5.64) and to the results of this subsection, as

$$k_{\mathrm{B}}T \sim \frac{D}{M\gamma} \sim \frac{\int_0^\infty \mathrm{d}\tau\ \langle \delta F(\tau)\delta F(0) + \delta F(0)\delta F(\tau)\rangle}{(\mathrm{i}/\hbar)\int_0^\infty \tau\,\mathrm{d}\tau\ \langle \delta F(\tau)\delta F(0) - \delta F(0)\delta F(\tau)\rangle}. \tag{5.83}$$

If the mean values of the anticommutator and commutator appearing, respectively, in the numerator and denominator of eq. (5.83) are of the same order, we predict that

$$k_{\mathrm{B}}T \sim \frac{\hbar}{\langle\tau\rangle}, \tag{5.84}$$

where $\langle\tau\rangle$ is on the order of the correlation time of the Langevin force operator $\delta\boldsymbol{F}$. We have seen in subsection 5.2.2 that the correlation function of $\delta\boldsymbol{F}$ is proportional to the correlation function of the atomic dipole moment d_z, so that $\langle\tau\rangle$ is on the order of an internal atomic time T_{int}. It follows that

$$k_{\mathrm{B}}T \sim \frac{\hbar}{T_{\mathrm{int}}}. \tag{5.85}$$

For a two-level atom, $T_{\mathrm{int}} \sim \Gamma^{-1}$, and we find again in eq. (5.85) the Doppler limit (5.67). Equation (5.85) suggests that much lower temperatures can be reached if internal times much longer than Γ^{-1} exist. Examples of such situations will be given in the second part of this course.

6. Basic physical processes in the perturbative limit

6.1. Introduction

At low saturation ($s \ll 1$), i.e., at low intensity or large detuning, photon–atom interactions can be analyzed perturbatively in terms of elementary absorption and emission processes. For an atom in a plane wave, such an analysis, combined with the basic conservation laws, provides a simple interpretation of the main features of radiative forces: mean value, velocity dependence, fluctuations (see sections 3.3, 4.1 and subsection 5.2.3).

The situation becomes more complicated when the laser wave is a superposition of several plane waves. Because of the phase relations which exist between these waves, their contributions cannot be added independently. There are interference effects which make, for example, atomic motion in a laser standing wave more difficult to analyze than in a plane running wave. An example of such difficulties is given by the very intriguing behavior of an atom put in a node of a standing wave. In such a place, there is no light and no photon absorption, so that one would expect the atomic momentum diffusion coefficient D to vanish. However, such a naïve prediction is not confirmed by the calculation of D, which predicts that D is as large at the nodes as at the antinodes! (See subsection 5.2.3.)

The motivation of this chapter is to try to get new physical insights in these problems in terms of quantum interferences between different scattering amplitudes. Instead of treating the laser field classically, as in the previous sections, we consider here single photon states, which are linear combinations of states with different momenta, and we study how such states are scattered by well localized atomic wave packets. Although such an approach is limited to the low saturation limit, it presents some advantages in comparison with the usual approaches, where one "traces" over the field variables to get reduced equations of motion for the atom. Here, we keep the state vector of the *whole* system A+F (atom + field), so that it is much easier to see if the atom–field correlations play an important role. One can also follow the evolution of the incident photon and see if it disappears (absorption process replacing the incident photon by a fluorescence photon appearing in an initially empty mode), or if it is transferred from one initially excited mode to another initially excited mode (redistribution process).

The idea of interfering scattering amplitudes is first introduced in the simplest possible case of an atom in a laser plane wave (section 6.2). Studying the evolution of the initial state allows us to show that the photon absorption results from an interference between the incident field and the

field scattered by the atom in the forward direction. We then consider (section 6.3) an atomic wave packet localized in a node of a standing wave, the corresponding one-photon state being a linear superposition of two states with opposite momenta $+\hbar\boldsymbol{k}_{\mathrm{L}}$ and $-\hbar\boldsymbol{k}_{\mathrm{L}}$. We show that the atomic momentum diffusion which persists in the nodes is due to more subtle interference effects involving forward and backward scattering amplitudes and leading to a photon redistribution between the modes $+\boldsymbol{k}_{\mathrm{L}}$ and $-\boldsymbol{k}_{\mathrm{L}}$, which is correlated with the atomic momentum. Another important feature of such a "correlated redistribution" is that it is dissipative, varying with the laser detuning as a Lorentz absorption curve. Using the same formalism of interfering scattering amplitudes, we show in section 6.4 that the usual redistribution responsible for the dipole forces appearing out of a node in a standing wave is quite different from the one discussed in section 6.3, insofar as it is reactive and not correlated with atomic momentum. Finally, we consider in section 6.5 the case of an atom moving in a standing wave and we determine when it is possible to neglect the interferences between forward and backward scattering amplitudes, a situation which then allows the radiation pressures of the two waves to be added independently.

6.2. Simple case of an atom in a laser plane wave

At time $t = 0$, the global system A+F (atom + field) is in the state

$$|\Psi(0)\rangle = |\psi_{\mathrm{A}}\rangle \otimes |\psi_{\mathrm{F}}\rangle = |g, \boldsymbol{p}\,; \boldsymbol{k}_{\mathrm{L}}\epsilon_{\mathrm{L}}\rangle, \tag{6.1}$$

where $|\psi_{\mathrm{A}}\rangle = |g, \boldsymbol{p}\rangle$ is the atomic state describing A in g with a momentum $\boldsymbol{p}$, and $|\psi_{\mathrm{F}}\rangle = |\boldsymbol{k}_{\mathrm{L}}\epsilon_L\rangle$ is the field state describing a single photon with momentum $\hbar\boldsymbol{k}_{\mathrm{L}}$ and polarization ϵ_{L}. The time evolution of A+F is governed by the Hamiltonian

$$H = H_{\mathrm{A}} + H_{\mathrm{F}} + V_{\mathrm{AF}} \tag{6.2}$$

where H_{A} and H_{F} are the atomic and field Hamiltonians given in eqs. (2.2) and (2.3). We treat here the incident field quantum mechanically, so that the two interaction terms V_{AL} and V_{AV} of eq. (2.1) are replaced by a single atom-field interaction term $V_{\mathrm{AF}} = -\boldsymbol{d} \cdot \boldsymbol{E}(\boldsymbol{R})$, where $\boldsymbol{E}(\boldsymbol{R})$ is the total (incident + vacuum) field operator given by an expression analogous to (2.6)

$$V_{\mathrm{AF}} = -\mathrm{i}\boldsymbol{d} \cdot \sum_{\boldsymbol{k}\epsilon} \sqrt{\frac{\hbar\omega}{2\epsilon_0 L^3}}\, \epsilon\, a_{\boldsymbol{k}\epsilon}\, \mathrm{e}^{\mathrm{i}\boldsymbol{k}\cdot\boldsymbol{R}} + \mathrm{h.c.} \tag{6.3}$$

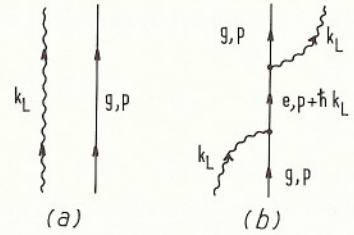

Fig. 9. Diagrammatic representation of the processes contributing to the amplitude (6.5).

After a time T, the state vector of A+F becomes, in the interaction representation with respect to $H_A + H_F$,

$$|\Psi(T)\rangle = c(T)|g, \boldsymbol{p}\,; \boldsymbol{k}_L \epsilon_L\rangle + |\Psi_\perp(T)\rangle, \tag{6.4}$$

where $|\Psi_\perp(t)\rangle$ describes the projection of $|\Psi(t)\rangle$ on states orthogonal to the initial state (6.1). Such a projection involves states containing fluorescence photons $\boldsymbol{k}_F \epsilon_F$ with $\boldsymbol{k}_F \neq \boldsymbol{k}_L$ or $\epsilon_F \neq \epsilon_L$, or atomic excited states. We are interested here in the amplitude

$$c\,(T) = \langle g, \boldsymbol{p}\,; \boldsymbol{k}_L \epsilon_L \mid U(T) \mid g, \boldsymbol{p}\,; \boldsymbol{k}_L \epsilon_L\rangle, \tag{6.5}$$

where $U(T)$ is the evolution operator, and which describes how the initial state (6.1) disappears.

Since V_{AF} describes only single photon absorption or emission processes, there are only two amplitudes contributing to eq. (6.5) to order 2 in V_{AF}, which are represented by the two diagrams a and b of fig. 9. They represent, respectively, processes where nothing happens (diagram a of order 0 in V_{AF}), and where the incident photon is absorbed and re-emitted (diagram b of order 2).

Using the well known results of scattering theory (see for example ref. [2], Complement A_I), we get for the zeroth and second order terms in the expansion of $c(T)$ in powers of V_{AF}

$$c^{(0)}(T) = 1, \tag{6.6}$$

$$c^{(2)}(T) = -2\pi \mathrm{i}\ \delta^{(T)}(E_{fin} - E_{in}) \frac{|\ \langle e, \boldsymbol{p} + \hbar \boldsymbol{k}_L\,; 0 \mid V_{AF} \mid g, \boldsymbol{p}\,; \boldsymbol{k}_L \epsilon_L\rangle\ |^2}{E_{g,\boldsymbol{p}\,;\boldsymbol{k}_L} - [E_{e,\boldsymbol{p}+\hbar\boldsymbol{k}_L\,;0} - \mathrm{i}\hbar(\Gamma/2)]}, \tag{6.7}$$

In eq. (6.7), $\delta^{(T)}(E_{fin} - E_{in})$ is a delta function expressing the conservation of energy. Such a function is actually a diffraction function with a width

$\delta E \sim \hbar/T$ associated with the finite duration T of the interaction

$$\delta^{(T)}(E) = \frac{1}{2\pi\hbar}\int_0^T \mathrm{d}\tau\ \mathrm{e}^{-\mathrm{i}E\tau/\hbar} = \mathrm{e}^{-\mathrm{i}E\tau/2\hbar}\ \frac{\sin ET/2\hbar}{\pi E}. \tag{6.8}$$

E_{fin} and E_{in} are the unperturbed energies of the initial and final states appearing in the amplitude (6.5). Since they coincide here, we have $E_{\mathrm{fin}} - E_{\mathrm{in}} = 0$, and we get for the limit $E \longrightarrow 0$ of eq. (6.8)

$$\delta^{(T)}(0) = \frac{T}{2\pi\hbar}. \tag{6.9}$$

The numerator of eq. (6.7) is the square of the matrix element of V_{AF} between the initial and intermediate states of diagram b of fig. 9 and is equal, using eq. (6.3), to

$$|\ \langle e, \boldsymbol{p} + \hbar\boldsymbol{k}_{\mathrm{L}}\,; 0\ |\ V_{\mathrm{AF}}\ |\ g, \boldsymbol{p}\,; \boldsymbol{k}_{\mathrm{L}}\boldsymbol{\epsilon}_{\mathrm{L}}\rangle\ |^2 = d^2\,\mathcal{E}^2_{\omega_{\mathrm{L}}} = d^2\,\frac{\hbar\omega_{\mathrm{L}}}{2\epsilon_0 L^3}, \tag{6.10}$$

where d is the matrix element of $\boldsymbol{\epsilon}_{\mathrm{L}} \cdot \boldsymbol{d}$ between e and g. In eq. (6.10), $\mathcal{E}^2_{\omega_{\mathrm{L}}}$ can be considered as the square of the electric field corresponding to a single photon $\boldsymbol{k}_{\mathrm{L}}\boldsymbol{\epsilon}_{\mathrm{L}}$. The denominator $\mathcal{D}$ of eq. (6.7) is the difference between the unperturbed energies of the initial and intermediate states of diagram b of fig. 9.

$$\begin{aligned}\mathcal{D} &= E_g + \hbar\omega_{\mathrm{L}} + \frac{\boldsymbol{p}^2}{2M} - \left(E_e - \mathrm{i}\hbar\frac{\Gamma}{2}\right) - \frac{(\boldsymbol{p} + \hbar\boldsymbol{k}_{\mathrm{L}})^2}{2M} \\ &= \hbar\left(\delta + \mathrm{i}\frac{\Gamma}{2}\right) - \frac{\hbar\boldsymbol{k}_{\mathrm{L}}.\boldsymbol{p}}{M} - \frac{\hbar^2 k_{\mathrm{L}}^2}{2M}.\end{aligned} \tag{6.11}$$

We have added -i$\hbar\Gamma/2$ to the unperturbed energy of the excited atomic state e, Γ being the natural width of e. Such a procedure is well known in resonance scattering theory and amounts to renormalizing the propagator of the excited state by taking into account its coupling with the vacuum field to all orders (see for example Complement B_{III} of ref. [2] and figs. 15 and 16 of this complement – we suppose here that the Lamb-shifts of e and g have been reincluced in E_e and E_g). The last two terms of the second line of eq. (6.11) represent the Doppler and recoil shifts. We assume here that these shifts are small compared to the natural width of e

$$\left|\frac{\boldsymbol{k}_{\mathrm{L}} \cdot \boldsymbol{p}}{M}\right|, \quad \frac{\hbar k_{\mathrm{L}}^2}{2M} \ll \Gamma, \tag{6.12}$$

so that

$$\mathcal{D} \simeq \hbar(\delta + \mathrm{i}\frac{\Gamma}{2}). \tag{6.13}$$

Using eqs. (6.9), (6.10) and (6.13) for rewriting eq. (6.7), we get for the amplitude (6.5), up to order 2 in V_{AF}

$$c(T) = 1 - \mathrm{i}\,T\,\frac{d^2\mathcal{E}_\omega^2/\hbar^2}{\delta + \mathrm{i}(\Gamma/2)} = 1 - \frac{\Gamma'}{2}T - \mathrm{i}\,\delta'\,T, \tag{6.14}$$

where

$$\Gamma' = \Gamma\,\frac{d^2\mathcal{E}_{\omega_\mathrm{L}}^2/\hbar^2}{\delta^2 + (\Gamma^2/4)} = \Gamma\frac{\Omega_1^2/4}{\delta^2 + (\Gamma^2/4)} = \Gamma\frac{s_0}{2}, \tag{6.15a}$$

$$\delta' = \delta\,\frac{d^2\mathcal{E}_{\omega_\mathrm{L}}^2/\hbar^2}{\delta^2 + \frac{\Gamma^2}{4}} = \delta\frac{\Omega_1^2/4}{\delta^2 + \frac{\Gamma^2}{4}} = \delta\frac{s_0}{2}. \tag{6.15b}$$

We have introduced the Rabi frequency $\Omega_1 = -2d\mathcal{E}_{\omega_\mathrm{L}}/\hbar$ associated with the single photon state $|\boldsymbol{k}_\mathrm{L}\boldsymbol{\epsilon}_\mathrm{L}\rangle$ and the corresponding saturation parameter s_0 given by eq. (3.6).

We now discuss the physical content of eq. (6.14). If T is not too long, (6.14) can be rewritten as *

$$c(T) \simeq \mathrm{e}^{-\left([\Gamma'/2] + \mathrm{i}\delta'\right)t}. \tag{6.16}$$

Taking the square of the modulus of eq. (6.16) then gives

$$|c(T)|^2 \simeq \mathrm{e}^{-\Gamma' t}, \tag{6.17}$$

which shows that Γ' can be considered as the rate at which the initial state disappears, or the absorption rate or, more precisely, the total scattering rate of the incident photon. It clearly appears from eq. (6.14) that Γ' is associated with an interference between the incident field and the imaginary part of the forward scattering amplitude. The dependence of Γ' on the detuning δ, which is the one of a Lorentz absorption curve, corresponds to what is expected for a dissipative process. In eq. (6.16), $\hbar\delta'$ appears as

* This result can actually be obtained rigorously by a resummation of the perturbation series. See for example ref. [2], chapter III.

an energy shift of the initial state, due to the atom–field coupling. Actually, such a shift is nothing but the light shift of the atomic ground state produced by the incident photon [50, 51]. According to eq. (6.14), δ' is associated with an interference between the incident field and the real part of the forward scattering amplitude. Its dependence on δ (Lorentz dispersion curve) corresponds to what is expected for a reactive process.

6.3. Atom in a node of a standing wave

6.3.1. Initial state of the atom + field system

We consider now a field mode, linearly polarized along Oz, with a spatial dependence given by $\sin k_L x$. The laser standing wave, written in eq. (5.53), which has a node in $x = 0$, corresponds to a quasi-classical excitation of such a field mode. We suppose here that this mode contains initially a single elementary excitation and we look first for the mathematical expression of this one-photon state in terms of states describing photons with well defined momenta. In order to keep the notation as simple as possible, we denote by $\pm k$ the running wave modes with wave vectors $\pm k\boldsymbol{\epsilon}_x$ and polarization $\boldsymbol{\epsilon}_z$.

Let $a_{\pm k}$ and $a^+_{\pm k}$ be the annihilation and creation operators for a photon in the modes $\pm k$. From these operators, we introduce the operators

$$b_k = \frac{1}{\sqrt{2}}(a_k - a_{-k}), \tag{6.18a}$$

$$c_k = \frac{1}{\sqrt{2}}(a_k + a_{-k}), \tag{6.18b}$$

and their adjoints. It is then easy to check that b_k and b_k^+ are annihilation and creation operators, since they satisfy

$$b_k|0\rangle = 0, \tag{6.19a}$$

$$[b_k, b_{k'}^+] = \delta_{kk'}. \tag{6.19b}$$

Similar relations hold for c_k and c_k^+, which in addition commute with b_k and b_k^+. If, in the expansion (2.6) of the electric field operator in running wave modes, we regroup the terms proportional to $a_{\pm k}$ and $a^+_{\pm k}$, we easily find that b_k and b_k^+ are multiplied by $\sin kx$, whereas c_k and c_k^+ are multiplied by $\cos kx$. This shows that b_k and b_k^+ (respectively c_k and c_k^+) are annihilation and creation operators for an elementary excitation of the standing wave mode $\sin kx$ (respectively $\cos kx$). The quantum state which

describes a single elementary excitation of the standing wave $\sin k_L x$ can thus be written

$$|\psi_F\rangle = b^+_{k_L}|0\rangle = \frac{1}{\sqrt{2}}\left[a^+_{k_L} - a^+_{-k_L}\right]|0\rangle = \frac{1}{\sqrt{2}}\left[|+k_L\rangle - |-k_L\rangle\right] \tag{6.20}$$

It is clearly a linear superposition (and not a statistical mixture!) of single photon states $|\pm k_L\rangle$ with well defined momenta $\pm\hbar k_L$. Note finally that the saturation parameter $s(x)$ associated with the single photon state (6.20) is

$$s(x) = 2s_0 \sin^2 k_L x = s_{max} \sin^2 k_L x, \tag{6.21}$$

where $s_0 = s_{max}/2$ is the saturation parameter used in eq. (6.15) and corresponding to a single photon in a running plane wave mode. Equations (6.21) and (5.56) differ by a factor 2 because the mean number of photons in each of the two counterpropagating plane wave modes appearing in eq. (6.21) is 1/2 and not 1.

For the initial atomic state $|\psi_A\rangle$, we take an atom in the ground state g, with its center of mass described by a wave packet very well localized near the node $x = 0$ of the standing wave $\sin k_L x$.

$$|\psi_A\rangle = \sum_p c_p |g, p\rangle. \tag{6.22}$$

As in the field state (6.20), we have used a simpler notation, p instead of $p\epsilon_x$, for the atomic momentum states along Ox. In eq. (6.22), c_p is a real, even function of p, centered about $p = 0$, so that, in position space, the wave packet is centered about $x = 0$, with zero global velocity. The width of the curve giving c_p versus p is denoted by Δp and is on the order of $\hbar/\Delta x$, where Δx is the width of the wave packet in position space. The localization assumption is equivalent to

$$\Delta x \ll \lambda_L \qquad \Longleftrightarrow \qquad \Delta p \gg \hbar k_L. \tag{6.23}$$

6.3.2. Amplitude to remain in one of the initially populated states

At $t = 0$, the global A+F system is in the initial state

$$\begin{aligned} |\Psi_{in}\rangle &= |\psi_A\rangle \otimes |\psi_F\rangle \\ &= \frac{1}{\sqrt{2}} \sum_p c_p \left[\, |g, p\,; +k_L\rangle - |g, p\,; -k_L\rangle \,\right], \end{aligned} \tag{6.24}$$

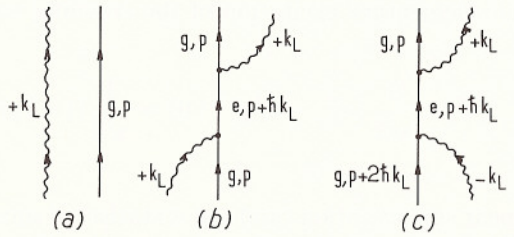

Fig. 10. Diagrammatic representation of the processes contributing to $\mathcal{A}_p^+$, up to order 2 in V_{AF}.

where only the field modes $+k_{\mathrm{L}}$ and $-k_{\mathrm{L}}$ are populated. After a time interval T, the system has evolved, the excitation of the modes $+k_{\mathrm{L}}$ and $-k_{\mathrm{L}}$ has changed, and modes, which were initially empty, have now a certain amplitude to be excited, which describes the appearance of fluorescence photons. In this subsection, we are interested in the evolution of the initially populated modes. More precisely, we want to calculate the amplitudes

$$\mathcal{A}_p^{\pm} = \langle g, p\,; \pm k_{\mathrm{L}} \mid U(T) \mid \Psi_{\mathrm{in}} \rangle \tag{6.25}$$

to find, at time $t = T$, the global system A+F in one of the states $|g, p; k_{\mathrm{L}}\rangle$ or $|g, p; -k_{\mathrm{L}}\rangle$.

Consider first the amplitude $\mathcal{A}_p^+$. Using the same diagrammatic representation as in section 6.2, one finds that, to order 2 in V_{AF}, $\mathcal{A}_p^+$ is a sum of three terms corresponding, respectively, to the three diagrams a, b, c of fig. 10.

Diagram a is of zeroth order, whereas diagrams b and c are of second order and describe respectively forward and backward scattering processes. Because of the conservation of the total linear momentum, which explicitly appears at each vertex in fig. 10, one easily checks that there are no other possible contributions to $\mathcal{A}_p^+$. Diagrams a and b are multiplied by the amplitude $\langle g, p; k_{\mathrm{L}} | \psi_{\mathrm{in}} \rangle = c_p/\sqrt{2}$ for the total system to be initially in the state $|g, p; k_{\mathrm{L}}\rangle$, whereas diagram c is multiplied by $\langle g, p + 2\hbar k_{\mathrm{L}}; -k_{\mathrm{L}} | \psi_{\mathrm{in}} \rangle = -c_{p+2\hbar k_{\mathrm{L}}}/\sqrt{2}$, which is the amplitude for A+F to be initially in $|g, p + 2\hbar k_{\mathrm{L}}; -k_{\mathrm{L}}\rangle$. The three diagrams of fig. 10, which end in the same final state, start from different initial states $|g, p; k_{\mathrm{L}}\rangle$ and $|g, p + 2\hbar k_{\mathrm{L}}; -k_{\mathrm{L}}\rangle$. They can interfere only because the initial state $|\psi_{\mathrm{in}}\rangle$, given in eq. (6.24), is a linear superposition of $|g, p; k_{\mathrm{L}}\rangle$ and $|g, p + 2\hbar k_{\mathrm{L}}; -k_{\mathrm{L}}\rangle$.

For diagrams a and b the initial and final states are the same, so that $E_{\mathrm{fin}} - E_{\mathrm{in}} = 0$ and we can use eq. (6.9). For diagram c, we have

$$E_{\mathrm{fin}} - E_{\mathrm{in}} = \frac{p^2}{2M} - \frac{(p + 2\hbar k_{\mathrm{L}})^2}{2M}$$

$$= -\frac{2\hbar k_{\mathrm{L}} p}{M} - \frac{2\hbar^2 k_{\mathrm{L}}^2}{M} \simeq -\frac{2\hbar k_{\mathrm{L}} \Delta p}{M}, \tag{6.26}$$

since $p \sim \Delta p \gg \hbar k_{\mathrm{L}}$ according to eq. (6.23). The $\delta^{(T)}(E_{\mathrm{fin}} - E_{\mathrm{in}})$ function multiplying the contribution of diagram c has a width $\hbar/T$. If

$$E_{\mathrm{fin}} - E_{\mathrm{in}} \simeq \frac{\hbar k_{\mathrm{L}} \Delta p}{M} \ll \frac{\hbar}{T} \tag{6.27}$$

one can thus replace $E_{\mathrm{fin}} - E_{\mathrm{in}}$ by 0 in the $\delta^{(T)}$ function and get the same result, $T/2\pi\hbar$, as in the case of diagram b. The physical meaning of eq. (6.27) is quite clear. Such a condition can be also written

$$\frac{\Delta p}{M} T \ll \frac{1}{k_{\mathrm{L}}} \sim \lambda\!\!\!^{-}_{\mathrm{L}}, \tag{6.28}$$

and means that T must not be too long, so that the spatial spreading of the wave packet during T, $\Delta p T/M$, remains small compared to the laser wavelength λ_{L}. Otherwise, it would no longer be possible to consider that the atom remains well localized in the node $x = 0$.

The calculation of the amplitudes associated with the three diagrams of fig. 10 is quite similar to the one presented in subsection 6.2. The matrix elements of V_{AF} are similar, as well as the energy denominators. We are interested in this section in the momentum diffusion coefficient, which, according to the results of subsection 5.2.3, is proportional to Γ'. So, in order to simplify the equations, we will suppose

$$\delta = 0 \qquad \longrightarrow \qquad \delta' = 0. \tag{6.29}$$

This leads for $\mathcal{A}_p^+$ to the following result

$$\begin{aligned} \mathcal{A}_p^+ &= \frac{1}{\sqrt{2}} c_p - \frac{1}{\sqrt{2}} c_p \frac{\Gamma' T}{2} + \frac{1}{\sqrt{2}} c_{p+2\hbar k_{\mathrm{L}}} \frac{\Gamma' T}{2} \\ &= \frac{1}{\sqrt{2}} \left[c_p - \frac{\Gamma' T}{2} (c_p - c_{p+2\hbar k_{\mathrm{L}}}) \right], \end{aligned} \tag{6.30}$$

where the first, second and third terms of the first line are, respectively, associated with diagrams a, b, c of fig. 10

In the limit $\Delta p \to \infty$, $c_p - c_{p+2\hbar k_{\mathrm{L}}} \to 0$ and $\mathcal{A}_p^+$ no longer depends on T. Such a result means that, for an atom perfectly localized in a node ($\Delta x \sim \hbar/\Delta p \to 0$), the interference between the contributions of diagrams b and c is perfectly destructive, which suppresses completely photon absorption.

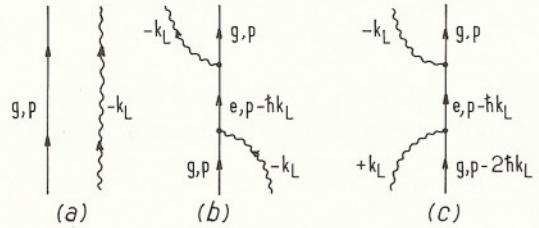

Fig. 11. Diagrammatic representation of the processes contributing to $\mathcal{A}_p^-$, up to order 2 in V_{AF}.

Actually, Δp cannot be taken infinite, since $|\psi_{\mathrm{A}}\rangle$ would have then an infinite norm (see also condition (6.27)). Expanding $c_p - c_{p+2\hbar k_{\mathrm{L}}}$ in powers of

$$\varepsilon = \frac{\hbar k_{\mathrm{L}}}{\Delta p} \sim \frac{\Delta x}{\lambda_{\mathrm{L}}} \tag{6.31}$$

allows one to transform eq. (6.30) into

$$\mathcal{A}_p^+ = \frac{1}{\sqrt{2}}\, c_p \left[1 + \Gamma' T \left(\hbar k_{\mathrm{L}} \frac{c_p'}{c_p} + \hbar^2 k_{\mathrm{L}}^2 \frac{c_p''}{c_p} + \cdots\right)\right]. \tag{6.32}$$

The amplitude $\mathcal{A}_p^-$ for remaining in the state $|g, p; -k_{\mathrm{L}}\rangle$ can be analyzed along the same lines. Figure 11 gives the interfering scattering amplitudes analogous to those of fig. 10.

Similarly, the equation corresponding to eqs. (6.30) and (6.32) is

$$\begin{aligned}\mathcal{A}_p^- &= -\frac{1}{\sqrt{2}}\, c_p + \frac{1}{\sqrt{2}}\, c_p \frac{\Gamma' T}{2} - \frac{1}{\sqrt{2}}\, c_{p-2\hbar k_{\mathrm{L}}} \frac{\Gamma' T}{2} \\ &= -\frac{1}{\sqrt{2}}\, c_p \left[1 - \Gamma' T \left(\hbar k_{\mathrm{L}} \frac{c_p'}{c_p} - \hbar^2 k_{\mathrm{L}}^2 \frac{c_p''}{c_p} + \cdots\right)\right].\end{aligned} \tag{6.33}$$

Combining eqs. (6.32) and (6.33), we finally get for the state vector of A+F at time T, to order 2 in V_{AF} and ε

$$\begin{aligned}|\Psi(T)\rangle = \sum_p c_p |g, p\rangle \\ \otimes \left\{ + \frac{1}{\sqrt{2}} \left(1 + \Gamma' T\, \hbar k_{\mathrm{L}} \frac{c_p'}{c_p} + \Gamma' T\, \hbar^2 k_{\mathrm{L}}^2 \frac{c_p''}{c_p}\right) |k_{\mathrm{L}}\rangle \right. \\ \left. - \frac{1}{\sqrt{2}} \left(1 - \Gamma' T\, \hbar k_{\mathrm{L}} \frac{c_p'}{c_p} + \Gamma' T\, \hbar^2 k_{\mathrm{L}}^2 \frac{c_p''}{c_p}\right) |-k_{\mathrm{L}}\rangle \right\} \\ + \text{ states involving modes other than } \pm k_{\mathrm{L}}\end{aligned} \tag{6.34}$$

The three first lines of eq. (6.34) give the projection of $|\psi(T)\rangle$ onto the subspace $\mathcal{E}_0$ subtended by the initially populated states $\{|g, p; \pm k_L\rangle\}$.

6.3.3. Physical discussion

It clearly appears in eq. (6.34), that after a time T each atomic state $|g, p\rangle$ becomes correlated with a photon state $|\psi_F(p, T)\rangle$ which depends on p and T and which is given by the expression inside the brackets of eq. (6.34). Since $|\psi_F(p, T)\rangle$ depends on p through c'_p/c_p and c''_p/c_p, the projection of $|\psi(T)\rangle$ onto $\mathcal{E}_0$ (given by the three first lines of eq. (6.34)) cannot be written as a product of an atomic state and a photon state. Quantum correlations have appeared between the atom and the field as a result of their interaction.

The square of the norm of $|\psi_F(p, T)\rangle$ is, to order 2 in V_{AF} and ε, given by

$$\langle\psi_F(p, T) \mid \psi_F(p, T)\rangle = 1 + 2\,\Gamma' T\,\hbar^2 k_L^2 \frac{c''_p}{c_p}. \tag{6.35}$$

In eq. (6.35), $\hbar^2 k_L^2 c''_p/c_p$ is on the order of $(\hbar k_L/\Delta p)^2 = \varepsilon^2$, so that photon absorption appears only in second order in ε. Such a result has a clear physical meaning. Because of its finite spatial width Δx, the atomic wave packet explores the neighborhood of the node over a distance Δx, where the intensity is no longer zero, but proportional to $\sin^2 k_L \Delta x \sim k_L^2 \Delta x^2 \sim \hbar^2 k_L^2/\Delta p^2 = \varepsilon^2$.

If we restrict ourselves to order 1 in ε, $|\psi_F(p, t)\rangle$ can be written

$$|\psi_F(p, T)\rangle = \frac{1}{\sqrt{2}}\left(1 + \Gamma' T\,\hbar k_L \frac{c'_p}{c_p}\right)|k_L\rangle - \frac{1}{\sqrt{2}}\left(1 - \Gamma' T\,\hbar k_L \frac{c'_p}{c_p}\right)|-k_L\rangle \tag{6.36}$$

and keeps a constant norm equal to 1 when T increases. The fact that no photon absorption occurs at order 1 in ε, does not mean however that nothing happens for the incident photon. We see from eq. (6.36) that the probability P_+ (respectively P_-) to have the photon in the mode $+k_L$ (respectively $-k_L$) changes in time from $P_\pm(0)$ to $P_\pm(T)$.

$$P_\pm(0) = \tfrac{1}{2} \;\longrightarrow\; P_\pm(T) = \tfrac{1}{2} \pm \Gamma' T\,\hbar k_L \frac{c'_p}{c_p}. \tag{6.37}$$

The probability of occupation of one of the modes $+k_L$ or $-k_L$ increases whereas the probability of occupation of the other mode decreases by the

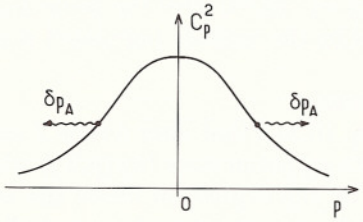

Fig. 12. Atomic momentum distribution. The arrows indicate how such a momentum distribution is modified by the correlated redistribution.

same amount. Such a phenomenon corresponds to a "redistribution" of the incident photon between the two initially populated modes $\pm k_L$ and produces a change δp_F of the mean field momentum given by

$$\delta p_F = 2\hbar k_L \left(\Gamma' T \hbar k_L \frac{c'_p}{c_p} \right) = 2\,\Gamma' T\,\hbar^2 k_L^2 \frac{c'_p}{c_p}. \tag{6.38}$$

Because of the conservation of the total momentum, there is a corresponding change δp_A of the mean atomic momentum given by

$$\delta p_A = -\delta p_F = -2\,\Gamma' T\,\hbar^2 k_L^2 \frac{c'_p}{c_p}. \tag{6.39}$$

A very important feature of the photon redistribution described by eq. (6.37) is that it depends on the atomic momentum p. We show now how such a correlated redistribution can explain the large momentum diffusion occurring in a node. Figure 12 gives the initial momentum distribution c_p^2 versus p. These variations are similar to those of c_p since c_p is assumed to be real and positive. Consider a positive value of p, where c'_p/c_p is negative. Equation (6.39) shows that, for such a value of p, the correlated redistribution produces a positive variation δp_A of p, represented by the arrow oriented to the right of fig. 12. Similarly, we find from eq. (6.39) that, for $p < 0$, there is a negative variation δp_A of p (arrow oriented to the left of fig. 12). Since δp_A is an odd function of p, we conclude from such an analysis that the atomic momentum distribution is broadened by the correlated photon redistribution, without any global shift.

The previous argument can be made more quantitative. For an atom with momentum $p_A = p$, the variation δp_A of p_A produces a variation of p_A^2 given by

$$\delta(p_A^2) = 2\,p_A \delta p_A = 2\,p\,\delta p_A = -4\,\Gamma' T\,\hbar^2 k_L^2\, p \frac{c'_p}{c_p}. \tag{6.40}$$

To average eq. (6.40) over $p_{\mathrm{A}} = p$, we multiply eq. (6.40) by the probability $c_p^2 \mathrm{d}p$ to have p_{A} between p and $p + \mathrm{d}p$ and we integrate over p, which gives

$$\overline{\delta p_{\mathrm{A}}^2} = \int_{-\infty}^{+\infty} \delta p_{\mathrm{A}}^2 c_p^2 \, \mathrm{d}p = -4 \, \Gamma' T \, \hbar^2 k_{\mathrm{L}}^2 \int_{-\infty}^{+\infty} p \, c_p c_p' \mathrm{d}p. \tag{6.41}$$

An integration by parts and the fact that c_p^2 is normalized finally gives

$$\overline{\delta p_{\mathrm{A}}^2} = 2DT, \tag{6.42}$$

where the momentum diffusion D is, according to eqs. (6.15) and (6.21), given by

$$D = \hbar^2 k_{\mathrm{L}}^2 \, \Gamma' = \hbar^2 k_{\mathrm{L}}^2 \, \Gamma \frac{s_0}{2} = \hbar^2 k_{\mathrm{L}}^2 \, \Gamma \frac{s_{\max}}{4}, \tag{6.43}$$

which quantitatively coincides with the value in a node of the Gordon–Ashkin result [8] given in eq. (5.58).

To conclude this section, we can summarize the results which have been established, concerning the behavior of an atom in a node of a standing wave.

(i) There is a photon redistribution which appears between the 2 modes $+k_{\mathrm{L}}$ and $-k_{\mathrm{L}}$, which is more important than photon absorption since it is of order 1 in $\varepsilon = \Delta x / \lambda_{\mathrm{L}}$ (instead of 2).

(ii) This redistribution, which is proportional to Γ' and not to δ', is related to the dissipative response of the atom and not to the reactive one.

(iii) Globally, this redistribution changes $\overline{p_{\mathrm{A}}^2}$ but not $\overline{p_{\mathrm{A}}}$. It produces a momentum diffusion, with zero mean force.

(iv) This redistribution is correlated with the atomic momentum. It is this correlation which explains why the rate of increase of $\overline{p_{\mathrm{A}}^2}$ does not vanish if $\Delta x \sim \hbar / \Delta p \longrightarrow 0$. In eq. (6.40) giving $\delta p_{\mathrm{A}}^2 = 2 p_{\mathrm{A}} \delta p_{\mathrm{A}}$, the fact that p_{A} can increase proportionally to Δp when Δp increases compensates for the decrease of δp_{A} which varies, according to eq. (6.39), as $c_p'/c_p \sim 1/\Delta p$. This compensation leads to a diffusion coefficient D which does not depend on Δp.

Note finally that the discussion in this subsection clearly shows the importance of the atom–field correlations which explicitly appear in expression (6.34) of the state vector of the total system $A+F$. This does not mean however that the usual treatments based on master equations describing only the reduced evolution of A neglect these correlations. They are taken into account in the derivation of the master equations. The fact that they

appear explicitly, and not implicitly, in eq. (6.34) explains why the physical effects responsible for the non-vanishing of D in a node can be more easily identified in the treatment presented here.

6.4. Atom at rest in any point of a standing wave

In section 3.4, we have mentioned that the dipole force which is experienced by an atom put in a spatially inhomogeneous light wave is a reactive force due to a redistribution of photons between the various plane waves making up the light wave. Since the formalism presented in this chapter seems well suited for investigating redistribution processes, it seems interesting to try to apply it to an atom put anywhere in a standing wave, and in particular out of a node. We will then be able to elucidate the differences which exist between the redistribution responsible for dipole forces and the correlated redistribution analyzed in the previous section. New insight will be also gained on the various processes which contribute to the momentum diffusion coefficient out of a node and on the origin of non-Poissonian effects in resonance fluorescence.

6.4.1. Initial atomic state

We consider now an atomic wave packet $\widetilde{\psi}(x)$, identical to the wave packet $\psi(x)$ of subsection 6.3.1, except that it is translated by an amount x_0, so that it describes an atom well localized around x_0

$$\widetilde{\psi}(x) = \psi(x - x_0). \tag{6.44}$$

Taking the Fourier transform of eq. (6.44) leads to

$$|\widetilde{\psi}_{\mathrm{A}}\rangle = \sum_p \widetilde{c}_p |g, p\rangle = \sum_p c_p \, \mathrm{e}^{-\mathrm{i}px_0/\hbar} \, |g, p\rangle, \tag{6.45}$$

which replaces eq. (6.22). The coefficients $\widetilde{c}_p$ of the expansion of $|\widetilde{\psi}\rangle$ in plane waves are no longer real.

The initial photon state (6.20) remains unchanged and describes an elementary excitation of the standing wave mode $\sin k_{\mathrm{L}} x$.

6.4.2. New expression for the state vector of A+F at time T

Since we are interested here in dipole forces, which vanish for $\delta = 0$, we no longer suppose that $\delta = 0$, so that eq. (6.29) is replaced by

$$\delta \neq 0 \qquad \longrightarrow \qquad \delta' = \delta \frac{s_0}{2} \neq 0. \tag{6.46}$$

All calculations leading to eqs. (6.30), (6.32) and (6.33) remain unchanged, provided that one makes the substitutions

$$\begin{aligned} c_p &\longrightarrow \widetilde{c}_p = c_p \, \mathrm{e}^{-\mathrm{i}px_0/\hbar}, \\ \frac{\Gamma'}{2} &\longrightarrow \frac{\Gamma'}{2} + \mathrm{i}\,\delta'. \end{aligned} \tag{6.47}$$

It follows that the expression giving the state vector of A+F at time T has the same structure as in eq. (6.34)

$$\begin{aligned} |\Psi(T)\rangle = &\sum_p \widetilde{c}_p |g,p\rangle \otimes |\psi_{\mathrm{F}}(p,T)\rangle \\ &+ \text{ states involving modes other than } \pm \mathrm{k_L}, \end{aligned} \tag{6.48}$$

where the photon state $|\psi_{\mathrm{F}}(p,T)\rangle$ is given by an expression which generalizes eq. (6.36). The substitution (6.47) changes the real part of the coefficients multiplying $|+k_{\mathrm{L}}\rangle$ and $|-k_{\mathrm{L}}\rangle$, which means that photon absorption and photon redistribution are not the same at $x=0$ and $x=x_0$. Imaginary parts also appear in these coefficients, which describe energy shifts. We will not study these imaginary parts here and we will focus on the modifications of absorption and redistribution. Keeping only the real parts of the coefficients of $|+k_{\mathrm{L}}\rangle$ and $|-k_{\mathrm{L}}\rangle$ in $|\psi_{\mathrm{F}}(p,T)\rangle$, we get, to order 2 in V_{AF} and 1 in ε

$$\begin{aligned} |\,\psi_{\mathrm{F}}(p,T)\,\rangle = & \\ &+\frac{1}{\sqrt{2}}\Bigg[1 - \Gamma' T \sin^2 k_{\mathrm{L}} x_0 + 2\hbar k_{\mathrm{L}} \delta' T \frac{c'_p}{c_p} \sin 2k_{\mathrm{L}} x_0 \\ &\qquad + \delta' T \sin 2k_{\mathrm{L}} x_0 + \hbar k_{\mathrm{L}} \delta' T \frac{c'_p}{c_p} \cos 2k_{\mathrm{L}} x_0 \Bigg] |+k_{\mathrm{L}}\rangle \\ &-\frac{1}{\sqrt{2}}\Bigg[1 - \Gamma' T \sin^2 k_{\mathrm{L}} x_0 + 2\hbar k_{\mathrm{L}} \delta' T \frac{c'_p}{c_p} \sin 2k_{\mathrm{L}} x_0 \\ &\qquad - \delta' T \sin 2k_{\mathrm{L}} x_0 - \hbar k_{\mathrm{L}} \delta' T \frac{c'_p}{c_p} \cos 2k_{\mathrm{L}} x_0 \Bigg] |-k_{\mathrm{L}}\rangle \\ &+ \text{ imaginary terms.} \end{aligned} \tag{6.49}$$

In eq. (6.49), the terms independent of c'_p/c_p lead to factorized atom–photon states in the expression (6.48) of $|\psi(T)\rangle$ since they do not depend

on p (the atomic state (6.45) can be factored out). By contrast, the terms proportional to c'_p/c_p depend on p and lead to entangled atom–photon states which contain non-separable quantum correlations.

From eq. (6.49), one deduces that the probabilities $P_+(T)$ (respectively $P_-(T)$) to have, at time $t = T$, the photon in the mode $+k_L$ (respectively $-k_L$) are given by

$$P_\pm(T) = \tfrac{1}{2} - \Gamma' T \sin^2 k_L x_0 + 2\hbar k_L \delta' T \frac{c'_p}{c_p} \sin 2k_L x_0 \pm \delta' T \sin 2k_L x_0 \pm \hbar k_L \Gamma' T \frac{c'_p}{c_p} \cos 2k_L x_0. \tag{6.50}$$

Adding $P_+(T)$ and $P_-(T)$ gives the probability of survival $P(T)$ of the incident photon in any one of the two initially populated modes $\pm k_L$

$$P(T) = 1 - 2\,\Gamma' T \sin^2 k_L x_0 + 4\,\hbar k_L \delta' T \frac{c'_p}{c_p} \sin 2k_L x_0. \tag{6.51}$$

Finally multiplying $P_+(T)$ by $+\hbar k_L$ and $P_-(T)$ by $-\hbar k_L$, and adding the two results gives the change δp_F of the mean momentum of the field after a time T, which is also equal to $-\delta p_A$ where δp_A is the change of the atomic momentum

$$\delta p_F = 2\hbar k_L \delta' T \sin 2k_L x_0 + 2\,\hbar^2 k_L^2 \Gamma' T \frac{c'_p}{c_p} \cos 2k_L x_0 = -\delta p_A. \tag{6.52}$$

6.4.3. Absorption of the incident photon

The disappearance of the incident photon is described by eq. (6.51). The last term of eq. (6.51), which describes an absorption correlated with the atomic momentum p, gives a zero contribution when multiplied by $c_p^2\,\mathrm{d}p$ and integrated over p. It is anyway of order 1 in ε and vanishes in the limit $\Delta x \sim \hbar/\Delta p \longrightarrow 0$.

So, we are left with the first term of eq. (6.51) which leads to an absorption rate $\Gamma'(x_0)$ in x_0 given by

$$\Gamma'(x_0) = 2\,\Gamma' \sin^2 k_L x_0 = \Gamma \frac{s(x_\circ)}{2}. \tag{6.53}$$

We have used $\Gamma' = \Gamma s_0/2$ (see eq. 6.15.a) and expression (6.21) of $s(x)$. The result (6.53) is in agreement with the usual absorption rate that one gets for an atom put in a place x_0 where the saturation parameter is $s(x_0)$.

6.4.4. Uncorrelated redistribution and dipole forces

The terms independent of c'_p/c_p, in eq. (6.52) come from the terms independent of c'_p/c_p which have opposite signs in $P_+(T)$ and $P_-(T)$. These terms describe a redistribution between the modes $+k_L$ and $-k_L$ which is reactive (proportional to δ') and which is not correlated with the atomic momentum p. They give rise to a mean force $\mathcal{F}$

$$\mathcal{F} = \frac{\delta p_A}{T} = -2\hbar k_L \delta' \sin 2k_L x_0, \tag{6.54}$$

which can be also written

$$\mathcal{F} = -\frac{d}{dx_0} \hbar\, \delta'(x_0), \tag{6.55}$$

where

$$\hbar\, \delta'(x_0) = 2\,\hbar\delta' \sin^2 k_L x_0 = \hbar\delta\, \frac{s(x_0)}{2} \tag{6.56}$$

is the light shift of the ground state in x_0. Such a force is nothing but the usual dipole force which derives from a potential which, at low intensity, coincides with the light-shifted energy of the ground state.

The term of eq. (6.52) which is proportional to c'_p/c_p describes a redistribution which is dissipative (proportional to Γ') and which is correlated with p. Such a redistribution is the same as the one studied in the previous section 6.3, except that δp_F is multiplied by $\cos 2k_L x_0$ which is equal to $+1$ at a node but which can take negative values elsewhere. It follows that such a correlated redistribution can produce a narrowing of the atomic momentum redistribution instead of a broadening, as in section 6.3. The corresponding "diffusion coefficient" can be written

$$D_{\text{correl. red.}} = \hbar^2 k_L^2\, \Gamma' \cos 2k_L x_0. \tag{6.57}$$

6.4.5. Total momentum diffusion coefficient

The change $\overline{\delta p_A^2}$ of p_A^2 is produced not only by the correlated redistribution, leading to eq. (6.57), but also by the absorption process.

According to expression (6.50) of $P_+(T)$, the probability of having one photon absorbed in the mode $+k_L$ during T (without redistribution in the mode $-k_L$) is equal to $\Gamma' T \sin^2 k_L x_0$. In such an absorption process, the atomic momentum changes from p to $p + \hbar k_L$ and the variation of p^2 is equal to $\hbar^2 k_L^2 + 2p\hbar k_L$. Similarly if the photon is absorbed in the mode $-k_L$,

with the same probability $\Gamma' T \sin^2 k_L x_0$ (see eq. (6.50)), the variation of p^2 is equal to $\hbar^2 k_L^2 - 2p\hbar k_L$. It follows that the mean change of p^2 due to absorption processes is given by

$$\begin{aligned}\overline{\delta p_A^2} &= \Gamma' T \sin^2 k_L x_0 [\hbar^2 k_L^2 + 2p\hbar k_L + \hbar^2 k_L^2 - 2p\hbar k_L] \\ &= 2T\hbar^2 k_L^2 \Gamma' \sin^2 k_L x_0, \end{aligned} \tag{6.58}$$

which can be written as $2D_{abs}T$ where

$$D_{abs} = \hbar^2 k_L^2 \Gamma' \sin^2 k_L x_0 \tag{6.59}$$

is the diffusion coefficient associated with absorption.

Adding eqs. (6.57) and (6.59) gives the total diffusion coefficient D_{las} associated with the laser field *

$$D_{las} = \hbar^2 k_L^2 \Gamma' \cos^2 k_L x_0 = \hbar^2 k_L^2 \Gamma \frac{s_{max}}{4} \cos^2 k_L x_0, \tag{6.60}$$

where we have used $\Gamma' = \Gamma s_0/2$. Such a result coincides with Gordon-Ashkin's result [8] given in eq. (5.58). It is easy to check that, in a standing wave, eq. (6.59) could be obtained by considering the mean number $\overline{N_+} = \overline{N_-}$ of photons absorbed in each of the counterpropagating waves forming the standing wave, and by assuming that $N_+ - N_-$ is a random variable following Poisson statistics. The result derived in this section thus shows that the correlated redistribution, which is responsible for the strange behavior of an atom put in a node of a standing wave, is also responsible for the corrections to Poisson statistics in the fluctuations of $N_+ - N_-$.

6.5. Atom moving in a standing wave

We suppose now that the atomic wave packet has a global velocity $v_0 = p_0/M$, so that, in momentum space, the momentum distribution is centered about p_0 instead of 0, as in section 6.3. We investigate in this last section a few physical effects which result from this non-zero value of p_0.

A first modification which must be introduced in the equations of the previous sections concerns the energy denominator $\mathcal{D}$ given in eq. (6.11)

* The uncorrelated redistribution analyzed in subsection 6.4.4 does not contribute to D_{las}, because the corresponding change $\overline{\delta p_A^2}$ is proportional to T^2 and not to T and because the average over p of $2p\,\delta p_A$ is zero in the absence of correlation between p and δp_A.

and which corresponds to the diagrams b of figs. 9, 10 and 11. The Doppler shift $-\hbar k_L p/M$ varies in a range $\hbar k_L \Delta p/M$ around $-\hbar k_L p_0/M$. We can still neglect $\hbar k_L \Delta p/M$ (and $\hbar^2 k_L^2/2M$) in comparison with $\hbar\Gamma$, but the mean Doppler shift $-k_L p_0/M = -k_L v_0$ is not necessarily small compared to the natural width Γ and we must keep it in eq. (6.13) which becomes

$$\mathcal{D} = \hbar\left(\delta - k_L v_0 + i\frac{\Gamma}{2}\right). \tag{6.61}$$

Similar considerations show that the energy denominator associated with the diagrams c of figs. 10 and 11 is equal to eq. (6.61) with $-k_L v_0$ replaced by $+k_L v_0$. These modifications of the energy denominators result in a v-dependence of the parameters Γ' and δ' given by equations (6.15), which physically describes how the absorption rate Γ' and the ground-state light shift $\hbar\delta'$ are modified by the Doppler effect.

The non-zero value of v_0 plays also an important role in the $\delta^{(T)}(E_{\text{fin}} - E_{\text{in}})$ functions describing the conservation of energy for the diagrams c of figs. 10 and 11 (recall that, for the diagrams b, the initial and final states are the same, so that we can use eq. (6.9)). Instead of eq. (6.26), we have now

$$\begin{aligned} E_{\text{fin}} - E_{\text{in}} &= \frac{p^2}{2M} - \frac{(p + 2\hbar k_L)^2}{2M} \\ &= -\frac{2\hbar k_L p}{M} - \frac{2\hbar^2 k_L^2}{M} \simeq -2\,\hbar k_L v_0. \end{aligned} \tag{6.62}$$

The delta functions which appear in the contributions of diagrams c are now evaluated, not at $E_{\text{fin}} - E_{\text{in}} = 0$, but at a value (6.62) of $E_{\text{fin}} - E_{\text{in}}$ which can be larger than the width $\hbar/T$ of the delta function, if v_0 is large enough. More precisely, if

$$\hbar k_L v_0 \gg \hbar/T \tag{6.63}$$

the contribution of diagrams c becomes negligible compared to the contribution of diagrams b and diagrams c can be ignored. Condition (6.63) can be also written as

$$v_0 T \gg 1/k_L = \lambda_L \tag{6.64}$$

and means that, during the interaction time T, the atom travels over several laser wavelengths λ_L. It then experiences a radiative force spatially averaged over λ_L.

The previous result indicates that the radiative force, spatially averaged over several λ_L is no longer sensitive to interference effects involving both forward and backward scattering amplitudes. Only forward scattering amplitudes can interfere with the incident field. One can understand in this way why, at low intensity, it is possible to add independently the effect of the two waves if one is interested only in the spatially averaged force. Since the two Doppler shifts are opposite for the two waves, the absorption rates will be different and one gets the usual well known physical picture for Doppler cooling as resulting from a Doppler induced imbalance between two radiation pressures.

7. Physical mechanisms in the high intensity limit

7.1. Introduction

In the previous sections, we have mentioned a few results concerning atomic motion in an intense laser standing wave, which do not seem to have an obvious physical interpretation. For example, the spatially averaged velocity dependent force has, for a given value of the detuning $\delta = \omega_L - \omega_A$ and in the low velocity limit ($k_L v_0 \ll \Gamma$), a sign which depends on the laser intensity. At low intensity ($s_0 \ll 1$), this force is a damping force for $\delta < 0$, a result which can be interpreted as a Doppler induced imbalance between the radiation pressures exerted by the two counterpropagating plane waves forming the standing wave (see section 6.5). But, when the intensity is increased, this friction force is transformed into an "antidamping" one, and such a change of sign cannot be interpreted with a diagrammatic approach, since perturbative expansions of the transition amplitudes, analogous to the ones used in the preceding chapter 6, no longer converge. Another example of an intriguing result concerns the momentum diffusion coefficient of an atom at rest in a laser standing wave, which does not saturate when the laser intensity is increased (see eq. (5.60)), contrarily to what happens for an atom in a laser plane wave. The purpose of this chapter is to present a different theoretical treatment of atomic motion in an intense laser light which provides simple physical pictures for such unexpected features.

Such a treatment is based on the "dressed-atom" approach * which has been first introduced for describing atoms interacting with strong radiofrequency fields [30, 31], and which has been then extended to the optical

* For a general review of the dressed-atom approach and its various applications, see ref. [2], chapter VI and Complements A_{VI} and B_{VI}.

domain in order to interpret resonance fluorescence [32–34] and photon correlations [34–38] in intense resonant or quasi-resonant laser beams. The principle of this approach, which is briefly sketched in section 7.2, is to consider, in a first step, the global system "atom + laser photons" interacting with each other as an isolated system having true energy levels (dressed states). Such an approximation is justified in the high intensity limit, since the atom–laser field coupling V_{AL} is much larger than the atom–vacuum field coupling V_{AV} (see fig. 1). Then, in a second step, the effect of V_{AV} is taken into account and described as a radiative relaxation mechanism which induces, for example, population transfers between dressed states with well defined rates. Resonance fluorescence thus appears, in this approach, as a radiative cascade of the dressed-atom.

As shown in ref. [39], the dressed-atom approach can be extended to a moving atom. If the mode function associated with the laser field varies in space, the Rabi frequency, and consequently the dressed-state energies, become position dependent, so that it is possible to define, for each dressed state, a position dependent potential energy and a corresponding force. As in the Stern–Gerlach effect, one gets a two-valued force that depends on the internal state of the dressed atom. Spontaneous radiative transitions, which occur at random times between the dressed states, change in a random way the sign of the instantaneous force experienced by the atom [8,39]. We show in section 7.3 how such a picture can provide a physical interpretation of the sign, mean value and fluctuations of dipole forces. We will restrict ourselves to qualitative considerations, since quantitative results may be found in ref. [39].

Applying these general ideas to an atom moving in an intense laser standing wave, we finally introduce in section 7.4 a new type of laser cooling mechanism, the "Sisyphus" cooling. Such a denomination comes from the fact that the atom, moving in the spatially undulating dressed-state potential curves runs up the hills more than down, as does Sisyphus in the Greek mythology. Here also, a detailed treatment of Sisyphus cooling is presented in ref. [39], and we will focus here on the physical ideas. Note finally that we will come back to the Sisyphus mechanism in chapter 9 in a different context. Instead of having, as here, a two-level atom in an intense laser beam, we will consider there an atom with several ground-state sublevels, moving in a weak intensity laser configuration.

7.2. The dressed-atom approach

The laser field is treated as a quasi-classical excitation of a single mode with frequency ω_L of the quantum radiation field. Such a mode, which is not in

general a plane wave mode since we want to investigate atomic motion in spatially inhomogeneous laser waves, can for example be considered as a mode of a fictitious cavity in which the atom is put. The local field "seen" by the atom inside the cavity must be the same as in the actual experience (same mean value, same spatial dependence...) and the cavity volume V must be large enough to avoid any modification of the spontaneous emission by cavity effects. The Hamiltonian H_{L} of the laser mode L is

$$H_{\mathrm{L}} = \hbar\omega_{\mathrm{L}} \left(a_{\mathrm{L}}^{+} a_{\mathrm{L}} + \tfrac{1}{2}\right), \tag{7.1}$$

where a_{L}^{+} and a_{L} are the creation and annihilation operators of a laser photon. The eigenstates $|N\rangle$ of H satisfy

$$H_{\mathrm{L}}|N\rangle = \left(N + \tfrac{1}{2}\right)\hbar\omega_{\mathrm{L}}|N\rangle \tag{7.2}$$

with $N = 0, 1, 2\ldots$ and describe a state with N photons in the mode L. The state of L is supposed to be a coherent state (see ref. [40] and ref. [41], Complement G_V), so that the mean value $\langle N\rangle$ of N and the dispersion ΔN of the values of N about $\langle N\rangle$ are related by

$$\Delta N = \sqrt{\langle N\rangle}. \tag{7.3}$$

Only the energy density $\langle N\rangle\hbar\omega_{\mathrm{L}}/V$ has a physical meaning. So we can take $\langle N\rangle$ and V very large, keeping $\langle N\rangle/V$ constant. In such a limit, we have

$$\langle N\rangle \gg \Delta N \gg 1,\ \Gamma T, \tag{7.4}$$

where ΓT gives the order of magnitude of the number of fluorescence photons emitted during the time T.

In this section, we suppose that the atom is at rest at a given point $\boldsymbol{r}$ and we first introduce the dressed states in $\boldsymbol{r}$. In the absence of coupling, the energy levels of the combined system "atom + laser photons" are labelled by two quantum numbers, e or g for the atom, N for the number of laser photons. Such "unperturbed" states are represented on the left side in fig. 13. When the laser frequency ω_{L} is close to the atomic one ω_{A}, these states are bunched into two-dimensional manifolds... $\mathcal{E}_N = \{|g, N+1\rangle, |e, N\rangle\}, \mathcal{E}_{N-1} = \{|g, N\rangle, |e, N-1\rangle\}\ldots$, the distance between the two levels of a manifold being $\hbar\delta = \hbar(\omega_{\mathrm{L}} - \omega_{\mathrm{A}})$ and the distance between two adjacent manifolds being $\hbar\omega_{\mathrm{L}}$. The atom–laser coupling V_{AL} connects the two states of a given manifold. For example, the atom in the ground

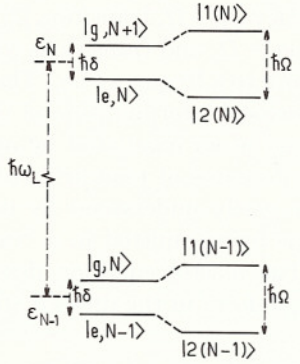

Fig. 13. Left part: unperturbed states of the combined "atom–laser photons" system, which are, in the absence of coupling, bunched into well-separated two-dimensional manifolds. Right part: dressed states resulting from the atom–laser coupling.

state g and in the presence of $N+1$ laser photons can absorb one laser photon and jump into the excited state e. This means that V_{AL} has a non-zero matrix element between the two states $|g, N+1\rangle$ and $|e, N\rangle$ of $\mathcal{E}_N$. Actually, one can show that, when N varies within ΔN around $\langle N \rangle$

$$\langle e, N \mid V_{\mathrm{AL}} \mid g, N+1 \rangle = \frac{\hbar}{2}\, \Omega_1(\boldsymbol{r})\, \mathrm{e}^{\mathrm{i}\phi(\boldsymbol{r})}, \tag{7.5}$$

where $\phi(\boldsymbol{r})$ and $\Omega_1(\boldsymbol{r})$ are the phase and the Rabi frequency corresponding to the quasi-classical state of the laser mode. This coupling gives rise to two perturbed states, $|1(N)\rangle$ and $|2(N)\rangle$ (for $\mathcal{E}_N$), represented on the right side of fig. 13. These dressed states are both linear combinations of the unperturbed states $|e, N\rangle$ and $|g, N+1\rangle$ and are separated by a splitting $\hbar\Omega$, where Ω is given by

$$\Omega(\boldsymbol{r}) = \sqrt{\delta^2 + \Omega_1^2(\boldsymbol{r})}. \tag{7.6}$$

Consider now the effect of spontaneous emission. Radiative transitions occur between the dressed states in fig. 13. The emission frequencies correspond to allowed transitions, i.e., to transitions between states connected by a non-zero matrix element of the atomic dipole operator d_z. In the uncoupled basis, d_z, which does not change the number of laser photons, connects only $|e, N\rangle$ and $|g, N\rangle$. Since both dressed states $|1(N)\rangle$ and $|2(N)\rangle$ of $\mathcal{E}_N$ are contaminated by $|e, N\rangle$, and since both dressed states $|1(N-1)\rangle$ and $|2(N-1)\rangle$ of $\mathcal{E}_{N-1}$ are contaminated by $|g, N\rangle$, there are 4 allowed transitions between $\mathcal{E}_N$ and $\mathcal{E}_{N-1}$: transition $|1(N)\rangle \rightarrow |2(N-1)\rangle$

corresponding to a frequency $\omega_L + \Omega$, transition $|2(N)\rangle \rightarrow |1(N-1)\rangle$ corresponding to a frequency $\omega_L - \Omega$, and transitions $|i(N)\rangle \rightarrow |i(N-1)\rangle$ (with $i = 1, 2$) corresponding both to a frequency ω_L. The dressed atom approach thus provides a straightforward interpretation of the "fluorescence triplet" [42] emitted by a two-level atom irradiated by an intense resonant laser beam. Similarly, various features of photon correlations observed on the fluorescence light can be easily understood by considering the sequence of fluorescence photons as being emitted in a "radiative cascade" by the dressed atom [34–38]. The master equation describing such a radiative cascade takes a very simple form in the dressed state basis in the limit

$$\Omega(\boldsymbol{r}) \gg \Gamma, \tag{7.7}$$

which is equivalent, according to eq. (7.6), to

$$|\delta| \gg \Gamma \qquad \text{or} \qquad \Omega_1 \gg \Gamma. \tag{7.8}$$

When condition (7.7) is fulfilled, one can neglect the coupling between the dressed state populations and the coherences between them (off-diagonal elements of the dressed-atom density matrix). Such a "secular approximation" then leads to equations of motion, which couple only populations to populations and coherences to coherences, and which can be simply interpreted in terms of spontaneous transition rates between dressed states. The dressed-atom approach is thus particularly well adapted to the limit (7.7), which implies well resolved lines in the fluorescence spectrum, or equivalently, according to eq. (7.8), to large detunings or high intensities.

7.3. Dressed-atom interpretation of dipole forces

We apply now the dressed-atom approach to the interpretation of dipole forces, which are associated with the intensity gradients of the laser beam.

In an inhomogeneous laser beam, the laser intensity is position dependent. It follows that $\Omega_1^2(\boldsymbol{r})$, and consequently $\Omega(\boldsymbol{r})$ according to eq. (7.6), vary in space. In fig. 14, we have represented the variations of the energies of the dressed states across a Gaussian laser beam. Out of the laser beam, the dressed levels coincide with the bare ones, and their splitting is just $\hbar\delta$. Inside the laser beam, each dressed level $|1(N)\rangle$ or $|2(N)\rangle$ is a linear superposition of $|g, N+1\rangle$ and $|e, N\rangle$ and the splitting between the two dressed states of a given manifold becomes $\hbar\Omega(\boldsymbol{r})$, which is larger than $\hbar|\delta|$.

Within each manifold, the energy diagram of fig. 14 is similar to that of a spin 1/2 magnetic moment in an inhomogeneous static magnetic field.

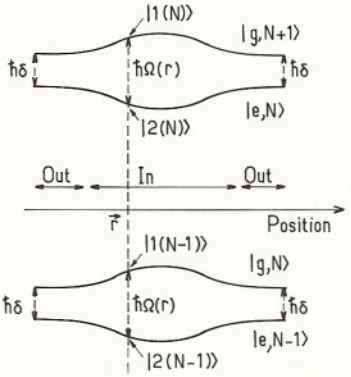

Fig. 14. Variations across a Gaussian laser beam of the dressed-atom energy levels. Out of the laser beam, the energy levels connect with the uncoupled states of fig. 13, separated by $\hbar|\delta|$. In the laser beam, the splitting between the dressed states is $\hbar\Omega(\boldsymbol{r}) > \hbar|\delta|$.

It follows that, in the absence of spontaneous emission, we can define a two-valued dressed state dependent force, equal to minus the gradient of the dressed state energy

$$\begin{aligned} \boldsymbol{f}_1 &= -\boldsymbol{\nabla} E_{1(N)}(\boldsymbol{r}) = -(\hbar/2)\boldsymbol{\nabla}\Omega(\boldsymbol{r}), \\ \boldsymbol{f}_2 &= -\boldsymbol{\nabla} E_{2(N)}(\boldsymbol{r}) = +(\hbar/2)\boldsymbol{\nabla}\Omega(\boldsymbol{r}) = -\boldsymbol{f}_1. \end{aligned} \tag{7.9}$$

As in the ordinary Stern and Gerlach effect, we have a force that depends on the internal state of the dressed atom, but the basic interaction occurs now between an optical dipole moment and an inhomogeneous laser electric field (optical Stern and Gerlach effect).

The effect of spontaneous emission is to produce, at random times, transitions between dressed states of type 1 and dressed states of type 2, or vice versa. This changes in a random way the sign of the instantaneous two-valued dressed state dependent force. Such a picture of an instantaneous force switching back and forth between two opposite values provides a simple understanding of the mean value and of the fluctuations of dipole forces.

Consider first the mean force. It can be written as

$$\boldsymbol{\mathcal{F}}_{\text{dip}} = \Pi_1 \boldsymbol{f}_1 + \Pi_2 \boldsymbol{f}_2, \tag{7.10}$$

where Π_i is the proportion of time spent in a dressed state of type i ($i = 1, 2$). For $\delta > 0$ (case of fig. 14), the unperturbed state $|g, N+1\rangle$ is above

$|e, N\rangle$, since $\omega_L > \omega_A$, and the dressed state $|1(N)\rangle$ is less contaminated by $|e, N\rangle$ than $|2(N)\rangle$ and is therefore more stable with respect to spontaneous emission. It follows that $\Pi_1 > \Pi_2$, and that the atom spends more time in dressed states of type 1 than in dressed states of type 2. We conclude that, for $\delta > 0$, the sign of the mean force is that corresponding to the level $|1(N)\rangle$: the atom is expelled from the high intensity regions. For $\delta < 0$, the conclusions are reversed. The dressed state $|2(N)\rangle$ connects to $|g, N+1\rangle$ out of the laser beam, is more populated than $|1(N)\rangle$ and it imposes its sign to the mean dipole force which attracts the atom towards the high intensity regions. Finally, for $\delta = 0$, the two dressed states contain the same admixture of $|e, N\rangle$, are equally populated ($\Pi_1 = \Pi_2$), so that the mean force vanishes. We understand in this way why the variations of the mean dipole force (for an atom initially at rest) versus the detuning $\delta = \omega_L - \omega_A$ are of a dispersive type. The argument given above is not only qualitative but also quantitative. If one calculates Π_1 and Π_2 from the master equation giving the spontaneous transition rates between the various dressed states, and if one puts their values in eq. (7.10), one gets the exact value of the mean dipole force, (to lowest order in Γ/Ω) [39].

We now try to get an order of magnitude of the momentum diffusion coefficient due to the fluctuations of the instantaneous force $\boldsymbol{F}$ switching back and forth between $\boldsymbol{f}_1$ and $\boldsymbol{f}_2 = -\boldsymbol{f}_1$. To simplify the discussion, we consider the resonant case where $\delta = 0$[8,39]. In such a case, both dressed states are equally populated so that $\boldsymbol{\mathcal{F}} = \langle \boldsymbol{F} \rangle = \boldsymbol{0}$. The variations with τ of the correlation function $C(\tau)$ of $\delta \boldsymbol{F} = \boldsymbol{F} - \langle \boldsymbol{F} \rangle = \boldsymbol{F}$, which is equal to $\langle \boldsymbol{F}(t) \cdot \boldsymbol{F}(t-\tau) \rangle$, are represented in fig. 15. For $\tau = 0$, $C(0) = \langle \boldsymbol{F}^2 \rangle$ takes the value

$$C(0) = \langle \boldsymbol{f}_1^2 \rangle = \langle \boldsymbol{f}_2^2 \rangle = (\hbar^2/4) \boldsymbol{\nabla} \Omega_1^2. \tag{7.11}$$

Then, $C(\tau)$ decreases with a characteristic time, which is the correlation time τ_{corr} of $\boldsymbol{F}(t)$, and which is on the order of the mean time between two successive changes of dressed states due to a spontaneous transition. Such a time is on the order of $2/\Gamma$. It follows that the integral from 0 to $+\infty$ of $C(\tau)$ which, according to eq. (5.36), gives an order of magnitude of the momentum diffusion coefficient D_{dip}, is on the order of

$$D_{dip} \sim C(0)\, \tau_{corr} \sim \frac{\hbar^2}{4} \boldsymbol{\nabla} \Omega_1^2 \frac{2}{\Gamma}. \tag{7.12}$$

Such an estimation is in agreement with the result given in eq. (5.60) for a standing wave, since in a standing wave $\boldsymbol{\nabla} \Omega_1 \sim k_L \Omega_1$. More quantitative calculations of $C(\tau)$ and D_{dip}, based on such a dressed atom picture, and not limited to the resonant case $\delta = 0$, may be found in ref. [39].

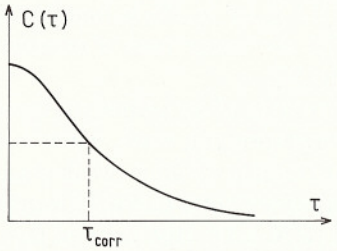

Fig. 15. Variation with τ of the correlation function $C(\tau)$ of the instantaneous dipole force.

7.4. Atomic motion in an intense laser standing wave – Sisyphus cooling

Atomic motion in a strong standing wave has been studied by several authors [8,14,15,39,43–45]. We present in this subsection a physical picture, based on the dressed atom approach, and which provides some physical insight in this problem.

In a plane standing wave, along Ox, the Rabi frequency $\Omega_1(x)$ is a periodic function of x

$$\Omega_1(x) = 2\Omega_1 \sin k_L x. \tag{7.13}$$

It follows that the two dressed states of a given manifold oscillate periodically in space since their splitting is according to eqs. (7.6) and (7.13).

$$\hbar\Omega(x) = \hbar\sqrt{\delta^2 + 4\Omega_1^2 \sin^2 k_L x}. \tag{7.14}$$

Figure 16 represents these dressed states for positive detuning (dashed lines). At a node of the standing wave ($z = 0, \lambda/2, \lambda \ldots$), $\Omega_1(x)$ vanishes and the two dressed states $|1(N)\rangle$ and $|2(N)\rangle$, respectively, coincide with the unperturbed states $|g, N+1\rangle$ and $|e, N\rangle$, separated by $\hbar\delta$ (dotted lines). Out of a node, $\Omega_1(x)$ is different from zero, the dressed states are linear combinations of $|g, N+1\rangle$ and $|e, N\rangle$ and their splitting is maximum at the antinodes ($z = \lambda/4, 3\lambda/4 \ldots$) where $\Omega_1(x)$ reaches its maximum value. Consider now the effect of spontaneous emission. As we have seen in section 7.2, an atom in level $|1(N)\rangle$ or $|2(N)\rangle$ can emit spontaneous a photon and decay to the levels $|1(N-1)\rangle$ or $|2(N-1)\rangle$. The key point is that, in a standing wave, the various rates for such spontaneous processes vary in space because of the x-dependence of the wave functions. For example, if δ is positive and if the atom is in the level $|1(N)\rangle$, its decay rate is zero at a node where $|1(N)\rangle = |g, N+1\rangle$ and maximum at an antinode where

the contamination of $|1(N)\rangle$ by $|e,N\rangle$ is maximum. On the contrary, for an atom in level $|2(N)\rangle$, the decay rate is maximum at the nodes where $|2(N)\rangle$ coincides with $|e,N\rangle$.

The previous considerations allow us now to understand why an atom is slowed down in an intense standing wave, when δ is positive, contrarily to what happens for usual Doppler cooling (weak standing wave). We can for example follow the "trajectory" of a moving atom starting at a node of the standing wave, in level $|1(N+1)\rangle$ (full lines of fig. 16). Starting from this valley, the atom climbs uphill until it approaches the top (antinode) where its decay rate is maximum. It may jump either into level $|1(N)\rangle$ (which does not change anything from a mechanical point of view if one neglects the recoil due to the spontaneously emitted photon) or into level $|2(N)\rangle$, in which case the atom is again in a valley. It has now to climb up again until it reaches a new top (node) where $|2(N)\rangle$ is the most unstable, and so on ... It is clear that the atomic velocity is decreased in such a process, since the atom sees on the average more "uphill" parts than "downhill" ones. Such a scheme can be actually considered as a microscopic realization of the "Sisyphus myth": every time the atom has climbed a hill, it may be put back at the bottom of a valley by spontaneous emission and it has to climb up again.

Such an approach has been used to derive quantitative results for the velocity dependence of the force acting upon the atom [39]. At very low velocities ($k_L v_0 \ll \Gamma$), we have a linear dependence with a slope which can be much higher than for usual radiation pressure molasses (by a factor on the order of Ω_1/Γ). The force reaches its maximum value for velocities such that $k_L v_0 \sim \Gamma$, or in other words, for situations in which, as in fig. 16, the atom travels over a distance on the order of a wavelength between two spontaneous emissions. The important point is that the magnitude of this friction force is directly related to the modulation depth of the dressed energy levels, i.e., to the Rabi frequency Ω_1. As a consequence, this force increases indefinitely with the laser intensity. After this maximum, when $k_L v_0$ becomes large compared to Γ, the force decreases as v_0^{-1} and finally, at very large velocities, resonances appear which are due to non-adiabatic Landau–Zener transitions between the two dressed states of each manifold [45].

To conclude this analysis, it may be useful to discuss the energy–momentum balance in the cooling processes associated with this Sisyphus effect. Between two spontaneous emission processes, the total energy (kinetic + potential) of the atom is conserved. When the atom climbs uphill, its kinetic energy is transformed into potential energy by stimulated emission processes which redistribute photons between the two counterpropa-

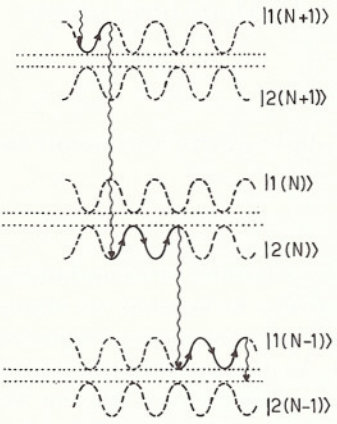

Fig. 16. Laser cooling in a strong standing wave with a blue detuning ($\delta > 0$). The dashed lines represent the spatial variations of the dressed atom energy levels which coincide with the unperturbed levels (dotted lines) at the node. The full lines represent the "trajectory" of a slowly moving atom. Because of the spatial variation of the dressed wave functions, spontaneous emission occurs preferentially at an antinode (node) for a dressed state of type 1 (2). Between two spontaneous emissions (vertical wavy lines), the atom sees on the average more uphill parts than downhill ones and is therefore slowed down.

gating waves at a rate Ω_1. Atomic momentum is therefore transferred to laser photons. The total atomic energy is then dissipated by spontaneous emission processes which carry away part of the atomic potential energy.

We finally mention that these large velocity dependent forces appearing in an intense laser standing wave with a blue detuning have been used to cool the transverse velocity spread Δv of a Cs atomic beam [47]. If $k\Delta v \sim \Gamma$, the cooling efficiency is very high and one can use interaction lengths much shorter than those required for usual Doppler cooling. Furthermore, if the kinetic energy of the atoms along the standing wave is smaller than the height of the hills of fig. 16, the atoms can be trapped near the nodes or the antinodes of the standing wave, depending whether the detuning δ is positive or negative. Such a "channeling" of atoms, which was first predicted in ref. [46], has been observed experimentally on Cs atoms [48]. It represents the first experimental demonstration of the possibility of confining neutral atoms in optical wavelength size regions.

II Multi-level atoms

8. Optical pumping, light shifts and mean radiative forces

8.1. Introduction

This part II of the course is devoted to atoms having several sublevels in the ground state. More precisely, we consider an atomic transition connecting two levels g and e with angular momenta, respectively, equal to J_g and J_e, and we suppose $J_g \neq 0$. As mentioned in the general introduction (chapter 1), such a situation gives rise to very efficient new cooling mechanisms which we now want to analyze.

Two physical effects, which have been known for a long time, play a basic role in the new cooling mechanisms. The first one is optical pumping which consists of a transfer of atoms from one sublevel g_μ of g to another one $g_{\mu'}$ by absorption–spontaneous emission cycles. The second one is an energy shift of the ground-state sublevels, which in general varies from one sublevel to the other and which is proportional to the light intensity. Such shifts are called light shifts or ac-Stark shifts. Up to now, these effects have been considered only in connection with the dynamics of the atomic internal degrees of freedom. Very recently, it has been realized that these effects play also a very important role in the dynamics of the atomic translational degrees of freedom. So we have thought it would be useful to recall in this chapter a few properties of optical pumping and light shifts which are needed for understanding the new cooling mechanisms, discussed in the following chapters.

We begin in section 8.2 by generalizing to multilevel atoms the equations of motion of the atomic density matrix σ and the expression of the mean force introduced in chapter 2 for two-level atoms. We then show in section 8.3 that these equations can be considerably simplified in the low saturation and low velocity limit ($s \ll 1, k_L v_0 \ll \Gamma$), which is precisely the limit where the new cooling mechanisms are the most efficient. The existence of two different time scales, the radiative lifetime τ_R of e and the optical pumping time τ_P in g, with $\tau_P \gg \tau_R$, allows one to adiabatically eliminate all fast variables and to get equations of motion involving only the ground-state density matrix. Such equations of motion contain two types of terms, terms corresponding to a Hamiltonian evolution and describing the light shifts in g, and terms describing a relaxation in g associated with optical pumping. The physical content of these two types of terms is analyzed, respectively,

in sections 8.4 and 8.5. Finally, we discuss in section 8.6 the new expression of the mean force in the limit $s \ll 1, k_L v_0 \ll \Gamma$, and we identify two types of terms related, respectively, to the light shifts of the ground-state sublevels and to the absorption rate from these sublevels.

8.2. Basic equations for multilevel atoms

8.2.1. Approximations

As in section 2.5, we use a semi-classical description where the position operator $\boldsymbol{R}$ of the center of mass is replaced by the c-number $\boldsymbol{r} = \boldsymbol{r}_0 + \boldsymbol{v}_0 t$.

Let P_g (respectively P_e) be the projector onto the subspace subtended by the various Zeeman sublevels of g (respectively e)

$$\begin{aligned} P_g &= \sum_{\mu=-J_g}^{+J_g} |J_g\,\mu\rangle\langle J_g\,\mu|, \\ P_e &= \sum_{m=-J_e}^{+J_e} |J_e\,m\rangle\langle J_e\,m|. \end{aligned} \tag{8.1}$$

The atomic density operator σ can be written as

$$\sigma = \sigma_{gg} + \sigma_{ge} + \sigma_{eg} + \sigma_{ee}, \tag{8.2}$$

where

$$\sigma_{ab} = P_a \sigma P_b \tag{8.3}$$

with $a, b = e$ or g. Note that σ_{ab} is now an operator and not a c-number. The two operators σ_{gg} and σ_{ee} are represented by square matrices. Their diagonal elements give the populations of the various Zeeman sublevels of g and e, whereas the off-diagonal elements describe "Zeeman coherences" which exist between them in e or g. Finally, σ_{ge} and $\sigma_{eg} = \sigma_{ge}^{\dagger}$ are represented by rectangular matrices consisting of off-diagonal elements between one sublevel of e and one sublevel of g, which are called "optical coherences".

The new expression of the atom–laser interaction Hamiltonian V_{AL}, which generalizes eq. (2.10), is given by

$$V_{AL} = -\boldsymbol{d}^{+} \cdot \boldsymbol{E}_L^{+}(\boldsymbol{r})\, \mathrm{e}^{-\mathrm{i}\omega_L t} - \boldsymbol{d}^{-} \cdot \boldsymbol{E}_L^{-}(\boldsymbol{r})\, \mathrm{e}^{+\mathrm{i}\omega_L t}, \tag{8.4}$$

where

$$\boldsymbol{d}^{+} = P_e \boldsymbol{d} P_g, \qquad \boldsymbol{d}^{-} = P_g \boldsymbol{d} P_e \tag{8.5}$$

and where $\boldsymbol{E}_{\mathrm{L}}^{+}(\boldsymbol{r})$ (respectively $\boldsymbol{E}_{\mathrm{L}}^{-}(\boldsymbol{r})$) are the positive (respectively negative) frequency components of the laser electric field.

$$\boldsymbol{E}_{\mathrm{L}}(\boldsymbol{r},t)=\boldsymbol{E}_{\mathrm{L}}^{+}(\boldsymbol{r})\,\mathrm{e}^{-\mathrm{i}\omega_{\mathrm{L}}t}+\boldsymbol{E}_{\mathrm{L}}^{-}(\boldsymbol{r})\,\mathrm{e}^{+\mathrm{i}\omega_{\mathrm{L}}t}\,. \tag{8.6}$$

As in eq. (2.10), the rotating wave approximation has been used.

It will be useful for the following to introduce the internal atomic operators $G^{\pm}(\boldsymbol{r})$ defined by:

$$\hbar G^{\pm}(\boldsymbol{r})=\boldsymbol{d}^{\pm}\cdot\boldsymbol{E}_{\mathrm{L}}^{\pm}(\boldsymbol{r}), \tag{8.7}$$

and to define dimensionless dipole operators $\widehat{\boldsymbol{d}}^{\pm}$ in the following way. Let

$$\boldsymbol{\epsilon}_{\pm}=\mp\frac{1}{\sqrt{2}}(\boldsymbol{\epsilon}_x\pm\mathrm{i}\boldsymbol{\epsilon}_y),\qquad\qquad \boldsymbol{\epsilon}_0=\boldsymbol{\epsilon}_z \tag{8.8}$$

be a spherical basis of polarization vectors, corresponding respectively to the $\sigma^{\pm}$ and π polarizations. The Wigner–Eckart theorem (ref. [49], Chap. XIII) applied to the vectorial operator $\boldsymbol{d}^{+}$ gives

$$\langle J_e\,m\mid\boldsymbol{\epsilon}_q\cdot\boldsymbol{d}^{+}\mid J_g\,\mu\rangle=\mathcal{D}\,\langle J_e\,m\mid J_g\,1\,\mu\;q\,\rangle, \tag{8.9}$$

where $\langle J_e m|J_g 1\mu q\rangle$ is a Clebsch–Gordan coefficient and where $\mathcal{D}$ is a reduced matrix element which can always be taken real with an appropriate choice of the relative phases of e and g, and which is independent of the magnetic quantum numbers, m, μ and q. We will put

$$\boldsymbol{d}^{+}=\mathcal{D}\,\widehat{\boldsymbol{d}}^{+}=\left(\boldsymbol{d}^{-}\right)^{\dagger}, \tag{8.10}$$

so that the matrix elements of $\boldsymbol{\epsilon}_q\cdot\widehat{\boldsymbol{d}}^{+}$ are just Clebsch–Gordan coefficients. We also introduce the polarization vector $\boldsymbol{\epsilon}(\boldsymbol{r})$ in $\boldsymbol{r}$

$$\boldsymbol{E}_{\mathrm{L}}^{+}(\boldsymbol{r})=\tfrac{1}{2}\boldsymbol{\epsilon}(\boldsymbol{r})\,\mathcal{E}_{\mathrm{L}}(\boldsymbol{r}), \tag{8.11}$$

the amplitude $\mathcal{E}_{\mathrm{L}}(\boldsymbol{r})$ being real. The (generally complex) polarization vector $\boldsymbol{\epsilon}(\boldsymbol{r})$ is normalized

$$\boldsymbol{\epsilon}^{*}(\boldsymbol{r})\cdot\boldsymbol{\epsilon}(\boldsymbol{r})=1. \tag{8.12}$$

From $\mathcal{D}$ and $\mathcal{E}_{\mathrm{L}}(\boldsymbol{r})$, we finally define the Rabi frequency in $\boldsymbol{r}$

$$\hbar\,\Omega_1(\boldsymbol{r})=-\mathcal{D}\,\mathcal{E}_{\mathrm{L}}(\boldsymbol{r}), \tag{8.13}$$

which corresponds to the Rabi frequency of a transition with Clebsch–Gordan coefficient equal to 1, excited by a laser field with amplitude $\mathcal{E}_{\mathrm{L}}(\boldsymbol{r})$.

8.2.2. Operator form of optical Bloch equations

The basic equations of motion, which generalize eq. (2.42) can be now written in operator form

$$\dot{\sigma}_{ab} = -\frac{\mathrm{i}}{\hbar} P_a \left[H_{\mathrm{A}}^{\mathrm{int}} + V_{\mathrm{AL}}, \sigma \right] P_b + \left(\frac{\mathrm{d}}{\mathrm{d}t} \sigma_{ab} \right)_{\mathrm{sp}}, \tag{8.14}$$

where V_{AL} is given in eq. (8.4) and where

$$H_{\mathrm{A}}^{\mathrm{int}} = \hbar \omega_{\mathrm{A}} P_e. \tag{8.15}$$

The last term of eq. (8.14) describes the damping due to spontaneous emission. For the excited state density matrix σ_{ee} and for the optical coherences σ_{eg} and σ_{ge} it has the same form as in eqs. (2.43.a), (2.43.c) and (2.43.d). Only the equation (2.43.b) describing the feeding of σ_{gg} from σ_{ee} by spontaneous emission has to be modified. One can show (see ref. [5], subsection 4.3.4) that, for an atom having a degenerate ground state, eq. (2.43.b) has to be replaced by

$$\left(\frac{\mathrm{d}}{\mathrm{d}t} \sigma_{gg} \right)_{\mathrm{sp}} = \Gamma \sum_{q=-1,0,+1} (\boldsymbol{\epsilon}_q^* \cdot \widehat{\boldsymbol{d}}^-)\, \sigma_{ee}\, (\boldsymbol{\epsilon}_q \cdot \widehat{\boldsymbol{d}}^+), \tag{8.16}$$

where the dimensionless operators $\widehat{\boldsymbol{d}}^{\pm}$ and the basic polarization vectors $\boldsymbol{\epsilon}_q$ have been defined above in eqs. (8.10) and (8.8). Note that the transfer by spontaneous emission satisfies the following selection rule

$$\begin{aligned} &\langle J_e\, m \mid \sigma \mid J_e\, m' \rangle \longrightarrow \langle J_g\, \mu \mid \sigma \mid J_g\, \mu' \rangle \\ &\qquad \text{with} \qquad \mu - \mu' = m - m', \end{aligned} \tag{8.17}$$

which is actually a consequence of the rotational invariance of the atom–vacuum field interaction Hamiltonian V_{AV}. According to eq. (8.16), the transfer rate associated with eq. (8.17) is just the product of Γ by the two Clebsh–Gordan coefficients connecting m to μ and m' to μ'.

Calculating the commutator of eq. (8.14), and using eqs. (8.15), (8.4), (2.43.a, c, d) and (8.16), we finally get

$$\dot{\sigma}_{ee} = -\Gamma \sigma_{ee} + \mathrm{i} \left[G^+(\boldsymbol{r})\, \widetilde{\sigma}_{ge} - \widetilde{\sigma}_{eg} G^-(\boldsymbol{r}) \right], \tag{8.18a}$$

$$\dot{\widetilde{\sigma}}_{eg} = -\left(\frac{\Gamma}{2} - \mathrm{i}\delta \right) \widetilde{\sigma}_{eg} + \mathrm{i} \left[G^+(\boldsymbol{r})\, \sigma_{gg} - \sigma_{ee} G^+(\boldsymbol{r}) \right], \tag{8.18b}$$

$$\dot{\sigma}_{gg} = \left(\frac{\mathrm{d}}{\mathrm{d}t} \sigma_{gg} \right)_{\mathrm{sp}} + \mathrm{i} \left[G^-(\boldsymbol{r})\, \widetilde{\sigma}_{eg} - \widetilde{\sigma}_{ge} G^+(\boldsymbol{r}) \right], \tag{8.18c}$$

where we have used

$$\widetilde{\sigma}_{eg} = \sigma_{eg}\ \mathrm{e}^{\mathrm{i}\omega_{\mathrm{L}}t} \tag{8.19}$$

instead of σ_{eg} in order to eliminate any explicit time dependence in the coefficients of the equations. Note that, if the atom is moving, there is an implicit time dependence through $\boldsymbol{r} = \boldsymbol{r}_0 + \boldsymbol{v}_0 t$.

8.2.3. Expression of the mean force

According to eqs. (2.30) and (8.4), the mean force can be written

$$\begin{aligned}\boldsymbol{\mathcal{F}}(\boldsymbol{r},t) &= -\langle \boldsymbol{\nabla} V_{\mathrm{AL}}(\boldsymbol{r},t)\rangle \\ &= +\sum_{i=x,y,z} \langle d_i^+\rangle\, \boldsymbol{\nabla} E_{Li}^+(\boldsymbol{r})\ \mathrm{e}^{-\mathrm{i}\omega_{\mathrm{L}}t} + \mathrm{h.c.}.\end{aligned} \tag{8.20}$$

Using eqs. (8.5) and (8.19), the mean value of d_i^+ which appears in eq. (8.20) can be re-expressed as

$$\langle d_i^+\rangle = \mathrm{Tr}\{P_e d_i P_g \sigma\} = \mathrm{Tr}\{d_i \sigma_{ge}\} = \mathrm{Tr}\{d_i \widetilde{\sigma}_{ge}\}\ \mathrm{e}^{\mathrm{i}\omega_{\mathrm{L}}t} \tag{8.21}$$

which, inserted into eq. (8.20), yields

$$\boldsymbol{\mathcal{F}}(\boldsymbol{r},t) = \sum_{i=x,y,z} \mathrm{Tr}\{d_i \widetilde{\sigma}_{ge}\}\, \boldsymbol{\nabla} E_{Li}^+(\boldsymbol{r}) + \mathrm{c.c.} \tag{8.22}$$

Equation (8.22) clearly shows that the mean radiative force only depends on the optical coherences $\widetilde{\sigma}_{eg}$ and $\widetilde{\sigma}_{ge}$.

8.3. Limit of low saturation and low velocity

8.3.1. New possible approximations

Except for the semi-classical and rotating wave approximations, equations (8.18) are exact. We consider now the low saturation limit ($s \ll 1$), which is the relevant limit for the new cooling mechanisms. In such a limit, the characteristic times for the evolution of the ground state become much longer than those of the excited state. It follows that σ_{gg} is a slow variable compared to $\widetilde{\sigma}_{eg}$ and σ_{ee}. After a short transient regime, lasting for a time on the order of $\tau_{\mathrm{R}} = \Gamma^{-1}$, σ_{gg} "slaves" the other variables by imposing its slow rate of variation on $\widetilde{\sigma}_{eg}$, $\widetilde{\sigma}_{ge}$ and σ_{ee}, so that one can write

$$|\dot{\sigma}_{ee}| \ll \Gamma\, \sigma_{ee}, \qquad |\dot{\widetilde{\sigma}}_{eg}| \ll \Gamma\, |\widetilde{\sigma}_{eg}|. \tag{8.23}$$

It is then possible to use the inequalities (8.23) to neglect the left-hand side of equations (8.18.a) and (8.18.b) in comparison with the damping terms $-\Gamma\sigma_{ee}$ and $-(\Gamma/2)\widetilde{\sigma}_{eg}$, which appear in the right-hand side. This yields algebraic equations allowing σ_{ee} and $\widetilde{\sigma}_{eg}$ to be re-expressed in terms of σ_{gg}. Such a procedure is called "adiabatic elimination of the fast variables" and leads for these fast variables to expressions describing how they adjust themselves at each time to the value taken at this time by the slowly varying variable.

Such an argument is in fact valid only for an atom at rest, the rate of variation of σ being only due to the absorption and emission processes. For a moving atom, one must not forget that the time derivatives $\dot{\sigma}_{ab}$ appearing on the left-hand side of eq. (8.18) are actually total time derivatives $\mathrm{d}/\mathrm{d}t = \partial/\partial t + \boldsymbol{v}_0 \cdot \boldsymbol{\nabla}$, so that one must also consider the order of magnitude of the terms $\boldsymbol{v}_0 \cdot \boldsymbol{\nabla}\sigma_{ab} \simeq k_{\mathrm{L}} v_0 \sigma_{ab}$. Actually, with the new cooling mechanisms, the typical r.m.s. steady-state velocities reach very low values, for which

$$\eta = \frac{k_{\mathrm{L}} v_0}{\Gamma} \ll 1. \tag{8.24}$$

This is why we will restrict ourselves in the remaining part of this course to calculations done in zeroth order in η. Such an approximation, which allows us to neglect $\dot{\sigma}_{ee}$ and $\dot{\widetilde{\sigma}}_{eg}$ in eq. (8.18), even for a moving atom, eliminates any possibility of taking into account Doppler cooling which appears in the first order in η, but we are interested now in new cooling mechanisms which are much more efficient than Doppler cooling, and the equations so obtained will be much simpler. Note finally that we do not neglect in eq. (8.18.c) $\partial\sigma_{gg}/\partial t$ and $\boldsymbol{v}_0 \cdot \boldsymbol{\nabla}\sigma_{gg}$, because σ_{gg} is a slow variable and the Doppler shift $k_{\mathrm{L}} v_0$ can no longer be neglected in comparison with the characteristic evolution frequencies of σ_{gg}.

8.3.2. Adiabatic elimination of the excited state

We first eliminate optical coherences. Neglecting $\dot{\widetilde{\sigma}}_{eg}$ in eq. (8.18.b) leads to

$$\widetilde{\sigma}_{eg} = -\frac{1}{\delta + \mathrm{i}(\Gamma/2)}\, G^{+}(\boldsymbol{r})\, \sigma_{gg}, \tag{8.25a}$$

$$\widetilde{\sigma}_{ge} = -\frac{1}{\delta - \mathrm{i}(\Gamma/2)}\, \sigma_{gg}\, G^{-}(\boldsymbol{r}). \tag{8.25b}$$

We have actually neglected the contribution of σ_{ee} to eq. (8.25). The reason is that σ_{ee} is at least of order 2 in the Rabi frequency Ω_1 (see eq. (8.28) below). Since σ_{ee} is multiplied in eq. (8.18.a) by G^{+}, which is of order 1 in

Ω_1, the contribution of σ_{ee} to eq. (8.25) is at least of order 3. We restrict ourselves here to calculations up to order 2 in Ω_1, more precisely to order 1 in the saturation parameter s given in eq. (3.6). This is why σ_{ee} does not appear in eq. (8.25).

Having re-expressed $\widetilde{\sigma}_{eg}$ and $\widetilde{\sigma}_{ge}$ in terms of σ_{gg}, we can now obtain a new expression for the mean force $\boldsymbol{\mathcal{F}}$. Inserting eq. (8.25) into eq. (8.22) yields

$$\begin{aligned}\boldsymbol{\mathcal{F}}(\boldsymbol{r}) &= \frac{-1}{\delta - \mathrm{i}(\Gamma/2)} \sum_{i=x,y,z} \mathrm{Tr}\left\{G^-(\boldsymbol{r})\, d_i^+\, \sigma_{gg}\right\} \boldsymbol{\nabla} E_{Li}^+(\boldsymbol{r}) \;+\; \text{c.c.} \\ &= \frac{-\hbar}{\delta - \mathrm{i}(\Gamma/2)} \left\langle G^-(\boldsymbol{r}) \left(\boldsymbol{\nabla} G^+(\boldsymbol{r})\right)\right\rangle + \text{c.c.} \end{aligned} \tag{8.26}$$

We have used eq. (8.7) and the simpler notation

$$\langle X \rangle = \mathrm{Tr}\left\{X \sigma_{gg}\right\}. \tag{8.27}$$

We turn now to equation (8.18.a) giving $\dot{\sigma}_{ee}$. Neglecting $\dot{\sigma}_{ee}$ and using eq. (8.25) for eliminating $\widetilde{\sigma}_{eg}$ and $\widetilde{\sigma}_{ge}$, we get

$$\begin{aligned}\sigma_{ee} &= -\frac{\mathrm{i}}{\Gamma} \frac{1}{\delta - \mathrm{i}(\Gamma/2)}\, G^+(\boldsymbol{r})\, \sigma_{gg}\, G^-(\boldsymbol{r}) \;+\; \text{h.c.} \\ &= \frac{1}{\delta^2 + (\Gamma^2/4)}\, G^+(\boldsymbol{r})\, \sigma_{gg}\, G^-(\boldsymbol{r}) \\ &= \frac{\Omega_1^2/4}{\delta^2 + (\Gamma^2/4)} \left(\boldsymbol{\epsilon}\,(\boldsymbol{r}) \cdot \widehat{\boldsymbol{d}}^+\right) \sigma_{gg} \left(\boldsymbol{\epsilon}^*(\boldsymbol{r}) \cdot \widehat{\boldsymbol{d}}^-\right). \end{aligned} \tag{8.28}$$

8.3.3. Equation of motion of the ground-state density matrix

It remains to transform the last equation (8.18.c) describing the evolution of σ_{gg}. Using eqs. (8.16), (8.25) and (8.28), we get

$$\begin{aligned}\dot{\sigma}_{gg} = {} & \frac{-\mathrm{i}}{\delta + \mathrm{i}\frac{\Gamma}{2}}\, G^-(\boldsymbol{r})\, G^+(\boldsymbol{r})\, \sigma_{gg} + \frac{\mathrm{i}}{\delta - \mathrm{i}(\Gamma/2)}\, \sigma_{gg}\, G^-(\boldsymbol{r})\, G^+(\boldsymbol{r}) \\ & + \frac{\Gamma}{\delta^2 + (\Gamma^2/4)} \sum_{q=-1,0,+1} \boldsymbol{\epsilon}_q^* \cdot \widehat{\boldsymbol{d}}^-\, G^+(\boldsymbol{r})\, \sigma_{gg}\, G^-(\boldsymbol{r})\, \boldsymbol{\epsilon}_q \cdot \widehat{\boldsymbol{d}}^+, \end{aligned} \tag{8.29}$$

which is a closed equation of motion for σ_{gg}, since it relates $\dot{\sigma}_{gg}$ only to σ_{gg}. The first line of eq. (8.29) describes the effect of the laser excitation, whereas the second line describes the effect of spontaneous emission.

We separate now the real and the imaginary parts of $1/(\delta \pm \mathrm{i}\Gamma/2)$. This allows one to transform the first line of eq. (8.29), which will be noted $(\dot{\sigma}_{gg})_{\mathrm{las}}$, as a sum of two terms, the first one involving a commutator and the second one an anticommutator

$$(\dot{\sigma}_{gg})_{\mathrm{las}} = -\,\mathrm{i}\,\frac{\delta}{\delta^2 + (\Gamma^2/4)}\,[\,G^-(\boldsymbol{r})\,G^+(\boldsymbol{r})\,,\,\sigma_{gg}] - \frac{\Gamma/2}{\delta^2 + (\Gamma^2/4)}\,\{\,G^-(\boldsymbol{r})\,G^+(\boldsymbol{r})\,,\,\sigma_{gg}\}_+. \tag{8.30}$$

In eq. (8.30), $\{X, Y\}_+$ means $XY + YX$. Note that the operator $G^-(\boldsymbol{r})G^+(\boldsymbol{r})$ is Hermitian and semi-positive since $G^- = (G^+)^\dagger$,

$$\big(\,G^-(\boldsymbol{r})\,G^+(\boldsymbol{r})\,\big)^\dagger = G^-(\boldsymbol{r})\,G^+(\boldsymbol{r}), \tag{8.31}$$

so that its eigenvalues are real and non-negative. Equations having the same structure as eqs. (8.30) and (8.29) have been derived for the first time in refs. [50] and [51] dealing with the quantum theory of the optical pumping cycle. The pumping light was not monochromatic, as it is the case here, but broad band incoherent light, so that equations (8.29) and (8.30) had to be averaged over the spectral distribution $I(\omega_{\mathrm{L}})$ of the incoming light.

Equations (8.29) and (8.30) can still be transformed, using eqs. (8.7), (8.10), (8.11) and (8.13). Introducing in G^-G^+ the Hermitian, semi-positive and dimensionless operator

$$\Lambda(\boldsymbol{r}) = \Big(\boldsymbol{\epsilon}^*(\boldsymbol{r}) \cdot \widehat{\boldsymbol{d}}^-\Big)\,\Big(\boldsymbol{\epsilon}\,(\boldsymbol{r}) \cdot \widehat{\boldsymbol{d}}^+\Big) \;=\; \Lambda^\dagger(\boldsymbol{r}) \tag{8.32}$$

and the parameters Γ' and δ' analogous to those defined in eq. (6.15),

$$\Gamma'(\boldsymbol{r}) = \Gamma\,\frac{\Omega_1^2(\boldsymbol{r})/4}{\delta^2 + (\Gamma^2/4)} = \Gamma\,\frac{s(\boldsymbol{r})}{2}, \tag{8.33a}$$

$$\delta'(\boldsymbol{r}) = \delta\,\frac{\Omega_1^2(\boldsymbol{r})/4}{\delta^2 + (\Gamma^2/4)} = \delta\,\frac{s(\boldsymbol{r})}{2}, \tag{8.33b}$$

where the saturation parameter $s(\boldsymbol{r})$ is given by

$$s(\boldsymbol{r}) = \frac{\Omega_1^2(\boldsymbol{r})/2}{\delta^2 + (\Gamma^2/4)}, \tag{8.34}$$

we get for σ_{gg} the following equation of motion

$$\dot{\sigma}_{gg} = -\,\mathrm{i}\,\delta'(\boldsymbol{r})\,[\Lambda(\boldsymbol{r})\,,\,\sigma_{gg}] - \frac{\Gamma'(\boldsymbol{r})}{2}\,\{\Lambda(\boldsymbol{r})\,,\,\sigma_{gg}\}_+ + \Gamma'(\boldsymbol{r}) \sum_{q=-1,0,+1} (\boldsymbol{\epsilon}_q^* \cdot \widehat{\boldsymbol{d}}^-)\left(\boldsymbol{\epsilon}\,(\boldsymbol{r}) \cdot \widehat{\boldsymbol{d}}^+\right) \sigma_{gg} \left(\boldsymbol{\epsilon}^*(\boldsymbol{r}) \cdot \widehat{\boldsymbol{d}}^-\right) (\boldsymbol{\epsilon}_q \cdot \widehat{\boldsymbol{d}}^+). \tag{8.35}$$

8.4. Light shifts of the ground-state sublevels

8.4.1. Hamiltonian part of the equations of motion

The terms involving a commutator in eqs. (8.30) and (8.35) can be written as $[H_{\mathrm{eff}}(\boldsymbol{r}), \sigma_{gg}]/\mathrm{i}\hbar$ where

$$H_{\mathrm{eff}} = \frac{\hbar\,\delta}{\delta^2 + (\Gamma^2/4)}\, G^-(\boldsymbol{r})\, G^+(\boldsymbol{r}) = \hbar\,\delta'(\boldsymbol{r})\,\Lambda(\boldsymbol{r}). \tag{8.36}$$

The corresponding rate of variation is the same as the one which would be induced by the effective Hamiltonian $H_{\mathrm{eff}}(\boldsymbol{r})$.

We will call $|g_\alpha(\boldsymbol{r})\rangle$ the eigenstates of $\Lambda(\boldsymbol{r})$ and $\lambda_\alpha(\boldsymbol{r})$ the corresponding eigenvalues, which are real and non-negative since $\Lambda(\boldsymbol{r})$ is Hermitian and semi-positive

$$\begin{aligned} &\Lambda(\boldsymbol{r})\,|g_\alpha(\boldsymbol{r})\rangle = \lambda_\alpha(\boldsymbol{r})\,|g_\alpha(\boldsymbol{r})\rangle, \\ &\quad \lambda_\alpha(\boldsymbol{r}) \quad \text{real} \quad \text{and} \quad \geqslant 0. \end{aligned} \tag{8.37}$$

If the term associated with eq. (8.36) was alone in the equation of motion of σ_{gg}, one would find that the Zeeman degeneracy in g is removed (if the λ_α are all different) and that the states $|g_\alpha(\boldsymbol{r})\rangle$ get a well defined energy shift δE_α, called light shift and equal to

$$\delta E_\alpha = \hbar\,\delta'\lambda_\alpha. \tag{8.38}$$

8.4.2. Properties of light shifts

The light shifts δE_α are, as δ', proportional to Ω_1^2, i.e., to the laser intensity I_{L}. Since the λ_α are positive (see eq. (8.37)), all the δE_α have the same sign, which is the sign of δ, according to eq. (8.33.b).

The variations with the detuning δ of the light shifts δE_α are those of a Lorentz dispersion curve, corresponding to a reactive effect. Recalling

the analysis of section 6.2, and in particular diagram b of fig. 9, one can also consider that the light shifts are associated with a virtual absorption and re-emission of the incident photon (contamination of $|g, \boldsymbol{p}; \boldsymbol{k}_{\mathrm{L}}\epsilon_{\mathrm{L}}\rangle$ by $|e, \boldsymbol{p} + \hbar\boldsymbol{k}_{\mathrm{L}}; 0\rangle$). Light shifts can be considered as the equivalent, for the absorption process, of the Lamb-shift (which is associated with the spontaneous virtual emission and reabsorption of a photon). Another equivalent picture for light shifts is to consider them as the polarization energy of the induced atomic dipole moment in the driving laser field, which explains the denomination "ac-Stark shifts" which is sometimes used.

The first observations of light shifts [52,53,51] predate the use of lasers in atomic physics. They were induced by the light coming from an ordinary discharge lamp (this is why they were called "Lamp-shifts" by Alfred Kastler, in a word play indicating their origin and their analogy with the Lamb-shift). The fact that the light shifts depend on the polarization of the light beam and vary from one ground-state sublevel to the other was essential for their observation. Because of the length of relaxation times in atomic ground states, magnetic resonance curves in atomic ground states are very narrow, and even if the light shifts of two ground-state sublevels differ only by a few Hz, such an effect can be easily detected as a shift of the magnetic resonance curve [52].

To conclude this subsection, we point out a few symmetry properties of the effective Hamiltonian (8.36). The two operators $\widehat{\boldsymbol{d}}^{\pm}$ appearing in expression (8.32) of Λ are vector operators. It follows that the expansion of H_{eff} in irreducible tensor operators $T_q^{(k)}$ of rank k can contain only terms with $k = 0, 1, 2$. The corresponding terms of H_{eff} describe, respectively, a global shift of the ground state ($k = 0$) and a removal of degeneracy equivalent to the one which would be produced by a fictitious magnetic ($k = 1$) or electric ($k = 2$) static field, the direction of these fictitious fields being determined by the polarization vector $\boldsymbol{\epsilon}(\boldsymbol{r})$. The interested reader may find more details in refs. [54] and [55].

8.5. Relaxation associated with optical pumping

8.5.1. Departure rates

The second term of eq. (8.35) describes how the atomic ground state is emptied by the absorption process. The contribution of this term to the rate of variation of the diagonal element of σ in the eigenstate $|g_\alpha\rangle$ of Λ can be written

$$(\langle g_\alpha \mid \dot{\sigma} \mid g_\alpha\rangle)_{\mathrm{abs}} = -\Gamma'_\alpha \langle g_\alpha \mid \sigma \mid g_\alpha\rangle, \tag{8.39}$$

where

$$\Gamma'_\alpha = \Gamma' \lambda_\alpha \tag{8.40}$$

can be interpreted as a rate of departure from the state $|g_\alpha\rangle$. Note that Γ'_α is non-negative as λ_α [see eq.(8.37)], is proportional to the laser intensity $I_L \sim \Omega_1^2$ (as Γ'), and varies with the detuning δ as a Lorentz absorption curve (dissipative effect).

The fact that the $\lambda'_\alpha s$ are not all equal means that the departure rates vary from one sublevel to the other. If one λ_α vanishes, there is no possibility for an atom in the corresponding sublevel $|g_\alpha\rangle$ to leave such a state by photon absorption. The sublevel $|g_\alpha\rangle$ then appears as a trap state.

8.5.2. Feeding of the ground state by spontaneous emission

The atoms which have left the ground state by photon absorption fall back in the ground state by spontaneous emission. Such an effect is described by the last term of eq. (8.35) which is, as the second one, proportional to Γ' (dissipative effect).

One can easily check that the trace of the second term of (8.35) is opposite to the trace of the third one.* This means that there are as many atoms leaving g per unit time as atoms falling back in g.

As a consequence of these absorption–spontaneous emission cycles, population differences can build up between the various Zeeman sublevels. This is the well known principle of optical pumping [6]. Such a process can be actually considered as a transfer of angular momentum from the incident polarized photons to the atoms. For example, if the incident light beam is propagating along Oz and has a right circular polarization σ^+, corresponding to photons having an angular momentum $+\hbar$ along Oz, one can easily show that optical pumping concentrates the atomic population in the Zeeman sublevel with the highest value of the magnetic quantum number along Oz. An example of such a situation will be given in chapter 9.

Optical pumping appears thus as a relaxation process, described by the last two terms of eq. (8.35), and leading the internal atomic state to a new equilibrium state, which generally is quite different from the thermodynamic equilibrium. The characteristic time constants of optical pumping are on the order of

$$\tau_P = \frac{1}{\Gamma'}. \tag{8.41}$$

* The trace of the first term of eq. (8.35), which is a commutator, vanishes. This means that light shifts (which are a reactive effect) cannot change the total population of the ground state.

The pumping time τ_P is inversely proportional to the laser intensity I_L and can become very long if $I_L \to 0$.

8.5.3. Zeeman coherence effects

It may happen that atoms are submitted to two perturbations with different symmetries. For example, a σ^+ polarized beam propagating along the Ox-axis, tends to create in the ground state a magnetization along Ox. If one applies a static magnetic field $\boldsymbol{B}$ along the Oz-axis, this magnetization starts to precess around Oz with a Larmor frequency Ω_B proportional to B. Such a precession will wash out the anisotropy along Ox introduced by the pumping beam if, during the characteristic damping time τ_g of the ground-state (pumping time τ_P, or more generally relaxation time including the effect of collisions, the finite duration of the interaction ...), the rotation angle $\Omega_B \tau_g$ is not small compared to 1. It follows that, when B is scanned around zero, the anisotropy introduced by the pumping beam in the ground state undergoes resonant variations which can be detected by changes in the light absorbed or emitted by the atoms. This is the well known Hanle effect which has been first observed in atomic excited states [56]. The interest of Hanle resonances in atomic ground states is that they are very narrow, since τ_g can be very long. These resonances may thus be used to detect very small magnetic fields, smaller than 10^{-9} Gauss [57,58]. Note that, since Hanle resonances correspond to resonant variations of the photon absorption rate when B is scanned, the momentum transferred to the atomic trajectories varies also in a resonant way. Hanle resonances have been recently detected in this way, by monitoring the deflection of an atomic beam [59].

In equation (8.35), the Hanle resonances appear as resonant variations of the Zeeman coherences (off-diagonal elements of σ in the basis of eigenstates of J_z). They represent an example, among others, of situations where optical pumping cannot be described only in terms of populations (see for example ref. [51]).

8.5.4. Case of a moving atom

All previous considerations suppose implicitly that the atom is at rest, so that it "sees " a pumping light with a constant intensity and a constant polarization. If the atom is moving, and if the laser configuration is such that the local polarization varies in space, the moving atom will "see", in its rest frame a time varying polarization. Since it reacts to these variations of optical pumping with a characteristic time on the order of τ_P, its internal state in $\boldsymbol{r}$ will lag behind the steady state of an atom which would be at rest at the same point. We will discuss later on the role played by such a time lag in the new cooling mechanisms.

8.6. General properties of the mean force

We come back now to the approximate expression (8.26) of the mean force, deduced from the general expression (8.22) after adiabatic elimination of the optical coherences. In this last subsection, we discuss the physical content of eq. (8.26), and we point out the connection which exists, in the low saturation and low velocity limit, between the mean force and the light shifts and absorption rates discussed in sections 8.4 and 8.5. Other similar treatments can be found in refs. [60] and [61].

8.6.1. Reactive component and dissipative component

In eq. (8.26), we split $1/(\delta - \mathrm{i}\Gamma/2)$ in its real and imaginary part. We will call reactive and dissipative respectively the components of the mean force proportional to these real and imaginary parts

$$\boldsymbol{\mathcal{F}}_{\text{react}}(\boldsymbol{r}) = -\hbar \frac{\delta}{\delta^2 + (\Gamma^2/4)} \Big[\langle G^-(\boldsymbol{r}) \big(\boldsymbol{\nabla} G^+(\boldsymbol{r})\big) \rangle + \langle \big(\boldsymbol{\nabla} G^-(\boldsymbol{r})\big)\, G^+(\boldsymbol{r}) \rangle \Big], \tag{8.42a}$$

$$\boldsymbol{\mathcal{F}}_{\text{dissip}}(\boldsymbol{r}) = \mathrm{i}\,\hbar \frac{\Gamma/2}{\delta^2 + (\Gamma^2/4)} \Big[\langle \big(\boldsymbol{\nabla} G^-(\boldsymbol{r})\big)\, G^+(\boldsymbol{r}) \rangle - \langle G^-(\boldsymbol{r}) \big(\boldsymbol{\nabla} G^+(\boldsymbol{r})\big) \rangle \Big]. \tag{8.42b}$$

The denomination reactive and dissipative comes from the δ-dependence of the real and imaginary parts of $1/(\delta - \mathrm{i}\Gamma/2)$. Note however that the δ-dependence of $\boldsymbol{\mathcal{F}}_{\text{react}}$ and $\boldsymbol{\mathcal{F}}_{\text{dissip}}$ is not entirely determined by the two terms which multiply the term in brackets of eqs. (8.42.a) and (8.42.b). The average values which appear inside the brackets depend on the ground-state density matrix σ_{gg} which is obtained by solving eq. (8.29). Such a solution is itself a function of δ and Γ, so that the final expressions of $\boldsymbol{\mathcal{F}}_{\text{react}}$ and $\boldsymbol{\mathcal{F}}_{\text{dissip}}$ will have a more complicated dependence on δ and Γ. Note also that, even if $|\delta| \gg \Gamma$, we must not conclude that $\boldsymbol{\mathcal{F}}_{\text{react}}$ is much larger than $\boldsymbol{\mathcal{F}}_{\text{dissip}}$, since the term in bracket of eq. (8.42.b) can be much larger than the term in bracket of eq. (8.42.a).

One can still give a useful equivalent expression for $\boldsymbol{\mathcal{F}}_{\text{react}}$ and $\boldsymbol{\mathcal{F}}_{\text{dissip}}$ by using an expansion of the laser electric field $\boldsymbol{E}_{\text{L}}$ in plane waves. If we use for the positive frequency component $\boldsymbol{E}_{\text{L}}^+$ the expansion

$$\boldsymbol{E}_{\text{L}}^+(\boldsymbol{r}) = \sum_{\mu} \boldsymbol{E}_{\mu}^+(\boldsymbol{r}), \tag{8.43}$$

where the $\mathbf{r}$-dependence of $\boldsymbol{E}_{\mu}^+$ is given by

$$\boldsymbol{E}_{\mu}^+(\boldsymbol{r}) \sim \mathrm{e}^{\mathrm{i}\boldsymbol{k}_{\mu}\cdot\boldsymbol{r}}, \tag{8.44}$$

then, we can write

$$\boldsymbol{\nabla} G^{\pm} = \pm \mathrm{i} \sum_{\mu} \boldsymbol{k}_{\mu} G^{\pm}_{\mu}, \tag{8.45}$$

where, according to eqs. (8.7) and (8.43)

$$\hbar\, G^{\pm}_{\mu} = \boldsymbol{d}^{\pm} \cdot \boldsymbol{E}^{\pm}_{\mu}(\boldsymbol{r}) \tag{8.46}$$

Inserting eq. (8.45) into eq. (8.42) finally gives

$$\boldsymbol{\mathcal{F}}_{\text{react}} = -\mathrm{i} \frac{\delta}{\delta^2 + (\Gamma^2/4)} \sum_{\mu} \sum_{\nu} \hbar\, \boldsymbol{k}_{\mu} \left[\langle G^{-}_{\nu} G^{+}_{\mu} \rangle - \langle G^{-}_{\mu} G^{+}_{\nu} \rangle \right], \tag{8.47a}$$

$$\boldsymbol{\mathcal{F}}_{\text{dissip}} = +\frac{\Gamma/2}{\delta^2 + (\Gamma^2/4)} \sum_{\mu} \sum_{\nu} \hbar\, \boldsymbol{k}_{\mu} \left[\langle G^{-}_{\nu} G^{+}_{\mu} \rangle + \langle G^{-}_{\mu} G^{+}_{\nu} \rangle \right]. \tag{8.47b}$$

8.6.2. Interpretation of the reactive component

Comparing the expression (8.42.a) of $\boldsymbol{\mathcal{F}}_{\text{react}}$ and the expression (8.36) of the effective Hamiltonian H_{eff} describing the light shifts of the ground state sublevels shows that $\boldsymbol{\mathcal{F}}_{\text{react}}$ can be written

$$\boldsymbol{\mathcal{F}}_{\text{react}} = -\langle\, \boldsymbol{\nabla} H_{\text{eff}} \,\rangle, \tag{8.48}$$

which clearly demonstrates the close connection which exists between the reactive component of the mean force and light shifts.

An equivalent expression of H_{eff} in terms of its eigenvalues E_{α} and eigenstates $|g_{\alpha}\rangle$ is

$$H_{\text{eff}} = \sum_{\alpha} E_{\alpha}(\boldsymbol{r}) |g_{\alpha}(\boldsymbol{r})\rangle\langle g_{\alpha}(\boldsymbol{r})|. \tag{8.49}$$

Taking the gradient of eq. (8.49) (and omitting $\boldsymbol{r}$ to simplify the notation) gives

$$\begin{aligned} \boldsymbol{\nabla} H_{\text{eff}} = & \sum_{\alpha} (\boldsymbol{\nabla} E_{\alpha})\, |g_{\alpha}\rangle\langle g_{\alpha}| \\ & + \sum_{\alpha} E_{\alpha} \Big[(\boldsymbol{\nabla} |g_{\alpha}\rangle) \langle g_{\alpha}| + |g_{\alpha}\rangle (\boldsymbol{\nabla} \langle g_{\alpha}|) \Big], \end{aligned} \tag{8.50}$$

which, inserted in eq. (8.48), leads to

$$\begin{aligned}\boldsymbol{\mathcal{F}}_{\text{react}} = &-\sum_{\alpha}(\boldsymbol{\nabla}E_{\alpha})\Pi_{\alpha} \\ &-\sum_{\alpha}E_{\alpha}\Big[\langle g_{\alpha}|\sigma(\boldsymbol{\nabla}|g_{\alpha}\rangle) + (\boldsymbol{\nabla}\langle g_{\alpha}|)\sigma|g_{\alpha}\rangle\Big],\end{aligned} \tag{8.51}$$

where

$$\Pi_{\alpha} = \langle g_{\alpha} \mid \sigma \mid g_{\alpha}\rangle \tag{8.52}$$

is the population of the ground-state sublevel $|g_{\alpha}\rangle$.

The first term of eq. (8.51) has a straightforward interpretation, analogous to the dressed atom interpretation of the mean dipole force given in section 7.3 for a two-level atom (see eq. (7.10)). This term is just the average value of the forces $-\boldsymbol{\nabla}E_{\alpha}$ associated with the spatial gradients of the light shifted ground-state sublevels, weighted by the probabilities of occupation Π_{α} of these sublevels.

In order to interpret the second line of (8.51), we suppose that the atom is displaced from $\boldsymbol{r}$ to $\boldsymbol{r} + \mathrm{d}\boldsymbol{r}$, and we calculate the work done against the reactive force

$$\begin{aligned}-\boldsymbol{\mathcal{F}}_{\text{react}} \cdot \mathrm{d}\boldsymbol{r} = &\sum_{\alpha}\Pi_{\alpha}\cdot\mathrm{d}E_{\alpha} \\ &+\sum_{\alpha}E_{\alpha}\Big[\langle g_{\alpha} \mid \sigma \mid \mathrm{d}g_{\alpha}\rangle + \langle \mathrm{d}g_{\alpha} \mid \sigma \mid g_{\alpha}\rangle\Big],\end{aligned} \tag{8.53}$$

where $\mathrm{d}E_{\alpha}$ and $|\mathrm{d}g_{\alpha}\rangle$, given by

$$\mathrm{d}E_{\alpha} = \mathrm{d}\boldsymbol{r}\cdot\boldsymbol{\nabla}E_{\alpha}, \tag{8.54a}$$

$$|\mathrm{d}g_{\alpha}\rangle = \mathrm{d}\boldsymbol{r}\cdot\boldsymbol{\nabla}|g_{\alpha}\rangle, \tag{8.54b}$$

represent the variations of E_{α} and $|g_{\alpha}\rangle$ between $\boldsymbol{r}$ and $\boldsymbol{r}+\mathrm{d}\boldsymbol{r}$. The second line of eq. (8.53), which originates from the second line of eq. (8.51), is associated with the spatial variations of the wave functions of the sublevels $|g_{\alpha}\rangle$. It can be written, to first order in $\mathrm{d}\boldsymbol{r}$

$$\sum_{\alpha}E_{\alpha}\,\mathrm{d}\Pi_{\alpha}^{\text{nonad}}, \tag{8.55}$$

where

$$\mathrm{d}\Pi_{\alpha}^{\text{nonad}} = \langle g_{\alpha}(\boldsymbol{r}+\mathrm{d}\boldsymbol{r}) \mid \sigma \mid g_{\alpha}(\boldsymbol{r}+\mathrm{d}\boldsymbol{r})\rangle - \langle g_{\alpha}(\boldsymbol{r}) \mid \sigma \mid g_{\alpha}(\boldsymbol{r})\rangle \tag{8.56}$$

is the non-adiabatic variation of the population of the state $|g_\alpha\rangle$ due to the spatial variations of the wave functions. It follows that the second line of eq. (8.51) represents the contribution of non-adiabatic transitions between the various ground-state sublevels, induced by atomic motion and due to the spatial variations of the wave functions of the light shifted ground-state sublevels.

Finally, we discuss the physical content of eq. (8.47.a), deduced from the plane wave expansion of the laser field. Since the force exerted by the laser beam comes from a disappearance of photons $\boldsymbol{k}_\mu$ from the various plane waves μ forming the laser wave, each of these photons carrying a momentum $\hbar\boldsymbol{k}_\mu$, one can interpret the coefficient of $\hbar\boldsymbol{k}_\mu$ in eq. (8.47.a) as the mean number of photons absorbed per unit time in the plane wave μ. The fact that this coefficient depends on ν means that the field $\boldsymbol{E}_\mu$ of the plane wave μ interacts with the atomic dipole induced by the wave ν. It follows that

$$\frac{\mathrm{d}N_{\mu\nu}^{\mathrm{react}}}{\mathrm{d}t} = -\mathrm{i}\frac{\delta}{\delta^2 + (\Gamma^2/4)}\left[\langle G_\nu^- G_\mu^+\rangle - \langle G_\mu^- G_\nu^+\rangle\right] \tag{8.57}$$

can be interpreted as the mean number of photons μ absorbed per unit time out of the wave μ interacting with the reactive component of the dipole moment induced by the wave ν. We take here the reactive component of the dipole moment because of the δ-dependence of eq. (8.57). From eq. (8.57), it follows that

$$\frac{\mathrm{d}N_{\mu\mu}^{\mathrm{react}}}{\mathrm{d}t} = 0, \tag{8.58a}$$

$$\frac{\mathrm{d}N_{\mu\nu}^{\mathrm{react}}}{\mathrm{d}t} = -\frac{\mathrm{d}N_{\nu\mu}^{\mathrm{react}}}{\mathrm{d}t}. \tag{8.58b}$$

Such a result is easy to understand. Reactive effects involving a single wave cannot lead to photon absorption. This is the meaning of eq. (8.58.a). But, according to eq. (8.58.b), photons can disappear from one wave, μ for example, and reappear in the other wave ν of the pair $\mu\nu$. This is a redistribution process. During such a process, the total energy of the field does not change, because the waves μ, ν have the same frequency. But since $\boldsymbol{k}_\mu \neq \boldsymbol{k}_\nu$, there is a change of momentum of the field. The corresponding change of the atomic momentum is at the origin of $\boldsymbol{\mathcal{F}}_{\mathrm{react}}$, which can be written according to eq. (8.57)

$$\boldsymbol{\mathcal{F}}_{\mathrm{react}} = \sum_{\text{pairs } \mu\nu} \hbar(\boldsymbol{k}_\mu - \boldsymbol{k}_\nu)\frac{\mathrm{d}N_{\mu\nu}^{\mathrm{react}}}{\mathrm{d}t}. \tag{8.59}$$

8.6.3. Interpretation of the dissipative component

Using the same type of argument as in the previous subsection, one shows from eq. (8.47.b) that

$$\frac{\mathrm{d}N_{\mu\nu}^{\mathrm{dissip}}}{\mathrm{d}t} = \frac{\Gamma/2}{\delta^2 + (\Gamma^2/4)} \left[\langle G_\nu^- G_\mu^+ \rangle + \langle G_\mu^- G_\nu^+ \rangle \right] \tag{8.60}$$

is the number of photons absorbed per unit time out of the wave μ interacting with the dissipative component of the dipole moment induced by the wave ν.

The equations corresponding to eq. (8.58) are now

$$\frac{\mathrm{d}N_{\mu\mu}^{\mathrm{dissip}}}{\mathrm{d}t} = \frac{\Gamma}{\delta^2 + (\Gamma^2/4)} \langle G_\mu^- G_\mu^+ \rangle \neq 0 \tag{8.61a}$$

$$\frac{\mathrm{d}N_{\mu\nu}^{\mathrm{dissip}}}{\mathrm{d}t} = + \frac{\mathrm{d}N_{\nu\mu}^{\mathrm{dissip}}}{\mathrm{d}t} \tag{8.61b}$$

The contribution of the wave μ alone to $\boldsymbol{\mathcal{F}}_{\mathrm{dissip}}$ is different from zero and equal to

$$\frac{\Gamma}{\delta^2 + (\Gamma^2/4)} \hbar \boldsymbol{k}_\mu \langle G_\mu^- G_\mu^+ \rangle. \tag{8.62}$$

Such a term represents the radiation pressure exerted by the wave μ independently of the other waves. Note however that eq. (8.62) depends implicitly on the other waves ν since the average values appearing in eq. (8.62) are taken in σ_{gg}, which itself is determined by the total laser field $\boldsymbol{E}_{\mathrm{L}}$, i.e., by the whole set of plane waves forming $\boldsymbol{E}_{\mathrm{L}}$.

There are also cross terms $\mu \neq \nu$ in the expression (8.47.b) of $\boldsymbol{\mathcal{F}}_{\mathrm{dissip}}$, the contribution of the pair (μ, ν) being equal to

$$\frac{\Gamma/2}{\delta^2 + (\Gamma^2/4)} \hbar (\boldsymbol{k}_\mu + \boldsymbol{k}_\nu) \left[\langle G_\nu^- G_\mu^+ \rangle + \langle G_\mu^- G_\nu^+ \rangle \right]. \tag{8.63}$$

Such terms describe interference effects between the waves μ and ν. The radiation pressure exerted by the wave μ is modified by the presence of the wave ν and vice versa. Equation (8.61.b) means that, if the absorption of the wave μ is modified by the presence of the wave ν, the absorption of the wave ν is modified by the same amount by the presence of the wave μ. Here we have not a redistribution process as in the previous subsection, but a similar increase (or decrease) of the absorption of both waves due to interference effects.

8.6.4. Particular case of one-dimensional molasses

Suppose that the laser configuration is formed by two counterpropagating plane waves 1 and 2, with

$$\boldsymbol{k}_1 = \boldsymbol{k}, \qquad \boldsymbol{k}_2 = -\boldsymbol{k}. \tag{8.64}$$

As shown in subsection 8.6.2, $\boldsymbol{\mathcal{F}}_{\text{react}}$ is a pure redistribution force, which does not contain single wave terms. Equation (8.59) becomes now, taking eq. (8.64) into account

$$\boldsymbol{\mathcal{F}}_{\text{react}} = \frac{\delta}{\delta^2 + (\Gamma^2/4)}\, 2\hbar\boldsymbol{k}\,\mathrm{i}\left[\langle G_1^- G_2^+\rangle - \langle G_2^- G_1^+\rangle\right]. \tag{8.65}$$

Since $\boldsymbol{k}_1 + \boldsymbol{k}_2 = \boldsymbol{0}$, the cross term (8.63) of $\boldsymbol{\mathcal{F}}_{\text{dissip}}$ vanishes. The radiation pressure of each wave is increased by the presence of the other wave, but these extra forces have the same modulus but opposite directions, so that they cancel out. We are left with a sum of single wave terms which can be written

$$\boldsymbol{\mathcal{F}}_{\text{dissip}} = \frac{\Gamma}{\delta^2 + (\Gamma^2/4)}\, \hbar\boldsymbol{k}\left[\langle G_1^- G_1^+\rangle - \langle G_2^- G_2^+\rangle\right]. \tag{8.66}$$

It follows that, for one-dimensional molasses, $\boldsymbol{\mathcal{F}}_{\text{dissip}}$ is just equal to the difference between the radiation pressures exerted separately by the two waves.

We will conclude with a remark concerning the polarizations $\boldsymbol{\epsilon}_1$ and $\boldsymbol{\epsilon}_2$ of the two counterpropagating waves. If we take $\boldsymbol{k}_1 = -\boldsymbol{k}_2$ along Oz, these polarization vectors are perpendicular to Oz, because of the transversality of the field, and can therefore be considered as linear superpositions of the right and left circular polarizations σ^+ and σ^-. It follows that all the matrix elements of $G_\mu^- G_\nu^+$, with $\mu, \nu = 1$ or 2, in the ground-state manifold, satisfy the selection rule $\Delta m = 0, \pm 2$, where m is the magnetic quantum number along Oz (G_μ^- and G_ν^+ change m by $+1$ or -1). Consequently, if the angular momentum J_g of the ground state is equal to $J_g = 1/2$, one concludes that all the $G_\mu^- G_\nu^+$ are diagonal in the basis of eigenstates of J_z, and also $G^- G^+$. In such a case, the eigenstates of the effective Hamiltonian H_{eff} which, according to eq. (8.36), is proportional to $G^- G^+$, are independent of z.

9. Low intensity Sisyphus cooling

9.1. Introduction

During the last few years, spectacular developments have allowed the performance of laser cooling to be improved by orders of magnitude. The

starting point of these developments was the demonstration, by the N.I.S.T. group at Gaithersburg, that the Doppler limit could be overcome [62]. For a discussion of this experiment and of the subsequent ones from various groups, we refer the reader to Phillips' course in this volume. The purpose of this chapter and the following one is to present a few new cooling mechanisms which, we think, are responsible for the very low temperatures which have been measured.

This chapter is devoted to the analysis of a low intensity version of the Sisyphus cooling mechanism presented in chapter 7 for a two-level atom moving in an intense laser standing wave. As in chapter 7, we have an atom moving in a bipotential, and jumping preferentially from the tops of the hills of one potential curve to the bottoms of the valleys of the other potential curve, so that, on the average, the atom is running up the hills more than down, as did Sisyphus in the Greek mythology. But, now, the bipotential is no longer associated with the two dressed states originating from the excited state e and the ground state g (more precisely from $|e, N\rangle$ and $|g, N+1\rangle$). It is associated with two ground-state Zeeman sublevels which undergo spatially modulated light shifts and between which optical pumping transitions occur with a rate which is also spatially modulated. We show that in this case a very efficient Sisyphus cooling can appear at very low intensity, when the saturation parameter s is very small.

We begin in section 9.2 by introducing a one-dimensional model consisting of a laser configuration exhibiting strong polarization gradients and of a simple atomic transition leading to a mean radiative force which is only due to the spatial gradients of light shifts. Using the results of chapter 8, we determine in section 9.3 the light shifts of the atomic ground state sublevels as well as the optical pumping transition rates between these sublevels. We then consider in section 9.4 a moving atom and we show how the spatial modulation of light shifts and optical pumping rates in the laser polarization gradient can conspire to produce a Sisyphus cooling. A more quantitative analysis is presented in section 9.5 in the traditional case where the internal times T_{int} are much shorter than the external times T_{ext}. We evaluate the friction coefficient and give an order of magnitude of the equilibrium temperature. Finally, some indications are given in section 9.6 on the less usual case where the external times become of the order of or shorter than the internal times. Such a case is actually important because it corresponds to the situation where the low intensity Sisyphus cooling reaches its limits.

We will follow here the presentation of refs. [63] and [64]. More details may be found in these references, and in ref. [65] which gives the results of a numerical integration of optical Bloch equations. A general review of

the field is presented in ref. [85].

9.2. Presentation of the model

9.2.1. Laser configuration

We consider two counterpropagating waves along Oz, with orthogonal polarizations $\boldsymbol{\epsilon}_x$ and $\boldsymbol{\epsilon}_y$, and the same amplitude $\mathcal{E}_0$ (fig. 17a). With an appropriate choice of the relative phases of the two waves, the laser electric field in z can be written

$$\boldsymbol{E}_{\mathrm{L}}(z,t) = \boldsymbol{E}_{\mathrm{L}}^{+}(z)\, \mathrm{e}^{-\mathrm{i}\omega_{\mathrm{L}}t} + \mathrm{c.c.} \tag{9.1}$$

with

$$\boldsymbol{E}_{\mathrm{L}}^{+}(z) = \tfrac{1}{2}(\boldsymbol{\epsilon}_x\, \mathrm{e}^{\mathrm{i}kz} - \mathrm{i}\,\boldsymbol{\epsilon}_y\, \mathrm{e}^{-\mathrm{i}kz})\, \mathcal{E}_0. \tag{9.2}$$

As in eq. (8.11), one can then write

$$\boldsymbol{E}_{\mathrm{L}}^{+}(z) = \tfrac{1}{2}\mathcal{E}_0\sqrt{2}\, \boldsymbol{\epsilon}\,(z) = \tfrac{1}{2}\mathcal{E}_{\mathrm{L}}\, \boldsymbol{\epsilon}\,(z), \tag{9.3}$$

where $\mathcal{E}_{\mathrm{L}}$ is a real amplitude which is independent of z and equal to $\mathcal{E}_0\sqrt{2}$ and where the normalized polarization vector $\boldsymbol{\epsilon}(z)$ is given by

$$\boldsymbol{\epsilon}\,(z) = \cos kz\, \boldsymbol{\epsilon}_- - \mathrm{i}\sin kz\, \boldsymbol{\epsilon}_+. \tag{9.4}$$

According to eq. (9.4), the laser polarization is an elliptical one which is particularly simple in certain places: σ^- in $z = 0$, linear along $(\boldsymbol{\epsilon}_x - \boldsymbol{\epsilon}_y)/\sqrt{2}$ in $z = \lambda/8$, σ^+ in $z = \lambda/4$, linear along $(\boldsymbol{\epsilon}_x + \boldsymbol{\epsilon}_y)/\sqrt{2}$ in $z = 3\lambda/8$, σ^- in $z = \lambda/2$ and so on (see fig. 17a).

The laser configuration of fig. 17a exhibits therefore a strong gradient of ellipticity along Oz, on a length scale equal to a fraction of the wavelength. Since the internal atomic state depends on the polarization of the pumping light, such a configuration leads, as will be shown below, to large non-adiabatic effects, since a moving atom has to respond to the variations of the laser polarization due to its motion with an internal response time (the optical pumping time) which becomes very long at low intensity. By contrast, if the two counterpropagating laser waves had the same polarization one would have just a gradient of intensity, without any polarization gradient. In the low intensity regime considered here, this would produce only a slight change of the total population in the ground state g (which remains close to 1), without any change of the anisotropy in g (characterized by the population differences between the ground-state sublevels and the Zeeman coherences between them).

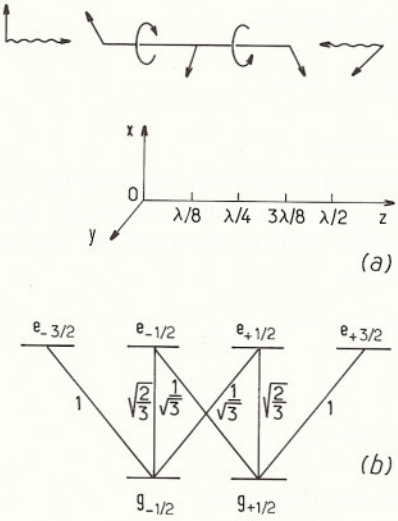

Fig. 17. (a) Lin ⊥ Lin laser configuration, exhibiting a strong polarization gradient along Oz. (b) Clebsch–Gordan coefficients for a $J_g = 1/2 \leftrightarrow J_e = 3/2$ transition.

9.2.2. Atomic transition. Simplifications for the mean force

As for usual laser cooling experiments, we consider a transition $J_g \to J_e = J_g + 1$. We take the simplest possible value of J_g leading to a degenerate ground state, i.e., $J_g = 1/2$. Figure 17b gives the various Clebsch–Gordan coefficients corresponding to a transition $J_g = 1/2 \to J_e = 3/2$.

Since there are only two Zeeman sublevels in the ground state, the matrix representing $G^- G^+$ in the ground-state manifold is diagonal (see end of subsection 8.6.4). It follows that the effective Hamiltonian H_{eff} describing the light shifts of the ground-state sublevels is diagonal in the basis $\{|g_{\pm 1/2}\rangle\}$ of eigenstates of J_z, so that the eigenstates of H_{eff}, which coincide with $|g_{\pm 1/2}\rangle$, are independent of z. One can thus, in the expression (8.51) of $\boldsymbol{\mathcal{F}}_{\text{react}}$, neglect the second line which is associated with the gradients of the wave functions, and write

$$\boldsymbol{\mathcal{F}}_{\text{react}} = -\Pi_{+1/2} \boldsymbol{\nabla} E_{+1/2} - \Pi_{-1/2} \boldsymbol{\nabla} E_{-1/2}, \tag{9.5}$$

where $\Pi_{\pm 1/2}$ and $E_{\pm 1/2}$ are the populations and the energies of $|g_{\pm 1/2}\rangle$.

Since we consider here one-dimensional molasses, we can use the expression (8.66) of $\boldsymbol{\mathcal{F}}_{\text{dissip}}$, which involves the radiation pressures exerted separately by the two counterpropagating waves. Here also, the matrices representing the two operators $G_1^- G_1^+$ and $G_2^- G_2^+$ appearing in eq. (8.66) are diagonal in the basis $\{|g_{\pm 1/2}\rangle\}$ of eigenstates of J_z (see end of subsection

8.6.4). Since both counterpropagating waves have a linear polarization, one can then easily show that $\langle G_1^- G_1^+ \rangle$ and $\langle G_2^- G_2^+ \rangle$ are equal and proportional to $\Pi_{-1/2} + \Pi_{+1/2} = 1$, i.e., independent of the internal atomic state. It follows that

$$\boldsymbol{\mathcal{F}}_{\text{dissip}} = \mathbf{0}. \tag{9.6}$$

The choice of the simple atomic transition of fig. 17b leads therefore to a mean force which is due only to the spatial variations of the light-shifted energies of the ground-state sublevels. This is why the new cooling mechanism analyzed in this chapter can be considered as a pure Sisyphus effect.

9.3. Dynamics of the internal degrees of freedom

9.3.1. Light shifts of the ground-state sublevels

The light shifts $E_{\pm 1/2}(z)$ of $|g_{\pm 1/2}\rangle$ can be written

$$E_{\pm\frac{1}{2}}(z) = \hbar\, \delta' \Lambda_{\pm\pm}(z), \tag{9.7}$$

where $\Lambda_{++}(z)$ and $\Lambda_{--}(z)$ are the diagonal elements of the operator $\Lambda(z)$ defined in eq. (8.32), which are the only non-zero matrix elements of this operator, and where δ' is given by eq. (8.33.b). Note that, since the laser amplitude in z, $\mathcal{E}_{\text{L}} = \mathcal{E}_0\sqrt{2}$, is independent of z (see eq. (9.3)), the Rabi frequency Ω_1, appearing in eq. (8.33.b) is also independent of z, so that the only z-dependence in eq. (9.7) comes from the matrix elements of Λ, and not from δ'. Note that δ' can be written

$$\delta' = \delta\, s/2 = \delta\, s_0, \tag{9.8}$$

where s is the saturation parameter associated with $\mathcal{E}_{\text{L}}$ and $s_0 = s/2$ the saturation parameter associated with $\mathcal{E}_0$, i.e., with each of the two counterpropagating waves.

Inserting eq. (9.4) into eq. (8.32), and using for the matrix elements of $\boldsymbol{\epsilon}_q \cdot \widehat{\boldsymbol{d}}_{\pm}$ the Clebsh–Gordan coefficients of fig. 17b (see eqs. (8.9) and (8.10)), we get

$$\Lambda_{++}(z) = \sin^2 kz + \tfrac{1}{3}\cos^2 kz = 1 - \tfrac{2}{3}\cos^2 kz, \tag{9.9a}$$

$$\Lambda_{--}(z) = \cos^2 kz + \tfrac{1}{3}\sin^2 kz = 1 - \tfrac{2}{3}\sin^2 kz. \tag{9.9b}$$

Figure 18 represents the spatial variations of $E_{\pm 1/2}(z)$. We have supposed $\delta < 0$, so that the light shifts are negative. At $z = 0, \lambda/2, \ldots$ where the

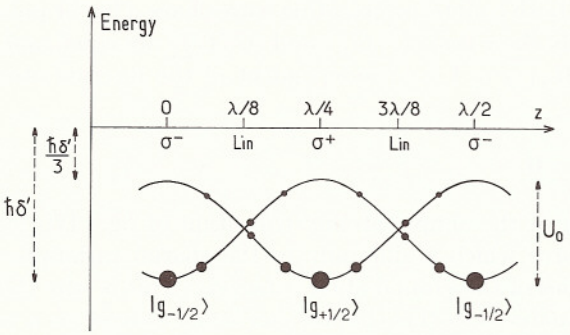

Fig. 18. Light shifts $E_{\pm 1/2}(z)$ of $|g_{\pm 1/2}\rangle$ versus z. The size of the solid circles is proportional to the steady state populations of $|g_{\pm 1/2}\rangle$ for an atom at rest in z. We have supposed $\delta < 0$.

polarization is σ^-, the sublevel $|g_{-1/2}\rangle$ is shifted downwards (with respect to the zero of energy, corresponding to the absence of the laser) three times more than the sublevel $|g_{+1/2}\rangle$, because the σ^- transition starting from $|g_{-1/2}\rangle$ is three times more intense that the σ^- transition starting from $|g_{+1/2}\rangle$. The situation is opposite in $z = \lambda/4$, where the polarization is σ^+, and where the sublevel $|g_{+1/2}\rangle$ is shifted three times more than $|g_{-1/2}\rangle$. Finally, in $z = \lambda/8, 3\lambda/8, \ldots$ where the polarization is linear, both sublevels undergo the same light shift.

Using eqs. (9.9) and (9.7), we can also write

$$E_{+1/2}(z) = -\frac{3U_0}{2} + U_0 \cos^2 kz, \tag{9.10a}$$

$$E_{-1/2}(z) = -\frac{3U_0}{2} + U_0 \sin^2 kz, \tag{9.10b}$$

where

$$U_0 = -\tfrac{2}{3}\hbar\,\delta' = -\tfrac{2}{3}\hbar\delta s_0 \tag{9.11}$$

is the depth of the potential wells associated with the spatial oscillations of $E_{+1/2}(z)$ and $E_{-1/2}(z)$. Equations (9.10) allow also the expression (9.5) of the reactive force, which coincides with the total mean force because of eq. (9.6), to be transformed into

$$\boldsymbol{\mathcal{F}}_{\text{react}}(z) = \boldsymbol{\mathcal{F}}(z) = \boldsymbol{\epsilon}_z k\, U_0 \mathcal{M}(z) \sin 2kz, \tag{9.12}$$

where

$$\mathcal{M}(z) = \Pi_{+1/2}(z) - \Pi_{-1/2}(z) \tag{9.13}$$

is the difference between the populations of the two sublevels.

9.3.2. Optical pumping rates

We first consider the departure rates from $|g_{\pm 1/2}\rangle$, $\Gamma'_{\pm 1/2}(z)$, associated with the anticommutator of eq. (8.35), and given by (see also eqs. (8.39) and (8.40))

$$\Gamma'_{+1/2}(z) = \Gamma' \Lambda_{++}(z) = \Gamma' \left(1 - \tfrac{2}{3}\cos^2 kz\right), \tag{9.14a}$$

$$\Gamma'_{-1/2}(z) = \Gamma' \Lambda_{--}(z) = \Gamma' \left(1 - \tfrac{2}{3}\sin^2 kz\right), \tag{9.14b}$$

where

$$\Gamma' = \Gamma s/2 = \Gamma s_0. \tag{9.15}$$

The last term of eq. (8.35), which describes how atoms return to the ground state after having absorbed one photon can be easily calculated, using the expression (9.4) of $\epsilon(z)$ and the Clebsh–Gordan coefficients of fig. 17b. Such a term couples populations only to populations, because the value 1/2 of J_g excludes any off-diagonal element $\langle g_m|\sigma_{gg}|g_{m'}\rangle$ of σ_{gg} with $m - m' = \pm 2$.

Adding the contributions of the last two terms of eq. (8.35), and using (9.14), we finally get, for the populations $\Pi_{\pm 1/2}$ of $|g_{\pm 1/2}\rangle$, the following rate equations describing the effect of optical pumping

$$\frac{\mathrm{d}}{\mathrm{d}t}\Pi_{+1/2}(z) = -\Gamma_{+\to -}(z)\,\Pi_{+1/2}(z) + \Gamma_{-\to +}(z)\,\Pi_{-1/2}(z), \tag{9.16a}$$

$$\frac{\mathrm{d}}{\mathrm{d}t}\Pi_{-1/2}(z) = -\Gamma_{-\to +}(z)\,\Pi_{-1/2}(z) + \Gamma_{+\to -}(z)\,\Pi_{+1/2}(z), \tag{9.16b}$$

where

$$\Gamma_{+\to -}(z) = \tfrac{2}{9}\,\Gamma' \cos^2 kz, \tag{9.17a}$$

$$\Gamma_{-\to +}(z) = \tfrac{2}{9}\,\Gamma' \sin^2 kz \tag{9.17a}$$

are, respectively, the optical pumping rates from $|g_{+1/2}\rangle$ to $|g_{-1/2}\rangle$ and from $|g_{-1/2}\rangle$ to $|g_{+1/2}\rangle$.

Subtracting eq. (9.16.b) from eq. (9.16.a) and using eqs. (9.13) and (9.17), we also get for $\mathcal{M}(z)$ the following equation

$$\frac{\mathrm{d}}{\mathrm{d}t}\mathcal{M}(z) = -\frac{1}{\tau_{\mathrm{P}}}[\,\mathcal{M}(z) + \cos 2kz\,], \tag{9.18}$$

where τ_P, given by

$$\tau_P = \frac{9}{2\Gamma'} = \frac{9}{2\Gamma s_0} \tag{9.19}$$

is the optical pumping time characterizing the time constant with which the population difference reaches its equilibrium value.

It is clear from (9.17) that, as the light shifts $E_{\pm 1/2}(z)$ given in eq. (9.10), the optical pumping rates from one sublevel to the other are spatially modulated. The same function of z, $\cos^2 kz$, appears in eqs. (9.10.a) and (9.17.a). There is therefore a perfect correlation between the spatial dependence of the light shift of $|g_{+1/2}\rangle$ and the spatial dependence of the optical pumping rate from $|g_{+1/2}\rangle$ to $|g_{-1/2}\rangle$. More precisely, $E_{+1/2}(z)$ and $\Gamma_{+\to -}(z)$ reach their maximal values for the same values of z, those for which $\cos^2 kz = 1$. A similar result holds for $E_{-1/2}(z)$ and $\Gamma_{-\to +}(z)$. This means that the transition rate from $|g_{+1/2}\rangle$ (respectively $|g_{-1/2}\rangle$) to $|g_{-1/2}\rangle$ (respectively $|g_{+1/2}\rangle$) is maximum at the places where the energy of $|g_{+1/2}\rangle$ (respectively $|g_{-1/2}\rangle$) is the highest. We will see in the next subsection that, for a moving atom, the most probable processes are those where the atom leaves one of the two oscillating potential curves of fig. 18 at the top of one hill and is transferred to the bottom of one valley of the other potential curve. This is the key point of the cooling mechanism discussed in this chapter.

9.3.3. Steady-state populations for an atom at rest

If we suppose that the atom is at rest in z, all coefficients of eq. (9.18) are time independent. This equation has therefore a steady-state solution given by

$$\mathcal{M}^{st}(z) = \Pi^{st}_{+1/2}(z) - \Pi^{st}_{-1/2}(z) = -\cos 2kz. \tag{9.20}$$

Combining this equation with the normalization condition $\Pi^{st}_{+1/2}(z) + \Pi^{st}_{-1/2}(z) = 1$, we get

$$\Pi^{st}_{+1/2}(z) = \sin^2 kz, \tag{9.21a}$$

$$\Pi^{st}_{-1/2}(z) = \cos^2 kz, \tag{9.21b}$$

The size of the solid circles of fig. 18 is proportional to these steady-state populations. For a given value of z, the most populated sublevel is the lowest one. At the top of the hills, the population is equal to zero whereas it is equal to 1 at the bottom of the valleys.

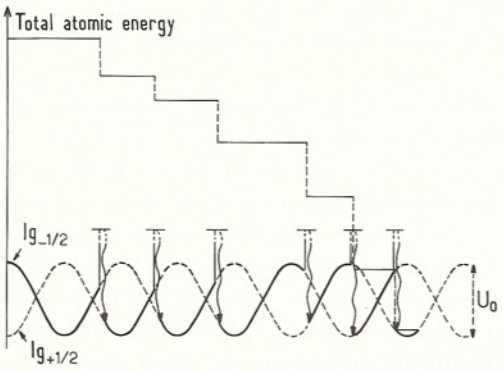

Fig. 19. Sisyphus effect for a moving atom. Because of the strong correlation between the spatial dependencies of light shifts and optical pumping rates, the atom loses potential energy when it jumps from one sublevel to the other. The upper part of the figure gives the corresponding variations of the total energy. The random path sketched here has been obtained for $\delta = -5\Gamma$, $\Omega_1 = 2.3\Gamma$, and for the cesium recoil shift $\hbar k^2/M\Gamma = 7.8 \times 10^{-4}$.

9.4. Cooling mechanism for a moving atom

9.4.1. Sisyphus effect

Consider an atom moving with velocity v along Oz in the bipotential $E_{\pm 1/2}(z)$ of fig. 18. We suppose that initially v is large enough

$$\tfrac{1}{2}Mv^2 \gg U_0, \tag{9.22a}$$

$$kv \gg \Gamma', \tag{9.22b}$$

so that, on the one hand, the atom is not trapped in one of the potential wells and, on the other hand, travels over several wavelengths before being optically pumped from one sublevel to the other. Note however that v is small enough so that we can still neglect kv in comparison with Γ (negligible Doppler cooling)

$$kv \ll \Gamma. \tag{9.23}$$

Condition (9.23), which can be written $v\Gamma^{-1} \ll \lambda$, means also that the atom travels over a distance very small compared to λ during the duration Γ^{-1} of a fluorescence cycle. In other words, each optical pumping cycle can be considered as occurring instantaneously in a given point of the Oz-axis.

Suppose that initially the atom is in the sublevel $|g_{-1/2}\rangle$ (fig. 19). As long as it remains in this sublevel, its total (kinetic + potential) energy,

represented in the upper part of fig. 19, remains constant. We neglect for the moment the recoil due to the absorbed and re-emitted photons in the fluorescence cycles $g_{-1/2} \rightarrow e_{+1/2}$ (or $e_{-3/2}$) $\rightarrow g_{-1/2}$ where the atom returns in $g_{-1/2}$. Because of the spatial dependence of the optical pumping rates, discussed at the end of subsection 9.3.2, the transfer by optical pumping from $g_{-1/2}$ to $g_{+1/2}$ will occur preferentially near the maxima of $E_{-1/2}(z)$, and the atom will jump suddenly from a point near the top of one hill of $E_{-1/2}(z)$ to a point near the bottom of one valley of $E_{+1/2}(z)$. The corresponding change δU of its potential energy will therefore be negative and on the order (in absolute value) of U_0. If we neglect here also the recoil of the absorbed and re-emitted photons, the total energy of the atom will decrease suddenly by an amount δU (first discontinuity in the curve represented in the upper part of fig. 19).

From there, the same sequence can be repeated. On the average, the atom is running up the hills more than down and its total energy decreases by a series of discontinuous steps until its kinetic energy becomes on the order of or smaller than U_0 (see for example the last jump of fig. 19). Such a qualitative analysis, which is confirmed by the results of more quantitative treatments, therefore shows that the kinetic energies which can be achieved by low intensity Sisyphus cooling are on the order of the depth U_0 of the potential wells associated with the spatially modulated light shifts: $Mv^2/2 \sim U_0$. For large detunings ($|\delta| \gg \Gamma$), which is the interesting case where the light shifts of the ground-state sublevels are larger than their widths, U_0 is on the order of $\hbar\Omega_1^2/|\delta|$, so that

$$k_B T \sim \frac{\hbar\Omega_1^2}{|\delta|}. \tag{9.24}$$

9.4.2. Threshold intensity – Cooling limit

According to equation (9.24), the temperature can be decreased by decreasing the laser intensity $I_L \sim \Omega_1^2$, or by increasing the detuning δ. Obviously, one cannot decrease I_L indefinitely. There must be therefore a threshold intensity below which equation (9.24) is no longer valid.

Actually, in deriving eq. (9.24), we have neglected the recoil due to the absorbed and re-emitted photons in each fluorescence cycle. We have thus implicitly assumed that the mean loss of potential energy at each optical pumping cycle, on the order of U_0, is much larger than mean increase of kinetic energy due to the recoil, on the order of $E_R = \hbar^2 k^2/2M$. If I_L is decreased, U_0 also decreases, and when U_0 becomes on the order of a few E_R, the cooling due to the Sisyphus effect is no longer sufficient to overcome

the heating due to the recoil. There is therefore a threshold intensity given by

$$(U_0)_{\rm thr} > \text{ a few } E_{\rm R}. \tag{9.25}$$

The previous analysis also shows that low intensity Sisyphus cooling cannot lead to minimum energies lower than a few $E_{\rm R}$. The characteristic energy is now the recoil energy $E_{\rm R}$, and not $\hbar\Gamma$ as was the case for Doppler cooling.

9.4.3. Comparison of internal and external times

In the cooling scheme discussed in this chapter, internal variables evolve with a characteristic time $T_{\rm int}$ equal to the optical pumping time $\tau_{\rm P}$

$$T_{\rm int} \simeq \tau_{\rm P} = \frac{9}{2\Gamma s_0}. \tag{9.26}$$

To characterize the evolution of external variables, we suppose that the atom has been cooled during a time long enough so that it is quasi-trapped in the potential wells of fig. 19, and we introduce the oscillation frequency $\Omega_{\rm osc}$ in these wells. Near the bottom of one potential well, for example near $z = 0$, we have, according to eq. (9.10.b)

$$E_{-1/2}(z) \simeq -\frac{3U_0}{2} + k^2 U_0^2 z^2 \qquad \text{for} \qquad |z| \ll 1/k, \tag{9.27}$$

so that $\Omega_{\rm osc}$ is given by

$$\Omega_{\rm osc} = k\sqrt{\frac{2U_0}{M}} = \sqrt{\frac{4\hbar|\delta|s_0}{3M}}. \tag{9.28}$$

The external time $T_{\rm ext}$ is on the order of the oscillation period:

$$T_{\rm ext} \simeq \frac{1}{\Omega_{\rm osc}}. \tag{9.29}$$

An important parameter for characterizing atomic motion is therefore

$$\Omega_{\rm osc}\,\tau_{\rm P} = \sqrt{\frac{27\hbar k^2|\delta|}{Ms_0\Gamma^2}} \simeq \frac{T_{\rm int}}{T_{\rm ext}}. \tag{9.30}$$

If $\Omega_{\rm osc}\tau_{\rm P} \ll 1$, the atom makes several transitions between $|g_{-1/2}\rangle$ and $|g_{+1/2}\rangle$ in a single oscillation period. In such a "jumping regime", internal variables are much faster than external variables. This is the usual

regime considered up to now in the semi-classical treatment of laser cooling. One can adiabatically eliminate the internal variables and describe atomic motion in terms of a velocity dependent force and a momentum diffusion coefficient. Such a treatment, which is given in detail in ref. [63], will be sketched in section 9.5.

If $\Omega_{\rm osc}\tau_{\rm P} \gg 1$, we are in the opposite situation where the atom makes several oscillations in a potential well before being optically pumped into the other sublevel. Such an "oscillating regime", where external variables are faster than internal variables, is quite unusual in laser cooling of free atoms. It is important here since, if one decreases Ω_1, at fixed δ, in order to decrease the temperature estimated in eq. (9.24), one sees from eq. (9.30) that one can go from the jumping regime to the oscillating regime. A few remarks on this regime will be given in section 9.6. More details may be found in refs. [64] and [66].

Before ending this subsection, we would like to mention other cooling mechanisms, closely related to the one discussed in this chapter, but which do not use polarization gradients [67,68]. Suppose for example that the laser configuration consists of two counterpropagating waves along Oz, with the same circular polarization σ^+. We have in this case a pure σ^+ standing wave. If we still consider a $J_g = 1/2 \leftrightarrow J_e = 3/2$ transition, the light shifts $E_{\pm 1/2}(z)$ of $|g_{\pm 1/2}\rangle$ oscillate in space (with $E_{+1/2} = 3E_{-1/2}$), the splitting between the two sublevels being equal to zero at the nodes of the standing wave and maximum at the antinodes. Because of optical pumping, all atoms are pumped into $|g_{+1/2}\rangle$ and the steady state population of this state for an atom at rest in z remains equal to 1 and independent of z, since, in the limit $s \ll 1$, the population of the excited state is negligible. Suppose now that one adds a small static magnetic field $\boldsymbol{B}_0$, perpendicular to Oz. If B_0 is small enough, its effect will be important only near the nodes where it mixes the sublevels $|g_{\pm 1/2}\rangle$, which become degenerate in such places. Consider then a moving atom, initially pumped in the sublevel $|g_{+1/2}\rangle$. When such an atom passes through a node, Landau–Zener transitions can transfer it to the other sublevel $|g_{-1/2}\rangle$, which is less light shifted than $|g_{+1/2}\rangle$. The atom will remain in this sublevel for a time on the order of $\tau_{\rm P}$ before being optically pumped back to $|g_{+1/2}\rangle$. One can then easily see that such a scheme provides a new example of situations where the atom is running up the hills of oscillating potential curves more than down.

9.5. The jumping regime ($\Omega_{osc}\tau_{\rm P} \ll 1$)

We suppose in this subsection that $\Omega_{\rm osc}\tau_{\rm P} \ll 1$, so that

$$T_{\rm int} \ll T_{\rm ext}. \tag{9.31}$$

It follows that during the time required by the internal variables to reach a steady-state, or more precisely a forced regime, the atomic velocity does not change appreciably. We can thus set

$$z = vt \tag{9.32}$$

in the equations of motion (9.16) of the internal variables and consider v as a constant when solving these equations.

9.5.1. Internal state for an atom with velocity v

Inserting eq. (9.32) into the equation of motion (9.18) of the population difference $\mathcal{M}$ leads to

$$\frac{\mathrm{d}}{\mathrm{d}t}\mathcal{M}(t) + \frac{1}{\tau_\mathrm{P}}\mathcal{M}(t) = -\frac{1}{\tau_\mathrm{P}}\cos 2kvt, \tag{9.33}$$

which is a linear differential equation with constant coefficients (since τ_P is, according to eq. (9.19), independent of z and thus of t) and with a source term modulated at angular frequency $2kv$. The forced regime solution of eq. (9.33) can be written

$$\mathcal{M}(t) = -\ \mathrm{Re}\ \frac{\tau_\mathrm{P}^{-1}}{2\mathrm{i}kv + \tau_\mathrm{P}^{-1}}\ \mathrm{e}^{2\mathrm{i}kvt} \tag{9.34}$$

that is also, recalling eq. (9.32)

$$\mathcal{M}(z) = -\frac{1}{1+(v/v_\mathrm{c})^2}\cos 2kz - \frac{v/v_\mathrm{c}}{1+(v/v_\mathrm{c})^2}\sin 2kz, \tag{9.35}$$

where v_c is a critical velocity defined by

$$v_\mathrm{c} = \frac{1}{2k\tau_\mathrm{P}} = \frac{\lambda}{4\pi\tau_\mathrm{P}} = \frac{\Gamma'}{9k}. \tag{9.36}$$

In order to get some physical insight in eq. (9.35), it will be useful to study the limit of this expression for $v \ll v_\mathrm{c}$. To order 1 in v/v_c, eq. (9.35) can be written using eq. (9.36) and the definition (9.20) of the population difference for an atom at rest in z

$$\begin{aligned}\mathcal{M}(z) &= -\cos 2kz - 2kv\tau_\mathrm{P}\sin 2kz \\ &= \mathcal{M}^\mathrm{st}(z) - v\tau_\mathrm{P}\frac{\mathrm{d}}{\mathrm{d}}z\mathcal{M}^\mathrm{st}(z) \\ &\simeq \mathcal{M}^\mathrm{st}(z - v\tau_\mathrm{P}).\end{aligned} \tag{9.37}$$

Such a result clearly shows that (after a transient regime) the internal state of an atom passing in z with a small velocity v lags behind the internal state of an atom which is at rest in z. Because of the finite response time τ_P of internal variables, $\mathcal{M}(z)$ does not adjust instantaneously to the variations of the laser polarization "seen" by the moving atom. There is a non-locality in the response of the atom which is characterized by the distance $v\tau_P$ travelled by the atom during the internal time τ_P.

9.5.2. Velocity dependent mean force. Friction coefficient

Inserting eq. (9.35) into the expression (9.12) of the mean force, and taking a spatial average, we get for the z-component of the spatially averaged force acting upon an atom moving with velocity v

$$\overline{\mathcal{F}_z(v)} = -\frac{kU_0}{2}\frac{v/v_c}{1+(v/v_c)^2} = -\frac{\alpha_S v}{1+(v/v_c)^2}, \tag{9.38}$$

where α_S is equal, according to eqs. (9.36), (9.11) and (9.19), to

$$\alpha_S = k^2 U_0 \tau_P = -3\hbar k^2 \frac{\delta}{\Gamma}. \tag{9.39}$$

For $v \ll v_c$, $\overline{\mathcal{F}_z(v)}$ can be written

$$\overline{\mathcal{F}_z(v)} = -\alpha_S v, \tag{9.40}$$

which shows that α_S is the friction coefficient associated with low intensity Sisyphus cooling. It is interesting to compare α_S with the friction coefficient α_D given in eq. (4.8) for a two-level atom moving in a laser plane wave. We have added the subscript D to α, given in eq. (4.8), to indicate that the friction mechanism is, in this case, due to the Doppler effect. A remarkable property of α_S, given in eq. (9.39), is that it is independent of the laser intensity I_L, whereas equation (4.8) shows that α_D is proportional to s, and thus to I_L, if $s \ll 1$. At first sight, such a result seems quite surprising, since decreasing I_L decreases the depth U_0 of the potential wells of fig. 18, and consequently the corresponding gradient forces. But equation (9.39) shows that α_S is proportional to the product of U_0 by τ_P, so that, when I_L decreases, the decrease of U_0, which varies as I_L, is compensated for by the increase of τ_P, which varies as $1/I_L$. In other words, at low intensity, the weakness of light shifts is compensated for by the length of the optical pumping times. Note also that, according to eq. (9.39), the value of α_S is, for $|\delta| \gg \Gamma$, larger than the optimal value of α_D which, according to eq. (4.9), is on the order of $\hbar k^2/4$.

When v increases, $\overline{\mathcal{F}_z(v)}$ reaches a maximum when $v = v_c$ and then decreases as $1/v$ when $v \gg v_c$. The critical velocity v_c, which is a velocity such that the atom, moving with this velocity, travels over a distance on the order of λ during the optical pumping time τ_P, can thus be considered as defining the velocity range, sometimes called "velocity capture range", over which low intensity Sisyphus friction is most efficient. According to eq. (9.36), v_c is proportional to $1/\tau_P$, i.e., to the laser intensity I_L. Such a result is to be contrasted with what happens for Doppler cooling, where the velocity capture range, given by the width of the curve of fig. 4 of chapter 4, is, for the optimal value $\delta = -\Gamma/2$ of the detuning, such that $kv_c \simeq \Gamma$, and is therefore independent of I_L.

To summarize the results derived in this section, one can say that, for low intensity Sisyphus cooling, the friction coefficient α_S remains constant, and very large, when I_L decreases, whereas the velocity capture range decreases. On the contrary, for Doppler cooling, the friction coefficient α_D decreases when I_L decreases, whereas the velocity capture range remains constant.

9.5.3. Equilibrium temperature

In order to evaluate the equilibrium temperature T_S associated with low intensity Sisyphus cooling, we must first find the order of magnitude of the momentum diffusion coefficient D for an atom at rest in z.

As in the case of a two-level atom, we have a contribution D_{vac} to D coming from the fluctuations of the momentum carried away by the spontaneously emitted photons, and a contribution D_{abs} coming from the fluctuations in the difference between the number of photons absorbed in each of the two counterpropagating waves. Considerations similar to those developed in subsection 5.2.3, show that these two contributions are, for $s_0 \ll 1$, which is the case considered in this chapter, on the order of

$$D_{vac} \simeq D_{abs} \simeq \hbar^2 k^2 \Gamma' = \hbar^2 k^2 \Gamma s_0. \tag{9.41a}$$

We have also a contribution D_{dip} to D coming from the fluctuations of the instantaneous dipole force oscillating back and forth between $-\boldsymbol{\nabla} E_{+1/2}$ and $-\boldsymbol{\nabla} E_{-1/2} = +\boldsymbol{\nabla} E_{+1/2}$ when the atom undergoes, at random times, optical pumping transitions between the two ground-state Zeeman sublevels at a rate $1/\tau_P$. A calculation, quite similar to the one presented in subsection 4*B* of ref. [39], gives for this contribution the following result

$$D_{dip} = 2\hbar^2 k^2 \frac{\delta^2}{\Gamma} s_0 \sin^4(2kz), \tag{9.41b}$$

whose spatial average is equal to

$$\overline{D_{dip}} = \frac{3}{4} \hbar^2 k^2 \frac{\delta^2}{\Gamma} s_0. \tag{9.41c}$$

Note that, according to eq. (9.41.b), D_{dip} vanishes in certain places. But, since the departure rates from $|g_{\pm 1/2}\rangle$ never vanish (see Equations (9.14)), D_{vac} and D_{abs} never vanish.

If $|\delta| \gg \Gamma$, $\overline{D_{\text{dip}}}$ is larger than D_{vac} and D_{abs} by a factor on the order of $\delta^2/\Gamma^2 \gg 1$, so that

$$D \simeq \overline{D_{\text{dip}}} = \frac{3}{4}\hbar^2 k^2 \frac{\delta^2}{\Gamma} s_0. \tag{9.42}$$

The equilibrium temperature T_{S} results from a competition between the cooling, described by the friction coefficient α_{S}, and the heating due to momentum diffusion. We have then, for $|\delta| \gg \Gamma$,

$$k_{\text{B}} T = \frac{D}{\alpha_{\text{S}}} \simeq -\frac{1}{4}\hbar\delta s_0 = \frac{3}{8} U_0. \tag{9.43}$$

This confirms the result predicted above in a qualitative way (see eq. (9.24)), according to which the equilibrium energy is on the order of the depth U_0 of the potential wells of fig. 18. Using the definition (3.6) of s_0, we have, for $|\delta| \gg \Gamma$,

$$k_{\text{B}} T \simeq \frac{\hbar \Omega_1^2}{8|\delta|}, \tag{9.44}$$

where Ω_1 is the Rabi frequency associated with each of the two counter-propagating waves. Experiments [69] done on cesium have given results showing that T depends linearly on $\Omega_1^2/|\delta|$ over a large range of values of the parameters. This agreement with eq. (9.44) is somewhat unexpected since the theory presented here is valid only in one dimension and for a $J_g = 1/2 \leftrightarrow J_e = 3/2$ transition, whereas the experiments are done in three dimensions on a $J_g = 4 \leftrightarrow J_e = 5$ transition.

One can finally ask under what condition the whole velocity distribution falls in the linear part of $\overline{\mathcal{F}_z(v)}$. Such a condition can be written

$$v_{\text{rms}} \ll v_{\text{c}} \;\Rightarrow\; \Omega_1 \gg \sqrt{\frac{\hbar k^2}{M}\frac{|\delta|^3}{\Gamma^2}} \tag{9.45}$$

and turns out to be equivalent to $\Omega_{\text{osc}} \tau_{\text{P}} \ll 1$, which is the condition of validity of the jumping regime considered in this section.

9.6. The limits of low intensity Sisyphus cooling

The treatment presented in the previous section relies on a semi-classical approximation (atomic spatial coherence length ξ_{A} much smaller than the

laser wavelength λ – see the discussion of subsection 2.3.2) and on the assumption that $T_{\text{int}} \ll T_{\text{ext}}$. Its predictions for the equilibrium temperature (9.44) are certainly wrong when Ω_1 becomes too small. In order to determine the lowest temperatures which can be reached by low intensity Sisyphus cooling, we need therefore a more precise theory.

9.6.1. Results of a full quantum treatment

Reference [64] presents a full quantum treatment of low intensity Sisyphus cooling, where both internal and external degrees of freedom are quantized. We will not give here the details of such calculations. We just present a few important results.

Consider first the predictions concerning the variations with U_0 of the mean kinetic energy $\langle P^2/2M \rangle$, for a fixed value of the detuning δ. For $U_0 \gg E_{\text{R}}$, the quantum result agrees with the semi-classical one, and one gets a straight line. When U_0 is decreased, $\langle P^2/2M \rangle$ decreases, passes through a minimum and then diverges (see fig. 3b of ref. [64]. This confirms the qualitative predictions of subsection 9.4.2 for the existence of a threshold for U_0. Two important results must be noted concerning the minimum $\langle P^2/2M \rangle_{\text{min}}$ of $\langle P^2/2M \rangle$. First, for the values of δ and U_0 corresponding to this minimum, the dispersion Δp of the possible values of p, characterized by $\Delta p \sim \langle P^2 \rangle^{1/2}$, remains always larger than $\hbar k$. Actually, the smallest possible value of $\langle P^2 \rangle^{1/2}$, which is achieved for $U_0 = 95 E_{\text{R}}$ and $|\delta| \gg \Gamma$, is equal to $5.5\hbar k$. This means that the semi-classical approximation is not too bad, since the coherence length $\xi_{\text{A}} \sim \hbar/\Delta p$ remains always smaller than $\lambda = 2\pi/k$. Second, for the values of U_0 corresponding to $\langle P^2/2M \rangle_{\text{min}}$, $\Omega_{\text{osc}} \tau_{\text{P}}$ is no longer small compared to 1. Actually the smallest possible value of $\langle P^2/2M \rangle_{\text{min}}$ is reached in the limit $\Omega_{\text{osc}} \tau_{\text{P}} \to \infty$. These results show that the optimum of Sisyphus cooling cannot be properly described by the treatment of section 9.5, not because of the semi-classical approximation, which is not bad, but because of the assumption $T_{\text{int}} \ll T_{\text{ext}}$, which has to be reversed.

Reference [64] presents a few approximations which can be done on the quantum equations of motion and which are still semi-classical in the sense that, as in section 5.3, the atomic Wigner functions are expanded in powers of $\hbar k/\Delta p$, up to order 2. The difference with the treatment of section 5.3 is that internal variables are no longer adiabatically eliminated. Some other approximations are then introduced. We will focus here on the limit $\Omega_{\text{osc}} \tau_{\text{P}} \gg 1$, where the so-called "secular approximation" allows one to describe laser cooling of neutral atoms with physical pictures quite similar to the ones used to describe laser cooling of trapped ions [21].

9.6.2. The oscillating regime ($\Omega_{osc}\tau_P \gg 1$)

In this regime, the atom oscillates several times in one of the potential wells of fig. 18 before being optically pumped into the other sublevel. One can therefore, in a first step, neglect the dissipative part of the atom–field coupling, which is responsible for the real absorption and emission of photons by the atom, and consider only the reactive part of this coupling which is the origin of light shifts. This amounts to considering an atom moving in a bipotential $E_{\pm 1/2}(z)$, without any dissipative process. As shown in ref. [66], the diagonalization of the corresponding Hamiltonian gives a series of energy levels, which are actually energy bands because of the periodicity of $E_{\pm 1/2}(z)$. The lowest bands are very narrow because of the smallness of the tunnel effect between two adjacent potential wells. For example, for $\delta = -20\Gamma$, $\Omega_1 = 1.5\Gamma$ and the cesium recoil shift, one finds $U_0 \simeq 100 E_R$, which gives 6 bound bands [66], the width of the lowest band being smaller than $10^{-6} E_R$ and the distance between two successive bands being on the order of $\hbar\Omega_{osc}$ with $\Omega_{osc}/2\pi \simeq 40$ kHz.

The second step of such an approach consists in introducing the effect of optical pumping, which induces transitions between different energy bands or inside a given band. Condition $\Omega_{osc}\tau_P \gg 1$ then allows one to neglect any "non-secular" coupling between the populations of the energy levels and the off-diagonal elements of the density matrix between different energy levels separated by an energy on the order of $\hbar\Omega_{osc}$. Reference [66] shows how such a "secular approximation" (supplemented by symmetry considerations) leads to a set of rate equations involving only the populations of the energy levels. Such equations have a clear physical meaning in terms of optical pumping rates and they are much easier to solve numerically than the full quantum equations written in the basis $|g_{\pm 1/2}, p\rangle$, where p is the atomic momentum along Oz. For example, one finds that, for the values of the parameters given above, more than 50% of the atoms are trapped in the two lowest bound bands, and the value obtained in this way for $\langle P^2/2M \rangle$ is in very good agreement with the result obtained in ref. [64].

Such an approach provides a description of laser cooling in terms of spontaneous anti Stokes Raman transitions between bound states, quite analogous to the one given for laser cooling of trapped ions [21]. It thus suggests new phenomena which could be observed on neutral atoms trapped in optical molasses. For example, one could hope to observe discrete sidebands in the fluorescence spectrum of the trapped atoms, with a frequency shift from ω_L on the order of $\pm\Omega_{osc}$. Such sidebands could be easily resolved since their distance from ω_L, Ω_{osc}, is much larger than their width, on the order of $1/\tau_P$. Their observation would represent direct evidence for the

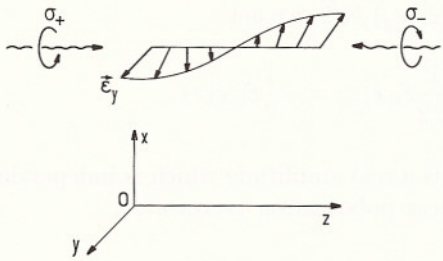

Fig. 20. σ^+–σ^- laser configuration. The resulting laser electric field has a linear polarization which rotates in space, forming a helix with a pitch λ.

quantization of atomic motion in optical molasses. Such effects have been recently observed experimentally [86] [87].

10. The σ^+–σ^- laser configuration – Semiclassical theory

10.1. Introduction

The purpose of this chapter is to present another example of a new laser cooling mechanism allowing one to beat the Doppler limit. As in the previous chapter, this mechanism is based on the existence of several ground state Zeeman sublevels, and on polarization gradients. The polarization gradient is however of a different nature and gives rise to physical processes which are quite different from the Sisyphus effect discussed in chapter 9. Another important motivation for studying the σ^+–σ^- configuration is that it will allow us to introduce, in the specific case of a $J_g = 1 \leftrightarrow J_e = 1$ transition, the idea of "coherent population trapping". This phenomenon is the basis of another cooling scheme, which will be analyzed in chapter 11, and which can lead to temperatures below the single photon recoil limit.

As in chapter 9, we consider two counterpropagating laser waves along Oz, with the same amplitude $\mathcal{E}_0$ and the same frequency ω_L. But instead of having orthogonal linear polarizations, the two waves have now orthogonal circular polarizations, σ^+ for the wave propagating along Oz, σ^- for the counterpropagating wave (see fig. 20).

With an appropriate choice of the relative phases of the two waves, the laser electric field in z can be written

$$\boldsymbol{E}_L(z,t) = \boldsymbol{E}_L^+(z)\, e^{-i\omega_L t} + \text{c.c.} \tag{10.1}$$

with

$$\boldsymbol{E}_L^+(z) = \tfrac{1}{2}\left(\boldsymbol{\epsilon}_+ e^{ikz} + \boldsymbol{\epsilon}_- e^{-ikz}\right) \mathcal{E}_0. \tag{10.2}$$

Using $\boldsymbol{\epsilon}_{\pm} = \mp (\boldsymbol{\epsilon}_x \pm \mathrm{i}\boldsymbol{\epsilon}_y)/\sqrt{2}$, we get

$$\boldsymbol{E}_{\mathrm{L}}^{+}(z) = -\frac{\mathrm{i}}{\sqrt{2}}\mathcal{E}_0\,\boldsymbol{\epsilon}(z) = -\frac{\mathrm{i}}{2}\mathcal{E}_{\mathrm{L}}\,\boldsymbol{\epsilon}(z)\,, \tag{10.3}$$

where $\mathcal{E}_{\mathrm{L}} = \mathcal{E}_0\sqrt{2}$ is a real amplitude which is independent of z, and where the normalized linear polarization vector $\boldsymbol{\epsilon}(z)$,

$$\begin{aligned}\boldsymbol{\epsilon}(z) &= \frac{\mathrm{i}}{\sqrt{2}}\left[\boldsymbol{\epsilon}_+\,\mathrm{e}^{\mathrm{i}kz} + \boldsymbol{\epsilon}_-\,\mathrm{e}^{-\mathrm{i}kz}\right] \\ &= \boldsymbol{\epsilon}_x \sin kz + \boldsymbol{\epsilon}_y \cos kz,\end{aligned} \tag{10.4}$$

is deduced from $\boldsymbol{\epsilon}_y$ by a rotation $\phi = -kz$ around Oz. It follows that the resulting laser electric field has, for all values of z, the same amplitude $\mathcal{E}_{\mathrm{L}}$ and a linear polarization $\boldsymbol{\epsilon}(z)$ which rotates when z varies, forming a helix with a pitch λ (fig. 20).

Since the laser electric fields at two different points z_1 and z_2 are deduced from each other by a pure rotation, the light shifts of the ground-state sublevels have the same magnitude in z_1 and z_2, whereas the corresponding wave functions are deduced from each other by a rotation. It follows that, contrary to the situation studied in chapter 9, the light-shifted energies do not exhibit any spatial gradient, whereas the wave functions of the ground-state Zeeman sublevels having a well defined light shift are position dependent. This shows that the light-shifted energies of the ground-state sublevels do not oscillate in space, which excludes any possibility of a Sisyphus effect for the σ^+–σ^- configuration. In such a configuration, the reactive component of the mean force, given in eq. (8.51), is entirely due to the spatial gradient of the wave functions. We have thus a situation which is, in some sense, complementary to the one analyzed in chapter 9.

The fact that the polarization $\boldsymbol{\epsilon}(z)$ of the laser electric field is linear has an important consequence. The light shifts, which have the same symmetry as dc-Stark shifts produced by a static electric field parallel to $\boldsymbol{\epsilon}(z)$, are the same for two Zeeman sublevels having opposite magnetic quantum numbers along $\boldsymbol{\epsilon}(z)$. It follows that, if we take $J_g = 1/2$, as in chapter 9, the Zeeman degeneracy of the ground state is not removed by light shifts, so that we have in this case neither energy gradients, nor gradients of wave functions. Since the radiation pressures of the two counterpropagating waves remain always equal for $J_g = 1/2$ (if we neglect Doppler cooling), we conclude that no new laser cooling mechanism can occur for $J_g = 1/2$. This is why we consider in this chapter two atomic transitions $J_g = 1 \leftrightarrow J_e = 2$ and $J_g = 1 \leftrightarrow J_e = 1$ having the simplest possible value of J_g leading to new

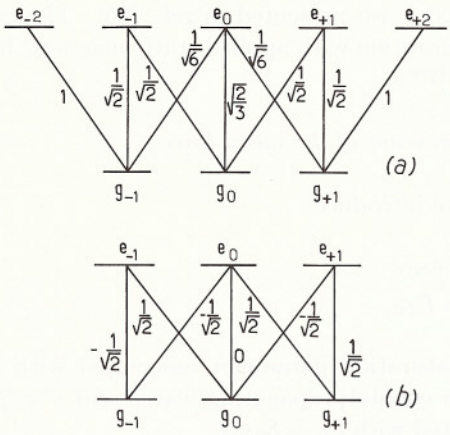

Fig. 21. Clebsch–Gordan coefficients for a transition $J_g = 1 \leftrightarrow J_e = 2$ (a) and $J_g = 1 \leftrightarrow J_e = 1$ (b).

cooling mechanisms in the σ^+–σ^- configuration (fig. 21). The first one is a standard transition $J_g \leftrightarrow J_e = J_g + 1$. The second one is considered here, in order to introduce in a simple way the idea of coherent population trapping.

We begin (section 10.2) by giving the general expression of the mean force, which is now the sum of a contribution due to the spatial gradients of the wave functions of the light-shifted Zeeman sublevels and of a contribution due to the difference between the radiation pressures exerted by the two counterpropagating waves. We then study in section 10.3 the light shifts and the steady-state populations of an atom at rest in z. For a moving atom, we show in section 10.4 that it is possible to introduce a moving rotating frame in which the evolution of the atom can be analyzed with a time independent Hamiltonian. Such a transformation then allows us in section 10.5 to interpret in a simple way the new cooling mechanism which appears for a $J_g = 1 \leftrightarrow J_e = 2$ transition. The important physical effect is essentially an ultra sensitive motion induced population difference which appears among the ground-state sublevels and which gives rise to an imbalance between the radiation pressures exerted by the two counterpropagating waves. Finally, we analyze in section 10.6 the case of a $J_g = 1 \leftrightarrow J_e = 1$ transition which gives rise to the phenomenon of coherent population trapping.

The σ^+–σ^- configuration has been considered from the beginning in the first explanations [70,71] proposed for the new laser cooling mechanisms. We will follow here the more quantitative presentation of ref. [63]. Some

numerical results are also presented in ref. [65]. The combination of the σ^+–σ^- laser configuration with applied static magnetic fields has been also considered in ref. [72].

10.2. General expression of the mean force

As in chapter 9, we introduce

$$\delta' = \delta s/2 = \delta s_0, \tag{10.5a}$$

$$\Gamma' = \Gamma s/2 = \Gamma s_0, \tag{10.5b}$$

where s_0 is the saturation parameter associated with the amplitude $\mathcal{E}_0$ of each of the two counterpropagating waves and $s = 2s_0$ the saturation parameter associated with $\mathcal{E}_L = \mathcal{E}_0\sqrt{2}$.

10.2.1. Effective Hamiltonian associated with light shifts
According to eq. (8.36), such an Hamiltonian can be written

$$H_{\text{eff}} = \hbar\delta' \sum_{m,m'} |g_m\rangle\langle g'_m| \ \langle g_m \mid \Lambda(z) \mid g'_m\rangle, \tag{10.6}$$

where $\Lambda(z)$ is given in eq. (8.32). Using the expansion (10.4) of $\epsilon(z)$ in ϵ_+ and ϵ_- and the Clebsch–Gordan coefficients of fig. 21, one can easily calculate the matrix elements of $\Lambda(z)$. Inserting them into eq. (10.6), one gets for a $J_g = 1 \leftrightarrow J_e = 2$ transition

$$\begin{aligned} H_{\text{eff}}\,(1 \leftrightarrow 2) = &+ \frac{\hbar\delta'}{2} \ |\, g_0\rangle\langle g_0 \,| + \frac{7\hbar\delta'}{12} \left[|\, g_1\rangle\langle g_1 \,| + |\, g_{-1}\rangle\langle g_{-1} \,| \right] \\ &+ \frac{\hbar\delta'}{12} \left[|\, g_1\rangle\langle g_{-1} \,| \, \mathrm{e}^{2\mathrm{i}kz} + |\, g_{-1}\rangle\langle g_1 \,| \, \mathrm{e}^{-2\mathrm{i}kz} \right] \end{aligned} \tag{10.7.a}$$

and for a $J_g = 1 \leftrightarrow J_e = 1$ transition

$$\begin{aligned} H_{\text{eff}}\,(1 \leftrightarrow 1) = &+ \frac{\hbar\delta'}{2} \ |\, g_0\rangle\langle g_0 \,| + \frac{\hbar\delta'}{4} \left[|\, g_1\rangle\langle g_1 \,| + |\, g_{-1}\rangle\langle g_{-1} \,| \right] \\ &- \frac{\hbar\delta'}{4} \left[|\, g_1\rangle\langle g_{-1} \,| \, \mathrm{e}^{2\mathrm{i}kz} + |\, g_{-1}\rangle\langle g_1 \,| \, \mathrm{e}^{-2\mathrm{i}kz} \right] \end{aligned} \tag{10.7.b}$$

It is clear in eq. (10.7) that the only non-zero off-diagonal elements of H_{eff} in the basis $\{|g_m\rangle\}$ of eigenstates of J_z are those connecting $|g_1\rangle$ to

$|g_{-1}\rangle$ or vice versa. This is a manifestation of the selection rule $\Delta m = \pm 2$ mentioned at the end of subsection 8.6.4. Note also that the only terms of eqs. (10.7) which depend on z are those where both $|g_1\rangle$ and $|g_{-1}\rangle$ appear. This is due to the fact that these terms involve both counterpropagating waves (redistribution processes) which have a relative phase which varies as $\exp(\pm 2ikz)$ when z varies.

10.2.2. Reactive force

Using the expression (8.48) of this force, we get, for a $J_g = 1 \leftrightarrow J_e = 2$ transition

$$\begin{aligned} \boldsymbol{\mathcal{F}}_{\text{react}}(1 \leftrightarrow 2) &= -\langle \boldsymbol{\nabla} H_{\text{eff}}(1 \leftrightarrow 2) \rangle \\ &= -\frac{\mathrm{i}}{6} \hbar k \, \delta' \, \boldsymbol{\epsilon}_z \Big[\sigma_{g_{-1}g_1} \, \mathrm{e}^{2ikz} - \sigma_{g_1 g_{-1}} \, \mathrm{e}^{-2ikz} \Big], \end{aligned} \tag{10.8a}$$

and for $J_g = 1 \leftrightarrow J_e = 1$ transition

$$\begin{aligned} \boldsymbol{\mathcal{F}}_{\text{react}}(1 \leftrightarrow 1) &= -\langle \boldsymbol{\nabla} H_{\text{eff}}(1 \leftrightarrow 1) \rangle \\ &= +\frac{\mathrm{i}}{2} \hbar k \, \delta' \, \boldsymbol{\epsilon}_z \Big[\sigma_{g_{-1}g_1} \, \mathrm{e}^{2ikz} - \sigma_{g_1 g_{-1}} \, \mathrm{e}^{-2ikz} \Big]. \end{aligned} \tag{10.8b}$$

It will be useful, for subsequent calculations, to introduce a new notation

$$\widetilde{\sigma}_{g_1 g_{-1}} = \sigma_{g_1 g_{-1}} \, \mathrm{e}^{-2ikz} = \widetilde{\sigma}^*_{g_{-1} g_1} \tag{10.9}$$

for the off-diagonal elements of the density matrix. The physical interpretation of the transformation relating $\sigma_{g_1 g_{-1}}$ to $\widetilde{\sigma}_{g_1 g_{-1}}$ will be given in section 10.4. Let C_{r} and C_{i} be the real and imaginary parts of $\widetilde{\sigma}_{g_1 g_{-1}}$

$$\widetilde{\sigma}_{g_1 g_{-1}} = C_{\mathrm{r}} + \mathrm{i} C_{\mathrm{i}}. \tag{10.10}$$

Using eqs. (10.9) and (10.10), one can rewrite eq. (10.8) as

$$\boldsymbol{\mathcal{F}}_{\text{react}}(1 \leftrightarrow 2) = -\frac{\hbar k}{3} \, \delta' \, C_{\mathrm{i}} \, \boldsymbol{\epsilon}_z, \tag{10.11a}$$

$$\boldsymbol{\mathcal{F}}_{\text{react}}(1 \leftrightarrow 1) = +\hbar k \, \delta' \, C_{\mathrm{i}} \, \boldsymbol{\epsilon}_z. \tag{10.11b}$$

It is clear from eq. (10.11) that the reactive component of the mean force is proportional to the imaginary part of the Zeeman coherence between g_1 and g_{-1}. This reflects the fact that the reactive force is a redistribution

force (see subsection 8.6.2) and that the two counterpropagating waves have orthogonal circular polarizations σ^+ and σ^-.

10.2.3. Dissipative force

Such a force, which is given by eq. (8.66), is the difference between the radiation pressures exerted by the two waves. Using the definition (8.46) of $G_\mu^\pm$ and the saturation parameter s_0 associated with each wave, one easily finds that the radiation pressure exerted by the wave 1 (with wave vector $k\boldsymbol{\epsilon}_z$ and polarization σ^+) is equal to the product of $(\hbar k \Gamma s_0/2)$ and the sum of the populations Π_m of the various Zeeman sublevels g_m weighted by the square of the Clebsch–Gordan coefficient of the σ^+ transition starting from g_m. A similar result holds for the radiation pressure exerted by wave 2, provided that one replaces $\boldsymbol{\epsilon}_z$ by $-\boldsymbol{\epsilon}_z$ and σ^+ by σ^-. This yields for a $J_g = 1 \leftrightarrow J_e = 2$ transition

$$\begin{aligned}\boldsymbol{\mathcal{F}}_{\text{dissip}}(1 \leftrightarrow 2) &= + \hbar k \frac{\Gamma'}{2} \boldsymbol{\epsilon}_z \\ &\quad \times \left[\Pi_1 + \frac{\Pi_0}{2} + \frac{\Pi_{-1}}{6} - \frac{\Pi_1}{6} - \frac{\Pi_0}{2} - \Pi_{-1} \right] \\ &= + \frac{5}{12} \hbar k \, \Gamma' \, \boldsymbol{\epsilon}_z \left[\Pi_1 - \Pi_{-1} \right],\end{aligned} \tag{10.12a}$$

and for a $J_g = 1 \leftrightarrow J_e = 1$ transition

$$\begin{aligned}\boldsymbol{\mathcal{F}}_{\text{dissip}}(1 \leftrightarrow 1) &= + \hbar k \frac{\Gamma'}{2} \boldsymbol{\epsilon}_z \\ &\quad \times \left[\frac{\Pi_0}{2} + \frac{\Pi_{-1}}{2} - \frac{\Pi_0}{2} - \frac{\Pi_1}{2} \right] \\ &= - \frac{1}{4} \hbar k \, \Gamma' \, \boldsymbol{\epsilon}_z \left[\Pi_1 - \Pi_{-1} \right].\end{aligned} \tag{10.12b}$$

It clearly appears in eqs. (10.12) that the dissipative component of the mean force is proportional to the population difference $\Pi_1 - \Pi_{-1}$ between the two Zeeman sublevels. Note also the change of sign between (10.12.a) and (10.12.b). It is due to the fact that the most intense σ^+ transition starts from g_1 for a $J_g = 1 \leftrightarrow J_e = 2$ transition, whereas it starts from g_{-1} for a $J_g = 1 \leftrightarrow J_e = 1$ transition (see fig. 21).

10.3. Internal state of an atom at rest

10.3.1. Light shifts

The effective Hamiltonians given in eqs. (10.7) are easy to diagonalize. First, the state $|g_0\rangle$ which is not coupled to any other state is obviously

an eigenstate of H_{eff}. Then, the 2×2 matrix representing H_{eff} in the manifold $\{|g_{\pm 1}\rangle\}$ has equal diagonal elements. It follows that the symmetric and antisymmetric linear combinations of $|g_1\rangle\ \mathrm{e}^{ikz}$ and $|g_{-1}\rangle\ \mathrm{e}^{-ikz}$ are also eigenstates of H_{eff}. If we put

$$|\psi_{\mathrm{S}}(z)\rangle = \frac{1}{\sqrt{2}}\Big[\,|g_1\rangle\ \mathrm{e}^{ikz} + |g_{-1}\rangle\ \mathrm{e}^{-ikz}\Big], \tag{10.13a}$$

$$|\psi_{\mathrm{A}}(z)\rangle = \frac{1}{\sqrt{2}}\Big[\,|g_1\rangle\ \mathrm{e}^{ikz} - |g_{-1}\rangle\,\mathrm{e}^{-ikz}\Big], \tag{10.13b}$$

we get for a $J_g = 1 \leftrightarrow J_e = 2$ transition

$$\begin{aligned} H_{\text{eff}}\,(1 \leftrightarrow 2)|g_0\rangle &= (\hbar\,\delta'/2)|g_0\rangle, \\ H_{\text{eff}}\,(1 \leftrightarrow 2)|\psi_{\mathrm{S}}(z)\rangle &= (2\hbar\,\delta'/3)|\psi_{\mathrm{S}}(z)\rangle, \\ H_{\text{eff}}\,(1 \leftrightarrow 2)|\psi_{\mathrm{A}}(z)\rangle &= (\hbar\,\delta'/2)|\psi_{\mathrm{A}}(z)\rangle, \end{aligned} \tag{10.14a}$$

and for a $J_g = 1 \leftrightarrow J_e = 1$ transition

$$\begin{aligned} H_{\text{eff}}\,(1 \leftrightarrow 1)|g_0\rangle &= (\hbar\,\delta'/2)|g_0\rangle, \\ H_{\text{eff}}\,(1 \leftrightarrow 1)|\psi_{\mathrm{S}}(z)\rangle &= 0\,|\psi_{\mathrm{S}}(z)\rangle, \\ H_{\text{eff}}\,(1 \leftrightarrow 1)|\psi_{\mathrm{A}}(z)\rangle &= (\hbar\,\delta'/2)|\psi_{\mathrm{A}}(z)\rangle. \end{aligned} \tag{10.14b}$$

As predicted above (see section 10.1), we find that the light shifts are independent of z, whereas the eigenstates of H_{eff} depend on z. Figure 22 represents for both transitions the light shifts of the ground-state Zeeman sublevels. As in chapter 9, we have supposed $\delta < 0$, so that light shifts are negative. Note that $|g_0\rangle$ and $|\psi_{\mathrm{A}}(z)\rangle$ have the same light shift so that they remain degenerate.

The results obtained in eq. (10.14) and represented in fig. 22 could have been found more quickly by noting that the laser polarization in z is linear and parallel to the unit vector $\boldsymbol{\epsilon}(z)$ given in eq. (10.4). It is then clear that the eigenstates of the component $\boldsymbol{\epsilon}(z)\cdot\boldsymbol{J}$ of the angular momentum $\boldsymbol{J}$ have a well defined light shift, which is equal to the product of $\hbar\delta'$ by the square of the Clebsch–Gordan coefficients of the π transitions of fig. 21. This gives immediately the eigenvalues written in eq. (10.14) and their degeneracy. One can also check that $|\psi_{\mathrm{S}}(z)\rangle$, given in eq. (10.13.a), coincides with the eigenstate of $\boldsymbol{\epsilon}(z)\cdot\boldsymbol{J}$ with eigenvalue 0, whereas $|g_0\rangle$ and $|\psi_{\mathrm{A}}(z)\rangle$ given in eq. (10.13.b) are two orthogonal linear combinations of the two eigenstates of $\boldsymbol{\epsilon}(z)\cdot\boldsymbol{J}$ with eigenvalues $+\hbar$ and $-\hbar$. It turns out however that the two states $|\psi_{\mathrm{S}}(z)\rangle$ and $|\psi_{\mathrm{A}}(z)\rangle$, which we have introduced for diagonalizing

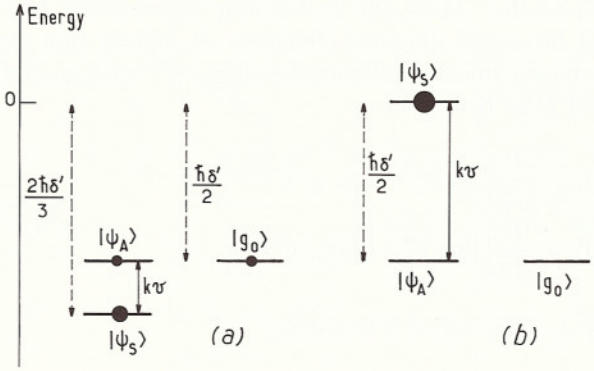

Fig. 22. Light shifts of the ground-state Zeeman sublevels for a $J_g = 1 \leftrightarrow J_e = 2$ transition (a) and for a $J_g = 1 \leftrightarrow J_e = 1$ transition (b). The size of the solid circles is proportional to the steady-state population of the corresponding sublevels for an atom at rest in z. We have supposed $\delta < 0$. The vertical arrows represent the motional coupling between $|\psi_S\rangle$ and $|\psi_A\rangle$, characterized by an angular frequency kv.

H_{eff}, will play an important role in the following sections and that they are more convenient to use than the eigenstates of $\boldsymbol{\epsilon}(z) \cdot \boldsymbol{J}$. First, we will see in section 10.4 that atomic motion couples only $|\psi_S\rangle$ to $|\psi_A\rangle$ and vice versa. Second, the states $|\psi_A(z)\rangle$ for a $J_g = 1 \leftrightarrow J_e = 2$ transition, $|\psi_S(z)\rangle$ for a $J_g = 1 \leftrightarrow J_e = 1$ transition, are linear combinations of $|g_{-1}\rangle$ and $|g_1\rangle$, which are not coupled to the excited state $|e_0\rangle$ by the laser–atom interaction Hamiltonian V_{AL} (for an atom at rest in z). One can easily check that

$$\langle e_0 \mid V_{AL}(1 \leftrightarrow 2) \mid \psi_A(z)\rangle = 0, \tag{10.15a}$$

$$\langle e_0 \mid V_{AL}(1 \leftrightarrow 1) \mid \psi_S(z)\rangle = 0. \tag{10.15b}$$

The physical interpretation of this result is that the absorption amplitudes for the absorption of a σ^+ photon from $|g_{-1}\rangle$ and for the absorption of a σ^- photon from $|g_{+1}\rangle$ can interfere destructively if the atom is in an appropriate linear superposition of $|g_{-1}\rangle$ and $|g_{+1}\rangle$. The difference of sign between the two non-coupled states (10.15.a) and (10.15.b) is due to the fact that the Clebsch–Gordan coefficients of the σ^+ and σ^- transitions arriving in e_0 are equal for a $J_g = 1 \leftrightarrow J_e = 2$ transition whereas they are opposite for a $J_g = 1 \leftrightarrow J_e = 1$ transition (see fig. 21). We will see later on that the non-coupled state (10.15.b) plays an essential role in the phenomenon of coherent population trapping.

10.3.2. Optical pumping and steady-state populations

The departure rates from $|g_0\rangle$, $|\psi_S(z)\rangle$, $|\psi_A(z)\rangle$ are well defined (see eq. (8.39)), and equal to the product of Γ' and the eigenvalues of Λ, which are

the coefficients of $\hbar\delta'$ in eq. (10.14). We get in this way

$$\begin{aligned} \Gamma'_0(1 \leftrightarrow 2) &= \Gamma'_{\mathrm{A}}(1 \leftrightarrow 2) = \frac{\Gamma'}{2}, \\ \Gamma'_{\mathrm{S}}(1 \leftrightarrow 2) &= \frac{2\Gamma'}{3}, \end{aligned} \tag{10.16a}$$

for a $J_g = 1 \leftrightarrow J_e = 2$ transition and

$$\begin{aligned} \Gamma'_0(1 \leftrightarrow 1) &= \Gamma'_{\mathrm{A}}(1 \leftrightarrow 1) = \frac{\Gamma'}{2}, \\ \Gamma'_{\mathrm{S}}(1 \leftrightarrow 1) &= 0, \end{aligned} \tag{10.16b}$$

for a $J_g = 1 \leftrightarrow J_e = 1$ transition. The vanishing of $\Gamma'_{\mathrm{S}}(1 \leftrightarrow 1)$ reflects the fact that $|\psi_{\mathrm{S}}(z)\rangle$ is a non-coupled state for a $J_g = 1 \leftrightarrow J_e = 1$ transition. For a $J_g = 1 \leftrightarrow J_e = 2$ transition, the state $|\psi_{\mathrm{A}}(z)\rangle$ is not coupled to e_0, but it remains coupled to $|e_{+2}\rangle$ and $|e_{-2}\rangle$, which explains why $\Gamma'_A(1 \leftrightarrow 2)$ does not vanish as $\Gamma'_{\mathrm{S}}(1 \leftrightarrow 1)$.

In order to find the steady-state density matrix for an atom at rest in z, which results from the competition between the departure rates and the return rates respectively associated with the second and third terms of the right-hand side of eq. (8.35), we use the basis of eigenstates of $\boldsymbol{\epsilon}(z) \cdot \boldsymbol{J}$, where the laser polarization can be considered as a π polarization and where the steady-state density matrix is diagonal. Consider first a $J_g = 1 \leftrightarrow J_e = 2$ transition. A simple detailed balance argument, expressing that the number of transitions from g_0 to g_{-1} by absorption of a π photon and spontaneous emission of a σ^+ photon must balance the number of transitions from g_{-1} to g_0 by absorption of a π photon and spontaneous emission of a σ^- photon, then shows that the populations of the eigenstates of $\boldsymbol{\epsilon}(z) \cdot \boldsymbol{J}$ with eigenvalues $-\hbar$, 0, $+\hbar$ are, respectively, equal to $4/17$, $9/17$, $4/17$. It follows that, in the basis $\{|g_0\rangle, |\psi_{\mathrm{S}}\rangle, |\psi_{\mathrm{A}}\rangle\}$, the density matrix is also diagonal, the corresponding populations being equal to

$$\begin{aligned} \Pi_0(1 \leftrightarrow 2) &= \Pi_{\mathrm{A}}(1 \leftrightarrow 2) = \frac{4}{17}, \\ \Pi_{\mathrm{S}}(1 \leftrightarrow 2) &= \frac{9}{17}. \end{aligned} \tag{10.17a}$$

These steady-state populations, which are independent of z, are represented by the solid circles in fig. 22a.

Consider now a $J_g = 1 \leftrightarrow J_e = 1$ transition. Since the departure rate from $|\psi_{\mathrm{S}}\rangle$ vanishes, all the atomic population will be optically pumped in

$|\psi_S\rangle$ where the atom remains trapped. It follows that

$$\begin{aligned} \Pi_0(1 \leftrightarrow 1) &= \Pi_A(1 \leftrightarrow 1) = 0, \\ \Pi_S(1 \leftrightarrow 1) &= 1. \end{aligned} \tag{10.17b}$$

Such a result can be also obtained by using the basis of eigenstates of $\epsilon(z)\cdot \boldsymbol{J}$. In such a basis, the atom is optically pumped into g_0 by absorption of a π photon and spontaneous emission of a σ^+ or σ^- photon, and it remains trapped in g_0 because of the vanishing of the Clebsch–Gordan coefficient of the π transition starting from g_0 (see fig. 21b).

10.4. Internal state for a moving atom

We consider now an atom moving with velocity v along Oz, so that

$$z = vt \tag{10.18}$$

and we suppose also that

$$T_{\text{int}} \ll T_{\text{ext}}, \tag{10.19}$$

so that we can neglect the variation of v during the time T_{int} required by internal variables to reach a steady-state.

10.4.1. Transformation to the moving rotating frame

Replacing z by vt in the expression (10.4) of $\epsilon(z)$, shows that, in its rest frame, moving with velocity v along Oz, the atom "sees" a laser field with a polarization rotating around Oz with an angular frequency $-kv$. This suggests the introduction, in the atomic rest frame, of a rotating frame such that, in this moving rotating frame, the laser field keeps a fixed direction.

Such a transformation is achieved by applying a unitary transformation

$$T(t) = \exp(-\mathrm{i}\, k\, v\, t J_z/\hbar) \tag{10.20}$$

One can easily check (see Appendix A of ref. [63]) that, in the new representation, the laser–atom interaction Hamiltonian describes the coupling of the atomic dipole moment with a laser electric field keeping a fixed linear polarization parallel to $\boldsymbol{\epsilon}_y$.

In the new representation, the atomic density matrix is equal to

$$\tilde{\sigma} = \exp(-\mathrm{i}\, k\, v\, t J_z/\hbar)\ \sigma\ \exp(+\mathrm{i}\, k\, v\, t J_z/\hbar), \tag{10.21}$$

which shows that the change of variables introduced above in eq. (10.9) corresponds to a transformation to the rotating frame. Note that the populations Π_{-1}, Π_0, Π_{+1} of the three Zeeman sublevels $|g_{-1}\rangle$, $|g_0\rangle$, $|g_{+1}\rangle$ are not modified by the transformation (10.20).

10.4.2. New Hamiltonian – new equations of motion

Since $T(t)$ depends on t, the dynamics in the new representation is governed by the Hamiltonian

$$\widetilde{H} = T(t)\, H\, T^{+}(t) + \mathrm{i}\hbar \left[\frac{\mathrm{d}T(t)}{\mathrm{d}t}\right] T^{+}(t), \tag{10.22}$$

where H is the Hamiltonian of the old representation. We have already mentioned that $T(t)HT^{+}(t)$ describes the dynamics of the atom coupled to a laser field with a fixed linear polarization parallel to $\boldsymbol{\epsilon}_y$. This dynamics is therefore described by equation (8.35) where $\boldsymbol{\epsilon}(\boldsymbol{r})$ is replaced by $\boldsymbol{\epsilon}_y$, and σ by $\widetilde{\sigma}$.

Using eq. (10.20), one can show that the last term of eq. (10.22) is equal to

$$\mathrm{i}\hbar \left[\frac{\mathrm{d}T(t)}{\mathrm{d}t}\right] T^{+}(t) = V_{\mathrm{rot}} = kvJ_z. \tag{10.23}$$

Such a term, which is time independent, has the same form as an interaction Hamiltonian with a static (fictitious) magnetic field $\boldsymbol{B}_f$, parallel to Oz, and having an amplitude such that the corresponding Larmor frequency is equal to kv. Actually, such a fictitious field is nothing but an inertial field appearing in the new frame because of its rotation (Larmor's theorem).

Finally, the dynamics of a moving atom is the same as the dynamics of an atom at rest in $z = 0$ submitted in addition to the effect of a static magnetic field $\boldsymbol{B}_f$ parallel to Oz. From eqs. (8.35) and (10.23), one deduces that the equation of motion of $\widetilde{\sigma}_{gg}$ in the new representation can be written

$$\begin{aligned}\dot{\widetilde{\sigma}}_{gg} = &-\mathrm{i}\,\delta'\,[\,\Lambda(z=0), \widetilde{\sigma}_{gg}\,] - \frac{\Gamma'}{2}\,\{\,\Lambda(z=0), \widetilde{\sigma}_{gg}\,\}_{+} \\ &+ \Gamma' \sum_{q=-1,0,+1} (\boldsymbol{\epsilon}_q^{*}\cdot\widehat{\boldsymbol{d}}^{-})\,(\boldsymbol{\epsilon}_y\cdot\widehat{\boldsymbol{d}}^{+})\,\widetilde{\sigma}_{gg}\,(\boldsymbol{\epsilon}_y^{*}\cdot\widehat{\boldsymbol{d}}^{-})\,(\boldsymbol{\epsilon}_q\cdot\widehat{\boldsymbol{d}}^{+}) \\ &- \mathrm{i}kv\,[\,J_z/\hbar, \widetilde{\sigma}_{gg}\,]\,.\end{aligned} \tag{10.24}$$

In eq. (10.24), $\Lambda(z)$ is the coefficient of $\hbar\delta'$ in eq. (10.7). Using eqs. (10.7), (10.10), and the Clebsch–Gordan coefficients of fig. 21, one can

deduce from eq. (10.24) a closed set of 5 equations for Π_{-1}, Π_0, Π_1, C_r, C_i which can be written

$$\begin{aligned}
\dot{\Pi}_1 &= -\frac{5\Gamma'}{72}\Pi_1 + \frac{9\Gamma'}{72}\Pi_0 + \frac{\Gamma'}{72}\Pi_{-1} - \frac{\Gamma'}{18}C_\mathrm{r} - \frac{\delta'}{6}C_\mathrm{i},\\
\dot{\Pi}_{-1} &= +\frac{\Gamma'}{72}\Pi_1 + \frac{9\Gamma'}{72}\Pi_0 - \frac{5\Gamma'}{72}\Pi_{-1} - \frac{\Gamma'}{18}C_\mathrm{r} + \frac{\delta'}{6}C_\mathrm{i},\\
\dot{\Pi}_0 &= -\left(\dot{\Pi}_1 + \dot{\Pi}_{-1}\right),\\
\dot{C}_\mathrm{r} &= +\frac{\Gamma'}{24}\Pi_1 + \frac{\Gamma'}{8}\Pi_0 + \frac{\Gamma'}{24}\Pi_{-1} - \frac{5\Gamma'}{12}C_\mathrm{r} + 2\,k\,v\,C_\mathrm{i},\\
\dot{C}_\mathrm{i} &= +\frac{\delta'}{12}\left(\Pi_1 - \Pi_{-1}\right) - 2\,k\,v\,C_\mathrm{r} - \frac{5\Gamma'}{12}C_\mathrm{i},
\end{aligned} \tag{10.25a}$$

for a $J_g = 1 \leftrightarrow J_e = 2$ transition, and

$$\begin{aligned}
\dot{\Pi}_1 &= -\frac{\Gamma'}{8}\Pi_1 + \frac{\Gamma'}{8}\Pi_0 + \frac{\Gamma'}{8}\Pi_{-1} + \frac{\delta'}{2}C_\mathrm{i},\\
\dot{\Pi}_{-1} &= +\frac{\Gamma'}{8}\Pi_1 + \frac{\Gamma'}{8}\Pi_0 - \frac{\Gamma'}{8}\Pi_{-1} - \frac{\delta'}{2}C_\mathrm{i},\\
\dot{\Pi}_0 &= -\left(\dot{\Pi}_1 + \dot{\Pi}_{-1}\right) = -\frac{\Gamma'}{4}\Pi_0,\\
\dot{C}_\mathrm{r} &= \frac{\Gamma'}{8} - \frac{\Gamma'}{4}C_\mathrm{r} + 2\,k\,v\,C_\mathrm{i},\\
\dot{C}_\mathrm{i} &= -\frac{\delta'}{4}\left(\Pi_1 - \Pi_{-1}\right) - 2\,k\,v\,C_\mathrm{r} - \frac{\Gamma'}{4}C_\mathrm{i},
\end{aligned} \tag{10.25b}$$

for a $J_g = 1 \leftrightarrow J_e = 1$ transition. The Zeeman coherences $\Delta m = \pm 1$ are not coupled to Π_0, $\Pi_{\pm 1}$, C_r, C_i because of the selection rule $\Delta m = 0, \pm 2$ followed by A and because the $|g_m\rangle$ are eigenstates of J_z. Since all coefficients of equations (10.25) are time independent, these equations have a steady-state solution.

The third equation (10.25.b) shows that, for a $J_g = 1 \leftrightarrow J_e = 1$ transition, Π_0 is damped with a rate $\Gamma'/4$. This is due to the fact that an atom initially in g_0 is optically pumped into $g_{\pm 1}$. From $g_{\pm 1}$, it can be re-excited to e_0 but it can then never fall back in g_0 because of the vanishing of the Clebsch–Gordan coefficient of the transition $e_0 \leftrightarrow g_0$ (see fig. 21b).

10.4.3. New expression of the mean force

Suppose that the atom has reached a steady-state so that all left-hand sides of equations (10.25) can be put equal to zero.

Consider first a $J_g = 1 \leftrightarrow J_e = 2$ transition. If one subtracts the second equation (10.25.a) from the first one, one gets

$$\text{for} \qquad J_g = 1 \leftrightarrow J_e = 2 \qquad \Pi_1 - \Pi_{-1} = -\frac{4\delta'}{\Gamma'} C_{\text{i}}. \tag{10.26}$$

Equation (10.26), combined with eqs. (10.11.a) and (10.12.a) implies that

$$\boldsymbol{\mathcal{F}}_{\text{dissip}}(1 \leftrightarrow 2) = 5\, \boldsymbol{\mathcal{F}}_{\text{react}}(1 \leftrightarrow 2). \tag{10.27}$$

The dissipative force is proportional to the reactive force, and 5 times more important, so that the total mean force is equal to

$$\boldsymbol{\mathcal{F}}(1 \leftrightarrow 2) = \tfrac{6}{5} \boldsymbol{\mathcal{F}}_{\text{dissip}}(1 \leftrightarrow 2) = \tfrac{1}{2} \hbar\, k\, \Gamma' \boldsymbol{\epsilon}_z (\Pi_1 - \Pi_{-1}). \tag{10.28}$$

For a $J_g = 1 \leftrightarrow J_e = 2$ transition, the main effect is therefore the imbalance between the radiation pressures exerted by the two counterpropagating waves. It may appear surprising that the reactive force is smaller than the dissipative force, even if $|\delta| \gg \Gamma$ (which implies $|\delta'| \gg \Gamma'$). This is due to the fact that the redistribution processes, which are the origin of the reactive force, are limited to a finite number of steps in the case of a σ^+–σ^- configuration. Starting from g_{-1}, the atom can absorb a σ^+ photon in the $k\boldsymbol{\epsilon}_z$ wave, jump into e_0, then make a stimulated emission of a σ^- photon in the $-k\boldsymbol{\epsilon}_z$ wave, which brings it into g_{+1}, then absorb again a σ^+ photon in the $k\boldsymbol{\epsilon}_z$ wave and jump into e_2. But, from e_2, it can no longer make a stimulated emission of a σ^- photon and the redistribution stops. This would not be the case if, as in chapter 9, the polarizations of the two counterpropagating waves both contain an admixture of σ^+ and σ^-.

Consider now a $J_g = 1 \leftrightarrow J_e = 1$ transition. Since Π_0 vanishes in steady state, the first two equations (10.25.b) are identical in steady-state and lead to

$$\text{for} \qquad J_g = 1 \leftrightarrow J_e = 1 \qquad \Pi_1 - \Pi_{-1} = +\frac{4\delta'}{\Gamma'} C_{\text{i}}, \tag{10.29}$$

which, combined with eqs. (10.11.b) and (10.12.b) gives

$$\boldsymbol{\mathcal{F}}_{\text{dissip}}(1 \leftrightarrow 1) = -\boldsymbol{\mathcal{F}}_{\text{react}}(1 \leftrightarrow 1). \tag{10.30}$$

This shows that the reactive and dissipative forces are equal and opposite. For a $J_g = 1 \leftrightarrow J_e = 1$ transition, the mean total radiative force always vanishes, even for a moving atom

$$\boldsymbol{\mathcal{F}}(1 \leftrightarrow 1) = \boldsymbol{\mathcal{F}}_{\text{react}}(1 \leftrightarrow 1) + \boldsymbol{\mathcal{F}}_{\text{dissip}}(1 \leftrightarrow 1) = \mathbf{0}. \tag{10.31}$$

There is therefore in this case no friction force. We will show, however, in the next chapter that a new cooling mechanism, not based on friction, but on momentum diffusion and velocity selective coherent population trapping, can appear for such a transition.

10.5. Friction force for a $J_g = 1 \leftrightarrow J_e = 2$ transition

10.5.1. Friction coefficient

In order to calculate the total mean force (10.28) experienced by the atom, we must solve equations (10.25.a) and find the steady-state value of $\Pi_1 - \Pi_{-1}$.

Consider first the limit of very small velocities. For an atom with $v = 0$ at $z = 0$, we know the steady-state density matrix which is given in eq. (10.17.a) and from which we can deduce the steady state values of Π_1, Π_0, Π_{-1}, C_r, C_i

$$\begin{aligned} \text{for} \qquad v = 0 \qquad & \Pi_1 = \Pi_{-1} = 13/34, \\ & \Pi_0 = 4/17, \\ & C_\mathrm{r} = 5/34, \\ & C_\mathrm{i} = 0. \end{aligned} \tag{10.32}$$

We can then use equations (10.25.a) with $v \neq 0$ to find the linear term in v of $\Pi_1 - \Pi_{-1}$ for an atom which is still at $z = 0$ in its moving rotating rest frame. Using eq. (10.26), we can transform the last equation (10.25.a) and express in steady-state $\Pi_1 - \Pi_{-1}$ as a function of C_r. Since C_r is already multiplied by kv in this equation, we can replace C_r by its zero order value given in eq. (10.32). We get in this way

$$\Pi_1 - \Pi_{-1} = \frac{240}{17} \, \frac{k\, v\, \delta'}{4\,\delta'^2 + 5\,\Gamma'^2}, \tag{10.33}$$

and consequently, when eq. (10.33) is inserted into eq. (10.28)

$$\frac{k\,v}{|\delta'|} \ll 1 \quad \longrightarrow \quad \mathcal{F}_z(1 \leftrightarrow 2) = -\alpha\, v, \tag{10.34}$$

where the friction coefficient α is given by

$$\alpha = -\frac{120}{17}\, \hbar\, k^2 \frac{\Gamma' \delta'}{4\,\delta'^2 + 5\,\Gamma'^2} = -\frac{120}{17}\, \hbar\, k^2 \frac{\Gamma \delta}{4\,\delta^2 + 5\,\Gamma^2}. \tag{10.35}$$

We have used eq. (10.5).

It is possible to give a more physical derivation of eq. (10.35) in the limit $|\delta| \gg \Gamma$, where $\Pi_1 - \Pi_{-1}$ and α are, according to eqs. (10.33) and (10.35), given by

$$|\delta| \gg \Gamma \quad \longrightarrow \quad \Pi_1 - \Pi_{-1} \simeq +\frac{60}{17}\,\frac{k\,v}{\delta'}, \tag{10.36a}$$

$$\alpha \simeq -\frac{30}{17}\,\hbar\,k^2\,\frac{\Gamma}{\delta}. \tag{10.36b}$$

We come back to fig. 22a giving the light shifts and steady-state populations of $|g_0\rangle$, $|\psi_S\rangle$ and $|\psi_A\rangle$ for an atom at rest and we try to understand the perturbation due to atomic motion, which is described by the Hamiltonian V_{rot} given in eq. (10.23). Since $J_z|g_0\rangle = 0$, V_{rot} cannot couple $|g_0\rangle$ to any other state. Furthermore, one can easily check, using eq. (10.13.a) (without the exponentials $\exp(\pm ikz)$ since the atom is at $z = 0$ in its moving rotating rest frame), that V_{rot} has no diagonal elements in $|\psi_S\rangle$ and $|\psi_A\rangle$. The only non-zero matrix element of V_{rot} is between $|\psi_S\rangle$ and $|\psi_A\rangle$ and is equal to

$$\langle \psi_S \mid V_{rot} \mid \psi_A \rangle = \hbar\,k\,v. \tag{10.37}$$

It is represented by the vertical arrow of fig. 22a. In the limit $kv \ll |\delta'|$, which is the condition of validity of eq. (10.36), leading to $|\Pi_1 - \Pi_{-1}| \ll 1$, the motional coupling $\hbar kv$ between ψ_S and ψ_A is small compared to the splitting $E_S - E_A$ which, according to eq. (10.14.a), is equal to

$$E_S - E_A = \tfrac{2}{3}\hbar\,\delta' - \tfrac{1}{2}\hbar\,\delta' = \frac{\hbar\,\delta'}{6}. \tag{10.38}$$

The effect of V_{rot} can thus be treated by perturbation theory. To lowest order in kv/δ', i.e., to order 1, the main effect of V_{rot} is to change the wave functions. The wave function ψ_A is contaminated by ψ_S and vice versa. If $\overline{|\psi_S\rangle}$ and $\overline{|\psi_A\rangle}$ are the perturbed states associated with $|\psi_S\rangle$ and $|\psi_A\rangle$, we have, to first order in kv/δ'.

$$\begin{aligned}\overline{|\psi_S\rangle} &= |\psi_S\rangle + \frac{\hbar\,k\,v}{E_S - E_A}\,|\psi_A\rangle = |\psi_S\rangle + \frac{6k\,v}{\delta'}\,|\psi_A\rangle \\ &= \frac{1}{\sqrt{2}}\Big[\Big(1 + \frac{6\,k\,v}{\delta'}\Big) \mid g_{+1}\rangle + \Big(1 - \frac{6\,k\,v}{\delta'}\Big) \mid g_{-1}\rangle\Big],\end{aligned} \tag{10.39a}$$

$$\begin{aligned}\overline{|\psi_A\rangle} &= |\psi_A\rangle + \frac{\hbar\,k\,v}{E_A - E_S}\,|\psi_S\rangle = |\psi_A\rangle - \frac{6k\,v}{\delta'}\,|\psi_S\rangle \\ &= \frac{1}{\sqrt{2}}\Big[\Big(1 - \frac{6\,k\,v}{\delta'}\Big)|g_{+1}\rangle - \Big(1 + \frac{6\,k\,v}{\delta'}\Big)|g_{-1}\rangle\Big].\end{aligned} \tag{10.39b}$$

Whereas $|\psi_S\rangle$ and $|\psi_A\rangle$ contain both the same proportion of $|g_1\rangle$ and $|g_{-1}\rangle$, this is no longer true for $|\psi_S\rangle$ and $|\psi_A\rangle$. For example, since $\delta' < 0$, the weight of $|g_{-1}\rangle$ in $|\psi_S\rangle$ is larger than the weight of $|g_1\rangle$. The conclusions are reversed for $|\psi_A\rangle$. Since the levels $|\psi_S\rangle$ and $|\psi_A\rangle$ have unequal populations, one understands how the motional coupling $\hbar kv$ between $|\psi_S\rangle$ and $|\psi_A\rangle$ can give rise to a motion induced difference between Π_1 and Π_{-1}. As in ref. [63], such an argument can be formulated in quantitative terms * and leads exactly to eq. (10.36). We want to emphasize here that the motion induced population difference $\Pi_1 - \Pi_{-1}$ varies as kv/δ', and not as kv/Γ, as is the case for Doppler cooling. Since $|\delta'| \ll \Gamma$ at low intensity, the new cooling mechanism discussed here is therefore much more sensitive to the velocity than Doppler cooling.

It is clear in eq. (10.35) that, as in chapter 9, the friction coefficient is independent of the laser intensity I_L. This results from a compensation in eq. (10.28) between the I_L-dependence of the absorption rate Γ', which decreases as I_L when I_L decreases, and the I_L-dependence of $\Pi_1 - \Pi_{-1}$, which increases as $1/I_L$ (see eqs. (10.33) and (10.36.a)). In particular, one sees on fig. 22a that, when I_L decreases, the distance between ψ_S and ψ_A decreases, which explains why the contamination of wave functions induced by the motional coupling $\hbar kv$ between ψ_S and ψ_A increases when I_L decreases. Note also that, according to eq. (10.36.b), α is on the order of $-(30/17)\hbar k^2\Gamma/\delta$ for $|\delta| \gg \Gamma$. Such a value is smaller than the corresponding value in eq. (9.39) of α_S found in chapter 9 by a factor of the order of Γ^2/δ^2, which is small for $|\delta| \gg \Gamma$. We will see however in subsection 10.5.3, that the momentum diffusion coefficient is reduced by the same factor Γ^2/δ^2, so that the equilibrium temperatures are on the same order for both σ^+-σ^- and Lin $\perp$ Lin configurations.

10.5.2. Velocity capture range

From now on, we will suppose that $|\delta| \gg \Gamma$. When kv is no longer small compared to $|\delta'|$, all perturbative calculations of the previous subsection, based on the smallness of kv/δ', are no longer valid. One must then go back to equations (10.25.a) and determine their exact steady-state solution, either numerically or analytically. One then finds that the variations with v of the mean force (10.28) are those of a dispersion curve, the maximum of the modulus of the force being reached for a critical velocity v_c, or velocity

* In ref. [63], the calculation is done in the basis of eigenstates of $\epsilon_y \cdot J$. The motional coupling V_{rot} has then two non-zero off-diagonal elements. Using the basis $\{|g_0\rangle, |\psi_S\rangle, |\psi_A\rangle\}$, as we do here, simplifies the calculations because only $|\psi_S\rangle$ and $|\psi_A\rangle$ are coupled by V_{rot}.

capture range, such that

$$k\,v_c \sim |\delta'|. \tag{10.40}$$

Figure 8 of ref. [63], which includes also the effect of Doppler cooling, gives an example of such a calculation.

As the velocity capture range (9.36) found for low intensity Sisyphus cooling, the value (10.40) of v_c is proportional to the laser intensity I_L. There is however an important difference between eqs. (9.36) and (10.40). For the Lin $\perp$ Lin configuration, kv_c is proportional to the absorption rate Γ', whereas for the σ^+–σ^- configuration, kv_c is proportional to the light shift δ'.

The discussion in this subsection can be presented in more physical terms by considering that the atom is submitted in the ground state to two perturbations with different symmetries. We have first the effect of the laser–atom interaction, which, in the moving rotating frame, has the symmetry of a static electric field parallel to ϵ_y and which is characterized by an Hamiltonian part, proportional to δ', and a relaxation part, proportional to Γ'. We have also the effect of atomic motion which has the symmetry of a magnetic field parallel to ϵ_z and which is proportional to kv. Depending on the relative values of kv and $|\delta'|$, one perturbation is predominant over the other. Both are of the same order for $v = v_c$. In this sense, there is a certain analogy between the narrow structures appearing in the variations with v of the mean force (10.28), and the narrow Hanle resonances which can be observed in atomic ground states (see subsection 8.5.3).

10.5.3. Order of magnitude of the equilibrium temperature

We first try to evaluate the momentum diffusion coefficient D for an atom at rest in z. Using the same notation and the same arguments as in subsection 9.5.3, we get for D_{vac} and D_{abs} the same result as in eq. (9.41.a). This amounts to assuming that D_{vac} and D_{abs} have the same order of magnitude as for a two-level atom (see subsection 5.2.3). We will see in the next subsection that this is not a good approximation for D_{abs}.

Since there is no spatial gradient of light shifts in the σ^+–σ^- configuration, there is no dipole force and no contribution D_{dip} to D as in eq. (9.41.b). It follows that

$$D \sim D_{vac} \sim D_{abs} \sim \hbar^2 k^2 \Gamma'. \tag{10.41}$$

Comparing eq. (10.41) to eq. (9.42), we see that D is smaller in the σ^+–σ^- configuration by a factor on the order of Γ^2/δ^2. This reduction of

D compensates for the reduction of α found above, so that the equilibrium temperature

$$k_B T \sim \frac{D}{\alpha} \sim \hbar |\delta'| \sim \frac{\hbar \Omega_1^2}{|\delta|} \tag{10.42}$$

is on the same order for both the σ^+-σ^- and the Lin $\perp$ Lin configurations.

10.5.4. Anomalous momentum diffusion

A quantum calculation of the momentum diffusion coefficient is done in ref. [73]. Such a calculation shows that D_{vac} has the order of magnitude given in eq. (10.41), but that D_{abs} can be much larger than D_{vac} for certain values of δ and kv. We discuss now the physical meaning of such an anomalous momentum diffusion. More details may be found in ref. [73]. See also refs. [63], [65] and [74].

The enhancement of D_{abs} is due to correlations between the directions of two successively absorbed photons. Because of optical pumping, just after the absorption of a σ^+ photon, the atom has a high probability to be in g_1 from where it has a higher probability to absorb a σ^+ photon than a σ^- one, since the σ^+ transition starting from g_1 is 6 times more intense than the σ^- one (see fig. 21a). It follows that the atom absorbs in sequence several σ^+ photons until it absorbs a σ^- photon which optically pumps it into g_{-1} from where it absorbs in sequence several σ^- photons and so on .... As a consequence, the steps of the random walk in momentum space (due to absorption) can be several $\hbar k$ instead of $\hbar k$ and this explains the increase of D_{abs}. Such an effect becomes more and more important for larger values of J_g.

Such an enhancement of D_{abs} occurs only if the eigenstates of J_z can be considered as stationary between two successive fluorescence cycles, separated by a time on the order of $\tau_P = 1/\Gamma'$. This is achieved, either for a moving atom with $kv \gg |\delta'|$, or for a slow atom if the detuning is small ($kv \ll |\delta'|$, $|\delta'| \ll \Gamma'$). In the first case ($kv \gg |\delta'|$), the perturbation $V_{rot} = kvJ_z$ predominates over the effect of light shifts described by H_{eff}, so that the eigenstates of J_z are quasi-stationary. In the second case, V_{rot} is negligible in comparison with H_{eff} (since $kv \ll |\delta'|$), but the precession induced by H_{eff} between the eigenstates of J_z occurs at a frequency $|\delta'|$, which is too small compared to the absorption rate Γ' to produce any observable effect between two fluorescence cycles.

The previous discussion explains why D_{abs} varies rapidly with kv for a given large value of δ. It is possible to understand in this way the profiles of the momentum distributions derived from a numerical integration of the

full quantum equations of motion [74]. The broad pedestal which appears in these distributions, which becomes more pronounced for larger values of J_g, reflects the increase of D_{abs} when v increases. Note however, that the width of the narrow peak around $p = 0$ appearing in these distributions remains large compared to $\hbar k$, so that the semi-classical approximation is not bad. But, for large values of J_g, the atom can make in sequence so many σ^+ transitions starting from the sublevel with the highest magnetic quantum number $m = J_g$, that it remains trapped in this sublevel for a time T_{int} which can become on the order of or even longer than T_{ext}. As in the case of low intensity Sisyphus cooling (see subsection 9.6.1), we find here a new example of a situation where usual treatments of laser cooling become questionable, not because of the semi-classical approximation, but because the usual assumption $T_{\text{int}} \ll T_{\text{ext}}$ is no longer valid.

10.6. Coherent population trapping for a $J_g = 1 \leftrightarrow J_e = 1$ transition

The fact that the mean total force vanishes for a $J_g = 1 \leftrightarrow J_e = 1$ transition (see eq. (10.31)), even if the atom is moving, does not mean that no interesting effect can occur for such a transition. We show in this section how atomic motion can induce spectacular changes in the internal dynamics.

10.6.1. Qualitative discussion

We have already mentioned at the end of subsection 10.4.2 that atoms initially in g_0 are optically pumped into $g_{\pm 1}$, from where they can never come back to g_0. Since there is no motional coupling between g_0 and $g_{\pm 1}$, we can thus completely ignore g_0, and consider that the ground state has only two relevant sublevels, g_1 and g_{-1}, or their linear combinations ψ_S and ψ_A given in eq. (10.13), with $z = 0$.

For $v = 0$, the total atomic population is optically pumped into $|\psi_S\rangle$ (see fig. 22b). When the atom is moving, a motional coupling $\hbar k v$ appears between the two states $|\psi_S\rangle$ and $|\psi_A\rangle$ (vertical arrow of fig. 22b), which are separated by a distance

$$E_S - E_A = -\frac{\hbar \delta'}{2}. \tag{10.43}$$

In the same way as for a $J_g = 1 \leftrightarrow J_e = 2$ transition, the wave functions of $|\psi_S\rangle$ and $|\psi_A\rangle$ are perturbed and this gives rise to a non-zero value of $\Pi_1 - \Pi_{-1}$. But we have now an additional spectacular effect which comes from the fact that, when $v = 0$, the absorption rate from $|\psi_S\rangle$ vanishes (see eq. (10.16.b)). The contamination of $|\psi_S\rangle$ by $|\psi_A\rangle$, induced by atomic motion, transfers to $|\psi_S\rangle$ a small part of the instability of $|\psi_A\rangle$, and the

absorption rate from the perturbed state $\overline{|\psi_S\rangle}$ corresponding to $|\psi_S\rangle$ no longer vanishes. In other words, the total fluorescence rate R_F, which vanishes when $v = 0$ because all atoms are in the non-absorbing state $|\psi_S\rangle$, reappears when the atom is moving because a slight absorption can take place from $\overline{|\psi_S\rangle}$. Such an effect is characterized by the perturbation parameter $kv/(E_S - E_A) \sim kv/\delta'$, so that the variations of R_F with v occur in a very small velocity range around $v = 0$, on the order of v_c given by eq. (10.40).

For the transition $J_g = 1 \leftrightarrow J_e = 2$, the motional coupling $\hbar kv$ between $|\psi_S\rangle$ and $|\psi_A\rangle$ also changes the absorption rates from these sublevels. In this case, it is the sublevel $|\psi_A\rangle$ which is not coupled to $|e_0\rangle$ (see eq. (10.15.a)) and which becomes partially coupled when contaminated by $|\psi_S\rangle$. The effect is however less spectacular because, even if $v = 0$, the state $|\psi_A\rangle$ can absorb light (see eq. (10.16.a)), since it is always coupled to e_2 and e_{-2}. One therefore expects variations of the total fluorescence rate when v is slightly varied around $v = 0$, but the fluorescence never stops completely, as it is the case for a $J_g = 1 \leftrightarrow J_e = 1$ transition.

Note also that, when the atom is moving with velocity v, it "sees" in its rest frame the two counterpropagating laser waves with opposite Doppler shifts $\pm kv$, so that these two waves have apparent frequencies $\omega_L \pm kv$, differing by a frequency shift $\Delta = 2kv$ which vanishes for $v = 0$. As long as one is interested only in the internal atomic dynamics, one would get the same equations and the same results by considering another problem where an atom, always at rest, interacts with two laser waves (not necessarily counterpropagating) having different frequencies, $\omega_L \pm \Delta/2$. When $\Delta = 0$, the atom gets trapped into $|\psi_S\rangle$ and the fluorescence stops. When Δ is slightly varied from zero, the fluorescence reappears. One can finally show that similar equations apply also to the situation where $g_1 = g$ and $g_{-1} = g'$ have different energies E and E', and where the two laser waves have different frequencies, ω_L for the wave exciting the transition $g \leftrightarrow e_0$, ω'_L for the wave exciting the transition $g' \leftrightarrow e_0$. The fluorescence stops when $E + \hbar\omega_L = E' + \hbar\omega'_L$, i.e., when the two detunings of the two laser excitations are equal, and reappears when ω'_L is slightly varied, ω_L, E and E' being fixed, or when $E - E'$ is slightly varied, ω_L and ω'_L being fixed. Such a phenomenon, called "coherent population trapping" was observed for the first time on sodium atoms irradiated by a bimodal laser and put in a gradient of a magnetic field [75]. Because of the corresponding spatial variation of the Zeeman effect, the fluorescence of the sodium cell was disappearing at certain places along the laser beam, where two Zeeman sublevels belonging to the two different hyperfine levels were separated by a frequency splitting equal to the mode spacing.

10.6.2. Velocity dependence of the total fluorescence rate

We now give a more quantitative description of coherent population trapping. Since the only excited Zeeman sublevel which can be reached from g_1 and g_{-1} is e_0 (see fig. 21b), the total fluorescence rate R_F is given by

$$R_F = \Gamma \sigma_{e_0 e_0}. \tag{10.44}$$

According to eq. (8.28), the population $\sigma_{e_0 e_0}$ of e_0 can be expressed in terms of the ground-state density matrix. Using eqs. (8.28), (10.4), (10.5) and the Clebsch–Gordan coefficients of fig. 21b, we get

$$R_F = \frac{\Gamma'}{4} \left[\Pi_1 + \Pi_{-1} - 2C_r\right] = \frac{\Gamma'}{4} (1 - 2C_r). \tag{10.45}$$

To evaluate C_r, we come back to equations (10.25.b). We know already that, in steady-state, $\Pi_1 - \Pi_{-1}$ and C_i are proportional (see eq. (10.29)). The last two equations thus couple only C_r and C_i and they allow one to calculate the steady-state value of C_r

$$C_r = \frac{1}{2} \frac{4\delta'^2 + \Gamma'^2}{4\delta'^2 + \Gamma'^2 + 64 k^2 v^2}, \tag{10.46}$$

which, inserted into eq. (10.45) yields

$$R_F(v) = \Gamma' \frac{16 k^2 v^2}{4\delta'^2 + \Gamma'^2 + 64 k^2 v^2}. \tag{10.47}$$

It is clear from eq. (10.47) that R_F vanishes for $v = 0$, and then increases when v increases, as an inverted Lorentz curve of amplitude $\Gamma'/4$ and of half-width at half maximum

$$\Delta v = \frac{\sqrt{4\delta'^2 + \Gamma'^2}}{8k}, \tag{10.48}$$

which decreases as I_L when I_L decreases. For $v \ll \Delta v$, R_F varies as

$$v \ll \Delta v \quad \longrightarrow \quad R_F(v) \simeq 16 k^2 v^2 \frac{\Gamma'}{4\delta'^2 + \Gamma'^2} = \frac{8 k^2 v^2 \Gamma}{\Omega_1^2}, \tag{10.49}$$

which no longer depends on the detuning δ (we have used eq. (10.5) and the definition of s_0 in terms of the Rabi frequency Ω_1, associated with each wave).

Calculations similar to the previous one and based on optical Bloch equations have been made [76] shortly after the discovery of coherent population trapping. Dressed atom interpretations, using coupled and uncoupled states analogous to the states $|\psi_A\rangle$ and $|\psi_S\rangle$ introduced here, have been also given (see for example refs. [77] and [78]).

10.6.3. Consequences for atomic motion

We come back to the external dynamics of the atom. Although the mean friction force vanishes, the fact that the fluorescence rate R_F varies very rapidly with v around $v = 0$ has interesting consequences for atomic motion.

First, one expects that the momentum diffusion coefficient varies also very rapidly with v around $v = 0$ and tends to zero when $v \to 0$, since such a phenomenon is due to the random exchanges of momentum associated with fluorescence cycles.

In all previous discussions, we have considered an atom with a fixed velocity v and we have ignored any change of v. This is usual in semi-classical treatments of laser cooling where one calculates the friction and diffusion coefficients for a fixed value of v. In fact, because of the random changes of momentum following a fluorescence cycle, the atomic velocity makes a random walk in velocity space. The important new feature which appears here, and which is not included in usual treatments, is that such a random walk can be profoundly perturbed by the strong velocity dependence of the fluorescence rate. After a fluorescence cycle, depending whether v gets closer or farther from $v = 0$, the next fluorescence cycle will occur after a longer or shorter delay. We will see in the next chapter how such a velocity dependent random walk can provide a new scheme for obtaining very narrow velocity distributions, i.e., very cold atoms.

11. Laser cooling below the single photon recoil limit

11.1. Introduction

11.1.1. The single photon recoil limit

All cooling mechanisms described in the previous chapters are based on a friction force which damps the atomic velocity. Spontaneous emission processes play also a basic role for dissipating the energy removed from the external degrees of freedom of the atom. For example, in the Sisyphus cooling mechanism, either at high (chapter 7) or low (chapter 9) intensity, spontaneous Raman anti Stokes processes dissipate the potential energy

gained by the atom (at the expense of its kinetic energy) when it climbs a potential hill. For Doppler cooling and for polarization gradient cooling in a σ^+–σ^- configuration it is a blue Doppler shift of the spontaneously emitted photons which explains the dissipation of energy (see discussion in subsection 3.B.6 in ref. [63]).

Since, in all these cooling mechanisms fluorescence cycles never stop, it seems impossible to avoid the random recoil due to spontaneously emitted photons and the corresponding single photon recoil energy

$$E_{\mathrm{R}} = \frac{\hbar^2 k^2}{2M} = k_{\mathrm{B}} T_{\mathrm{R}}. \tag{11.1}$$

The temperature T_{R} defined by eq. (11.1) is called the single photon recoil limit and appears as a fundamental limit for any cooling process using spontaneous emission. The corresponding velocity

$$v_{\mathrm{R}} = \frac{\hbar k}{M} \tag{11.2}$$

is called the recoil velocity. For sodium cooled on the resonance line, $T_{\mathrm{R}} \simeq 2.4$ μK and $v_{\mathrm{R}} \simeq 3$ cm/s. For cesium, we have $T_{\mathrm{R}} \simeq 0.13$ μK and $v_{\mathrm{R}} \simeq 3$ mm/s, and for helium cooled on the $2^3S_1 \leftrightarrow 2^3P_1$ transition at $\lambda = 1.08$ μm, $T_{\mathrm{R}} \simeq 4$ μK and $v_{\mathrm{R}} \simeq 9$ cm/s.

11.1.2. Velocity selective coherent population trapping

The previous discussion clearly shows that, in order to get temperatures lower than T_{R}, spontaneous emission processes must stop for the atoms we want to cool down to very small temperatures. Such a remark suggests the use of the phenomenon discussed in section 9.6 for a $J_g = 1 \leftrightarrow J_e = 1$ transition and a σ^+–σ^- laser configuration. We have seen in this case that the fluorescence rate R_{F} vanishes for atoms with zero velocity (see eqs. (10.47) and (10.49)), because atoms are optically pumped in a linear superposition of the ground-state sublevels which appears as a trapping non-absorbing state. This trap is perfect for $v = 0$ and less and less perfect when v increases. This is why such a phenomenon can be called velocity selective coherent population trapping. It selects very cold atoms, having very small velocities and protects them from the "bad" effects of spontaneous emission.

Actually, if we want to achieve cooling, we must also compress the velocity distribution around $v = 0$. It is not sufficient to find a velocity selection mechanism which consists here of quenching the fluorescence rate for atoms contained in a small velocity range δv around $v = 0$. One must also increase the density of atoms in this velocity range.

11.1.3. Optical pumping in velocity space

Because of the momentum transferred to the atom by the absorbed photon and because of the momentum carried away by the fluorescence photon, there is a random change of atomic momentum after each fluorescence cycle. It may happen than an atom with $v > \delta v$ undergoes such a cycle and ends up with $v < \delta v$. Momentum diffusion can thus be considered as an optical pumping process in velocity space which transfers atoms from the absorbing velocity classes into the non-absorbing velocity range δv around $v = 0$, where they remain trapped during the interaction time Θ and where they pile up, forming a narrow peak in the velocity distribution.

The new cooling mechanism we have just described, and which has been first proposed and demonstrated in refs. [79] and [80], differs radically from the other ones since it is not based on friction but on a combination of momentum diffusion and velocity selective coherent population trapping.* We show in the subsequent section that it is limited only by the interaction time Θ. Another important feature is that it does not depend on the sign of the detuning.

11.1.4. Failure of semi-classical treatments

The semi-classical treatment presented in chapter 10 considers atoms which are very well localized in the laser wave. For example, the state $|\psi_S(z)\rangle$ which we have introduced in eq. (10.13.a) for an atom "at rest in z" and which is a non-absorbing state for a $J_g = 1 \leftrightarrow J_e = 1$ transition (see eq. (10.15.b)), refers to the internal state of an atom whose center of mass is described a wave packet so well localized around z that it is not necessary to describe in fully quantum terms the evolution of such a wave packet. In eq. (10.13.a), z is considered as a fixed parameter. If the atom is moving with velocity v, z is replaced by the c-number vt (see eq. (10.18)).

If a cooling mechanism reduces the momentum spread δp of the atom below $\hbar k$, which is the case for laser cooling below the single photon recoil limit, the spatial coherence length $\xi_A \sim \hbar/\delta p$ becomes larger than the laser wavelength and it is no longer possible to consider the atom as well localized in the laser wave. A fully quantum treatment of all degrees of freedom is then required. Such a treatment is presented in the next subsection. We will see that the non-absorbing state is still given by eq. (10.13.a), but that $\psi_S(z)$ is no longer the internal state of a wave packet localized in z, but a two-component wave function of z.

* It has been also suggested that optical pumping in translation space might be used to cool the translational degrees of freedom below the recoil limit by velocity-selective recycling in a trap [81].

11.2. One-dimensional quantum treatment

We consider here a σ^+–σ^- laser configuration and $J_g = 1 \leftrightarrow J_e = 1$ transition.

11.2.1. Quantum atomic states uncoupled to the laser light

The atomic states are now labelled by two quantum numbers, one for the internal state, one for the external state. We have already seen in chapter 10 (see end of subsection 10.4.2) that, for a $J_g = 1 \leftrightarrow J_e = 1$ transition, the only relevant internal states are g_1 and g_{-1} in the ground state, e_0 in the excited state. For describing the external state, we will use the momentum p along Oz, so that a state such as $|g_1, p\rangle$ represents the atom in g_1 with a momentum p along Oz.

When the external degrees of freedom are quantized, the coordinate z of the center of mass, which appears in the expression (10.1) of the laser electric field $\boldsymbol{E}_{\mathrm{L}}(z,t)$, becomes an operator Z. The laser–atom interaction Hamiltonian (8.4) can then be written, using eq. (10.2), the Rabi frequency Ω_1 associated with $\mathcal{E}_0$ and the Clebsch–Gordan coefficients of fig. 21b

$$V_{AL} = \frac{\hbar\,\Omega_1}{2}\left[-\frac{1}{\sqrt{2}}\,\mathrm{e}^{\mathrm{i}kZ}\mid e_0\rangle\langle g_{-1}\mid + \frac{1}{\sqrt{2}}\,\mathrm{e}^{-\mathrm{i}kZ}\mid e_0\rangle\langle g_1\mid\right]\mathrm{e}^{-\mathrm{i}\omega_L t} + h.c. \tag{11.3}$$

The operators $\mathrm{e}^{\pm\mathrm{i}kZ}$ appearing in eq. (11.3) are translation operators in momentum space, so that

$$V_{\mathrm{AL}}|g_{-1}, p\rangle = -\frac{\hbar\,\Omega_1}{2\sqrt{2}}\,\mathrm{e}^{-\mathrm{i}\omega_{\mathrm{L}}t}\,|e_0,\, p + \hbar k\rangle, \tag{11.4a}$$

$$V_{\mathrm{AL}}|g_{+1}, p\rangle = +\frac{\hbar\,\Omega_1}{2\sqrt{2}}\,\mathrm{e}^{-\mathrm{i}\omega_{\mathrm{L}}t}\,|e_0,\, p - \hbar k\rangle. \tag{11.4b}$$

The interpretation of eq. (11.4.a) is very clear. Starting from g_{-1}, the atom can only go to e_0 by absorption of a photon which must be σ^+ (conservation of angular momentum). This σ^+ photon propagates along the positive direction of Oz (see fig. 20) and thus carries a momentum $+\hbar k$ which is transferred to the atom during the absorption process, so that the atomic momentum changes from p to $p + \hbar k$. Similar considerations apply to eq. (11.4.b).

Equations (11.4) suggest now to introduce the states

$$|\psi_{\mathrm{NC}}(p)\rangle = \frac{1}{\sqrt{2}}\left[\,|g_{-1},\, p - \hbar k\rangle + |g_{+1},\, p + \hbar k\rangle\,\right], \tag{11.5}$$

which are not coupled to the laser light since

$$V_{\mathrm{AL}}|\psi_{\mathrm{NC}}(p)\rangle = \frac{\hbar\Omega_1}{4}\,\mathrm{e}^{-\mathrm{i}\omega_{\mathrm{L}}t}\,[-|e_0,\,p\rangle + |e_0,\,p\rangle\,] = 0. \tag{11.6}$$

The two absorption amplitudes, starting from $|g_{-1}, p-\hbar k\rangle$ and from $|g_1, p+\hbar k\rangle$ and ending both in the same final state $|e_0, p\rangle$ interfere destructively. Equations (11.5) and (11.6) generalize the equations (10.13.b) and (10.15.b) of the previous chapter, where the external degrees of freedom were not quantized. Note that different atomic momenta $p-\hbar k$ and $p+\hbar k$ appear in the two states, which are linearly superposed in eq. (11.5). This is due to the fact that the photons which can be absorbed by an atom in g_{-1} or g_1 have opposite momenta $+\hbar\mathrm{k}$ and $-\hbar k$. Since the final state must be the same for the two paths, the two initial states corresponding to g_{-1} and g_1 must have momenta which differ by $2\hbar k$.

It is of course possible to introduce also the states

$$|\psi_{\mathrm{C}}(p)\rangle = \frac{1}{\sqrt{2}}\,[-|g_{-1},\,p-\hbar k\rangle + |g_{+1},\,p+\hbar k\rangle\,], \tag{11.7}$$

i.e., the linear combinations of $|g_{-1}, p-\hbar k\rangle$ and $|g_1, p+\hbar k\rangle$ which are orthogonal to the non-coupled states (11.5). For such states, the two absorption amplitudes, starting from $|g_{-1}, p-\hbar k\rangle$ and $|g_1, p+\hbar k\rangle$ and ending in $|e_0, p\rangle$ interfere constructively rather than destructively, so that these states are coupled to the laser

$$V_{\mathrm{AL}}|\psi_{\mathrm{C}}(p)\rangle = \frac{\hbar\Omega_1}{2}\,\mathrm{e}^{-\mathrm{i}\omega_{\mathrm{L}}t}\,|e_0,\,p\rangle. \tag{11.8}$$

It is easy to check that V_{AL} couples $|e_0, p\rangle$ only to $|\psi_{\mathrm{C}}(p)\rangle$

$$V_{\mathrm{AL}}|e_0,\,p\rangle = \frac{\hbar\Omega_1}{2}\,\mathrm{e}^{-\mathrm{i}\omega_{\mathrm{L}}t}\,|\psi_{\mathrm{C}}(p)\rangle, \tag{11.9}$$

so that the only non-zero matrix elements of V_{AL} are

$$\langle e_0,\,p\mid V_{\mathrm{AL}}\mid\psi_{\mathrm{C}}(p)\rangle = \frac{\hbar\Omega_1}{2}\,\mathrm{e}^{-\mathrm{i}\omega_{\mathrm{L}}t} = \langle\psi_{\mathrm{C}}(p)\mid V_{\mathrm{AL}}\mid e_0,\,p\rangle^*. \tag{11.10}$$

11.2.2. Couplings induced by atomic motion

When the external degrees of freedom are quantized, the atomic Hamiltonian H_{A} contains a contribution H_A^{ext} which describes the kinetic energy

of the center of mass motion. The equation which generalizes eq. (2.2) for a multilevel atom is

$$H_{\mathrm{A}} = H_{\mathrm{A}}^{\mathrm{ext}} + H_{\mathrm{A}}^{\mathrm{int}} = \frac{P^2}{2M} + \hbar\omega_{\mathrm{A}} P_e, \tag{11.11}$$

where P_e is the projector onto the manifold of excited Zeeman sublevels, since we suppose here that the ground-state Zeeman sublevels have all the same internal energy, taken equal to 0. In eq. (11.11), P is the atomic momentum operator along Oz, since we restrict ourselves in this section to a one-dimensional treatment.

The states $|g_{\pm 1}, p \pm \hbar k\rangle$ are eigenstates of H_{A}

$$H_{\mathrm{A}}|g_{\pm 1}, p \pm \hbar k\rangle = \frac{(p \pm \hbar k)^2}{2M}|g_{\pm 1}, p \pm \hbar k\rangle, \tag{11.12}$$

the corresponding eigenvalues being the kinetic energies associated with the values $p \pm \hbar k$ of the atomic momentum. From eq. (11.12), one deduces

$$\begin{aligned} H_{\mathrm{A}}|\psi_{\mathrm{NC}}(p)\rangle &= \frac{1}{\sqrt{2}}\left[\frac{(p-\hbar k)^2}{2M}|g_{-1}, p-\hbar k\rangle + \frac{(p+\hbar k)^2}{2M}|g_1, p+\hbar k\rangle\right] \\ &= \left(\frac{p^2}{2M} + E_{\mathrm{R}}\right)|\psi_{\mathrm{NC}}(p)\rangle + \frac{\hbar k\, p}{M}|\psi_{\mathrm{C}}(p)\rangle, \end{aligned} \tag{11.13a}$$

$$H_{\mathrm{A}}|\psi_{\mathrm{C}}(p)\rangle = \left(\frac{p^2}{2M} + E_{\mathrm{R}}\right)|\psi_{\mathrm{C}}(p)\rangle + \frac{\hbar k\, p}{M}|\psi_{\mathrm{NC}}(p)\rangle. \tag{11.13b}$$

Such a result shows that H_{A} shifts the two states $|\psi_{\mathrm{NC}}(p)\rangle$ and $|\psi_{\mathrm{C}}(p)\rangle$ by the same amount $(p^2/2M) + E_{\mathrm{R}}$, where E_{R} is the recoil energy given in eq. (11.1), and introduces a "motional coupling" between these two states

$$\langle\psi_{\mathrm{C}}(p) \mid H_{\mathrm{A}} \mid \psi_{\mathrm{NC}}(p)\rangle = \frac{\hbar k\, p}{M} \tag{11.14}$$

characterized by an angular frequency equal to the Doppler shift kp/M associated with the velocity p/M.

11.2.3. Decay rates due to spontaneous emission

As long as spontaneous emission is ignored, the three states $|e_0, p\rangle$, $|g_1, p+\hbar k\rangle$, $|g_{-1}, p-\hbar k\rangle$ form a three-dimensional subspace, or family, which we denote $\mathcal{F}(p)$, and which remains stable under the effect of the atom–laser coupling V_{AL} and the atomic Hamiltonian H_{A}. Without spontaneous emission, an atomic state, which belongs initially to $\mathcal{F}(p)$, cannot leave $\mathcal{F}(p)$. Since $|\psi_{\mathrm{C}}(p)\rangle$ and $|\psi_{\mathrm{NC}}(p)\rangle$ are linear combinations of

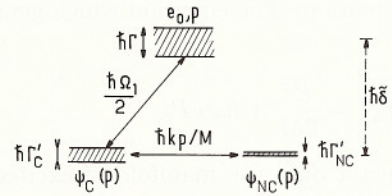

Fig. 23. Various couplings between the three states $|e_0, p\rangle$, $|\psi_C(p)\rangle$ and $|\psi_{NC}(p)\rangle$ of the family $\mathcal{F}(p)$. The energy separation between $|e_0, p\rangle$ and $|\psi_C(p)\rangle$ (or $|\psi_{NC}(p)\rangle$) is $-(\hbar\delta + E_R) = -\hbar\tilde{\delta}$ (after elimination of the time dependence of V_{AL}). The two states $|e_0, p\rangle$ and $|\psi_C(p)\rangle$ are coupled by V_{AL}(matrix element $\hbar\Omega_1/2$), whereas the two states $|\psi_C(p)\rangle$ and $|\psi_{NC}(p)\rangle$ are coupled by H_A (matrix element $\hbar kp/M$). In the absence of V_{AL} and H_A, the only radiatively unstable state of the family is $|e_0, p\rangle$ (natural width or departure rate Γ). Because of the contamination of $|\psi_C(p)\rangle$ and $|\psi_{NC}(p)\rangle$ by $|e_0, p\rangle$, due to V_{AL} and H_A, the two states $|\psi_C(p)\rangle$ and $|\psi_{NC}(p)\rangle$ also acquire finite widths, or departure rates, which are denoted Γ'_C and Γ'_{NC}.

$|g_{\pm 1}, p \pm k\rangle$, $\mathcal{F}(p)$ can also be considered as subtended by the three orthogonal states $|e_0, p\rangle$, $|\psi_C(p)\rangle$, $|\psi_{NC}(p)\rangle$

$$\begin{aligned}\mathcal{F}(p) &= \Big\{ |e_0, p\rangle, |g_{+1},\, p + \hbar k\rangle, |g_{-1},\, p - \hbar k\rangle \Big\} \\ &= \Big\{ |e_0, p\rangle, |\psi_C(p)\rangle, |\psi_{NC}(p)\rangle \Big\}.\end{aligned} \tag{11.15}$$

Figure 23 represents these three states and the various couplings which exist between them and which are due to V_{AL} (matrix element $\hbar\Omega_1/2$ between $|e_0, p\rangle$ and $|\psi_C(p)\rangle$) and to H_A (matrix element $\hbar kp/M$ between $|\psi_C(p)\rangle$ and $|\psi_{NC}(p)\rangle$). We have eliminated the exponentials $\exp(\pm i\omega_L t)$ appearing in expression (11.3) by using the transformation (8.19) (or by quantizing the laser mode), which amounts to replacing ω_A by $\omega_A - \omega_L = -\delta$. If one includes the diagonal elements of H_A in the unperturbed energies of the three states of $\mathcal{F}(p)$, the energy separation between $|e_0, p\rangle$ and $|\psi_C(p)\rangle$ (or $|\psi_{NC}(p)\rangle$) is $-\hbar\tilde{\delta}$ where

$$\hbar\,\tilde{\delta} = \hbar\,\delta + E_R. \tag{11.16}$$

In this subsection, we investigate the departure rates from $\mathcal{F}(p)$ due to spontaneous emission. If we ignore V_{AL} and H_A, the only radiatively unstable state of $\mathcal{F}(p)$ is $|e_0, p\rangle$ since no real* spontaneous emission process can occur from any one of the two ground-state sublevels $|g_1\rangle$ and $|g_{-1}\rangle$.

* Photons can be virtually emitted and reabsorbed from g_1 and g_{-1}, when the rotating

The departure rate from $|e_0, p\rangle$ is equal to the natural width Γ of $|e_0, p\rangle$. As long as one is interested only in the decay amplitude of an initial state belonging to $\mathcal{F}(p)$, and not in the final states resulting from this spontaneous decay, one can show* that the quantum evolution within $\mathcal{F}(p)$ is correctly described if one just adds an imaginary part $-i\hbar\Gamma/2$ to the energy of $|e_0, p\rangle$. The quantum evolution within $\mathcal{F}(p)$ is thus governed by the following 3×3 non-Hermitian effective Hamiltonian

$$H_{\text{eff}} = \hbar \begin{pmatrix} -\widetilde{\delta} - i\Gamma/2 & \Omega_1/2 & 0 \\ \Omega_1/2 & 0 & kp/M \\ 0 & kp/M & 0, \end{pmatrix} \tag{11.17}$$

which has in general three complex eigenvalues having different imaginary parts. This means that there are in general three different spontaneous decay modes from $\mathcal{F}(p)$. We want here to discuss the physical meaning of these modes in the perturbative limit where the couplings $\hbar\Omega_1/2$ and $\hbar kp/M$ due to V_{AL} and H_{A} are sufficiently small.

Consider first the particular case where $p = 0$. It is clear from fig. 23 that the state $|\psi_{\text{NC}}(p = 0)\rangle$, given by

$$|\psi_{\text{NC}}(p = 0)\rangle = \frac{1}{\sqrt{2}}\left[\, |g_{-1}, -\hbar k\rangle + |g_{+1}, +\hbar k\rangle \,\right] \tag{11.18}$$

is completely isolated from the other two states of $\mathcal{F}(p = 0)$ since the coupling $\hbar kp/M$ between $|\psi_{\text{NC}}(p)\rangle$ and $|\psi_{\text{C}}(p)\rangle$ vanishes for $p = 0$. This means that an atom which is put at $t = 0$ in $|\psi_{\text{NC}}(p = 0)\rangle$ will remain there indefinitely. The state $|\psi_{\text{NC}}(p = 0)\rangle$, given in eq. (11.18), is therefore a perfect trap. The departure rate $\Gamma'_{\text{NC}}(p = 0)$ from $|\psi_{\text{NC}}(p = 0)\rangle$ is strictly zero

$$\Gamma'_{\text{NC}}(p = 0) = 0. \tag{11.19}$$

---

wave approximation is not made in the atom–vacuum field interaction Hamiltonian V_{AV} appearing in eq. (2.1). One can show that these "virtual" processes give rise to energy shifts of g_1 and g_{-1} which are the same for these two sublevels as a consequence of the rotational invariance of V_{AV}. These Lamb-shifts of g_{-1} and g_1, as well as the Lamb-shift of e_0, are supposed here to be reincluded in the atomic frequency ω_{A}.

* One possible method for demonstrating such a result is to study the restriction of the resolvent operator within the subspace subtended by the three states of $\mathcal{F}(p)$ (see for example ref. [2], Chap. III).

The other two departure rates from $\mathcal{F}(p=0)$ may be found by using eq. (11.17), which splits up into two submatrices when $p=0$, one 1×1 submatrix corresponding to $|\psi_{\mathrm{NC}}(p=0)\rangle$, and one 2×2 submatrix

$$\hbar\begin{pmatrix} -\widetilde{\delta}-\mathrm{i}\Gamma/2 & \Omega_1/2 \\ \Omega_1/2 & 0 \end{pmatrix} \tag{11.20}$$

in the subspace $\{|e_0,p=0\rangle,\ |\psi_{\mathrm{C}}(p=0)\rangle\}$. If

$$\Omega_1 \ll \sqrt{\widetilde{\delta}^2+(\Gamma^2/4)}, \tag{11.21}$$

i.e., if $\Omega_1 \ll \Gamma$ or $\Omega_1 \ll \left|\widetilde{\delta}\right|$, the eigenvalues of eq. (11.20) can be found perturbatively. The eigenvalue which tends to zero when $\Omega_1 \to 0$ is given by the well know second order perturbative expression

$$\frac{(\hbar\Omega_1/2)^2}{\hbar(\widetilde{\delta}+\mathrm{i}(\Gamma/2))} = \hbar\left(\delta'_{\mathrm{C}}-\mathrm{i}\frac{\Gamma'_{\mathrm{C}}}{2}\right) \tag{11.22}$$

where

$$\Gamma'_{\mathrm{C}} = \Gamma\frac{(\Omega_1/2)^2}{\widetilde{\delta}^2+(\Gamma^2/4)}, \tag{11.23a}$$

$$\delta'_{\mathrm{C}} = \widetilde{\delta}\frac{(\Omega_1/2)^2}{\widetilde{\delta}^2+(\Gamma^2/4)}. \tag{11.23b}$$

Such a result means that, under the effect of V_{AL}, the state $|\psi_{\mathrm{C}}(p=0)\rangle$ is light shifted by $\hbar\delta'_{\mathrm{C}}$ and gets a finite width Γ'_{C}, which can be also considered as the photon scattering rate from $|\psi_{\mathrm{C}}(p=0)\rangle$. This departure rate from $|\psi_{\mathrm{C}}(p=0)\rangle$ is obviously due to the "contamination", induced by V_{AL}, of $|\psi_{\mathrm{C}}(p=0)\rangle$ by $|e_0,p=0\rangle$. The other eigenvalue of eq. (11.20) is very close to $-\hbar\widetilde{\delta}-\mathrm{i}\hbar\Gamma/2$.

Suppose now that p is different from zero, but very small. More precisely, the coupling $\hbar kp/M$ between $|\psi_{\mathrm{NC}}(p)\rangle$ and $|\psi_{\mathrm{C}}(p)\rangle$ is assumed to be very small compared with the light shift or the width of $|\psi_{\mathrm{C}}(p)\rangle$ calculated above for $p=0$

$$\frac{k|p|}{M} \ll |\delta'_{\mathrm{C}}| \quad \text{or} \quad \Gamma'_{\mathrm{C}}. \tag{11.24}$$

Two of the three eigenvalues of eq. (11.17) are then still very close to the two eigenvalues of eq. (11.20), i.e., to $-\hbar\widetilde{\delta}-\mathrm{i}\hbar(\Gamma/2)$ and $\hbar\delta'_{\mathrm{C}}-\mathrm{i}\hbar\Gamma'_{\mathrm{C}}/2$.

As for the third one, one can get it by applying second order perturbation theory to the coupling $\hbar kp/M$ induced by $H_{\rm A}$ between $|\psi_{\rm NC}(p)\rangle$ and the perturbed state $|\psi_{\rm C}(p)\rangle$ resulting from the coupling $\hbar\Omega_1/2$ induced by $V_{\rm AL}$ between $|\psi_{\rm C}(p)\rangle$ and $|e_0, p\rangle$. One gets in this way, using eq. (11.23)

$$\frac{(\hbar kp/M)^2}{\hbar(-\delta'_{\rm C} + \mathrm{i}\frac{\Gamma'_{\rm C}}{2})} = \hbar\left(\delta'_{\rm NC} - \mathrm{i}\frac{\Gamma'_{\rm NC}}{2}\right), \tag{11.25}$$

where

$$\delta'_{\rm NC}(p) = \frac{(kp/M)^2}{{\delta'_{\rm C}}^2 + ({\Gamma'_{\rm C}}^2/4)}\,\delta'_{\rm C} = \frac{4k^2p^2}{M^2\Omega_1^2}\,\widetilde{\delta}, \tag{11.26a}$$

$$\Gamma'_{\rm NC}(p) = \frac{(kp/M)^2}{{\delta'_{\rm C}}^2 + ({\Gamma'_{\rm C}}^2/4)}\,\Gamma'_{\rm C} = \frac{4k^2p^2}{M^2\Omega_1^2}\,\Gamma. \tag{11.26b}$$

In eq. (11.25), $\hbar\delta'_{\rm NC}(p)$ is the light shift of $|\psi_{\rm NC}(p)\rangle$, whereas $\Gamma'_{NC}(p)$ is the departure rate from $|\psi_{\rm NC}(p)\rangle$, more precisely from the eigenstate $|\psi_{\rm NC}(p)\rangle$ of eq. (11.17), which tends to $|\psi_{\rm NC}(p)\rangle$ when $p \to 0$ ($|\psi_{\rm NC}(p)\rangle$ is a linear superposition of the three states (11.15) where $|\psi_{\rm NC}(p)\rangle$ has the largest weight). Here also, the departure rate from $|\psi_{\rm NC}(p)\rangle$ is due to the contamination of $|\psi_{\rm NC}(p)\rangle$ by $|e_0, p\rangle$. But this contamination results now from two contaminations: the contamination induced by $V_{\rm AL}$ between $|\psi_{\rm C}(p)\rangle$ and $|e_0, p\rangle$, which gives rise to a perturbed state $|\psi_{\rm C}(p)\rangle$ containing a small admixture of $|e_0, p\rangle$, and the contamination induced by $H_{\rm A}$ between $|\psi_{\rm NC}(p)\rangle$ and $|\psi_{\rm C}(p)\rangle$.

It is clear from eq. (11.26.b) that the departure rate $\Gamma'_{\rm NC}(p)$ is very small when p is small, and vanishes for $p = 0$*. This means that an atom, which is put in $|\psi_{\rm NC}(p)\rangle$ at time $t = 0$, can remain there for a very long time if p is small enough, on the order of $(\Gamma'_{\rm NC}(p))^{-1}$. Conversely, for a given interaction time Θ, we can find a range δp of values of p around $p = 0$, such that if $|p| < \delta p$, an atom in $|\psi_{\rm NC}(p)\rangle$ has a high probability to remain trapped in $|\psi_{\rm NC}(p)\rangle$ during the whole interaction time Θ. The corresponding value of δp is given by the condition

$$\Gamma'_{\rm NC}(\delta p)\,\Theta < 1, \tag{11.27}$$

* The spontaneous decay rate $\Gamma'_{\rm NC}(p)$ is equal to half the semi-classical fluorescence rate $R_{\rm F}(v = p/M)$ found in eq. (10.49). The factor 1/2 is due to the fact that, in steady-state, the state $|\psi_{\rm C}(p)\rangle$ is also populated and contributes equally to the fluorescence rate.

which, using eq. (11.26.b), leads to

$$\delta p < \frac{M}{2k\sqrt{\Gamma}} \frac{\Omega_1}{\sqrt{\Theta}}. \tag{11.28}$$

The previous analysis thus demonstrates the existence of a velocity selection mechanism. The set of states $\overline{|\psi_{\mathrm{NC}}(p)\rangle}$ with $|p| < \delta p$ can be considered as protected from the "bad" effects of spontaneous emission, since a spontaneous decay process from such states, during a time interval Θ, is very unlikely. We have thus been able to give a correct full quantum description of the phenomenon of velocity selective coherent population trapping, introduced semi-classically in section 10.6. We see now that the correct trapping states are linear superpositions of states which differ not only in the internal state g_1 or g_{-1}, but also in the linear momentum which is $p+\hbar k$ for g_1 and $p-\hbar k$ for g_{-1}. We see also that δp can be as small as we want, and in particular smaller than $\hbar k$, provided that Θ is long enough, since according to eq. (11.28), δp varies as $1/\sqrt{\Theta}$.

11.2.4. Spontaneous transfers between different families

In the previous subsection, we have studied how an atom leaves a family $\mathcal{F}(p)$ by spontaneous emission. We show now that after a spontaneous emission process the atom can move into a new family. This diffusion in momentum space is essential for transferring atoms into the trapping states $\overline{|\psi_{\mathrm{NC}}(p)\rangle}$ with $|p| \ll \delta p$.

Suppose that, at time t, an atom whose state is described by a ket $|\psi(t)\rangle$ of $\mathcal{F}(p)$ spontaneously emits a photon with a momentum $\hbar\boldsymbol{k}$ having a component $\hbar k_z = u$ along Oz. Such an emission is possible only if $|\psi(t)\rangle$ contains a certain admixture of the unstable state $|e_0, \boldsymbol{p}\rangle$. We momentarily use a vector $\boldsymbol{p}$ for the atomic momentum and not only the component p of $\boldsymbol{p}$ along Oz. Just after the spontaneous emission process, the atom is in a linear superposition of $|g_1, \boldsymbol{p} - \hbar\boldsymbol{k}\rangle$ and $|g_{-1}, \boldsymbol{p} - \hbar\boldsymbol{k}\rangle$ which is determined by the direction of $\boldsymbol{k}$ and the polarization of the spontaneously emitted photon. If one is not interested in the x and y components of the atomic momentum, i.e., if one takes the trace of the final density matrix over these quantum numbers, keeping $\hbar k_z = u$ fixed, and if one averages over the polarization of the emitted photon and on the azimuthal direction of $\boldsymbol{k}$, one finds that the final atomic density matrix is a statistical mixture with equal weights, of $|g_1, p-u\rangle$ and $|g_{-1}, p-u\rangle$. Such a result is a clear manifestation of the conservation of the total linear momentum along Oz.

Figure 24 represents the three states $|g_1, p+\hbar k\rangle$, $|g_{-1}, p-\hbar k\rangle$ and $|e_0, p\rangle$ of $\mathcal{F}(p)$ and the two possible final states $|g_1, p-u\rangle$ (a) and $|g_{-1}, p-u\rangle$ (b) of the statistical mixture obtained after the spontaneous emission of a

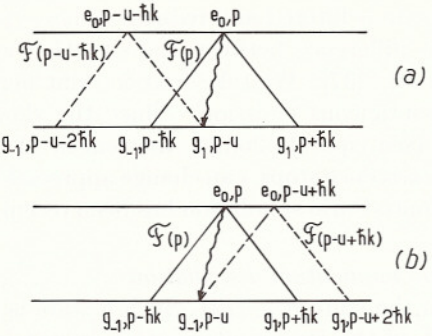

Fig. 24. Transfers between families due to spontaneous emission. Starting from $|e_0, p\rangle$ which belongs to $\mathcal{F}(p)$, the atom can, by spontaneous emission of a photon with momentum u along Oz, go either into $|g_1, p-u\rangle$ which belongs to $\mathcal{F}(p-u-\hbar k)$ (a), or into $|g_{-1}, p-u\rangle$ which belongs to $\mathcal{F}(p-u+\hbar k)$ (b).

photon with momentum u along Oz. According to eq. (11.5), $|g_1, p-u\rangle$ belongs to $\mathcal{F}(p-\hbar k-u)$ whereas $|g_{-1}, p-u\rangle$ belongs to $\mathcal{F}(p+\hbar k-u)$. Since u can take any value between $-\hbar k$ and $+\hbar k$, this shows that spontaneous transfers can occur from $\mathcal{F}(p)$ to $\mathcal{F}(p')$ with $p-2\hbar k \leqslant p' \leqslant p+2\hbar k$.

Combining the results of this subsection and the previous one, it would be possible to make a Monte-Carlo simulation of the time evolution of an atom. Just after a spontaneous emission process one knows the state of the atom, which is for example the state $|g_1, p-u\rangle$ or $|g_{-1}, p-u\rangle$. Knowing this initial state and the effective Hamiltonian (11.17) corresponding to the family of this initial state, one can then calculate the probability that the *next* spontaneous photon will be emitted after a time t. When such a process occurs, one knows the new initial state of the atom and the new family, and so on. There is a certain analogy between the calculation sketched here and the calculation of the delay function used for interpreting the phenomenon of intermittent fluorescence and quantum jumps (see ref. [37] and ref. [2], Chap. VI, subsection E.3.c). In the two situations, one calculates the distribution of the time delays between two *successive* emissions of photons by the same atom, and the existence of very slow decay rates explains why the fluorescence can stop for a very long time. Such an analysis explains also the mechanism for entering into the trapping state $|\psi_{\mathrm{NC}}\rangle$. Just after a spontaneous emission process the atom is for example in $|g_1, p-u\rangle$, which is a linear superposition of the three eigenstates of the effective Hamiltonian corresponding to the family $\mathcal{F}(p-u-\hbar k)$ to which $|g_1, p-u\rangle$ belongs. But these three states decay with quite different rates so that, if no spontaneous emission process has occurred after a time long

enough, the initial state is filtered and reduces to $\overline{|\psi_{NC}(p-\hbar k-u)\rangle}$. Note finally an important difference between the situation analyzed here and the one analyzed in ref. [37]. We take into account here the momentum change following spontaneous emission. Since the slow decay rates are very sensitive to p (see eq. (11.26.b)), the length of the dark periods, during which the fluorescence stops, can change appreciably during the time evolution. Such a Monte-Carlo simulation has been recently performed [88].

11.2.5. Expected final momentum distribution

Consider an atom in the state $|\psi_{NC}(p)\rangle$. Such a state is not an eigenstate of the component P_z of the atomic momentum operator $\boldsymbol{P}$. According to eq. (11.5), a measurement of P_z of an atom in $|\psi_{NC}(p)\rangle$ gives two possible results, $p-\hbar k$ and $p+\hbar k$, with equal probabilities. After an interaction time Θ, a notable fraction of the atoms will be trapped in the states $\overline{|\psi_{NC}(p)\rangle}$ (which are very close to $|\psi_{NC}(p)\rangle$) with $|p| \ll \delta p$, δp being related to Θ by eq. (11.28). One therefore expects to see in the final atomic momentum distribution (i.e., after an interaction time Θ) two peaks centered around $+\hbar k$ and $-\hbar k$, each of these two peaks having a width δp. If Θ is large enough so that δp is smaller than $\hbar k$, one expects these two peaks to be well resolved. Increasing Θ should decrease their width, and hopefully increase their weight, since atoms will have a longer time to diffuse in momentum space towards $p = 0$.

All these predictions are quantitatively confirmed * by a numerical integration of the quantum equations of motion [80]. The interested reader may find in ref. [80] a detailed description of such calculations and of their conclusions. In particular, the prediction (11.28) that the width δp of the two peaks at $\pm\hbar k$ should vary as $\Omega_1/\sqrt{\Theta}$ is very well confirmed. We just mention here that the quantum equations of motion cannot be transformed, as in subsection 5.3.3, into coupled Fokker–Planck equations. Since the atomic momentum distribution contains sharp peaks, with a width δp which can become smaller than $\hbar k$, it is no longer possible to make an expansion of the density matrix elements in powers of $\hbar k/\delta p$.

Note finally that one-dimensional laser cooling of the type described in this section was recently demonstrated on a beam of metastable ^{4}He atoms [79]. Two counterpropagating σ^+ and σ^- laser beams were exciting perpendicularly the atomic beam on the $2^3S_1 \leftrightarrow 2^3P_1$ transition of ^{4}He at $\lambda = 1.08$ nm. Double peak structures with a width δp smaller than

* Note however that the problem of the evolution of the weight of the peaks in the long time limit is still open.

$\hbar k$ were observed on the final momentum distribution, corresponding to a one-dimensional temperature of 2 μK, smaller than the recoil limit of 4 μK corresponding to this transition of ^{4}He.

11.3. Generalization to higher dimensions

In this last section, we present possible extensions to higher dimensions of the one-dimensional cooling scheme analyzed in the previous section. A few proposals have been published, extending the idea of velocity selective coherent population trapping to two dimensions [80,82] or three dimensions [82,83]. We will follow here the presentation of ref. 83, restricting ourselves to the particular case of a $J_g = 1 \leftrightarrow J_e = 1$ transition. Other transitions have been also considered in the literature [84].

11.3.1. Equivalent expression for the absorption amplitude

At two or three dimensions it is no longer possible to ignore the ground-state sublevel g_0 and the two excited Zeeman sublevels e_{-1} and e_1. In the position representation, the most general wave function representing the quantum state of the atom (both internal and external) in the lower state g can be written

$$\Psi_g(\boldsymbol{r}) = \psi_{-1}(\boldsymbol{r})|g_{-1}\rangle + \psi_0(\boldsymbol{r})|g_0\rangle + \psi_{+1}(\boldsymbol{r})|g_{+1}\rangle. \tag{11.29}$$

It is in fact a three-component wave function, one wave function $\boldsymbol{\psi}_m(\boldsymbol{r})$ being associated with each of the three Zeeman sublevels $|g_m\rangle$ of g. Changing from the spherical basis $\{|g_m\rangle\}$ to the Cartesian basis

$$\begin{aligned} |\, g_x\rangle &= -\frac{1}{\sqrt{2}}\,(\,|\, g_{+1}\rangle - |\, g_{-1}\rangle\,)\,, \\ |\, g_y\rangle &= +\frac{1}{\sqrt{2}}\,(\,|\, g_{+1}\rangle + |\, g_{-1}\rangle\,)\,, \\ |\, g_z\rangle &= +\,|\, g_0\rangle \end{aligned} \tag{11.30}$$

transforms eq. (11.29) into

$$\Psi_g(\boldsymbol{r}) = \psi_x(\boldsymbol{r})|g_x\rangle + \psi_y(\boldsymbol{r})|g_y\rangle + \psi_z(\boldsymbol{r})|g_z\rangle, \tag{11.31}$$

where $\psi_x(\boldsymbol{r})$, $\psi_y(\boldsymbol{r})$, $\psi_z(\boldsymbol{r})$ are three wave functions which are transformed by rotation as the three components of a vector field $\boldsymbol{\psi}_g(\boldsymbol{r})$

$$\boldsymbol{\psi}_g(\boldsymbol{r}) = \{\, \psi_x(\boldsymbol{r}),\, \psi_y(\boldsymbol{r}),\, \psi_z(\boldsymbol{r})\,\}. \tag{11.32}$$

A similar argument shows that the most general quantum state in the upper state e is described by a vector field $\boldsymbol{\phi}_e(\boldsymbol{r})$

$$\boldsymbol{\phi}_e(\boldsymbol{r}) = \{\, \phi_x(\boldsymbol{r}),\, \phi_y(\boldsymbol{r}),\, \phi_z(\boldsymbol{r}) \,\}. \tag{11.33}$$

We consider now the probability amplitude $\mathcal{A}$ for the atom to be excited from the state $\boldsymbol{\psi}_g(\boldsymbol{r})$ to the state $\boldsymbol{\phi}_e(\boldsymbol{r})$ by absorption of one laser photon. Such an amplitude depends not only on the initial and final states $\boldsymbol{\psi}_g(\boldsymbol{r})$ and $\boldsymbol{\phi}_e(\boldsymbol{r})$, but also on the laser electric field $\boldsymbol{E}_{\mathrm{L}}^{+}(\boldsymbol{r})$, which is, as $\boldsymbol{\psi}_g(\boldsymbol{r})$ and $\boldsymbol{\phi}_e(\boldsymbol{r})$, a vector field. From the Clebsch–Gordan coefficients of a $J_g = 1 \leftrightarrow J_e = 1$ transition, one can show that

$$\mathcal{A} = \langle \Phi_e \mid V_{\mathrm{AL}} \mid \Psi_g \rangle = C \int \mathrm{d}^3 r\, \boldsymbol{\phi}_e(\boldsymbol{r}) \cdot \left[\boldsymbol{E}_{\mathrm{L}}^{+}(\boldsymbol{r}) \times \boldsymbol{\psi}_g(\boldsymbol{r}) \right], \tag{11.34}$$

where C is a constant. In fact, the structure of eq. (11.34) can be easily understood if one notes that the only vector field which can be constructed from the two vector fields $\boldsymbol{\psi}_g(\boldsymbol{r})$ and $\boldsymbol{E}_{\mathrm{L}}^{+}(\boldsymbol{r})$ is $\boldsymbol{E}_{\mathrm{L}}^{+}(\boldsymbol{r}) \times \boldsymbol{\psi}_g(\boldsymbol{r})$.

11.3.2. Conditions for having a trapping state

Recalling the approach followed in the previous section, we can now identify two general conditions which must be fulfilled by an atomic state $\boldsymbol{\psi}_g^{\mathrm{T}}(\boldsymbol{r})$ in g if one wants this state to be a perfectly trapping state, i.e., such that, if an atom is put in $\boldsymbol{\psi}_g^{\mathrm{T}}(\boldsymbol{r})$ at time $t = 0$ it remains there indefinitely.

First, this state must be insensitive to the laser light. More precisely, one must have

$$V_{\mathrm{AL}} |\Psi_g^{\mathrm{T}}\rangle = 0, \tag{11.35}$$

which generalizes eq. (11.6), or equivalently, according to eq. (11.34)

$$\int \mathrm{d}^3 r\, \boldsymbol{\phi}_e(\boldsymbol{r}) \cdot \left[\boldsymbol{E}_{\mathrm{L}}^{+}(\boldsymbol{r}) \times \boldsymbol{\psi}_g^{\mathrm{T}}(\boldsymbol{r}) \right] = 0 \qquad \forall\, \boldsymbol{\phi}_e(\boldsymbol{r}). \tag{11.36}$$

Secondly, the atomic Hamiltonian H_{A} must not couple Ψ_g^{T} to any other state which could be coupled to the laser light. Such a condition implies that Ψ_g^{T} must be an eigenfunction of H_{A}, or equivalently that Ψ_g^{T} is a stationary state with respect to H_{A}. In the absence of a magnetic field, the three Zeeman sublevels of g have the same internal energy so that the requirement for Ψ_g^{T} to be an eigenfunction of H_{A} can be replaced by

$$H_{\mathrm{A}}^{\mathrm{ext}} |\Psi_g^{\mathrm{T}}\rangle = \frac{\boldsymbol{P}^2}{2M} |\Psi_g^{\mathrm{T}}\rangle = \frac{\boldsymbol{p}^2}{2M} |\Psi_g^{\mathrm{T}}\rangle, \tag{11.37}$$

where $\boldsymbol{P}$ is the atomic momentum operator and where the eigenvalue $\boldsymbol{p}^2/2M$ is a c-number.

11.3.3. Finding a trapping state

We show now that a very simple way to satisfy both conditions (11.36) and (11.37) is to take

$$\boldsymbol{\psi}_g^{\mathrm{T}}(\boldsymbol{r}) = \mu\, \boldsymbol{E}_{\mathrm{L}}^{+}(\boldsymbol{r}), \tag{11.38}$$

where μ is a constant. Equation (11.38) defines an atomic state in g whose wave function is described by the same vector field as the laser electric field. It is first clear that eq. (11.36) is fulfilled since

$$\boldsymbol{E}_{\mathrm{L}}^{+}(\boldsymbol{r}) \times \boldsymbol{\psi}_g^{\mathrm{T}}(\boldsymbol{r}) = \mu\, \boldsymbol{E}_{\mathrm{L}}^{+}(\boldsymbol{r}) \times \boldsymbol{E}_{\mathrm{L}}^{+}(\boldsymbol{r}) = \boldsymbol{0}. \tag{11.39}$$

Secondly, we note that, the laser field being monochromatic with frequency ω_{L}, $\boldsymbol{E}_{\mathrm{L}}^{+}(\boldsymbol{r})$ is necessarily a superposition of plane waves with wave vectors having all the same modulus $k_{\mathrm{L}} = \omega_{\mathrm{L}}/c$, so that

$$\boldsymbol{\nabla}^2 \boldsymbol{E}_{\mathrm{L}}^{+} = -k_{\mathrm{L}}^2 \boldsymbol{E}_{\mathrm{L}}^{+}. \tag{11.40}$$

Since $\boldsymbol{P} = -\mathrm{i}\hbar\boldsymbol{\nabla}$, we then deduce from eqs. (11.38) and (11.40) that

$$\frac{\boldsymbol{P}^2}{2M}\boldsymbol{\psi}_g^{\mathrm{T}} = -\frac{\mu\hbar^2}{2M}\,\boldsymbol{\nabla}^2 \boldsymbol{E}_{\mathrm{L}}^{+} = \frac{\hbar^2 k_{\mathrm{L}}^2}{2M}\,\boldsymbol{\psi}_g^{\mathrm{T}}, \tag{11.41}$$

which shows that $\boldsymbol{\psi}_g^{T}$ also satisfies eq. (11.37) since it is an eigenfunction of $\boldsymbol{P}^2/2M$ with the eigenvalue $E_{\mathrm{R}} = \hbar^2 k_{\mathrm{L}}^2/2M$.

It should be noted however that conditions (11.36) and (11.37), which must necessarily be fulfilled by a three-dimensional trapping state, are not sufficient for defining such a state. Consider for example a laser configuration which is formed by three coplanar plane waves whose wave vectors $\boldsymbol{k}_1$, $\boldsymbol{k}_2$, $\boldsymbol{k}_3$ are all in the $x\mathrm{O}y$ plane, with

$$|\boldsymbol{k}_1| = |\boldsymbol{k}_2| = |\boldsymbol{k}_3| = k_{\mathrm{L}} = \omega_{\mathrm{L}}/c \tag{11.42}$$

Suppose now that, instead of taking a constant μ in eq. (11.38), we replace μ by $\mathrm{e}^{\mathrm{i}\kappa z}$, so that we take for $\boldsymbol{\psi}_g^{T}$

$$\boldsymbol{\psi}_g^{\mathrm{T}}(\boldsymbol{r}) = \exp(\mathrm{i}\kappa z)\, \boldsymbol{E}_{\mathrm{L}}^{+}(\boldsymbol{r}). \tag{11.43}$$

It is clear that eq. (11.43) still fulfills eq. (11.36) since $\boldsymbol{\psi}_g^{\mathrm{T}} \times \boldsymbol{E}_{\mathrm{L}}^{+}$ is still equal to zero. On the other hand, the multiplication by $\mathrm{e}^{\mathrm{i}\kappa z}$ in eq. (11.43)

amounts to adding to the wave vectors $\boldsymbol{k}_i$ $(i = 1, 2, 3)$ of the three plane waves forming $\boldsymbol{E}_{\mathrm{L}}^{+}$ the vector $\boldsymbol{\kappa} = \kappa \boldsymbol{\epsilon}_z$. It follows that the vector wave function (11.43) is now the sum of three de Broglie plane waves with wave vectors $\boldsymbol{k}_i + \boldsymbol{\kappa}$ $(i = 1, 2, 3)$. Since $\boldsymbol{\kappa}$, which is parallel to Oz, is perpendicular to $\boldsymbol{k}_1$, $\boldsymbol{k}_2$, $\boldsymbol{k}_3$, which are all in the xOy plane, the three wave vectors $\boldsymbol{k}_i + \boldsymbol{\kappa}$ have the same modulus $\left(k_{\mathrm{L}}^2 + \kappa^2\right)^{1/2}$, so that eq. (11.43) is still an eigenstate of $\boldsymbol{P}^2/2M$ with eigenvalue $\hbar^2 \left(k_{\mathrm{L}}^2 + \kappa^2\right)/2M$.

$$\frac{\boldsymbol{P}^2}{2M} \exp(\mathrm{i}\kappa z) \boldsymbol{E}_{\mathrm{L}}^{+}(\boldsymbol{r}) = \frac{\hbar^2 (k_{\mathrm{L}}^2 + \kappa^2)}{2M} \exp(\mathrm{i}\kappa z)\, \boldsymbol{E}_{\mathrm{L}}^{+}(\boldsymbol{r}). \tag{11.44}$$

We have thus demonstrated that eq. (11.43) still satisfies eqs. (11.36) and (11.37). But, since κ can take any value, eq. (11.43) defines now a whole set of trapping states which differ from each other by the value of the momentum along Oz. In other words, with a laser configuration formed by three coplanar plane waves, taking ψ_T^g proportional to $\boldsymbol{E}_{\mathrm{L}}^{+}$ does not lead to a three-dimensional trapping state, since there are an infinite number of trapping states which differ by the momentum perpendicular to the plane of the three waves. We have only a two-dimensional trapping.

The previous discussion suggests that, in order to get a unique 3-D trapping state, one must take a laser configuration consisting of at least four plane waves $\boldsymbol{k}_i$ $(i = 1, 2, 3, 4)$, the directions of the four wave vectors $\boldsymbol{k}_i$ being such that there exists a single sphere (of radius $k_{\mathrm{L}} = \omega_{\mathrm{L}}/c$) centered on 0 and containing the extremities of the $\boldsymbol{k}_i$'s. Any translation $\boldsymbol{\kappa}$ then destroys the equality between the modulus of the four vectors $\boldsymbol{k}_i + \boldsymbol{\kappa}$. A 3-D atomic trapping state (for a $J_g = 1 \leftrightarrow J_e = 1$ transition) must therefore be a superposition of at least four states $|g_i, \boldsymbol{k}_i\rangle$, (with $|\boldsymbol{k}_i| = k_{\mathrm{L}}$), differing not only in the direction $\boldsymbol{k}_i/k_i$ of the momentum, but also in the internal state g_i. Since, according to eq. (11.38), each state $|g_i, \boldsymbol{k}_i\rangle$ is the replica of a laser plane wave, and since such light waves are transverse, the internal atomic state g_i must be also transverse with respect to $\boldsymbol{k}_i$.

It would be very interesting to try to demonstrate the existence of such 3-D trapping states which exhibit non-separable quantum correlations between internal and external degrees of freedom. A certain number of problems remain to be investigated. For example, one must get rid of gravity. Also, the filling efficiency of the trapping state, which depends on momentum diffusion, could be much smaller in three dimensions than in one dimension and it would probably be helpful to supplement the method by other schemes increasing the momentum diffusion towards the low values of p.

Acknowledgements

I warmly thank all my colleagues of the Ecole Normale Supérieure, in particular Jean Dalibard, for many helpful discussions and comments about this course. I am also very grateful to Paul Lett for a careful reading of the manuscript and to Michèle Sanchez and Isabelle Gazan for their help in the preparation of these lecture notes.

References

[1] B.R. Mollow, Phys. Rev. **A 12**, (1975) 1919.
[2] C. Cohen-Tannoudji, J. Dupont-Roc and G. Grynberg, Processus d'interaction entre photons et atomes (InterEditions et Editions du CNRS, Paris, 1988). English translation: Atom-Photon Interactions. Basic Processes and Applications (Wiley, New York, 1992).
[3] C. Cohen-Tannoudji, in Les Houches, Session XXXVIII, 1982 - New trends in atomic physics, eds. G. Grynberg and R. Stora (Elsevier Science Publishers B.V., Amsterdam, 1984).
[4] C. Cohen-Tannoudji, J. Dupont-Roc and G. Grynberg, Photons et atomes, Introduction à l'electrodynamique quantique (InterEditions et Editions du CNRS, Paris, 1987). English translation: Photons and Atoms, Introduction to Quantum Electrodynamics (Wiley, New York, 1989).
[5] C. Cohen-Tannoudji, in Les Houches, Session XXVII, 1975 - Frontiers in laser spectroscopy, eds. R. Balian, S. Haroche and S. Liberman (North-Holland, Amsterdam, 1977).
[6] A. Kastler, J. Phys. Rad. **11** (1950) 255.
[7] J. Dalibard, S. Reynaud and C. Cohen-Tannoudji, J. Phys. **B 17** (1984) 4577.
[8] J.P. Gordon and A. Ashkin, Phys. Rev. **A 21** (1980) 1606.
[9] J.R. Ackerhalt and J.H. Eberly, Phys. Rev. **D 10** (1974) 3350.
[10] J. Dalibard, J. Dupont-Roc and C. Cohen-Tannoudji, J. Phys. **43** (1982) 1617; **45** (1984) 637.
[11] R.J. Cook, Phys. Rev. **A 20** (1979) 224.
[12] E. Joos and H.D. Zeh, Z. Phys. **B 59** (1985) 223.
[13] T.W. Hansch and A.L. Schawlow, Opt. Commun. **13** (1975) 68.
[14] V.G. Minogin and T. Serimaa, Opt. Commun. **30** (1979) 373.
[15] E. Kyrola and S. Stenholm, Opt. Commun. **22** (1977) 123.
[16] N.G. van Kampen, Stochastic Processes in Physics and Chemistry (North-Holland, Amsterdam, 1981).
[17] J. Dalibard and C. Cohen-Tannoudji, J. Phys. **B 18** (1985) 1661.
[18] M. Lax, Phys. Rev. **172** (1968) 350.
[19] L. Mandel, Opt. Lett. **4** (1979) 205.
[20] J. Dalibard, S. Reynaud and C. Cohen-Tannoudji, Opt. Commun. **47** (1983) 395.
[21] D. Wineland and W. Itano, Phys. Rev. **A 20** (1979) 1521.
[22] S. Stenholm, Rev. Mod. Phys. **58** (1986) 699.
[23] J. Dalibard, Phys. Scr., **T 12** (1986) 28.

[24] E.P. Wigner, Phys. Rev. **40** (1932) 749.
[25] V.S. Letokhov and V.G. Minogin, Phys. Rep. **73** (1981) 1.
[26] R.J. Cook, Phys. Rev. **A 22** (1980) 1078.
[27] A.P. Kazantsev, G.I. Surdutovitch and V.P. Yakovlev, J. Phys. (Paris) **42** (1981) 1231.
[28] S. Stenholm, Phys. Rev. **A 27** (1983) 2513.
[29] P. Martin, in Many-Body Physics, eds. C. de Witt and R. Balian, (Gordon and Breach, New-York, 1968) p. 37.
[30] C. Cohen-Tannoudji, in Cargese Lectures in Physics, Vol. 2, p. 347, M.Levy ed. (Gordon and Breach, New York, 1968).
[31] S. Haroche, Thesis, Paris 1971, published in Ann. Phys. (Paris) **6** (1971) 189 and 327.
[32] C. Cohen-Tannoudji and S. Reynaud, J. Phys. **B 10** (1977) 345.
[33] C. Cohen-Tannoudji and S. Reynaud, in Multiphoton processes, eds. J. Eberly and P. Lambropoulos (Wiley, New York, 1978) p. 103.
[34] S. Reynaud, Thesis, Paris 1981, published in Ann. Phys. (Paris) **8** (1983) 315 and 371.
[35] C. Cohen-Tannoudji and S. Reynaud, Philos. Trans. R. Soc. London, **A 293** (1979) 233.
[36] A. Aspect, G. Roger, S. Reynaud, J. Dalibard and C. Cohen-Tannoudji, Phys. Rev. Lett. **45** (1980) 617.
[37] C. Cohen-Tannoudji and J. Dalibard, Europhys. Lett. **1**, (1986) 441.
[38] S. Reynaud, J. Dalibard and C. Cohen-Tannoudji, IEEE J. Quantum Electron. **24** (1988) 1395.
[39] J. Dalibard and C. Cohen-Tannoudji, J.O.S.A. **B 2** (1985) 1707. An extension of the method described here to multilevel atoms may be found in E. Bonderup and K.Mølmer, J.O.S.A. **B 6** (1989) 2125.
[40] R.J. Glauber, in Quantum Optics and Electronics, Les Houches (1964), eds. C. de Witt, A. Blandin and C. Cohen-Tannoudji (Gordon and Breach, New York, 1968) p. 63.
[41] C. Cohen-Tannoudji, B. Diu and F. Laloë, Quantum Mechanics (Wiley and Hermann, Paris, 1977).
[42] B.R. Mollow, Phys. Rev. **188** (1969) 1969.
[43] A.P. Kazantsev, Zh. Eksp. Teor. Fiz. **66** (1974) 1599 [Sov. Phys. JETP **39** (1974) 784].
[44] A.P. Kazantsev, Sov. Phys. Usp. **21** (1978) 58.
[45] A.P. Kazantsev, V.S. Smirnov, G.I. Surdutovitch, D.O. Chudesnikov and V.P. Yakovlev, J.O.S.A. **B 2** (1985) 1731. See also K. Mølmer, Thesis, University of Aarhus (1990).
[46] V.S. Letokhov, Pis'ma Zh. Eksp. Teor. Fiz. **7** (1968) 348 [JETP Lett. **7** (1968) 272].
[47] A. Aspect, J. Dalibard, A. Heidmann, C. Salomon and C. Cohen-Tannoudji, Phys. Rev. Lett. **57** (1986) 48.
[48] C. Salomon, J. Dalibard, A. Aspect, H. Metcalf and C. Cohen-Tannoudji, Phys. Rev. Lett. **59** (1987) 1659. An indirect manifestation of channeling was also reported in M.G. Prentiss and S. Ezekiel, Phys. Rev. Lett. **56** (1986) 46.
[49] A. Messiah, Quantum Mechanics (North-Holland, Amsterdam, 1962).
[50] J.P. Barrat and C. Cohen-Tannoudji, J. Phys. Rad. **22** (1961) 329 and 443.
[51] C. Cohen-Tannoudji, Thesis, Paris (1962), Ann. Phys. **7** (1962) 423 and 469.

[52] C. Cohen-Tannoudji, C. R. Acad. Sci. **252** (1961) 394.
[53] M. Arditi and T.R. Carver, Phys. Rev. **124** (1961) 800.
[54] W. Happer and S. Mathur, Phys. Rev. **163** (1967) 12.
[55] C. Cohen-Tannoudji and J. Dupont-Roc, Phys. Rev. **A 5** (1972) 968.
[56] W. Hanle, Z. Phys. **30** (1924) 93 and Z. Phys. **35** (1926) 346.
[57] J. Dupont-Roc, S. Haroche and C. Cohen-Tannoudji, Phys. Letters **A 28** (1969) 638.
[58] C. Cohen-Tannoudji, J. Dupont-Roc, S. Haroche and F. Laloë, Phys. Rev. Lett. **22** (1969) 758.
[59] R. Kaiser, N. Vansteenkiste, A. Aspect, E. Arimondo and C. Cohen-Tannoudji, Z. Phys. **D 18** (1991) 17.
[60] G. Nienhuis, Proceedings of Light Induced Kinetic Effects, eds. L. Moi, S. Gozzini, C. Gabbanini, E. Arimondo and F. Strumia (ETS Editrice, Pisa, 1991).
[61] H. Wallis, Thesis, Bonn (1990).
[62] P. Lett, R. Watts, C. Westbrook, W.D. Phillips, P. Gould and H. Metcalf, Phys. Rev. Lett. **61** (1988) 169.
[63] J. Dalibard and C. Cohen-Tannoudji, J.O.S.A. **B 6** (1989) 2023.
[64] Y. Castin, J. Dalibard and C. Cohen-Tannoudji, Proceedings of Light Induced Kinetic Effects, eds. L. Moi, S. Gozzini, C. Gabbanini, E. Arimondo and F. Strumia (ETS Editrice, Pisa, 1991).
[65] P.J. Ungar, D.S. Weiss, E. Riis and S. Chu, J.O.S.A. **B 6** (1989) 2058.
[66] Y. Castin and J. Dalibard, Europhys. Lett. **14** (1991) 761.
[67] D.S. Weiss, E. Riis, Y. Shevy, P.J. Ungar and S. Chu, J.O.S.A. **B 6** (1989) 2072.
[68] B. Sheehy, S.Q. Shang, P. van der Straten, S. Hatamian and H. Metcalf, Phys. Rev. Lett. **64** (1990) 858.
[69] C. Salomon, J. Dalibard, W.D. Phillips, A. Clairon and S. Guellati, Europhys. Lett. **12** (1990) 683. See also C. Monroe, W. Swann, H. Robinson and C. Wieman, Phys. Rev. Lett. **65** (1990) 1571.
[70] J. Dalibard, C. Salomon, A. Aspect, E. Arimondo, R. Kaiser, N. Vansteenkiste and C. Cohen-Tannoudji, in Atomic Physics 11, eds. S. Haroche, J.C. Gay and G. Grynberg (World Scientific, Singapore, 1989) p. 199.
[71] S. Chu, D.S. Weiss, Y. Shevy and P.J. Ungar, in Atomic Physics 11, eds. S. Haroche, J.C. Gay and G. Grynberg (World Scientific, Singapore, 1989) p. 636.
[72] H.J. Metcalf, Proceedings of Light Induced Kinetic Effects, eds. L. Moi, S. Gozzini, C. Gabbanini, E. Arimondo and F. Strumia (ETS Editrice, Pisa, 1991).
[73] Y. Castin and K. Mølmer, J. Phys. **B 23** (1990) 4101.
[74] Y. Castin, K. Mølmer, J. Dalibard and C. Cohen-Tannoudji, in Laser Spectroscopy IX, eds. M. Feld, J. Thomas and A. Mooradian (Academic Press, San-Diego, 1989).
[75] G. Alzetta, A. Gozzini, L. Moi and G. Orriols, Nuovo Cimento **B 36** (1976) 5.
[76] E. Arimondo and G. Orriols, Lett. Nuovo Cimento, **17** (1976) 333.
[77] P.M. Radmore and P.L. Knight, J. Phys. **B 15** (1982) 561.
[78] J. Dalibard, S. Reynaud and C. Cohen-Tannoudji, in Interaction of Radiation with Matter, a Volume in Honor of A. Gozzini, Scuola Normale Superiore, Pisa (1987).
[79] A. Aspect, E. Arimondo, R. Kaiser, N. Vansteenkiste and C. Cohen-Tannoudji, Phys. Rev. Lett. **61** (1988) 826.
[80] A. Aspect, E. Arimondo, R. Kaiser, N. Vansteenkiste and C. Cohen-Tannoudji, J.O.S.A. **B 6**, (1989) 2112.

[81] D.E. Pritchard, K. Helmerson, V.S. Bagnato, G.P. Lafyatis and A.G. Martin, in Laser Spectroscopy VIII, eds. S. Svanberg and W. Persson (Springer Verlag, Heidelberg, 1987) p. 68.

[82] F. Mauri, F. Papoff and E. Arimondo, Proceedings of Light Induced Kinetic Effects, eds. L. Moi, S. Gozzini, C. Gabbanini, E. Arimondo and F. Strumia (ETS Editrice, Pisa, 1991).

[83] M.A. Ol'shanii and V.G. Minogin, Proceedings of Light Induced Kinetic Effects, eds. L. Moi, S. Gozzini, C. Gabbanini, E. Arimondo and F. Strumia (ETS Editrice, Pisa, 1991).

[84] F. Papoff, F. Mauri and E. Arimondo, J.O.S.A. **B 9** (1992) 321.

[85] C. Cohen-Tannoudji and W.D. Phillips, Physics Today, October 1990, p. 33.

[86] P. Verkerk, B. Lounis, C. Salomon, C. Cohen-Tannoudji, J.Y. Courtois and G. Grijnberg, Phys. Rev. Lett. **68** (1992) 3861.

[87] P.S. Jessen, C. Gerz, P.D. Lett, W.D. Phillips, S.L. Rolston, R.J.C. Spreeuw and C.I. Westbrook, Phys. Rev. Lett. **69** (1992) 49.

[88] C. Cohen-Tannoudji, F. Bardou and A. Aspect, in Laser Spectroscopy X, eds. M. Ducloy, E. Giacobino and G. Camy (World Scientific, Singapore, 1992) p. 3.